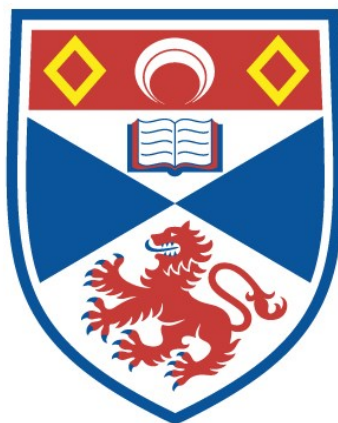


THE CO-ORDINATION AND REARRANGEMENT OF
PHOSPHORUS MIXED ANHYDRIDES OF
DIPHENYLPHOSPHINOUS AND ACRYLIC ACIDS

Derek John Irvine

A Thesis Submitted for the Degree of PhD
at the
University of St Andrews



1990

Full metadata for this item is available in
St Andrews Research Repository
at:

<http://research-repository.st-andrews.ac.uk/>

Please use this identifier to cite or link to this item:

<http://hdl.handle.net/10023/14937>

This item is protected by original copyright

**The Coordination and Rearrangement of Phosphorus
Mixed Anhydrides of Diphenylphosphinous and
Acrylic acids**

a thesis presented by

DEREK JOHN IRVINE

to the

UNIVERSITY OF ST. ANDREWS

in application for

THE DEGREE OF DOCTOR OF PHILOSOPHY

St. Andrews

April 1990



ProQuest Number: 10167029

All rights reserved

INFORMATION TO ALL USERS

The quality of this reproduction is dependent upon the quality of the copy submitted.

In the unlikely event that the author did not send a complete manuscript and there are missing pages, these will be noted. Also, if material had to be removed, a note will indicate the deletion.



ProQuest 10167029

Published by ProQuest LLC (2017). Copyright of the Dissertation is held by the Author.

All rights reserved.

This work is protected against unauthorized copying under Title 17, United States Code
Microform Edition © ProQuest LLC.

ProQuest LLC.
789 East Eisenhower Parkway
P.O. Box 1346
Ann Arbor, MI 48106 – 1346

th 12/13

Copyright

In submitting this thesis to the University of St. Andrews I understand that I am giving permission for it to be made available for use in accordance with the regulations of the University library for the time being in force, subject to any copyright vested in the work not being affected thereby. I also understand that the title and abstract will be published, and that a copy of the work may be made and supplied to any *bona fide* library or research worker.

Declaration

I, Derek John Irvine, hereby certify that this thesis has been composed by myself, that it is a record of my work, and that it has not been accepted in partial or complete fulfilment of any other degree or professional qualification.

Signed Date 3/7/90

I was admitted to the Faculty of Science of the University of St Andrews under Ordinance General No. 12 on 5th OCT 1986
and as a candidate for the degree of Ph. D on 5th OCT 1987

Signed Date

I hereby certify that the candidate has fulfilled the conditions of the Resolution and Regulations appropriate to the degree of Ph. D.

Signature of Supervisor

Date

" How often have I told you that when you have eliminated the impossible, whatever remains, however improbable, must be the truth. "

The Sign of Four

Sir Authur Conan Doyle

To my Family

They have had to put up with a great deal in the last 25
years

Contents

Page

Acknowledgements

Abbreviations

Abstract and Note

Chapter 1 Transition Metal Complexes of Mono-alkenes **A Literature Survey**

1.1	Introduction	1
1.2	Historical Overview	2
1.3	Theories on the π Bonding Model	3
1.3.1	Initial Observations Upon Alkene Coordination	3
1.3.2	Resonance Hybrid Model Based on Valence Bond Theory	4
1.3.3	Dewar, Chatt, Duncanson Model	5
1.3.4	Treatment of Alkenes with Highly Electronegative Substituents	8
1.4	Properties Which Effect the Stability of the π Alkene Complexes	9
1.4.1	Steric Properties	9
1.4.2	Electronic Properties	10
1.4.3	Properties of Metal	11
1.4.4	Effects of Non-Olefinic Ligands	11
1.4.5	Effects of Cyclic Ligands	12
1.5	The Development of Chelate Mono-Alkenes	13
1.5.1	Chelate Olefin Ligands Containing Phosphorus	24

1.5.1	Chelate Olefin Ligands Containing Phosphorus Donor Atoms	24
1.5.2	Phosphorus Mixed Anhydrides Ligands and their Rhodium Complexes	39
1.6	Catalysis Involving Metal Complexes	40
1.6.1	Asymmetric Synthesis	44
1.6.2	Early Work on Metal Ligand Stereoselectivity	46
1.6.3	Mechanism of Bidentate Ligand Stereoselectivity	47
1.7	Catalytic Studies with Phosphorus Mixed Anhydrides	48

Chapter 2 Complexation of the Mixed Anhydrides of Acrylic and Phosphinic Acids to Wilkinson's Catalyst

2.1	Introduction	52
2.2	Production of the Mixed Anhydride Ligands ($\text{Ph}_2\text{PO}_2\text{CCR}=\text{R}'\text{R}'$)	53
2.3	Coordination Study of the Mixed Anhydride Derived from Crotonic Acid and Wilkinson's Catalyst and Spectral Data for $[\text{RhCl}(\text{PPh}_3)(\text{Ph}_2\text{PO}_2\text{CCH}=\text{CHMe})]$	56
2.3.1	Infra-red Data	58
2.3.2	^{31}P n.m.r. Data	59
2.3.3	^1H n.m.r. Data	61
2.4	Explanation of fluxionality and Non Room Temperature n.m.r. Studies of the CAA/Wilkinson's Catalyst Complex	64
2.4.1	Solution Infra red Study	64
2.4.2	High Temperature n.m.r. Studies	65

2.4.3	Low Temperature ^{31}P n.m.r. Studies	65
2.5	Reaction of $[\text{RhCl}(\text{PPh}_3)(\text{Ph}_2\text{PO}_2\text{CCH}=\text{CHMe})]$ and $[\text{K}^+][^-\text{O}_2\text{CCH}=\text{CHMe}]$	73
2.5.1	Infra-red Data	74
2.5.2	^{31}P n.m.r. Data	80
2.5.3	^1H n.m.r. Data	81
2.6	Reaction of Wilkinson's Catalyst and the Mixed Anhydride Derived from Acrylic Acid	82
2.6.1	Spectral Data for $[\text{RhCl}(\text{PPh}_3)(\text{Ph}_2\text{PO}_2\text{CCH}=\text{CH}_2)]$	82
2.6.2	Spectroscopic Properties of $[\text{RhCl}(\text{PPh}_3)(\text{Ph}_2\text{PO}_2\text{CCH}=\text{CH}_2)]$	89
2.6.3	The Reaction of the Mixed Anhydrides with Triphenylphosphine	89
2.7	Structural Trends of the Bidentate Anhydride Complexes of Wilkinson's Catalyst and Computer Studies on the Crotonic and Acrylic Derivatives	95
2.7.1	Chem-X Computer Study	98
2.7.2	$[\text{RhCl}(\text{PPh}_3)(\text{Ph}_2\text{PO}_2\text{CCH}=\text{CH}_2)]$ Conclusions	99
2.7.3	$[\text{RhCl}(\text{PPh}_3)(\text{Ph}_2\text{PO}_2\text{CCH}=\text{CHMe})]$ Conclusions	99
2.8	Reaction of Wilkinson's Catalyst and the Mixed Anhydride Derived from Vinylacetic Acid	100
2.8.1	Mechanism of Double Bond Migration	103
2.9	Catalytic Studies Involving $[\text{RhCl}(\text{CAA})(\text{PPh}_3)]$	104
2.9.1	Results of the Catalytic Studies	106
2.10	Experimental	110

Chapter 3 **Investigations into the Rearrangements Resulting
in the Formation of $\text{Ph}_2\text{PP}(\text{O})\text{Ph}_2$ and
 $[\text{RhCl}(\text{PPh}_3)(\text{Ph}_2\text{POPPh}_2)]$**

3.1	Investigation into the Rearrangement of $\text{Ph}_2\text{PO}_2\text{CCH}=\text{CH}_2$ to $\text{Ph}_2\text{POPPh}_2$	116
3.2	The 2:1 Mole Reaction of the $\text{Ph}_2\text{PO}_2\text{CCH}=\text{CH}_2$ and Wilkinson's Catalyst	121
3.2.1	Spectral Data of $[\text{RhCl}(\text{PPh}_3)(\text{Ph}_2\text{POPPh}_2)].\text{thf}$	122
3.3	Formation of the Tdpdp Complexes	124
3.3.1	Proposed Mechanism for the Metal Promoted Rearrangement of $\text{Ph}_2\text{PO}_2\text{CCH}=\text{CH}_2$	124
3.3.2	Reaction of Wilkinson's Catalyst and Tetraphenyldiphosphine Monoxide	129
3.4	Reaction of $[\text{RhCl}(\text{PPh}_3)(\text{Ph}_2\text{POPPh}_2)]$ and TiPF_6	131
3.4.1	Spectroscopic Data of $[\text{Rh}(\text{PPh}_3)_2(\text{Ph}_2\text{POPPh}_2)][\text{PF}_6]$ and $[\text{Rh}(\text{PPh}_3)_2(\text{Ph}_2\text{POPPh}_2)][\text{Cl}]$	133
3.5	Reaction of $[\text{RhCl}(\text{PPh}_3)_3]$ and $2(\text{Ph}_2\text{PO}_2\text{CCH}=\text{CH}_2)$ in the Presence of TiPF_6	137
3.5.1	Spectroscopic Data for $[\text{Rh}(\text{PPh}_3)_3(\text{Ph}_3\text{PCH}_2\text{CH}_2\text{CO}_2)][\text{PF}_6]$	138
3.6	Spectroscopic properties of $[\text{Rh}(\text{PPh}_3)_3(\text{thf})][\text{PF}_6]$ $[\text{Rh}(\text{PPh}_3)_3(\text{CH}_2=\text{CHCO}_2)]$	140
3.6.1	Reaction of $[\text{Rh}(\text{PPh}_3)_3\text{Cl}]$ and TiPF_6 in THF	140
3.6.2	Spectral Data on $[\text{Rh}(\text{PPh}_3)_3(\text{thf})][\text{PF}_6]$	141
3.6.3	Reaction of $[\text{Rh}(\text{PPh}_3)_3\text{Cl}]$, TiPF_6 and $\text{K}^+\text{O}_2\text{CCH}=\text{CH}_2$	144
3.6.4	Spectral Data on $[\text{Rh}(\text{PPh}_3)_3(\text{CH}_2=\text{CHCO}_2)]$	144
3.7	Experimental	191

**Chapter 4 Reactions of the Mixed Anhydrides and Rhodium
Chlorine Bridged Dimers**

4.1	General Method for the Anhydride/Dimer Reactions	155
4.2	Spectroscopic Details of the Anhydride/Dimer Complexes	156
4.2.1	Infra red Data	156
4.2.2	^{31}P n.m.r. Spectra	156
	A) $\text{Ph}_2\text{PO}_2\text{CCH}=\text{CHMe}$ Dimer	156
	B) $\text{Ph}_2\text{PO}_2\text{CCH}=\text{CH}_2$ Dimer	160
	C) $\text{Ph}_2\text{PO}_2\text{CCH}_2\text{CH}=\text{CH}_2$ Dimer	160
4.2.3	Summary of ^{31}P n.m.r. Conclusions	163
4.2.4	^1H n.m.r. Spectra	163
4.3	Effects of Altering the Mole Ratio of the $\text{Ph}_2\text{PO}_2\text{CCH}=\text{CH}_2$ /Octene Dimer Reaction and the Spectral Evidence for $[(\text{RhCl}(\text{Ph}_2\text{PO}_2\text{CCH}=\text{CH}_2))_2(\text{Ph}_2\text{POPPh}_2)]$	164
4.4	The Reaction of $\text{Ph}_2\text{PO}_2\text{CCH}=\text{CH}_2$ with $[\text{Rh}_2\text{Cl}_2(\text{CH}_2=\text{CH}_2)_2]$ and the Spectral Evidence for $[\text{RhCl}(\text{Ph}_2\text{PO}_2\text{CCH}=\text{CH}_2)_2]$	172
4.4.1	Summary of the Results Obtained by Altering the Mole Ratios and the Dimeric Substrate in the Anhydride/Dimer Reactions	181
4.5	Reactions of $[\text{RhCl}(\text{Ph}_2\text{PO}_2\text{CCH}=\text{CH}_2)_2]$	182
4.5.1	Reaction of $[\text{RhCl}(\text{Ph}_2\text{PO}_2\text{CCH}=\text{CH}_2)_2]$ with Triphenylphosphine	182
4.5.2	Mechanism to Produce $[(\text{RhCl}(\text{Ph}_2\text{PO}_2\text{CCH}=\text{CH}_2))_2(\text{Ph}_2\text{POPPh}_2)]$	184
4.6	Experimental	191

**Chapter 5 The Reaction of Selected Mixed Anhydride
And $[\text{RuCl}_2(\text{PPh}_3)_4]$**

5.1	Introduction	195
5.2	The 1:1 Mole Reaction of $\text{Ph}_2\text{PO}_2\text{CCH}=\text{CMe}_2$ and $[\text{RuCl}_2(\text{PPh}_3)_4]$	196
5.3	The 1:1 Mole Reactions of $\text{Ph}_2\text{PO}_2\text{CCH}=\text{CH}_2$ and $\text{Ph}_2\text{PO}_2\text{CCH}=\text{CHMe}$ with $[\text{RuCl}_2(\text{PPh}_3)_4]$	200
5.3.1	Product 1	200
5.3.2	Product 2	201
5.3.3	Structural Conclusions on Product 1	202
5.4	Discussion on the Coordination Exhibited by the Ruthenium Complexes	210
5.5	The 2:1 Mole Reaction of $\text{Ph}_2\text{PO}_2\text{CCH}=\text{CH}_2$ and $[\text{RuCl}_2(\text{PPh}_3)_4]$	211
5.6	Experimental	221

**Chapter 6 Reflux Reactions of Platinum Metal Complexes
 $[\text{RhCl}(\text{PPh}_3)_3]$ and $[\text{MCl}_2(\text{PPh}_3)_4]$ and
 $\text{Ph}_2\text{POPPH}_2$ Where $\text{M} = \text{Ru}$ or Os**

6.1	Introduction	223
6.1.1	Literature Routes to Complexes Containing Chelate $\text{Ph}_2\text{POPPH}_2$ ligands	223
6.1.2	Literature Examples of Complexes of Diphenylphosphinous acid and Secondary Phosphites	227
6.2	Reflux reactions of $\text{Ph}_2\text{POPPH}_2$ with $[\text{RhCl}(\text{PPh}_3)_3]$.	

[RuCl ₂ (PPh ₃) ₄] and [OsCl ₂ (PPh ₃) ₄]	233
6.2.1 Reflux Reaction of [RhCl(PPh ₃) ₃] and Ph ₂ POPPPh ₂ in THF	233
6.2.2 Reflux Reaction of [RuCl ₂ (PPh ₃) ₄] and Ph ₂ POPPPh ₂ in THF	234
6.2.3 Reflux Reaction of [OsCl ₂ (PPh ₃) ₄] and Ph ₂ POPPPh ₂ in THF	238
6.3 Experimental	248

Chapter 7 Crystal Structure Determinations

7.1 Method of Structure Solution	251
7.2 Molecular Structure of [RhCl(PPh ₃)(Ph ₂ POPPPh ₂)]	258
7.2.1 Experimental	258
7.2.2 Discussion of Results	259
7.3 Molecular Structure of [RhCl ₂ (Ph ₂ PO) ₃ H][Et ₃ NH]	267
7.3.1 Experimental	267
7.3.2 Structural Features in [RhCl ₂ (Ph ₂ PO) ₃ H][Et ₃ NH]	267

References	280
-------------------	-----

Summary

Appendix 1

Appendix 2

Acknowledgements

I would like to express my deepest thanks to Professor David Cole-Hamilton for his encouragement and guidance during the course of my postgraduate studies. I also would like to thank my industrial supervisor Dr. Philip Hodgson for his invaluable assistance and discussions, especially during my brief period at B.P. Sunbury.

Special tanks also goes to :-

Dr. John Barnes and John Patton of the University of Dundee, for inspiring my interest in Crystallography and supervising my first tottering steps in the field. Also Dr. Alan Howie of the University of Aberdeen, for collecting the data sets.

Dr. K. Bare of B.P. International p.l.c., for the F.A.B. Mass Spectral results.

Dr. C. Glidewell, for some MNDO calculations.

Dr. Ray Mackie, for his guidance on N.M.R. hardware and theory.

Nigel, for being a great friend and a fellow conspirator.

Alistair, for putting up with me in varying flats over a three year period. A glutton for punishment.

All my friends in St. Andrews for making the last three years so

memorable and enjoyable. It wouldn't have been the same without you all.

Peter, Marjory, Neil, Amed and the rest of the lab crew for making Lab 337/8 such a pleasant place to work. Well perhaps work is too strong a word.

Pilar, the Spanish Contessa, gone back to Spain but not forgotten. Also Professor Ernesto Carmona and his group who made my stay in Seville such an enjoyable one.

Dr. A. Borowski, the gentle Pole who could crystallise almost anything

Dr. Joe Crayston who relieved the boredom of many a night in the department with a chat.

All the technical staff of the chemistry department. Especially Colin Smith, Sylvia Smith and Melanja Smith (no they are not related), who most regularly had to deal with my samples or my glassware requests.

Sheila Wilson, one of the most patient typists known to man

Abbreviations

AAA	$\text{Ph}_2\text{PO}_2\text{CCH}=\text{CH}_2$
Anhydride (mixed anhydride)	Phosphorus mixed anhydride (e.g. AAA)
AP	(2-allylphenyl)diphenylphosphine
Asym	Antisymmetric
Bbp	Bis(but-3-enyl)phenylphosphine
Bdpp	Bis(-o-diphenylphosphino)stilbene
CAA	$\text{Ph}_2\text{PO}_2\text{CCH}=\text{CMeH}$
COD	Cyclooctadiene
DAA	$\text{Ph}_2\text{PO}_2\text{CCH}=\text{CMe}_2$
DCD	Dewar, Chatt and Duncanson bonding model
Dppm	Diphenylphosphinomethane
Dppp	(Diphenylprop-2-enyloxo)phosphine
%ee	Enantiomeric excess
EPV	$\text{Ph}_2\text{PCH}_2\text{CH}_2\text{CH}=\text{CH}_2$
F.A.B.	Fast atom bombardment
J	Coupling constant
Mbp	But-3-enyldiphenylphosphine
Mpp	Diphenylpent-4-diphosphine
N.B.A.	Nitrobenylalcohol
P.A.N.I.C.	N.m.r. simulation program
PP	(2-cispropenyl)diphenylphosphine
σ/π	Bidentate coordination via one σ

	bond to a remote donor atom and one π bond to the olefin moiety
SP	2 vinylphenyl(diphenyl)phosphine
Sym	Symmetric
Tdp	Tetraphenyldiphosphoxane
VAA	$\text{Ph}_2\text{PO}_2\text{CCH}_2\text{CH}=\text{CH}_2$
(300MHz)	On labeled N.M.R. spectra indicates that the data was collected on a Bucker Associates A.M. 300 N.M.R. spectrometer

Abstract

The reactions of acrylic and vinylacetic acids with Ph_2PCl and Et_3N give $\text{Ph}_2\text{PO}_2\text{CCH}=\text{CH}_2$ (AAA) and $\text{Ph}_2\text{PO}_2\text{CCH}_2\text{CH}=\text{CH}_2$ (VAA) respectively. Both are found to undergo a facile rearrangement to give $\text{Ph}_2\text{PP}(\text{O})\text{Ph}_2$ and AAA is also found to react with PPh_3 to give $\text{Ph}_3\text{P}^+\text{CH}_2\text{CH}_2\text{CO}_2^-$.

Their reaction (1 mole ligand to 1 mole Rh) with $[(\text{RhCl}(\text{1,5 COD}))_2]$, gives complexes of the form $[(\text{RhCl}(\text{L})_2)]$, where L is AAA or VAA, in which the mixed anhydride ligands are bound via the phosphorus atom and the double bond. With AAA in a 1:2 mole reaction with $[(\text{RhCl}(\text{1,5 COD}))_2]$ or a 1:1 mole reaction with $[(\text{RhCl}(\text{C}_2\text{H}_4)_2)_2]$, the major products are $[(\text{RhCl}(\text{AAA}))_2 (\text{Ph}_2\text{POPPh}_2)]$ and $[\text{RhCl}(\text{AAA})_2]$, in which the mixed anhydride is bound as described above and the $\text{Ph}_2\text{POPPh}_2$ is a bridging ligand.

Reaction (1:1) of AAA with $[\text{RhCl}(\text{PPh}_3)_3]$ led to the formation of $[\text{RhCl}(\text{AAA})(\text{PPh}_3)]$; anhydride coordination is as above and the phosphorus atoms are mutually *trans*. This complex is, however, found to revert back to $[\text{RhCl}(\text{PPh}_3)_3]$ on standing. The (1:1) reaction with VAA produces $[\text{RhCl}(\text{PPh}_3)(\text{Ph}_2\text{PO}_2\text{CCH}=\text{CHMe})]$ ($\text{Ph}_2\text{PO}_2\text{CCH}=\text{CHMe} = \text{CAA}$), an example of a metal promoted double bond migration. Subsequent study shows that at ambient pressure and temperature this complex (with 3 butenoic, oleic and

hexa-4-enoic acids) is involved in stoichiometric and not catalytic reactions. $[\text{RhCl}(\text{CAA})(\text{PPh}_3)]$ exhibits fluxionality at room temperature, ^{31}P and ^1H n.m.r. studies on this complex (223-263K) and on $[\text{Rh}(\text{CAA})(\text{O}_2\text{CCH}=\text{CHMe})(\text{PPh}_3)]$ (298K) has determined the fluxionality to be a fast exchange between the *cis* and *trans* forms and led to the calculation of the thermodynamic parameters for this process .

The 1:2 mole reaction of $[\text{RhCl}(\text{PPh}_3)_3]$ and AAA gives $[\text{RhCl}(\text{PPh}_3)(\text{Ph}_2\text{POPPh}_2)]$, which contains a chelate tetraphenyl diphosphoxane ligand (tpdp) formed via a metal promoted rearrangement of the AAA ligand. Subsequent reaction of this complex with TiPF_6 results in $[\text{Rh}(\text{PPh}_3)_2(\text{tpdp})][\text{PF}_6]$. However if the $[\text{RhCl}(\text{PPh}_3)(\text{tpdp})]$ complex is not isolated, then the major product is $[\text{Rh}(\text{PPh}_3)_3(\text{Ph}_3\text{PCH}_2\text{CH}_2\text{CO}_2)][\text{PF}_6]$. Further tpdp complexes have been formed by refluxing $\text{Ph}_2\text{PP}(\text{O})\text{Ph}_2$ with $[\text{RhCl}(\text{PPh}_3)_3]$, $[\text{RuCl}_2(\text{PPh}_3)_4]$ and $[\text{OsCl}_2(\text{PPh}_3)_4]$ in THF. However the reaction of $[\text{RhCl}(\text{PPh}_3)_3]$ with excess $\text{Ph}_2\text{PP}(\text{O})\text{Ph}_2$ gives several products, one of which, namely $[\text{RhCl}_2((\text{PPh}_2\text{O})_2)\text{H}(\text{PPh}_2\text{O})][\text{HNEt}_3]$, has been crystallographically characterised.

The reaction (1:1) of $[\text{RuCl}_2(\text{PPh}_3)_4]$ with $\text{Ph}_2\text{PO}_2\text{CCHCMe}_2$ (DAA) produces $[\text{RuCl}_2(\text{PPh}_3)_2(\text{DAA})]$, in which the mixed anhydride is bound via the phosphorus atom and the oxygen atom of the carbonyl group. The 1:1 mole reactions of CAA and AAA give similar

complexes as minor products whilst the structure of the major product is, however, not known at this point in time. The 1:2 mole reaction was found to produce $[\text{RuCl}_2(\text{tpdp})(\text{AAA})(\text{PPh}_3)]$ in which the mixed anhydride is bound via the phosphorus atom alone.

Note

All ^{31}P n.m.r. spectra discussed have their chemical shifts quoted relative to H_3PO_4 .

CHAPTER 1

Transition Metal Complexes of Mono-alkenes

A literature Survey

1.1 Introduction

The study of π bonded alkene complexes of transition metals has received a great deal of attention in recent years. The interest in this area primarily stems from the isolation of a number of both useful and industrially applicable catalysts ^(1,2), in which the metal complex acts as a template upon which reactions of prochiral reagents occur. Although many alkenes readily coordinate to transition metals, others (for example highly substituted alkenes) require the metal-alkene bond to be stabilised by other coordinating groups which are connected to the alkene species involved in the π bond and result in a bi or tri dentate alkene ligand system. The increased structural rigidity invoked upon formation of the chelate alkene ligand has also been observed to have important stereochemical implications in a large number of metal mediated alkene transformations.

The brief of the project is to manufacture new mono olefinic catalysts which, by chelate stabilized coordination of the mono olefin, will lead to a high degree of face discrimination when other optically active ligands are present in the coordination sphere. This in turn should lead to highly stereospecific reactions although it is possible that the products obtained may derive from coordination of the less favoured face of the alkene.

1.2 Historical Overview

In the years around 1830 the first complexes utilizing neutral molecules as complex ligands were isolated, an example being $[\text{Pt}(\text{NH}_3)_4][\text{PtCl}_4]$, referred to as Magnus' Salt⁽³⁾. The first π complexes were isolated by W. C. Zeise. Zeise actually produced 3 main types of platinum-ethylene complexes, however the existence of these complexes, $\text{K}[(\text{C}_2\text{H}_4)\text{PtCl}_3] \cdot \text{H}_2\text{O}$ ⁽⁴⁾ (Zeise's Salt), $[(\text{C}_2\text{H}_4)\text{PtCl}_2]_2$ ⁽⁴⁾ and $[(\text{C}_2\text{H}_4)\text{-PtCl}_2\text{-NH}_3]$ ⁽⁴⁾, was not accepted by his contemporaries. Undaunted Zeise went on to produce the first complex in which the olefin contained a functional group close to the coordinated double bond. This complex, $[\text{PtCl}_2 \cdot \text{C}_6\text{H}_{10}\text{O}]$, called "acechlorplatin"⁽⁵⁾ was the result of the reaction of PtCl_4^{2-} and acetone. Corroborating evidence for Zeise's assignments was provided several decades later when two of these species were reproduced by alternative methods, Bimbaum isolating $\text{K}[(\text{C}_2\text{H}_4)\text{PtCl}_3]\text{H}_2\text{O}$ ^(6,7) whilst Pendtl and Hofmann produced $[\text{PtCl}_2\text{C}_6\text{H}_{10}\text{O}]$ ⁽⁸⁾. In the years following Zeise's initial discoveries a large number of olefin complexes were reported using, for example, mercury, iron and copper as the metal centre. However this work proved to be far less successful both in the number of complexes isolated when compared to the number of reactions attempted and in the number of these isolated complexes which were claimed, at the time, to be similar olefin complexes but have since proved not to be.

Throughout this period these complexes proved to be

highly controversial due to the lack of a theory which could adequately explain the bonding within them and an analytical method which could be confidently relied upon to detect them. These two problems persisted until the advent and development of the π bonding theory and the nuclear magnetic resonance spectrometer, the discovery and development of which signalled the beginning of the explosion in metal olefin chemistry which has occurred during the last twenty to thirty years.

1.3 Theories on the π Bonding Model

1.3.1 Initial Observations Upon Alkene Coordination

Following Zeise's work many attempts were made to explain the coordination of the olefin ligands in such complexes by applying the sigma theories of bonding. Although these models could explain a large percentage of the various physical⁽⁹⁾ and qualitative observations made on such complexes they did not provide answers for them all. The main properties which could not be explained are summarized in the following six points.

1) The ability to coordinate alkenes is found to vary considerably with the double bond substituents. Furthermore the coordinated alkene can exist as a mono alkene ligand (e.g. ethylene) or as part of a bi or tridentate system (e.g. α amido acrylic acids).

2) On coordination the alkene systems generally do not exhibit isomerisations or rearrangements but in many cases undergo rapid exchange with uncoordinated alkenes.

3) The alkenes possessing two different substituents become asymmetric centres upon coordination.

4) A coordinated alkene interacts with other ligands involved in the complex. These interactions although exhibited by other ligands are far greater for alkene ligands.

5) With coordinated monodentate alkenes rotation about the metal-alkene bond axis is possible but is found to require an energy of activation. If alkene coordination was via a σ bond the complex would exhibit free rotation around the sigma bond.

6) The alkenes structure is modified upon coordination; for example the C=C bond length is increased, the bond hybridization of the carbon atoms moves from sp^2 towards sp^3 hybridization (i.e. toward that of the corresponding alkane) and the alkenes substituents initially coplanar in the free alkene all bend away from the metal.

All these properties could be explained, however, by theories which utilized the concept of π coordination of alkenes to metals. The two most widely accepted of these theories are described in the following sections.

1.3.2 Resonance Hybrid Model Based on Valence Bond Theory

The resonance hybrid concept was developed by Winstein and Lucas^(10,11) in collaboration with Pauling in 1938 and was later modified by Douglas⁽¹²⁾ in 1953 to take into account the back

bonding from the metal to the alkene and so describe adequately the donor-acceptor π bonding model. This model explains the π coordination by writing down several valence bond structures, the full set drawn by Douglas to describe the anion of Zeise's Salt are shown in Figure 1.1.

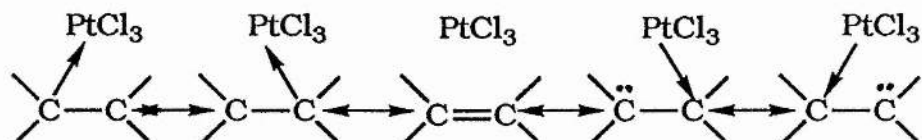


Fig. 1.1

1.3.3 The Dewar-Chatt-Duncanson Bonding Model

Though the valence bond model adequately explained the bonding observations described in Section 1.3.1 the theory did not give much insight into the actual processes which produced the π bond. A better model in this respect was tendered by the Dewar, Chatt and Duncanson (the DCD model). Dewar made the suggestion⁽¹³⁾ that the metal alkene bond involves electron donation from the π bond of the alkene into a vacant metal orbitals of d symmetry. J. Chatt and L. Duncanson⁽¹⁴⁾ in 1953 applied Dewar's initial description to Zeise's salt and related molecules. From these two studies it was concluded that the alkene is π bound to the metal as shown in Figure 1.2.

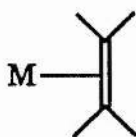


Fig. 1.2

This π bond is the combination of two independent processes. The first is σ overlap between the filled π orbital of the alkene and a suitably directed vacant hybrid metal orbital, and is referred to as the electron pair donor bond. This is shown diagrammatically in Figure 1.3a. The second component acts in support of the first and results from the overlap of a filled metal d orbitals with the vacant antibonding orbitals of the alkene (Figure 1.3b). Due to this cooperative type of bonding where one of the branches is supported by the other and vice versa it was dubbed the Synergic bonding model, the π symmetry of the orbitals with respect to the bonding axis allowing the second form of bonding to occur. It is the flexibility found to be a characteristic of this bonding model that allows the experimental observations mentioned in Section 1.3.1 to be rationalized⁽¹⁵⁾.

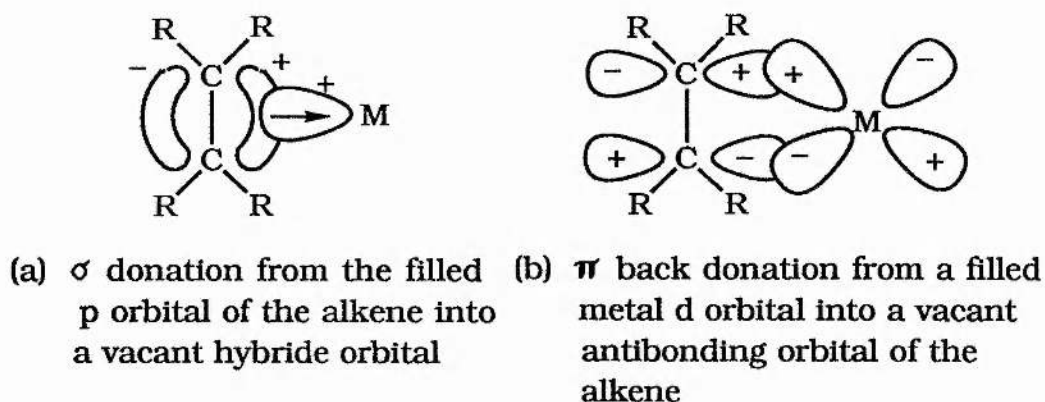


Fig. 1.3

Very accurate SCF-Xa-SW calculations have confirmed the reliability of the DCD model for Zeise's Salt⁽¹⁶⁾, and have produced very approximate values for the relative sizes of the two bonding components, 75% of the total bonding energy being allocated to the

forward donation component.

Furthermore this synergic bonding model was also found to explain the alterations in the structure of monolefinic complexes. These alterations are found to be dependent on specific properties of the metal or the alkene⁽¹⁷⁻²²⁾. The most important of these are listed below.

1) The lower valent a transition metal complex is the higher the relative percentage of the total binding is allocated to the back bonding.

2) The lower valent transition metal complexes due to the increase in back bonding are noted to exhibit larger changes in the geometry of the alkene upon coordination.

3) Altering the substituents on the alkene changes the degree by which the alkene loses its planarity. In all cases, as stated in Section 1.3.1, the planarity of the double bond and its substituents observed in the free alkene is lost upon coordination. The substituents are found to bend away from the metal producing a quasi-tetrahedral geometry for the olefinic carbon atoms. The synergic bonding model explains the movement toward pseudo sp^3 hybridization of the olefinic carbon atoms as being due to the alterations in both π and π^* entailed in forming the synergic bond. The degree of movement from planarity is found to be smallest when the substituents are all hydrogen atoms and in general is found to increase as the electronegativity of the substituent increases. This movement towards sp^3 hybridization also produces an associated lengthening of the alkene carbon to carbon bond, this increase however does not show any strong or predictable trend.

4) If an unsymmetrically substituted alkene is complexed, the metal carbon bond lengths are generally found to vary greatly⁽²³⁻³²⁾. In general the metal-carbon interatomic distance to a substituted alkene carbon atom is longer than that to an unsubstituted carbon. This effect is thought to be sterically controlled because it is noted with both net π acceptor and π donor alkene substituents and is usually manifested in the form of slippage of the alkene. In square planar complexes this means the centre point of the alkene's double bond is found to lie above or below the plane defined by the metal and the other ligands.

1.3.4 Treatment of Alkenes with Highly Electronegative Substituents

The synergic donor bonding model can be relied upon to predict the trends in spectroscopic and structural effects or provide a theoretical explanation for these effects in almost all situations. However one area where it cannot be applied reliably is when the alkene ligand possesses substituents of high electronegativity and the metal is found to be in a low oxidation state. In these systems a better stratagem is to treat the complex as a metallacycle bound to the alkene via two σ bonds^(33,34), a situation which can be viewed as an extreme form of the DCD theory in which the σ donation component of the synergic bond has a negligible value.

1.4 Properties which Effect the Stability of the π Alkene Complexes

1.4.1 Steric Properties

With π metal complexes it is hard to separate the steric and electronic properties of a substituent. For example replacing a hydrogen atom by a methyl group causes a decrease in the stability constant. The methyl is sterically different and is the closest electronically to the hydrogen atom but although close in electron character, unlike the hydrogen, the methyl group is a weak σ donor. However of these two effects it is the unfavourable enthalpy term due to the increased steric bulk which results in the decrease in stability⁽³⁵⁻⁴²⁾. A general study of substituted alkenes shows that the introduction of any substituent to a double bond creates an unfavourable, sterically induced effect on the stability of the metal-alkene bond. The appearance of steric effects is put down to the presence of bulkier substituents both preventing the alkene from approaching the metal centre at the optimum bonding angle⁽⁴³⁾ and imposing greater physical restrictions to ligand movement in any complex formed^(44,45).

The presence of steric effects also means that the coordination of *cis* and *trans* isomers must be considered separately. Generally complexes of *cis* alkenes are found to be more stable than those of their *trans* isomers, this is attributed to a sizeable enthalpy difference in favour of the *cis* isomer. This enthalpy difference is firstly due to less strain being induced by the lengthening of the alkene double bond upon coordination⁽⁴⁶⁾ and

secondly the *cis* isomer will be able to approach the metal closer to the ideal situation and thus will achieve greater π orbital overlap and hence a stronger bond⁽⁴⁷⁻⁵⁰⁾.

1.4.2 Electronic Properties

It has been already stated that it is hard to separate these from the steric effects. They have therefore been gauged by comparing complexes whose ligands are almost of identical size but of differing electronic properties⁽⁵¹⁾. The metals are found to fall into two groups.

1) Those, such as Ag(I) and Cu(I), which display a decrease in the stability as the electronegativity of the substituent increases.

2) Those, such as Pt(0) and Rh(I), which show increases in stability as electronegativity increases.

This effect is related to an alteration in the enthalpy term which decreases for group (1) and increases for group (2). The difference in behaviour is related to which of the components is the most important in the synergic bond. In group (1) the σ component is the more important. Therefore electron withdrawing substituents, which reduce the ease with which electrons can take part in this σ bond, decrease bond stability. In the second group the major component is found to be the π back bonding. Thus the increase in the π acceptor ability of the alkene caused by electron withdrawing substituents strengthens the metal alkene bond.

1.4.3 Properties of the Metal

Metal-alkene complexes are produced only when the d-orbitals of the metal of π symmetry are full, thus transition metals with d-electron configurations d^{10} , d^8 , d^6 or d^4 fit this criteria. The differing π bond stabilities exhibited within this group are due to the ability of the metal to donate electron density to the alkene via the π metal alkene bond, increasing this ability increases the π bond stability⁽⁵²⁾. The ionization potential of the metal gives a rough guide to the ability to donate electrons. An increase in ionisation potential is found to be mirrored in the stability of the complexes. It is essential when studying this effect that there is no steric or electronic differences thus the complexes compared must have identical ligand systems, for example the complexes $[L_2M(C_2H_4)]$ where $M = Ni, Pd$ and Pt have been studied.

1.4.4 Effects of Non-Olefinic Ligands

The non olefinic ligands present will also effect the stability of the π bond. A stable complex is more likely to be formed if the non olefinic ligands are soft ligands^(53,54). This situation results in an increase in the energy of highest occupied molecular orbital on the metal, reducing the ΔE value between it and π^* orbital of the alkene. As a result the interaction between these orbitals is increased and so the strength of the metal-alkene bond is increased⁽⁵⁵⁾ (see example of orbital diagram, Figure 1.4).

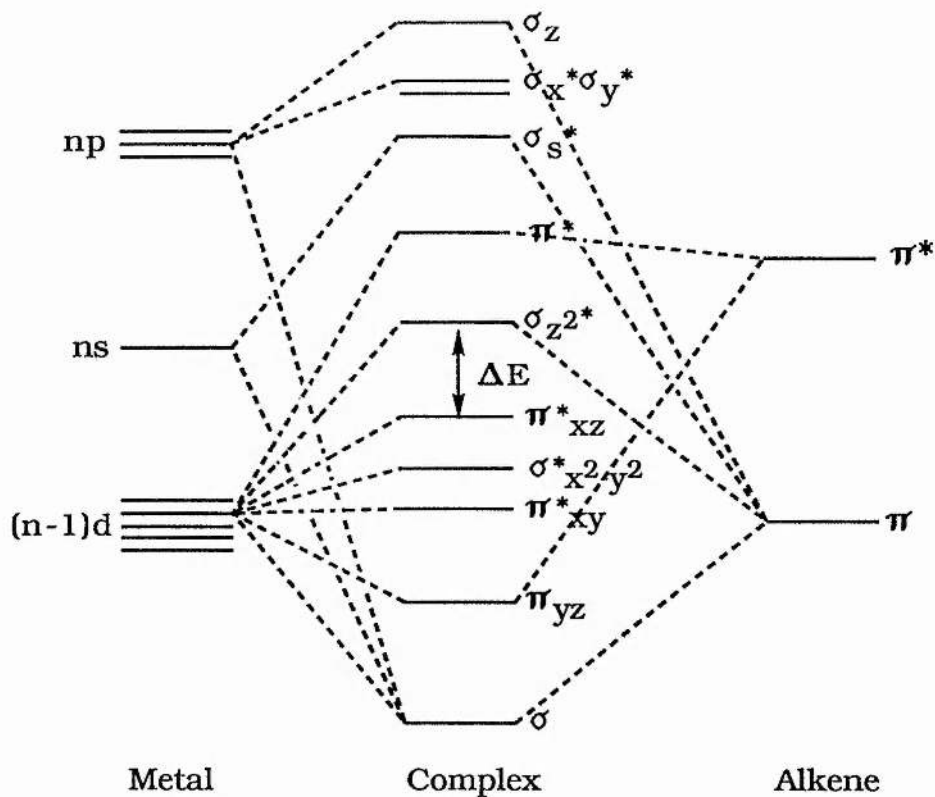


Fig. 1.4

Molecular orbital scheme for platinum(II)-palladium(II) alkene complexes. Only the alkene ligand orbitals have been shown.

1.4.5 Effects of Cyclic Ligands

The effect of introducing cyclic ligands is mainly steric but as ring formation also effects the electronic environment of the alkene, electronic effects will also be of some significance. Five membered rings provide the most stable complexes, the full order shown by ring alkene complexes being $C_5 > C_7 > C_6 > C_8$ ⁽⁵³⁾. This difference is linked to enthalpy effects due to firstly the weakening of the multiple bond that occurs in an attempt to relieve

ring strain by lengthening of the double bond, secondly the ring strain producing deformations of the π orbital which enhances complex stability and thirdly the transannular hydrogen atoms are also found to promote complex stability although the method by which this occurs is not fully understood⁽⁵⁶⁾.

1.5 The Development of Chelate Mono-Alkenes

As already stated the development of an adequate bonding theory and reliable methods of identification in the 1950's led to the rapid expansion of the chemistry of π bound alkenes. Such has been the increase in the volume of mono olefinic complexes isolated and their related organic applications that one review could not adequately cover the whole topic. Thus this section will deal almost entirely with the discovery and early development of complexes containing alkenes for which the coordination is stabilised by chelation.

Despite the attention given to olefinic ligands and the study of their coordination to transition metals, interest in the coordination and use of alkenes containing functional groups has been comparatively recent. Although the first complex isolated and determined to have a functional group close to the alkene group was "acechlorplatin" isolated by Zeise during the last century⁽⁵⁾, it was not until the years following 1960 that interest in this area really exploded. Furthermore it was observed that if the olefinic substituents contained a second moiety which possessed a lone pair of electrons then coordination was possible, in many cases, via both the double bond and the lone pair donor to produce a chelate mono

olefin system, π and σ bound to the metal respectively.

Chelate olefin coordination was first noted with unsaturated amine ligands. Both Rubinshtein and Derbisher⁽⁵⁷⁾ and Gelman and Essen⁽⁵⁸⁾ showed that reaction of diallylamine and ammonium tetrachloroplatinate (11) produced two isolable complexes, PtLCl_2 and $(\text{PtLCl}_2)_2$ where L = diallylamine. The dimer was determined to be $[(\text{Pt}-(\text{diallylamine})_2)\text{PtCl}_4]$ whereas the monomer was discovered to be $[\text{Pt}-(\text{diallylamine})\text{Cl}_2]$. Furthermore the diallylamine ligand was observed to be bound in a chelate fashion via the two olefin species as seen in Figure 1.5.

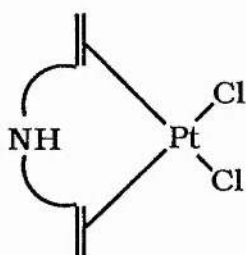


Fig. 1.5

Such chelate diolefin complexes were found to produce examples of chelate mono olefinic ligands by subsequent nucleophilic reactions. The reaction (A) shown in Figure 1.6 shows nucleophilic attack of an alkoxide ion at one of the olefinic carbon atoms resulting in σ attachment. However the reaction process did not end at this point. The nucleophilic attack, in this example, was found to be accompanied by the loss of a chlorine atom leading to the dimerization (B), and ultimately the isolation of a chlorine bridged

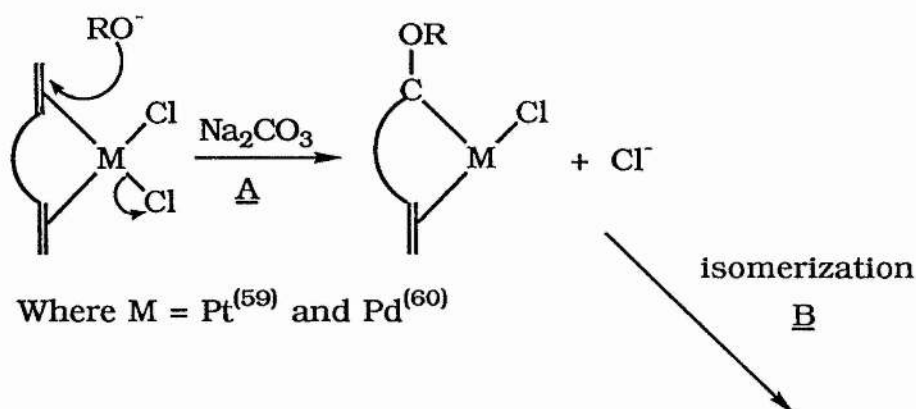


Fig. 1.6

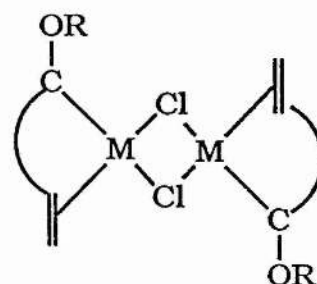


Fig. 1.6

mono olefin dimer. Mono olefinic ligands bound through a nitrogen moiety were discovered in 1963 during a study of the coordination of secondary allylamines, all of which had exhibited polymeric structures. The N-octyl derivative was found to be an exception, however, producing a dimeric structure in which the allylamine ligand is a bridging ligand, σ bound to one metal centre and π bound to the second⁽⁶¹⁾ as shown in Figure 1.7. This was closely followed by the characterization of complexes with chelate nitrogen containing olefins. For example, complexes of

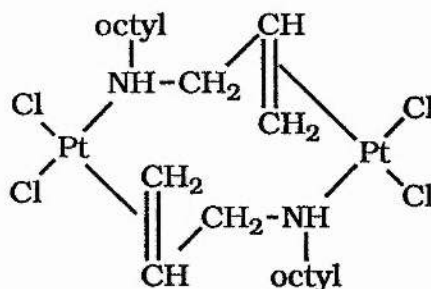
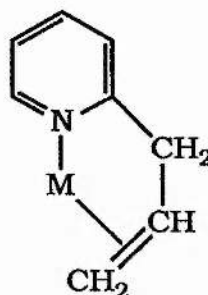


Fig. 1.7

of the form shown in Figure 1.8 were isolated by Yingst and Douglas⁽⁶²⁾.



where M = Cu(I), Ag(I) or Pt(II)

Fig. 1.8

Further examples of complexes which utilized carbon as the remote electron donor but which didn't rely on nucleophilic reactions for their formation were isolated by M. Dubeck⁽⁶³⁾. He found that the reaction of nickelocene and the dimethyl ester of acetylene dicarboxylic acid gave a Diels Alder adduct shown in Figure 1.9, a complex of the dimethyl ester of 2,5 norbornadiene 2-3 dicarboxylic acid and nickel cyclopentadiene. Complexes of similar form, in which the carbon is the remote donor atom, were isolated in the studies of fluoro olefins.

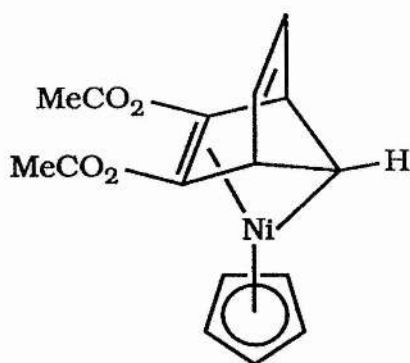


Fig 1.9

The example closest to Figure 1.9 is shown in Figure 1.10,

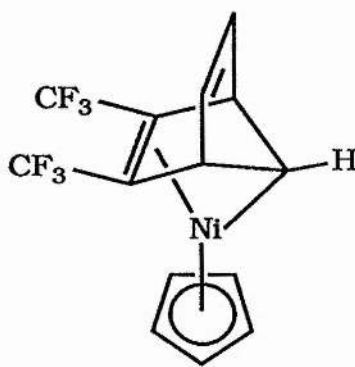


Fig. 1.10

it was isolated from the reaction of hexafluoro-2-butyne and nickelocene and, as in the carboxylic acid case, was concluded to have the norbornadiene ligand both π and σ attached to the nickel centre⁽⁶⁴⁾. Similar species involving iron⁽⁶⁵⁾, rhodium⁽⁶⁶⁾ and cobalt⁽⁶⁷⁾ were reported around this period involving π and σ bonding to ligands such as C_4F_6 , C_6F_8 and C_5F_6 . The complementary fluoro olefin bridging complexes were also discovered, for example Clark and Tsai⁽⁶⁸⁾ isolated a dimeric manganese carbonyl compound containing bridging groups which proved to be perfluoroethane π bound to one metal centre and σ to the other (Figure 1.11).

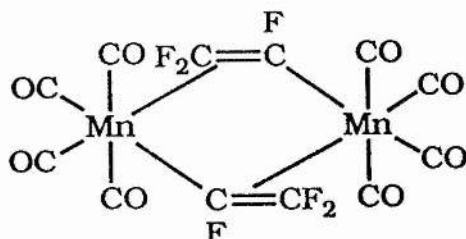


Fig. 1.11

In 1959 ⁽⁶⁹⁾ an attempt to produce palladium analogies of "acetochlorplatin" ($\text{C}_6\text{H}_{10}\text{O}.\text{PtCl}_2$), first isolated by Zeise from the reaction of mesityl oxide and PtCl_2 , resulted in the isolation of a stable complex concluded to bond via the π allylic system. This was shown by Wilkinson and Parshall⁽⁷⁰⁾ not to be the monomeric structure proposed by the initial study of Moiseev et al (Figure 1.12a) but a chlorine bridged dimer as shown in Figure 1.12b.

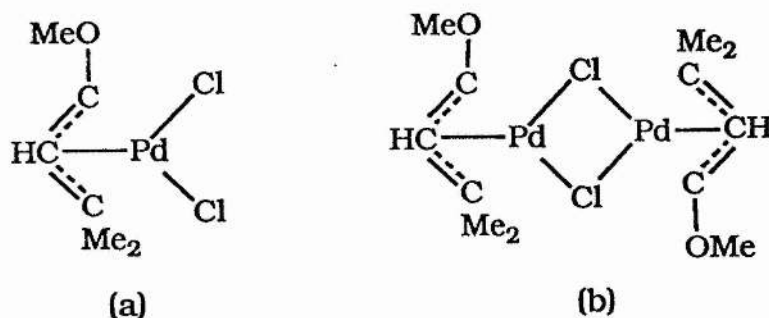


Fig. 1.12

In the same work Wilkinson and Parshall also concluded that the platinum complex isolated by Zeise was in fact a polymeric structure in which the mesityl oxide ligand is a bridge between metal centres bound σ through the ketonic oxygen and π through the alkene moiety (Figure 1.13).

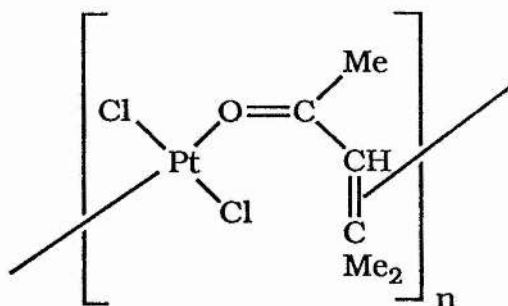


Fig. 1.13

Other complexes of oxygen containing ligands were isolated about this time exhibiting both chelate and bridged structures. However in these cases the bonding was found not to be through the remote oxygen atom but by a π bond to the carbon oxygen double bond. An example of this type results from the reaction of methyl vinyl ketone and $(\text{CH}_3\text{CN})_3\text{W}(\text{CO})_3$ ⁽⁷¹⁾, the complex isolated contained three ketonic ligands resulting in the metal centre being in an octahedral environment (Figure 1.14).

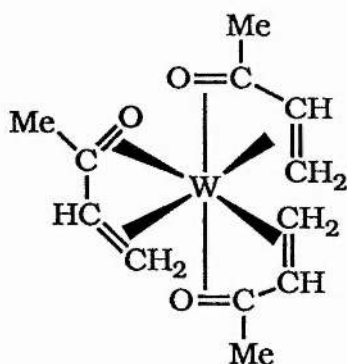


Fig. 1.14

The similar complexes possessing oxygen containing bridging ligands, such as methylvinylketone and crotonaldehyde, all led to similar but polymeric structures. Since this initial period of study many complexes which utilize the oxygen atom as a true donor atom have been isolated. Examples of which are the complexes of

α -amidoacrylic acids such as that shown in Figure 1.15(72, 73).

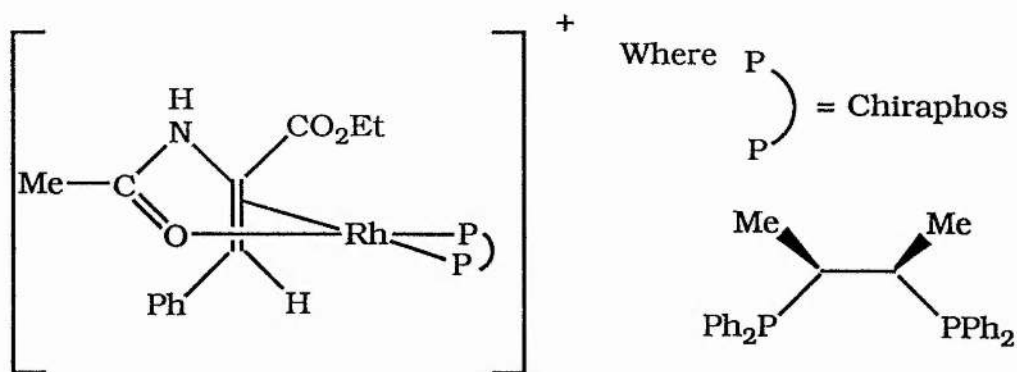


Fig. 1.15

Furthermore ligands which are coordinated via remote oxygen atoms have provided a high degree of success in the coordination of highly substituted alkene species. As has already been stated the more highly substituted an alkene species becomes, the lower the stability constant of the resultant complexes are found to be. Consequently the number of reported complexes containing π coordinated, highly substituted alkenes is small in comparison to those containing mono or disubstituted alkene species. Examples of complexes which contain such systems using oxygen as the remote donor are shown in figures 1.15 - 1.18.

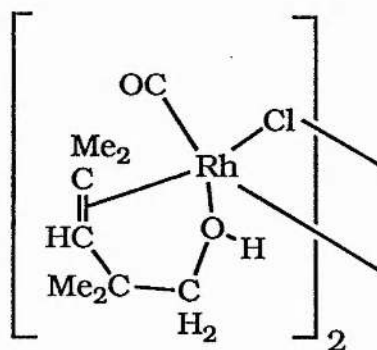


Fig. 1.16

The complex in Figure 1.16 was isolated from the reaction of

$[(\text{Rh}(\text{CO})_2\text{Cl})_2]$ and $\text{Me}_2\text{C}=\text{CHC}(\text{Me})_2\text{CH}_2\text{OH}$ in benzene ⁽⁷⁴⁾. That in Figure 1.17 was isolated from the reaction of $[\text{Ir}(\text{CO})_3(\text{PPh}_3)_2]^+$ and cinnamic alcohol ($\text{PhCH}=\text{CH}-\text{CH}_2\text{OH}$) in the presence of potassium hydroxide ⁽⁷⁵⁾. The complex is formed as a result of nucleophilic attack by the alcohol on a carbonyl group.

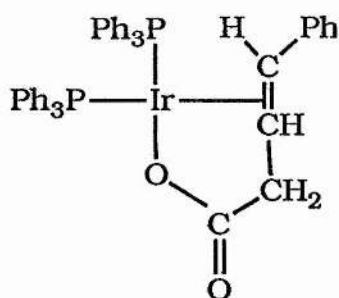


Fig. 1.17

The complex in Figure 1.18 was produced from the reaction of $\text{Me}_2\text{C}=\text{CHC}(\text{Me})_2\text{CH}_2\text{OH}$ and PtCl_2 in dimethyl formamide ⁽⁷⁴⁾.

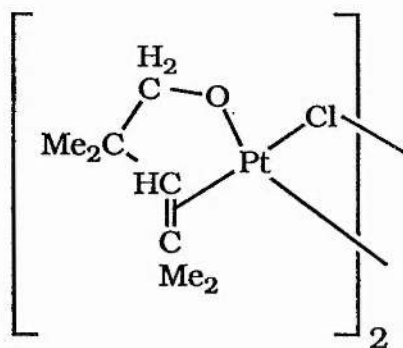


Fig. 1.18

Similar coordination to that exhibited by the carbonyl containing ligands, where π coordination is preferred over the electron donor abilities of the oxygen atom had also been observed with nitrogen containing ligands. Bogdanovic in 1965⁽⁷⁶⁾ reported the complex shown in Figure 1.19.

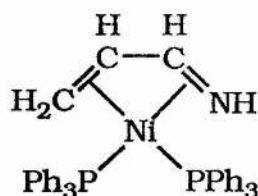


Fig. 1.19

Acrylonitrile was also shown to produce π/π chelate products where chelation is via the $C=C$ and $C\equiv N$ bonds and compounds exhibiting σ/π coordination through the nitrogen atom and the double bond, an example being,⁽⁷⁷⁾

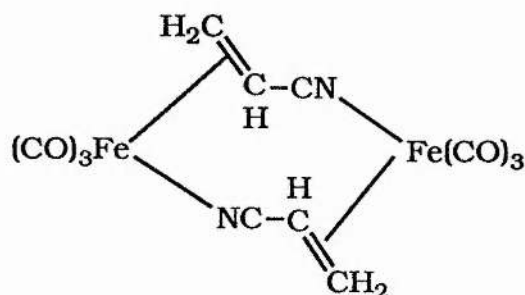


Fig 1.20

Thus five types of nitrogen ligand coordination have been observed, these being

- i) π bonding through the olefin moiety alone
- ii) π bonding through the nitrile triple bond alone
- iii) σ bonding through the nitrogen atom alone
- iv) Chelate binding via (i) and (ii)
- v) Chelate binding via (i) and (iii).

The most efficient types of ligand for chelate coordination are those containing phosphorus or arsine atoms as the remote donor. Complexes involving these species were first reported in 1961 by Kouwenhoven, Lewis and Nyholm⁽⁷⁸⁾, the reaction of

dimethyl-4-phenylarsine with platinum and mercury salts resulting in the isolation of σ/π chelate complexes e.g. Figure 1.21.

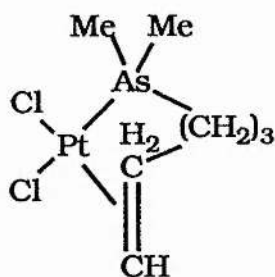


Fig. 1.21

The analogous phosphorus containing complex was formed by the reaction of dimethyl-4-pentenylphosphine and potassium chloroplatinate⁽⁷⁹⁾. Further examples of the phosphorus complexes isolated in the following years will be discussed in Section 1.5.1.

Thus the early study of alkene complexes showed that a substantial number of donor atoms could be used to produce chelate mono olefinic ligands σ bound via the donor atom and π bound via the alkene. However several of these atoms proved only to have limited use as donors, for example the acrylonitrile which proved only to have limited application in the area of chelate σ/π coordination. Ligands containing phosphorus donor atoms, however, have found wide application in catalysis and organic transformations. Because of this and their direct relevance to this study, the chemistry of chelate phosphorus containing ligands will now be discussed in greater detail.

1.5.1 Chelate Olefin Ligands Containing Phosphorus Donor Atoms

To recap, the early studies into the coordination of π bound mono alkenes discussed in Section 1.5, result in complexes which generally fall into one of three main forms as shown in Figure 1.22.

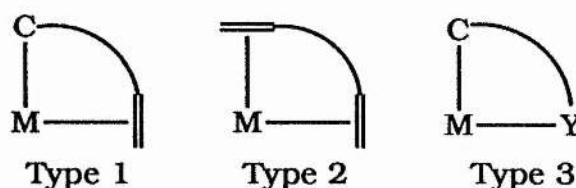
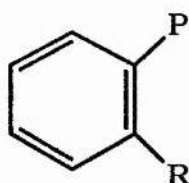


Fig. 1.22

It is type 3 which is of relevance to this study where the bond from Y (the hetero donor atom) to the metal centre is a σ bond and the double bond is π bound to the metal; this section deals with ligands where Y is a phosphorus atom. The initial successes in this area centred on substituted benzyl compounds of the form shown in Figure 1.23



where R is an alkene species

Fig. 1.23

An example of this style of compound is 2-vinylphenyl(diphenyl)phosphine, which during the early 1960's was found to produce five membered ring species upon reaction

with metal reagents via insertion of the double bond into an M-H bond (see Figure 1.24)^(80,81). However if all addition species, such as hydrogen or halogens, were removed from the reaction system it was possible to isolate products containing five and a half membered rings (see Chapter 2 for a description of these rings).

The 2-vinylphenyl(diphenyl)phosphine ligand bound to the metal

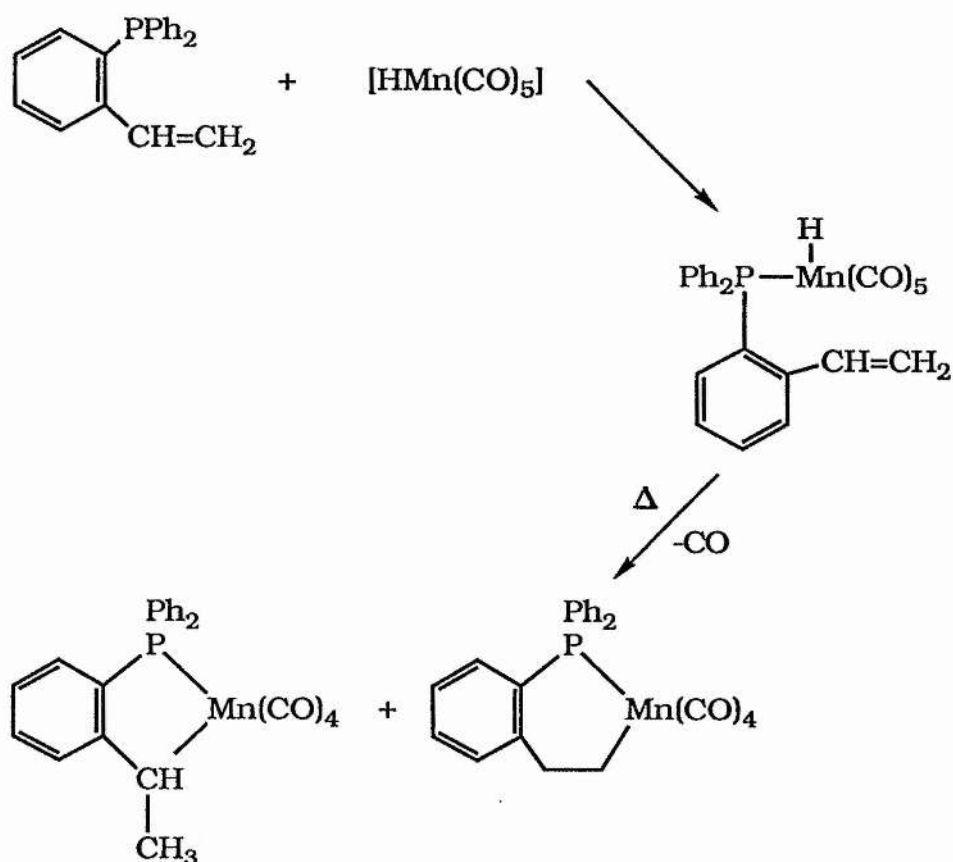


Fig. 1.24

centre via a σ bond to the phosphorus atom and a π bond to the alkene. Examples of complexes isolated via this method are shown in Figure 1.25⁽⁸²⁾. Following analogous methods similar chelate phosphorus containing alkene complexes of several different

transition metals were isolated. For example, in the case of iron, alkene complexes up to this point in time had proved to be thermally unstable and air sensitive except when the double bond carried strongly electron withdrawing substituents^(83,84). However the presence of a phosphorus donor atom in the alkene resulted in the isolation of complexes containing either the alkene ligand bound through the phosphorus atom alone or in a bidentate fashion via the phosphorus atom and the double bond, the chelate binding stabilising the coordination of the olefinic π bond. For example reaction of

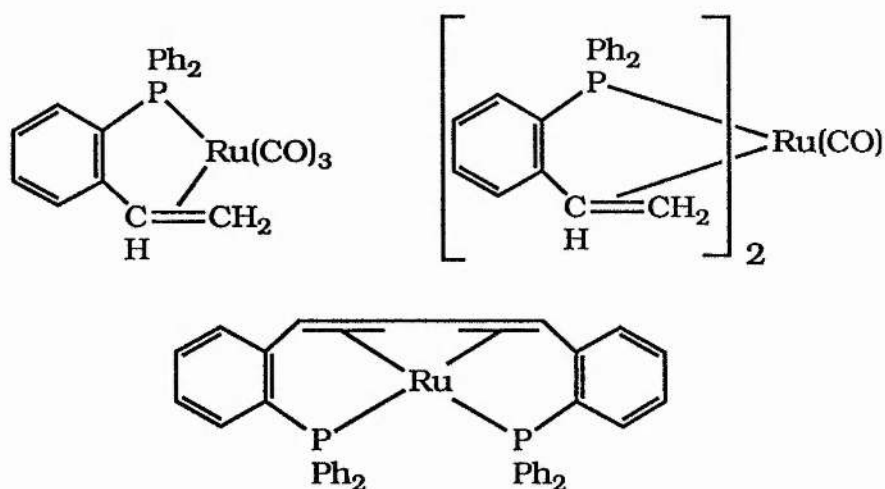


Fig. 1.25

$\text{Fe}_3(\text{CO})_{12}$ and 2-vinylphenyl(diphenyl)phosphine (SP) gives rise to two products, $[\text{Fe}(\text{CO})(\text{SP})]$ (Figure 1.27) and $[\text{Fe}(\text{CO})_2(\text{SP})_2]$ in yields of approximately 20% and 60% respectively. The structure of $[\text{Fe}(\text{CO})_2(\text{SP})_2]$ was confirmed by x-ray analysis (Figure 1.28).^(85,86) Complex 1.27 is thought to be derived from 1.26 by substitution of an axial CO ligand. Similar σ/π bidentate coordination was observed

for SP complexes of Pt⁽⁸⁷⁾, Cr, Mo, W⁽⁸⁸⁾, Mn, Re⁽⁸⁹⁾ and Ru⁽⁷⁹⁾.

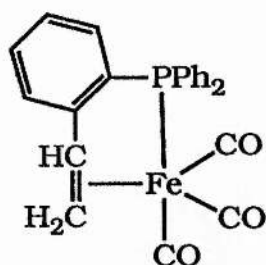


Fig. 1.26

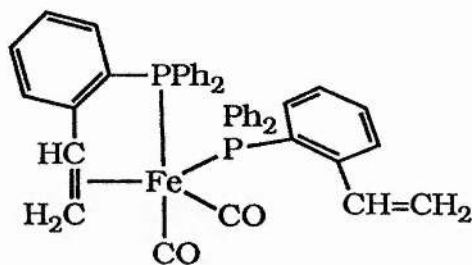
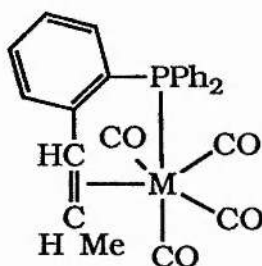


Fig. 1.27

However, prior to this work, group VI metal complexes of (2-allylphenyl)diphenylphosphine (AP) and (2-cispropenyl)diphenyl phosphine (PP) of general formula $[M(CO)_4L]$ were reported. AP is very similar to SP, the difference being that the benzyl groups vinyl substituent is replaced by a propenyl group. The products isolated from the reaction of AP and zero valent group VI metals, however, were shown to be of the form shown in Figure 1.28^(90,91)



Where $M = Cr, Mo, W$

Fig. 1.28

where the AP ligand has undergone isomerization to the PP ligand upon coordination.

A similar isomerization is described in Chapter 2 which reports the metal promoted isomerization of $[Ph_2PO_2CH_2CH=CH_2]$ to $[Ph_2PO_2CH=CHMe]$ (see Chapter 2, Section 2.8). A complex

containing unisomerized AP was produced with platinum as the metal centre by reaction of AP with platinum (II) bromide in refluxing chloroform^(90,91) (Figure 1.29).

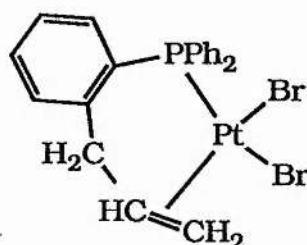


Fig. 1.29

As already stated the SP ligand was also found to produce platinum metal complexes in which the ligand is bound via the donor atom and the double bond. For example the complex shown in Figure 1.30 is the result of the reaction of $[(\text{RhCl}(\text{C}_8\text{H}_{14})_2)_2]$ with SP or alternatively of treatment of $[(\text{RhCl}(\text{CO})_2)_2]$ with two mole equivalents of SP which initially gives a 5 coordinated cationic complex $[\text{Rh}(\text{CO})(\text{SP})_2]\text{Cl}$ but subsequently loses CO to give the final product.⁽⁹²⁾

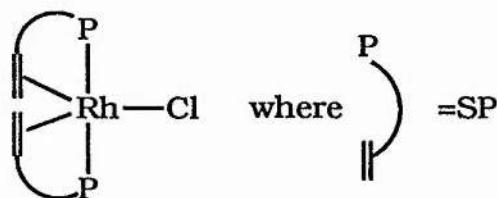


Fig. 1.30

Similar five coordinate Pt and Ru complexes have subsequently been produced⁽⁹³⁾. A further example of a five coordinate rhodium complex is the (tri-*o*-vinylphenyl)⁽⁹⁴⁾ complex shown in Figure 1.31. The structure has been confirmed by x-ray

analysis as trigonal bipyramidal. Similar structures have also been postulated for $[X(o\text{-vinylphenyl})_3\text{PRh}]$ ($X = \text{Cl, I}$) and $[\text{Cl}(3\text{-butenyl})_3\text{PRh}]$ ⁽⁹⁵⁾.

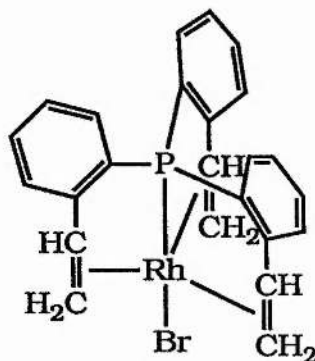


Fig. 1.31

It is in this area of platinum metal complexes that the bulk of chelate phosphine research has been centred due to both the relative compatibility of the metal and ligand systems and because of the catalytic properties exhibited by such complexes. For example early observations indicated that mono olefins containing two donor atoms did not produce a π metal to alkene bond, Platinum metal phosphorus containing mono olefin systems have proved to be exceptions to this rule. Several types of bisphosphino ligand, among them bis-(*o*-diphenylphosphino) stilbene (BDPP), have produced tridentate complexes containing a π bond with platinum metals ⁽⁹⁶⁾. The example shown in Figure 1.32a results from the reaction of BDPP and $[(\text{MCl}(1,5\text{COD}))_2]$ dimers where $\text{M} = \text{Rh}$ or Ir . The complexes of form (a) can, in turn, react with ligands such as CO , $\text{CH}_2=\text{CH}_2$, Cl_2 and HCl to produce π bound complexes with five or six coordinate metal centres⁽⁹⁷⁾ (Figure 1.32b).

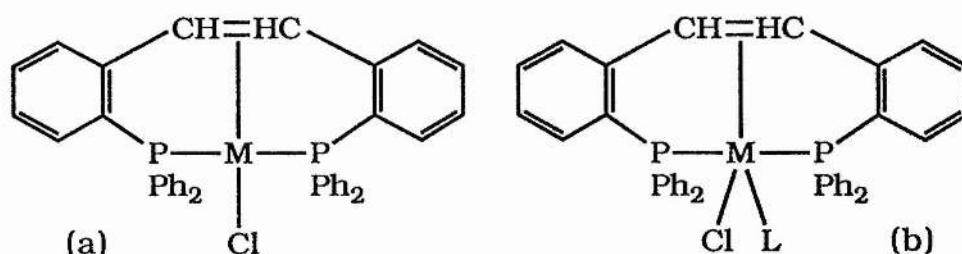
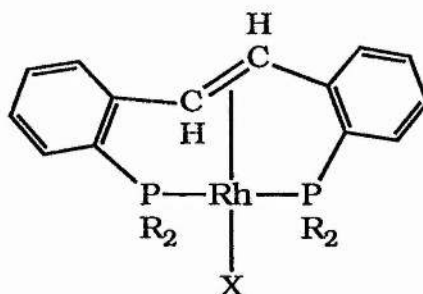


Fig. 1.32

Similar complexes with rhodium centres have been produced using several methods. For example prolonged reaction of rhodium trichloride with a six fold molar excess of tri-o-tolylphosphine in 2-methoxyethanol or 2-(2-methoxyethoxy)ethanol produces a yellow diamagnetic complex of apparent formula $[\text{RhCl}((\text{o-tolyl})_3\text{P})_2]$ which upon secondary reaction leads to the isolation of the complexes in Figure 1.33⁽⁹⁸⁾.



where $\text{X} = \text{Cl}, \text{Br}, \text{NCS}$
 $\text{R} = \text{Ph or Tol}$

Fig. 1.33

A similar product where X is chlorine is also shown to be the chief product of the reaction of rhodium (III) chloride with diphenyl-o-tolylphosphine in refluxing 2-methoxyethanol for 3 hours, the complex undergoing dehydrogenation and then coupling of the phosphine ligands to result in the final product. Similar

dimerization is noted in reflux reactions of SP to give the product shown in Figure 1.34.⁽⁹⁹⁾

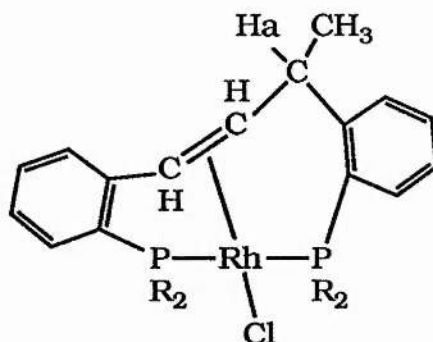


Fig. 1.34

However if the new ligand formed above ([1,3 bis[(o-diphenylphosphino)phenyl]-trans-1-butene]) and rhodium trichloride are reacted utilizing the same conditions the product, is not the compound shown in Figure 1.34. Rather via deprotonation and coordination of the double bond it gives rise to a η^3 -allyl tridentate complex (Figure 1.35)⁽⁹⁹⁾. Similar complexes of Ni, Pd and Pt were subsequently produced. Iridium⁽⁹⁹⁾, however, proved to be an exception as proton Ha (Figure 1.34)

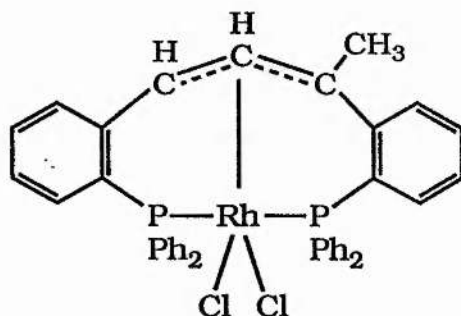


Fig. 1.35

remains intact and the complex isolated is the coordinated alkene product similar to that shown in Figure 1.34.

Such ring biphosphine complexes which do not contain an

aromatic ring as part of the organic backbone of the ligand have also been obtained. For example Shaw and McDonald et al produced, by reaction of $\text{RhCl}_3 \cdot 3\text{H}_2\text{O}$ and $\text{Bu}^t_2\text{PCH}_2\text{CH}_2\text{-CHMeCH}_2\text{CH}_2\text{P}^t\text{Bu}_2$, the complex shown in Figure 1.36.⁽¹⁰¹⁾

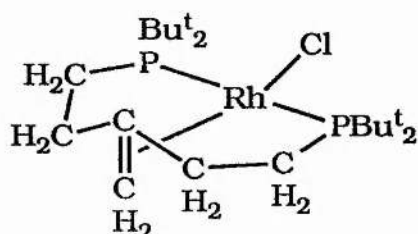


Fig. 1.36

Other tridentate complexes can be produced by the insertion of alkynes into M-C bonds in reactions of the type shown in Figure 1.37.^(102,103)

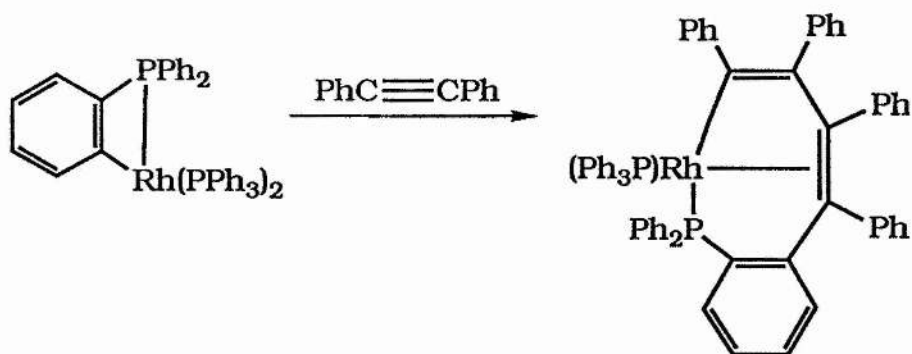


Fig. 1.37

Or, as shown in Figure 1.38, they can be isolated from the reaction of a bisacetylenephosphane compound and RhL_3Cl , where $\text{L} = \text{PPh}_3$ ⁽¹⁰⁴⁾. Subsequent reaction of the complex shown in Figure 1.38 with reagents like PMe_3 leads to the isolation of the bidentate complexes shown in Figure 1.39.

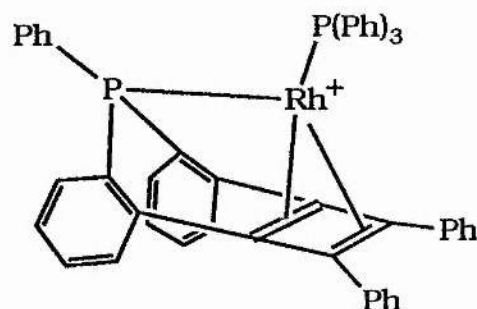


Fig. 1.38

The first of which (1.39a) is σ/π chelate through the phosphorus atom and the double bond⁽¹⁰⁵⁾.

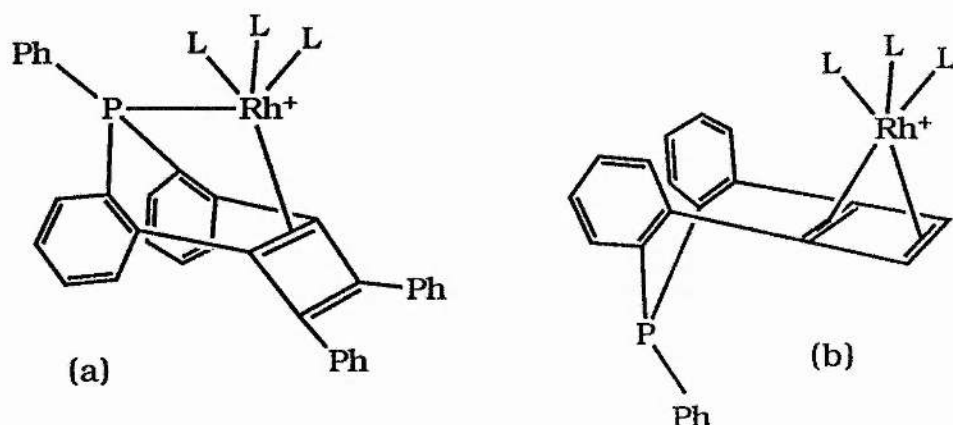


Fig. 1.39

One of the other main routes to chelate σ/π bound phosphine ligands is via alkenylphosphines. Alkenylphosphine complexes which possessed these σ/π structures were first isolated in the mid 1960's (see section 1.5.1). In 1970 Clark and Hartwell produced a trigonal bipyramidal alkenylphosphine complex $\text{RhX}[(\text{PPh}_2(\text{CH}_2)_n\text{CH}=\text{CH}_2)_3]$ where $n = 2, 3$ and $\text{X} = \text{Cl}$ or Br , or in the case of Iridium $\text{X} = \text{Cl}$ ^(95,106). Analogous in structure to the p-vinylphenyl complex shown in Figure 1.31, these complexes contained a tetradentate phosphine with three equivalent

rhodium-alkene π bonds as shown in Figure 1.40. The X-ray crystal structure⁽¹⁰⁷⁾ showed that, although several structures of five coordinate rhodium with either trigonal or square based pyramidal coordination were reported to be distorted from the ideal five coordinate geometry, this structure appears

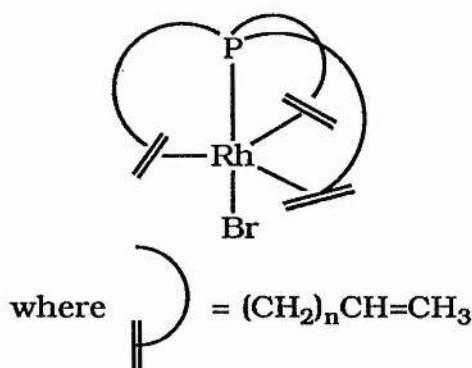


Fig. 1.40

to be a nearly perfect example of trigonal bipyramidal coordination.

The σ/π coordination of alkenyl ligands which only contain one olefin species such as $(\text{C}_2\text{H}_5)_2\text{PCH}_2\text{CH}_2\text{CH}=\text{CH}_2$ (EPV) is also possible. The reaction of $[(\text{Rh}(\text{C}_2\text{H}_4)_2\text{Cl})_2]$ and (EPV) results in $[\text{RhCl}(\text{EPV})_2]$ a complex found to be monomeric and five coordinate in the solid state, with each alkene occupying a coordination site⁽¹⁰⁸⁾. Also discovered were a series of compounds of the general formula $[(\text{RhCl}(\text{CO})(\text{Ph}_2\text{P}(\text{CH}_2)_n\text{CH}=\text{CH}_2)_2]$ where $n = 0-3$ ⁽¹⁰⁹⁻¹¹⁰⁾ in which the mono alkene is σ/π chelate bound. The similar complex of diphenylpent-3-enylphosphine ($\text{Ph}_2\text{PCH}_2\text{CH}_2\text{CH}=\text{CHCH}_3$) was subsequently isolated by isomerization of $[\text{RhCl}(\text{CO})$

$(\text{Ph}_2\text{P}(\text{CH}_2)_3\text{CH}=\text{CH}_2)]$, the only complex in the series to show such

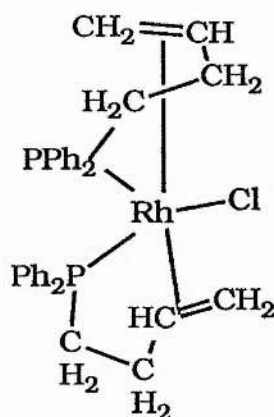


Fig 1.41

an isomerization⁽¹¹⁰⁾. The Br and I analogues of these compounds have also been isolated. Other such complexes isolated with alkenylphosphines are $[\text{Rh}_2\text{Cl}_2(\text{mbp})_2]$ and $[\text{Rh}_2\text{Cl}_2(\text{mpp})_2]$ ⁽¹¹⁰⁾ (where mbp = but-3-enyldiphenylphosphine and mpp = diphenylpent-4-enyldiposphine) in which both the alkene ligands are bound via the phosphorus atom and the alkene to the metal centre. The chlorine ligands are present as bridges between the metal centres. In the same work complexes containing both a σ/π chelated phosphine ligand and a tetraphenylborate ligand which was

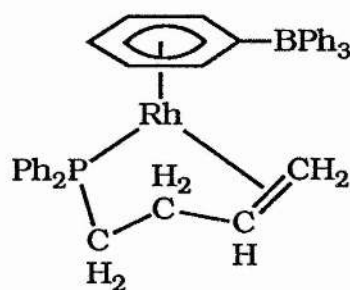


Fig. 1.42

bound in an η^6 fashion were also reported⁽¹¹¹⁾ (Figure 1.42). π bound bisalkenylphosphines have also been prepared, for example complexes of the form $[\text{Rh}_2\text{X}_2(\text{bbp})_2]$ where bbp = bis(but-3-enyl)phenyl phosphine and $\text{X} = \text{Cl}, \text{Br}, \text{I}$, the proposed structure being⁽¹¹²⁾ Figure 1.43.

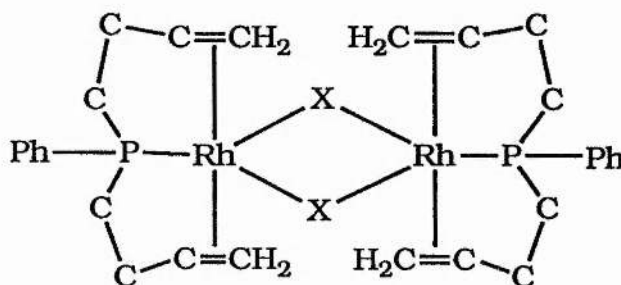


Fig. 1.43

These dimers will react with CO to produce the associated monomeric compounds with the structure shown in Figure 1.44⁽¹¹²⁾.

Also isolated were similar complexes of Pd^{II} and Pt^{II} , these having the formula $\text{MX}_2(\text{L})$ where $\text{X} = \text{Cl}, \text{Br}, \text{I}$ and $\text{L} = \text{Ph}_n\text{P}(\text{CH}_2\text{CH}_2\text{CH}=\text{CH}_2)_{3-n}$; $n = 0-2$ ⁽¹¹³⁾. A range of alkenyl phosphines bound σ/π through the phosphorus atom and the double bond has also been produced with ligands of the form

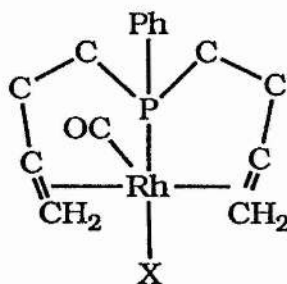


Fig. 1.44

$\text{Ph}_n\text{P}(\text{CH}_2\text{CH}_2\text{CH}=\text{CH}_2)_{3-n}$ where $n = 0, 1, 2$ and molybdenum is the metal centre⁽¹¹⁴⁾. In these cases however although chelate products are formed, the maximum coordinating ability of each ligand is not realized during the coordination of the alkenes. The species formed contain an increased number of carbonyls or polymerise due to metal alkene bond formation in preference to chelation. Examples of some of the structures produced in these studies are shown in Figure 1.45.

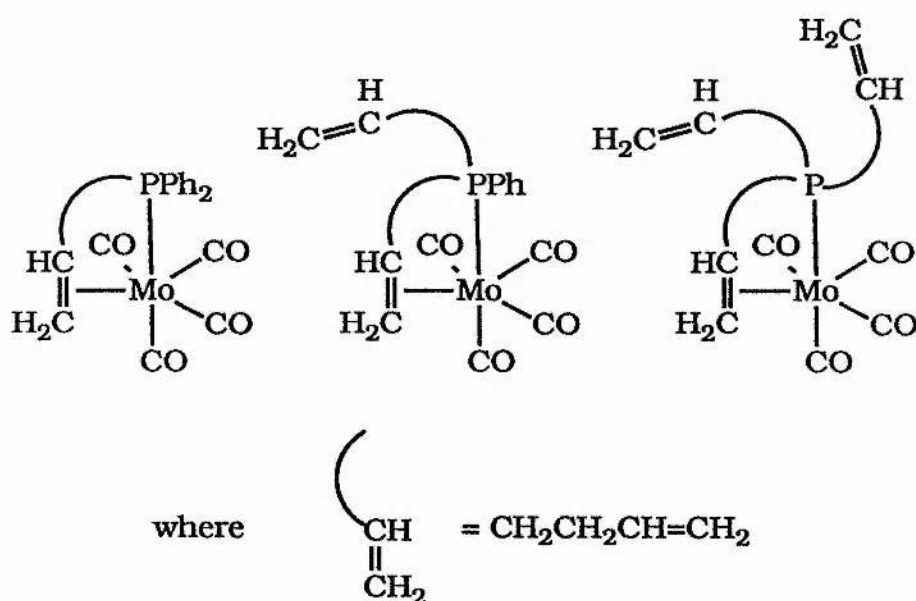
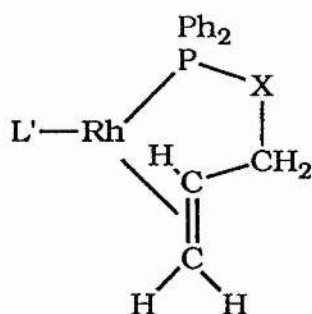


Fig. 1.45

Complexes of ligands containing unsaturated phosphinites have also been isolated. Diphenyl(prop-2-enyloxo) phosphine ($\text{Ph}_2\text{POCH}_2\text{CH}=\text{CH}_2 = \text{dppp}$) is found to produce σ/π complexes bound through the phosphorus atom and the double bond (Figure 1.46)⁽¹¹⁵⁾.

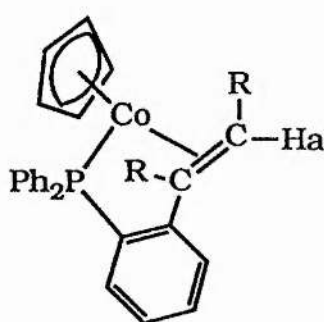


$L' = \text{cp or acac}$

$X = \text{O or CH}_2 \text{ (O for dppp)}$

Fig. 1.46

This work has led to the isolation of other complexes of oxygen containing phosphine ligands, these ligands taking the form of mixed anhydrides derived from acrylic and diphenylphosphinous acids. Furthermore complexation of these mixed anhydride ligands has also provided a new route to π coordination of highly substituted alkenes. Few complexes of chelate phosphorus ligands containing π bound, highly substituted alkene species have been reported. One of the few examples is shown in Figure 1.47⁽¹¹⁶⁾.



where $R = \text{CO}_2\text{Me}$

Fig. 1.47

The formation of these new ligands and the resultant complexes are discussed in the following section.

1.5.2 Phosphorus Mixed Anhydride Ligands and their Rhodium Complexes

The reaction of acrylic acids and allyl alcohols ($R^1R^2C=CR^3XOH$) with Ph_2PCl in the presence of Et_3N results in the formation of phosphorus mixed anhydrides of the form $[Ph_2PYCR^3=CR^2R^1]$ where $Y = OCH_2$ or O_2C ⁽¹⁰⁸⁾. The products show no signs of decomposition or oxygen migration if stored under dinitrogen at 0°C. The mixed anhydrides have been isolated in the following cases (see Table 1.1 for spectral details).

$X = CO$	$R^1 = Me$	$R^2 = R^3 = H$	
$X = CO$	$R^1 = R^2 = Me$	$R^3 = H$	
$X = CH_2$	$R^1 = R^2 = Me$	$R^3 = H$	
$X = CO$	$R^1 = MeCH = CH$	$R^2 = R^3 = H$	
$X = CO$	$R^1 = Ph$	$R^2 = H$	$R^3 = Me$

Upon their reaction at room temperature with rhodium chloride bridged dimers of the form $[(RhClL_2)_2]$, where $L = C_2H_4$ or cyclo octene, they are found to give rise to dimeric products. These resultant complexes without exception exhibit coordination of the mixed anhydride ligand through the phosphorus atom and the double bond, producing chlorine bridged structures of the form shown in Figure 1.48⁽¹¹⁷⁾. A second reaction attempting to coordinate the phosphorus mixed anhydride ligand derived from dimethylacrylic acid ($Ph_2POCOCH=CMe_2$) to Wilkinson's Catalyst ($[(RhClPPh_3)]$) has resulted in a complex in which this ligand is

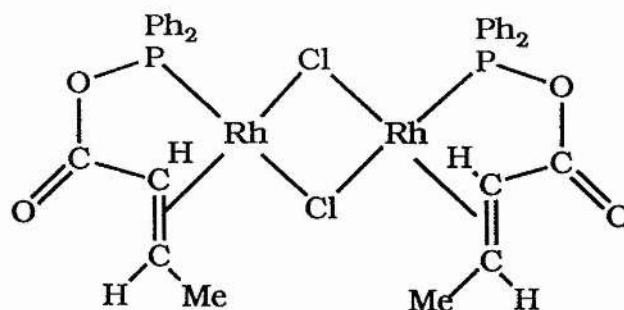


Fig. 1.48

bound only through the phosphorus atom⁽¹¹⁸⁾ (Figure 1.49).

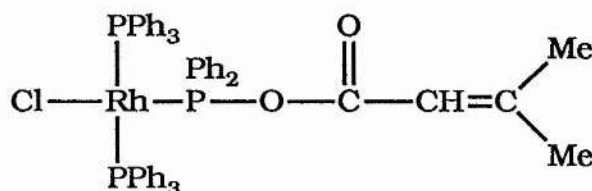


Fig. 1.49

A third mode of mixed anhydride coordination has been observed following halide abstraction reactions involving both $[\text{RhCl}(\text{Ph}_2\text{PO}_2\text{CCHCHMe})(\text{PPh}_3)]$ and $[\text{RhCl}(\text{PPh}_3)(\text{Ph}_2\text{PO}_2\text{CCHCMe}_2)]$ and TiPF_6 . The same form of product, $[\text{Rh}(\text{PPh}_3)_2(\text{Ph}_2\text{PO}_2\text{CHCYMe})][\text{PF}_6]$ ($\text{Y} = \text{H}$ or Me), is obtained in both cases and is found to exhibit coordination of the mixed anhydride via the phosphorus atom and oxygen atom of the carbonyl group^(119,120) (see Figure 3.16). This reaction of $[\text{RhCl}(\text{Ph}_2\text{PO}_2\text{CCHCHMe})(\text{PPh}_3)]$ is further discussed in Chapter 3, Section 3.4.

Tables 1.2-1.3 contain a summary of the spectral data of selected rhodium/mixed anhydrides complexes exhibiting all three modes of coordination discussed above.

Table 1.1 Spectral Data for The Mixed Anhydrides						
Compound	IR (cm ⁻¹)		³¹ P (ppm)	¹ H (ppm)		
	ν (c=O)	ν (c=c)		∂ Me	∂ H	
CH ₃ CO ₂ PPh ₂	1740sst	—	99.1s	2.0s	----	
Me ₂ ^{a,b} CCCH ^c CO ₂ PPh ₂	1692sst	1640s	96.2s	a 1.83, b 2.0d	c 5.7	
Me ^a CH ^b CH ^c CO ₂ PPh ₂	1705sst	1645s	98.9s	a 1.92d	b 7.1, c 6.0	
Me ₂ ^{a,b} CCCH ^c CH ₂ ^{d,e} OPPh ₂	-----	1660s	112.3s	a 2.0, b 2.1	c 5.8, d 4.7, e 4.68	
Me ^a CH ^b CH ^c CH ^d CH ^e CO ₂ PPh ₂	1692sst	1638s, 1608s	99.6s	a 1.83	b 6.2, c 7.3, d 6.2, e 5.8	
PhCH ^b CMe ^a CO ₂ PPh ₂	1685sst	1620m	100.6s	a 2.2	b 4.4	

† run as neat film between CsI plates § N.M.R.'s run in CD₂Cl₂ at 25°C

Table 1.2 | I.R. and ^1H n.m.r. Spectral Data for The Rhodium Mixed Anhydride Complexes

Compound	I.R. (cm^{-1})		$\delta^1\text{H}(\text{ppm})$	
	$\nu(\text{C}=\text{O})$	$\nu(\text{C}=\text{C})$	$\nu(\text{Rh}-\text{Cl})$	$\delta \text{ H}$
$[\text{RhCl}(\text{Ph}_2\text{PO}_2\text{CCH}^{\text{c}}=\text{CMe}_2^{\text{a,b}})_2]$	1748sst	-----	276	a1.3, b1.45d c2.75
$[\text{RhCl}(\text{Ph}_2\text{PO}_2\text{CCMe}^{\text{a}}=\text{CHPh}^{\text{b}})_2]$	1745sst	-----	265	a 1.6s b4.4s
$[\text{RhCl}(\text{PPh}_3)_2(\text{Ph}_2\text{PO}_2\text{CCH}^{\text{c}}=\text{CMe}_2^{\text{a,b}})]$	1708 ^a	1635 ^a	290 ^a	a1.9, b2.1s c5.7q
$[\text{RhCl}(\text{PPh}_3)_2(\text{Ph}_2\text{PO}_2\text{CCMe}^{\text{a}}=\text{CHPh}^{\text{b}})]$	1685	1620	----	a 1.48s ,
$[\text{Rh}(\text{PPh}_3)_2(\text{Ph}_2\text{PO}_2\text{CCH}^{\text{c}}=\text{CMe}_2^{\text{a,b}})]^{\dagger}$	1585	1628	----	a1.1d, b1.75d c5.7
$[\text{Rh}(\text{PPh}_3)_2(\text{Ph}_2\text{PO}_2\text{CCMe}^{\text{a}}=\text{CHPh}^{\text{b}})]^{\dagger}$	1565br	1613	----	a 1.8s ,

a in CD_2Cl_2 δ N.M.R.'s run in CD_2Cl_2 at 25°C \dagger obscured by phenyl region

Table 1.3		$^{31}\text{P}^3$ Spectral Data for the Rhodium Mixed Anhydride Complexes										
Compound		Chemical Shifts			Coupling Constants(Hz)							
		Pa	Pb	Pc	RhPa	RhPb	RhPc	PaPb	PaPc	PbPc		
$[\text{RhCl}(\text{Ph}_2\text{PO}_2\text{CCH}=\text{CMe}_2)_2]$		134.5d	---	----	188	---	---	---	---	---		
$[\text{RhCl}(\text{Ph}_2\text{PO}_2\text{CCMe}=\text{CHPh})_2]$		132.0d	----	----	174	---	---	---	---	---		
$[\text{RhCl}(\text{PPh}_3)_2(\text{Ph}_2\text{PO}_2\text{CCH}=\text{CMe}_2)]$		32.4dd	49.1dt	----	143	191	---	38	---	---		
$[\text{RhCl}(\text{PPh}_3)_2(\text{Ph}_2\text{PO}_2\text{CCMe}=\text{CHPh})]$		31.7dd	48.4dt	----	145	193	---	---	---	---		
$[\text{Rh}(\text{PPh}_3)_2(\text{Ph}_2\text{PO}_2\text{CCH}=\text{CMe}_2)]^+$		28.7ddd	52.0ddd	173.8ddd	137	185	162	37	320	37		
$[\text{Rh}(\text{PPh}_3)_2(\text{Ph}_2\text{PO}_2\text{CCMe}=\text{CHPh})]^+$		27.0ddd	48.5ddd	175.2ddd	136	185	164	36	323	36		

§ N.M.R.'s run in CD_2Cl_2 at 25°C

1.6 Catalysis Involving Metal Complexes

As stated one of the major driving forces behind the study of metal complexes of the form discussed in this chapter is their application to catalysis and the high degree of stereochemical selectivity often displayed in such reactions. Platinum metal complexes have exhibited both academic and industrial importance in these areas, especially in the latter. Generally transition metal compounds tend to try to achieve an $18e^-$ electron configuration in their outer valence shell ("inert gas" form). However platinum metals compounds (d^8 configuration) favour square planar arrangements which have 16 outer valence shell electrons. As a direct result complexes of these metals can be activated by either, oxidative addition or coordination of previously neutral molecules. The coordinated reagents then react by insertion and the modified products finally isolated by reductive elimination. A further point noted with alkenes is that upon coordination the synergic interaction involved in the formation of the π bond results in considerable weakening of the unsaturated linkage increasing their susceptibility to nucleophilic attack and attack of small molecules.

1.6.1 Asymmetric Synthesis

An asymmetric synthesis has been defined as a "kinetically controlled asymmetric transformation"⁽¹²¹⁾, in that normally it can be achieved only by the reaction proceeding through two diastereomeric transition states or intermediates at markedly different rates. There are a number of diastereomeric combinations

of the transition metal complex and the substrate possible which, eventually, will lead to an asymmetric synthesis. For example, the combination of a chirally modified transition metal complex and an achiral substrate molecule. The interaction consists of two parts, the total interaction and that part of the total interaction which leads to the asymmetric synthesis, namely the diastereotropic interaction. This interaction is defined as the free energy difference between the diastereomeric transition states of the asymmetric synthesis $\Delta\Delta G^\ddagger$ (122). The differences in these free energies are usually small, a difference in the region of 12 KJ/mol being large enough to result in an optically pure product. It follows that if the efficiency of the asymmetric synthesis is to be high, it is $\Delta\Delta G^\ddagger$, the diastereotropic interaction, that must be maximized; not necessarily the total interaction. The enantiomeric purity of a chiral compound obtained from such a synthesis is defined by its enantiomeric excess (% ee), calculated by applying the formula.

$$\frac{(\text{R})\text{enantiomer} - (\text{S})\text{enantiomer}}{(\text{R})\text{enantiomer} + (\text{S})\text{enantiomer}} \times 100 = \%ee.$$

The %ee is determined in the first irreversible step involving the diastereomeric transition states, this step is called the enantioselective step. A chiral auxilliary is associated with the catalyst and discriminates between the prochiral features of the bound substrate by differences in the reaction rates associated with the production of one or other of the enantiomers.

1.6.2 Early Work on Metal Catalysis

Before 1968 there were few examples of non-enzymatic catalytic studies and even after this period design of catalysts proved to be largely empirical. However several rules were developed to help guide catalyst design.

1) The chiral ligand should not drastically decrease the catalytic activity.

2) Due to structural modifications on the ligands, it should be expected that the reaction mechanism of the known achiral catalyst could be altered.

3) The chiral ligand has to remain coordinated to the metal during the step in which the asymmetric centre is created on the substrate.

4) The synthesis of the ligand should be easy and flexible, allowing the use of cheap, natural products. Thus a resolution step is avoided and many analogues and quasi-enantiomeric ligands become available.

5) Predictions and rational approaches are expected from information on the reaction mechanism and the structure of the various catalytic species.

The majority of initial studies were mainly concerned with tertiary phosphines chiral at phosphorus. Subsequent research proved that greater stereoselectivity could be obtained by utilizing bidentate phosphine ligands which were not chiral at the phosphorus but in the carbon backbone. This increase was assigned to the increased conformational rigidity attained due to the

bidentate nature of the ligand. Therefore interest in the chelating monoalkene ligands where phosphorus is the hetero donor atom centred on increasing the knowledge and scope of such bidentate ligands and thus develop better and more efficient catalysts which would hopefully produce highly stereoselective reactions. These ligands could be chiral at the phosphorus, the carbon or both.

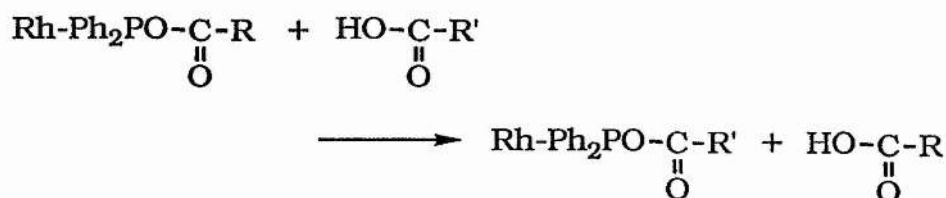
1.6.3 Mechanism of Bidentate Ligand Stereoselectivity

As stated high stereoselectivity became associated with bidentate coordination of both the chiral ligand and the substrate alkene via the double bond and the hetero donor atom. Halpern⁽¹²³⁾ showed, by X-ray crystallography that with α -amino acid precursors both the alkene moiety and the oxygen of the amide group are coordinated to the metal. The chelate ring formed stabilizes the metal-alkene interaction⁽¹²⁴⁾. Thus this system contains (1) a chiral ligand which allows face discrimination of the alkene (2) the alkene species as part of a bidentate ring which stabilizes the π bond, increases the steric interactions which result in the chiral recognition and adds to the conformational rigidity of the complex. These effects culminate, as suggested by Halpern, in the absolute configuration of the products observed⁽¹²⁵⁾. Very few systems are found to fulfil these criteria, thus few prochiral alkenes produce such high optical yields. A system which does are derivatives of itaconic acid, $[\text{CH}_2=\text{C}(\text{CO}_2\text{H})\text{CH}_2\text{CO}_2\text{H}]$ for which the high optical

yields⁽¹²⁶⁾ are attributed to similar coordination through a remote oxygen atom.

1.7 Catalytic Studies with Phosphorus Mixed Anhydrides

It was hoped that the rhodium complexes containing chelating phosphorus mixed anhydride ligands described in Section 1.5.2 could find applications as bifunctional catalysts. This is because the phosphorus is a good coordinating group, alkene coordination is favoured by chelate ring formation and the phosphinite group can be removed by hydrolyses or by a transesterification step which is found to be base catalysed and shown in Figure 1.50 (118).



where R and R' are alkene species

Fig. 1.50

Precedent for this transesterification step is provided⁽¹²⁷⁾ by the stoichiometric reaction of $[\text{Mo}(\text{CO})_4(2\text{-Me}_2\text{POC}_5\text{H}_4\text{N})]$ with $\text{LiOCH}_2\text{CR}=\text{CR}'\text{R}''$ to give $[\text{Mo}(\text{CO})_4(\text{Me}_2\text{POCH}_2\text{CR}=\text{CR}'\text{R}'')]$. The work with these mixed anhydrides has initially centred on hydrogenation reactions of a range of acrylic acids⁽¹¹⁸⁾. The mechanism proposed at the time of this study is shown in Figure 1.51 but this has subsequently been revised to the mechanism shown in Figure 1.52.

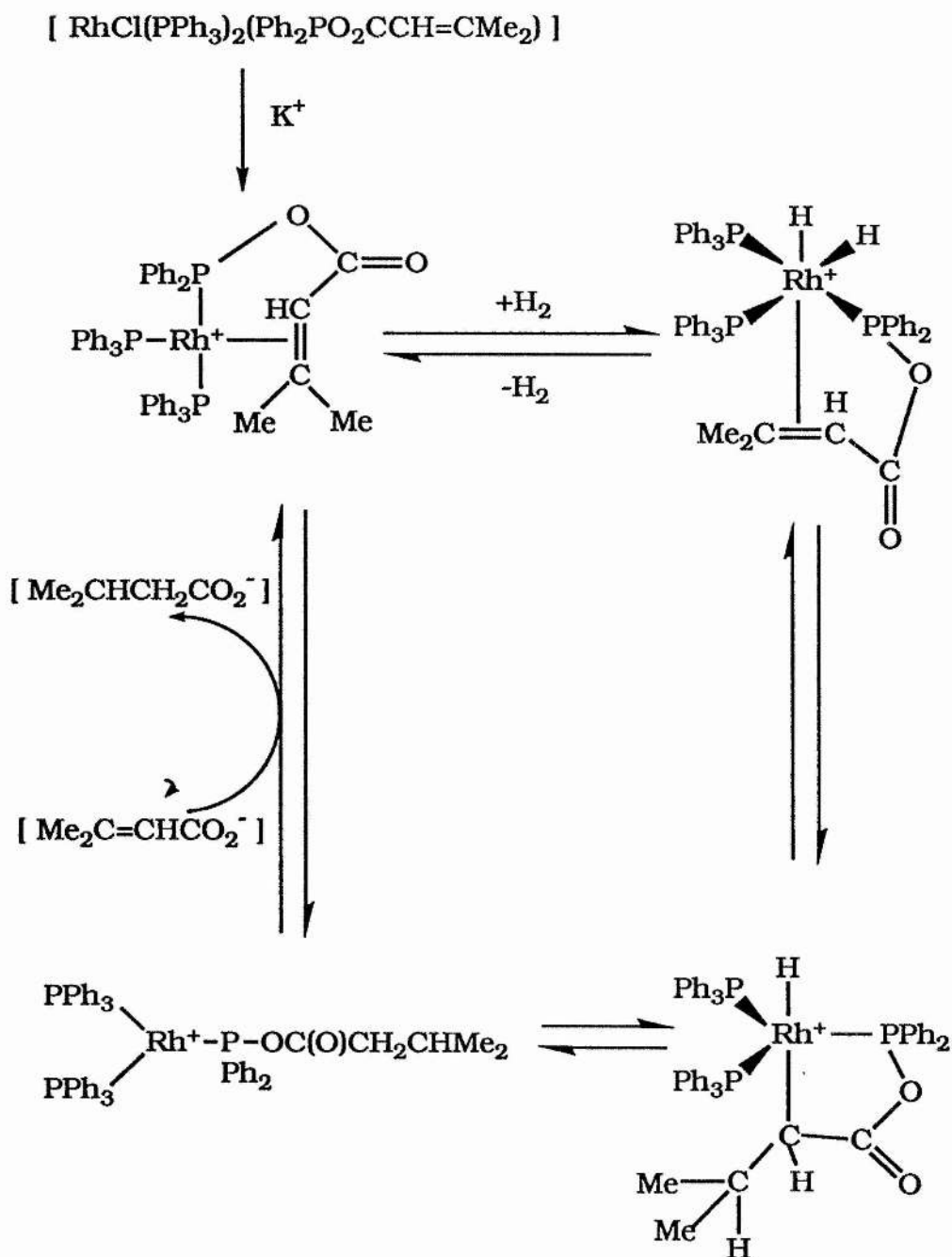


Fig. 1.51

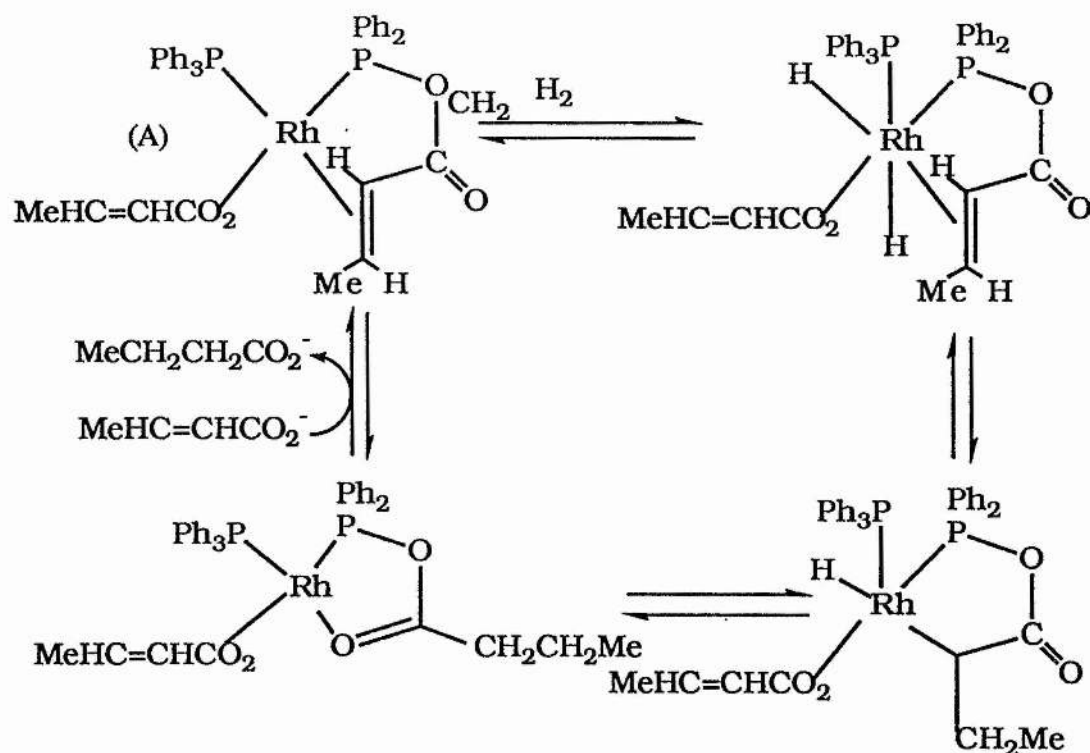


Fig. 1.52

The species (A) has been shown to be the catalytically active species. The mechanism is similar to those proposed for simple hydrogenations of alkenes using cationic rhodium catalysts up to the transesterification step. Strong support for the mechanism comes from the results of hydrogenating hexa-2,4-dienoic acid⁽¹¹⁸⁾. Normally this acid is fully hydrogenated to hexanoic acid⁽¹²⁸⁾, alternatively hydrogen adds across the diene to give hex-3-enoic acid or across the C4 double bond to give hex-2-enoic acid^(129,130). With [RhCl(PPh₃)(Ph₂PO₂CCH=CMe₂)] the hydrogenation of hexa-2,4-dienoic acid is found not only to be catalytic but exhibits an increased rate of hydrogenation relative to that exhibited by [RhCl(PPh₃)₃].

Furthermore the major product is hex-4-enoic acid arising from hydrogen addition across the C2 double bond which supports the proposed chelate binding of $\text{Ph}_2\text{PO}_2\text{CCH}_2\text{CH}=\text{CHCH}=\text{CHMe}$ by the phosphorus atom and the C2 double bond during the catalytic cycle. The increase in the rate of hydrogenation gained with this catalyst in the hydrogenation of hex-2,4-enoic acid when compared to other homogeneous catalysts is found to be a general trend exhibited in the hydrogenation of a range of acrylic acids as shown in Table 1.4.⁽¹¹⁸⁾ where Wilkinson's catalyst is used as a comparison.

Table 1.4 Substrate	% Conversion	
	$[\text{RhCl}(\text{PPh}_3)_3]$	$[\text{RhCl}(\text{PPh}_3)_2(\text{L})]$
$\text{Me}_2\text{C}=\text{CHCO}_2\text{H}$	26.7	80.0
$\text{PhCH}=\text{CMeCO}_2\text{H}$	57.6	68.2
$\text{MeCH}=\text{CHCO}_2\text{H}$	75.8	100
$\text{MeCH}=\text{CHCH}=\text{CHCO}_2\text{H}$	10.6	64.7

Where L is $\text{Ph}_2\text{PO}_2\text{CCH}=\text{CMe}_2$

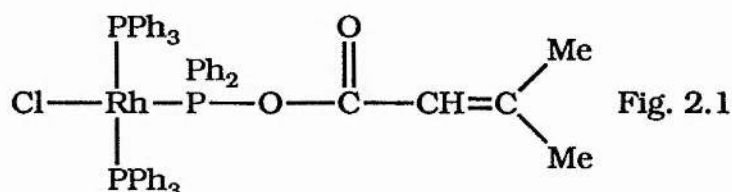
Thus with these encouraging hydrogenation results it is anticipated that the chelate stabilized coordination will lead to a high degree of face discrimination in the presence of other optically active ligands which would in turn lead to stereoselective reactions. Reactions of interest with such complexes includes attack of nucleophiles such as OMe^- , OH^- , SCN^- and NH_2^- in a stereo specific manner and lead to, for example, chiral amino acids and methoxyacids.

CHAPTER 2

Complexation of Mixed Anhydrides of Acrylic and Phosphinic Acids to Wilkinson's Catalyst

2.1 Introduction

As discussed in the introductory chapter, the initial work concerned with the coordination of the mixed anhydride ligands with the general formula $[\text{Ph}_2\text{PO}_2\text{CCR}=\text{CR}'\text{R}"]$ to a rhodium centre which used Wilkinson's Catalyst as the metal containing starting material, involved the reaction of Wilkinson's Catalyst and the mixed anhydride derived from dimethylacrylic acid $(\text{Ph}_2\text{PO}_2\text{CCH}=\text{CMe}_2)^{(118,119)}$. This work resulted in the isolation of a rhodium complex containing a mixed anhydride bound only through the phosphorus atom (Figure 2.1).



This result was found to be in contrast with similar work done on the coordination of these mixed anhydrides where rhodium chloride bridged dimers of the general form $[\text{Rh}_2\text{Cl}_2\text{L}_2]$, where L is octene or ethylene, were used as the metal containing reagents^(117,131). In these cases the mixed anhydride ligands were found to bind through both the phosphorus atom and the double bond as in Figure 2.2. Both these reaction types have now been extended to include the coordination studies on the anhydrides derived from crotonic,

acrylic and vinylacetic acids, investigating how the degree of alkene substitution effects the mode of anhydride coordination.

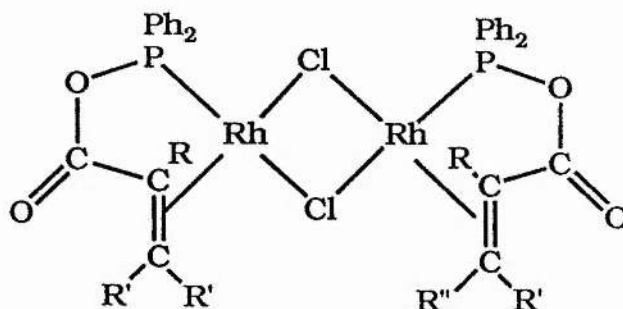


Fig. 2.2

The results from the work with the dimeric starting materials are reported in Chapter 4 whilst this chapter relates the observations and conclusions from the reactions with Wilkinson's Catalyst.

2.2 Production of the Mixed Anhydride Ligands

(Ph₂PO₂CCR=CR'R'')

The result of reacting either crotonic, acrylic or vinylacetic acids with chlorodiphenylphosphine and triethylamine under dinitrogen and at 0°C is found to be the production of Ph₂PO₂CCH=CHMe, Ph₂PO₂CCH=CH₂ and Ph₂PO₂CCH₂CH=CH₂ respectively as the major products. If the crotonic acid case is considered, the full reaction is as shown in Figure 2.3⁽¹³¹⁾.

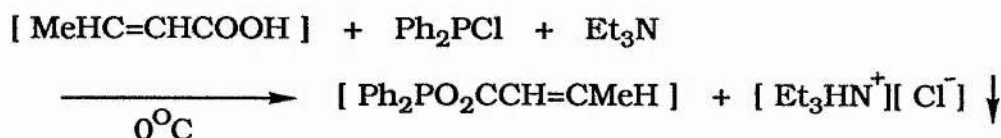


Fig. 2.3

The resultant mixed anhydride from this reaction is found, as in all other examples possessing greater than monosubstituted alkene moieties, to be stable for long periods of time if stored free from any solvent, at 0°C and under dinitrogen. The substituted mixed anhydrides (from this point the term mixed anhydride shall be reduced to just anhydride) display no tendency to undergo oxygen migration or Arbuzov rearrangements⁽¹³¹⁾. The experimental method used for the isolation of the substituted anhydrides has been reported in chapter 1.

As already stated, similar reactions to that shown in Figure 2.3 but utilizing acrylic and vinylacetic as the parent acids proceed in exactly the same manner producing the relevant anhydrides. In these cases however the anhydrides have only been identified and characterized by n.m.r. spectroscopy as attempts to isolate these anhydrides have resulted in the procurement of a colourless solid which analyses to be tetraphenyldiphosphine monoxide ($\text{Ph}_2\text{PP}(\text{O})\text{Ph}_2$), the product of an intermolecular rearrangement of the anhydrides as shown in Figure 2.4.

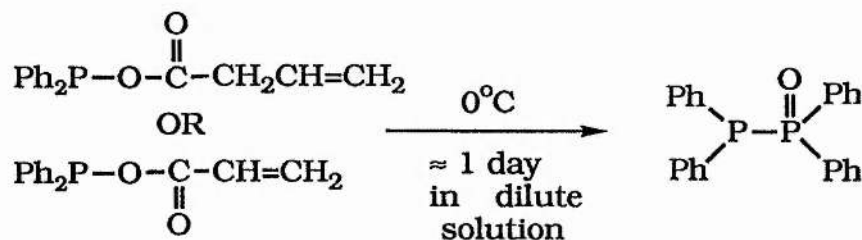


Fig. 2.4

The nature, time period of the rearrangement and relevant n.m.r. spectra will be fully discussed in chapter 3, it suffices to state

at this point that the isolation of solid samples of these monosubstituted anhydrides is impossible. Rather the extreme temperature and atmospheric sensitivity of these anhydrides coupled with their tendency toward further rearrangement has required an alteration to be made to the set method of production for these ligands.

In the case of the acrylic and vinylacetic anhydrides 1 molar solutions of the reactants were prepared in tetrahydrofuran, the required volume of these solutions was then added, under nitrogen, to a precooled (0°C - 10°C) constantly stirring quantity of tetrahydrofuran or diethyl ether. This resulted in the immediate appearance of the expected byproduct $[\text{HEt}_3\text{N}^+][\text{Cl}^-]$ as a white precipitate. After approximately five minutes the ligand solution was filtered straight into the metal-ligand reaction vessel which already contained a similarly precooled, predissolved solution of the metal reactant. In all future reactions reported during this study, involving the anhydrides derived from acrylic or vinylacetic acid, the anhydride ligand will have been introduced using this "in-situ" method. Tetrahydrofuran has been used in preference to diethyl ether as the solvent for the "in-situ" method because chlorodiphenylphosphine is found to decompose if diethyl ether is used as a dilutant. This change makes little difference to the overall method as $[\text{NEt}_3\text{H}^+][\text{Cl}^-]$ is also insoluble in tetrahydrofuran and can still be efficiently removed.

2.3 Coordination Study of the Mixed Anhydride Derived From Crotonic Acid and Wilkinsons Catalyst and Spectral Data for $[\text{RhCl}(\text{PPh}_3)(\text{Ph}_2\text{PO}_2\text{CCH}=\text{CHMe})]$

The initial work involving metal reagents in this study concerned the attempt to coordinate the crotonic acid anhydride to a rhodium centre using Wilkinsons Catalyst as the metal containing starting material⁽¹²⁰⁾. This reaction had been carried out prior to this study and crystals of X-ray quality had been obtained by recrystallization from a dichloromethane-diethyl ether solution⁽¹²⁰⁾. The X-ray crystal structure solution had subsequently shown that the anhydride ligand was bound via the phosphorus atom and the double bond. A diagram of the final structure is shown in Figure 2.5, in which one of the phenyl groups has been removed so that the ring can be viewed more easily.

The acquisition of the X-ray data proved that the reaction of the crotonic acid anhydride, to be known from this point as CAA, followed the path shown in Figure 2.6.

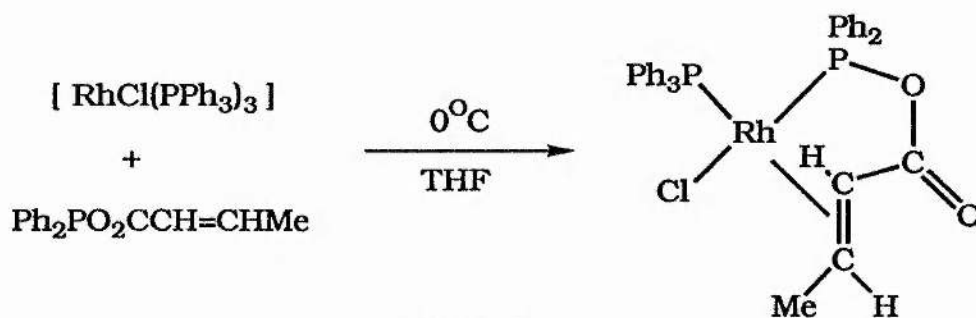


Fig. 2.6

Moreover the spectral data of this bidentate complex was found to contain several features which can both be explained by and be used as pointers in assigning bidentate coordination.

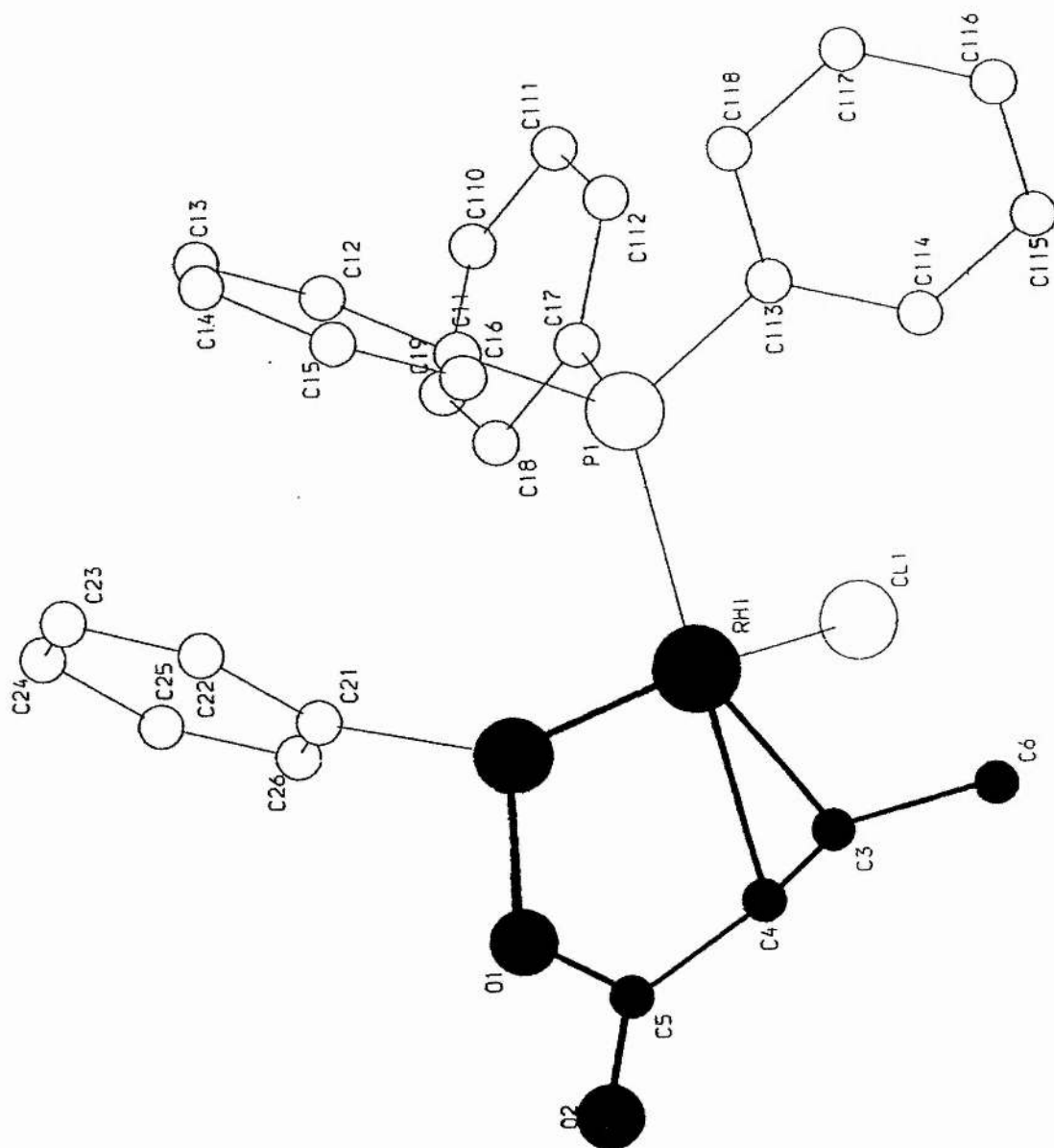


Fig. 2.5 $[\text{RhCl}(\text{Ph}_2\text{PO}_2\text{CCH}=\text{CHMe})(\text{PPh}_3)]$ x-ray crystal structure solution

2.3.1 Infra-red Data

If the complex contained the anhydride ligand only bound through the phosphorus atom, then as in the example of the dimethylacrylic acid anhydride the infrared bands, $\nu(\text{C}=\text{C})$ and $\nu(\text{C}=\text{O})$, would be in approximately the same position as observed for the free ligand. However the CAA complex has a carbonyl band located at 1740cm^{-1} and the absorbance assigned to the $\text{C}=\text{C}$ has been lost from the free ligand region of $\approx 1600\text{cm}^{-1}$. The carbonyl shift to higher frequency can be explained by considering the carbonyl to be one member of a five and a half membered ring. Study of the documented cases of 5 and 6 membered lactone rings exhibited carbonyl absorbances at $\approx 1700\text{cm}^{-1}$ and $\approx 1800\text{cm}^{-1}$ respectively⁽¹³²⁾, thus the new shifted carbonyl position of 1740cm^{-1} for the CAA complex is due to a structural arrangement between the 5 and 6 membered ring situations. Furthermore the lack of a band in the 1600cm^{-1} region upon complexation indicates that the environment of the double bond has also altered. A shift of this size, namely over 100cm^{-1} from the free ligand position could not be explained by a simple change in the mesomeric effects resulting from the anhydride binding to the metal from a site near the double bond, rather it is more likely that this large shift is a product of π coordination to the metal center in a manner described by the Dewar, Chatt and Duncanson bonding model (section 1.3.3). These two separate conclusions are complementary as the π coordination will induce the ligand into the 5 and a half membered ring expected from the carbonyl position and thus lead to the assignment of the

structure shown in Figure 2.7.

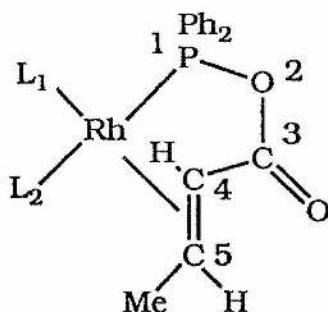


Fig 2.7

2.3.2. ^{31}P n.m.r. Data

The n.m.r. data for this complex was more complex than expected on the basis of structure 2.7. The expected ^{31}P n.m.r. spectrum for the CAA complex would consist of two doublets of doublets as in Figure 2.8.



Fig 2.8

Each phosphorus atom in a unique environment will give rise to a unique resonance which will be split firstly by a coupling to rhodium and secondly by mutual phosphorus coupling. In pictorial form this is shown in Figure 2.9. The experimentally observed spectrum (Figure 2.10) is not like the above, rather it contains a small broad signal at 140 ppm and a doublet at 25.5 ppm. Thus the complex would appear to be fluxional in some way so as to lose the information on one of the rhodium phosphorus couplings and the

mutual phosphorus coupling.

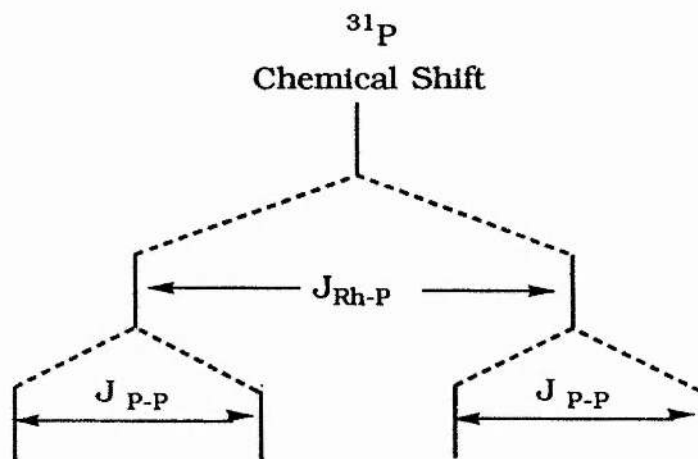


Fig. 2.9

There are however two pieces of information which can be obtained from the room temperature ^{31}P spectra. The first is that the anhydride ligand is bound in a chelate fashion which in the ^{31}P spectrum is shown by the movement to lower field of the ^{31}P resonance of the anhydride from the free ligand position of 98.9 ppm to the complexed position at 140 ppm. This CAA resonance shift is due to the appearance of ring contributions⁽¹³³⁾. These contributions produce a shift in the phosphorus resonance to lower field and, as their name suggests, occur upon formation of a bidentate ring by the ligand containing the phosphorus atom concerned. Furthermore the size of the contribution is found to be related to the size of the ring formed, in general the smaller the ring formed the greater the low field shift. Δ_R is the designated symbol for these contributions and the size of the contribution is simply calculated as

$$\left(\text{Resonance position of complex} \right)_{\text{containing ring}} - \left(\text{Resonance position of the same complex with bidentate ring now} \right)_{\text{monodentate}} = \Delta_R$$

If a complex containing the relevant ligand bound in a monodentate fashion is not available then some idea of Δ_R can be obtained by subtracting the ppm value of a similar monodentate complex. The contribution is usually connected to the size of the C-P-M angle, a change in this angle producing a change in the Δ_R value.

The second piece of information regards the fluxionality of the complex. Because almost all information about the 140 ppm resonance is lost as opposed to the loss of only the mutual phosphorus coupling for the triphenylphosphine resonance (25.5 ppm), the $J_{\text{Rh-P}}$ coupling of the latter clearly being displayed on the form of the retained doublet, it is concluded that the CAA species is the fluxional ligand (see section 2.4).

2.3.4 ^1H n.m.r. Data

The room temperature proton n.m.r. spectrum (Figure 2.11) contains little information due to the fluxionality broadening the observed resonances. However as in the ^{31}P data it can also be concluded that the anhydride ligand is bound through the phosphorus and the double bond. Evidence for this comes from the shift in the ^1H n.m.r. resonances for the vinylic protons to higher field. This high field shift is due to the π coordination driving the carbon atoms of the alkene double bond towards a pseudo sp^3

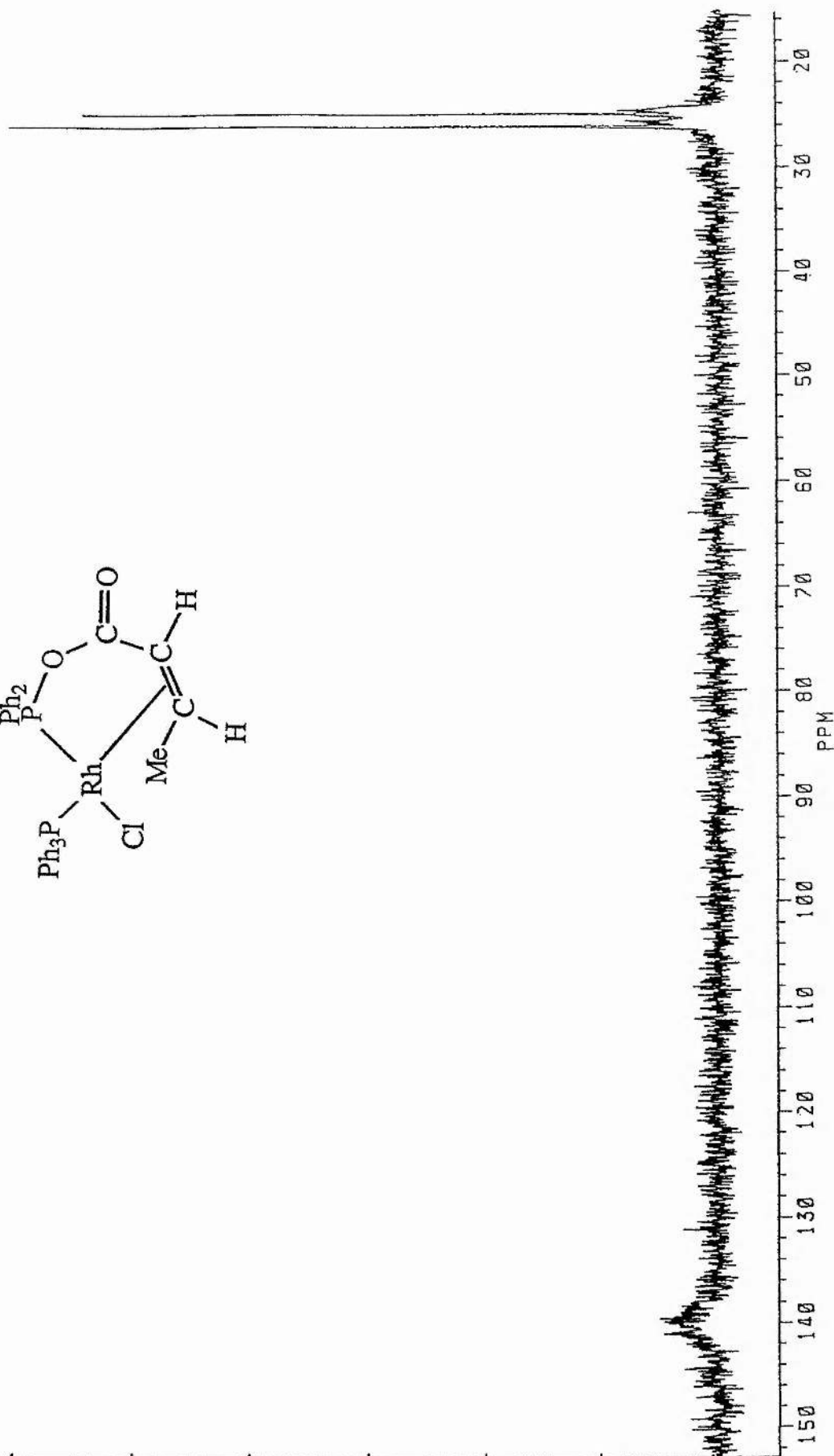
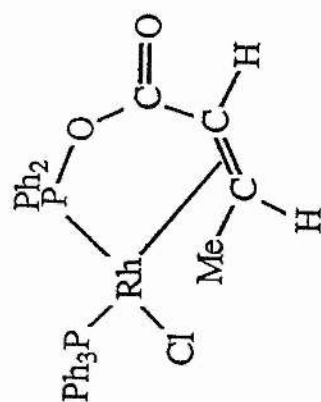


Fig. 2.10 ^{31}P n.m.r. spectrum (300 MHz) of $[\text{Rh}(\text{PPh}_3)(\text{HMeC}=\text{CHO}_2\text{PPh}_2)\text{Cl}]$

$(\text{CD}_2\text{Cl}_2, 25^\circ\text{C})$

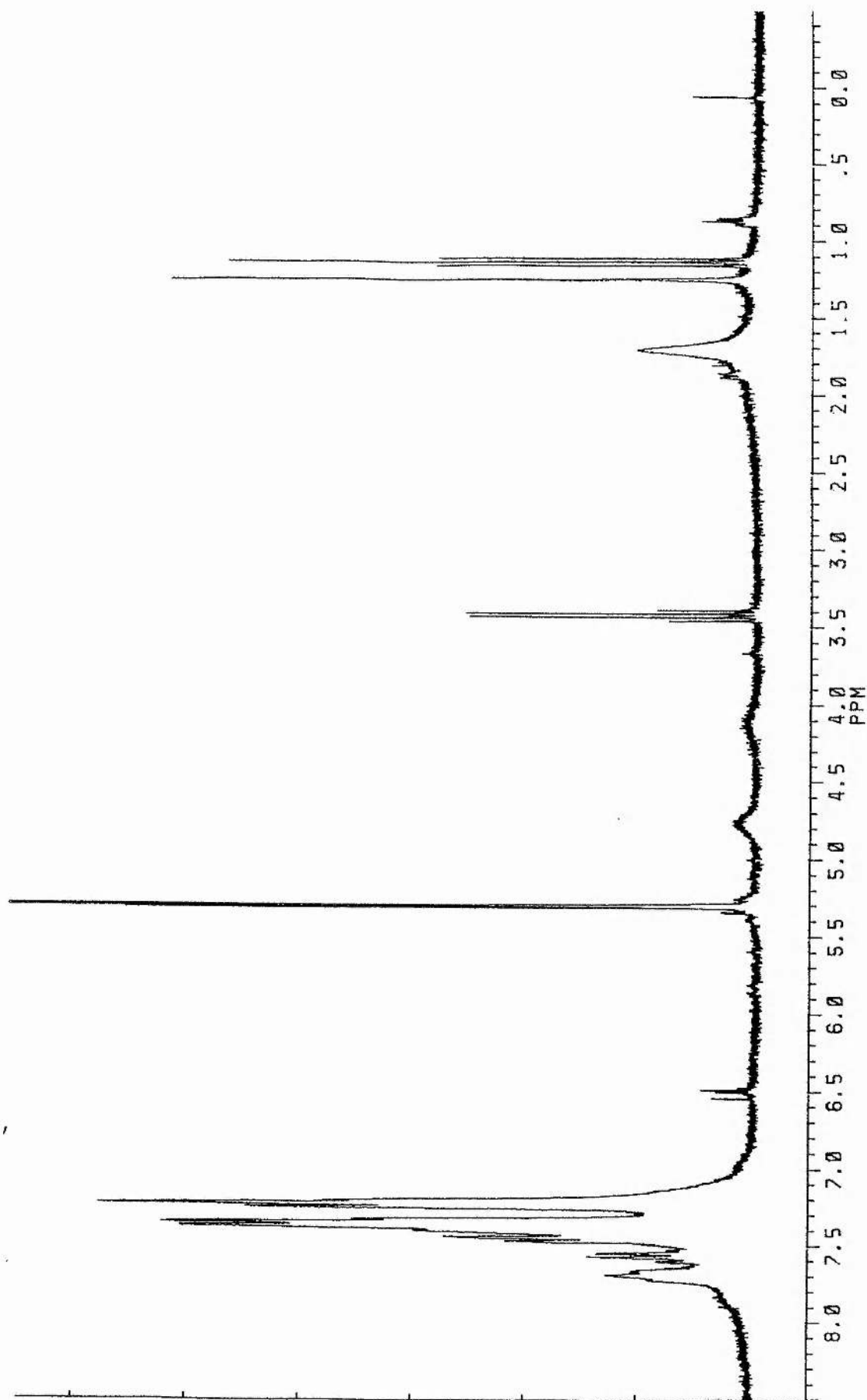


Fig. 2.11 ^1H n.m.r. spectrum (300 MHz) of $[\text{Rh}(\text{PPh}_3)(\text{MeHC}=\text{CHO}_2\text{PPh}_2)\text{Cl}]$

$(\text{CD}_2\text{Cl}_2, 25^\circ\text{C})$

hybridisation state, the reasons for this are explained by the Dewar, Chatt and Duncanson bonding model as described in section 1.3.3. This move to sp^3 hybridisation results in the protons of the alkene group becoming more shielded and so leads to them resonating at lower frequencies than when in the free ligand⁽¹³⁴⁾. Shifts of 2-4 ppm are usually taken as definite evidence of the π coordinations of an alkene to a metal⁽¹³⁴⁾. In the CAA/Wilkinson's Catalyst complex discussed here the vinylic protons are found to move from $\delta 7.08$ ppm and $\delta 6.02$ ppm to $\delta 4.75$ ppm and $\delta 4.07$ ppm respectively upon complexation, a shift of 2-2.5 ppm.

2.4 Explanation of Fluxionality and Non-Room Temperature

N.M.R. Studies on the CAA/Wilkinson's Catalyst Complex

In an attempt to explain the fluxionality shown by the CAA complex, solution infra-red and non-room temperature n.m.r. spectra were obtained to further study the nature of the CAA coordination and fluxionality.

2.4.1 Solution Infra-Red Study

Infra-red data is collected over a much shorter time period than n.m.r. data⁽¹³⁵⁾ thus the solution infra-red spectrum of the CAA complex would be expected to contain new peaks not viewed in the solid infra-red spectrum arising from the fluxionality. However no new peaks are observed indicating that the fluxionality doesn't

involve disconnection of the CAA ligand as this would mean the appearance of bands in similar positions to the free ligand.

2.4.2 High Temperature n.m.r. Studies

Although it was not possible to obtain the high temperature limiting spectra for $[\text{RhCl}(\text{PPh}_3)(\text{CAA})]$ because of extreme decomposition, the fact that the chemical shifts of the CAA phosphorus atom and vinylic protons do not alter greatly from conditions of slow exchange to those of an intermediate exchange rate suggest that the CAA ligand remains bound to the metal via both the phosphorus atom and the double bond in both exchange forms.

2.4.3 Low Temperature ^{31}P n.m.r. Study

By studying the low temperature (-25°C) spectra of this complex the fluxionality could be quenched and the theoretically expected spectra obtained. From the ^{31}P spectrum (figure 2.12) the complex is assigned the structure shown in figure 2.13

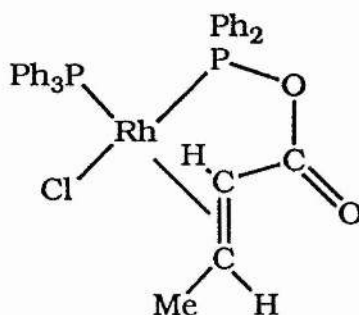
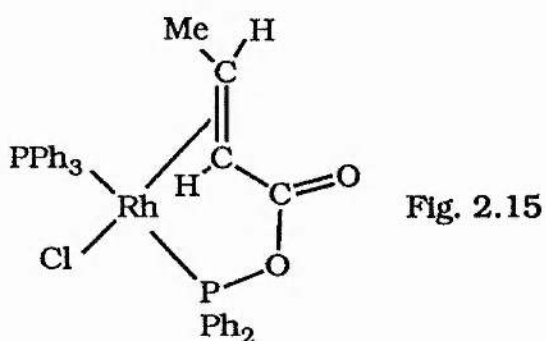


Fig 2.13

giving rise to two doublets of doublets, the anhydride resonance present at 142.1 ppm and that of PPh_3 at 25.5 ppm. The value of the J_{pp} indicates mutually *cis* phosphorus atoms as in figure 2.13. However if this spectrum is studied closely a second complex is observed to be present in very small quantities. This complex, marked as complex 2 on figure 2.12 and enlarged in 2.14, also exhibits an experimental spectrum of two doublets of doublets, the J_{pp} in this case is found to be very large (424 Hz) suggesting that it contains two mutually *trans* phosphorus atoms. Furthermore the fact that its resonances exchange with those of *cis* $[\text{RhCl}(\text{PPh}_3)(\text{CAA})]$ at higher temperatures suggests that complex 2 also has the formula $[\text{RhCl}(\text{PPh}_3)(\text{CAA})]$. The chemical shift of complex 2's mixed anhydride phosphorus atom is in the region expected for coordination through the phosphorus atom and double bond and so it is assigned the structure shown in figure 2.15.



The fluxional process must involve a complete rotation of the ligand, as there is no evidence from either n.m.r. or infra-red sources indicating that decomplexation occurs. Thus it is concluded that the *trans* and *cis* isomers are involved in a reversible

exchange process (figure 2.16).

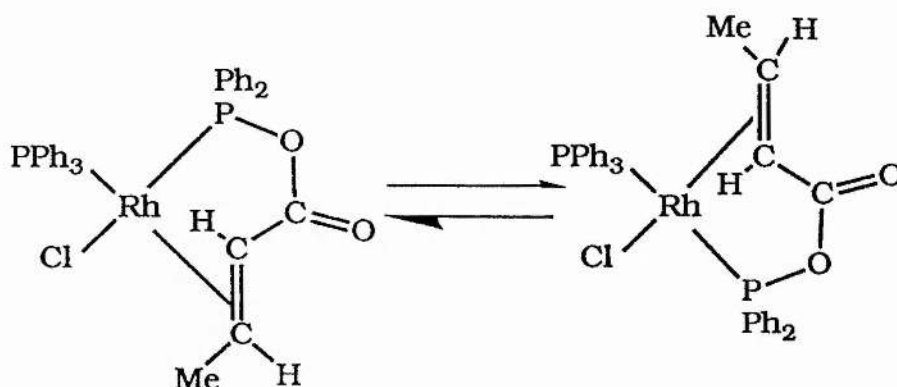


Fig 2.16

This process would not account for all the observed data, however, as it would be expected that coupling between the phosphorus atoms should be retained even under the conditions of fast exchange. Under these conditions J_{PP} should have a value which is the weighted mean of the values for the *trans* and *cis* isomers. By measuring the relative concentrations of the *trans* and *cis* forms of $[\text{RhCl}(\text{PPh}_3)(\text{Ph}_2\text{O}_2\text{CCH}=\text{CHMe})]$ at different temperatures (223-263K) it is possible to calculate the thermodynamic parameters for the *trans* and *cis* isomerisation processes. Figure 2.17 shows the plot of $-\ln K$ vs $1/T$ and from the application of the formulae I and II below the thermodynamic parameters can simply be obtained.

$$\Delta G = \Delta H - T\Delta S \dots\dots\dots \text{I}$$

$$\text{where } \Delta G = -RT \ln K \dots\dots\dots \text{II}$$

therefore

$$-\ln K = \Delta H/RT - \Delta S/R$$

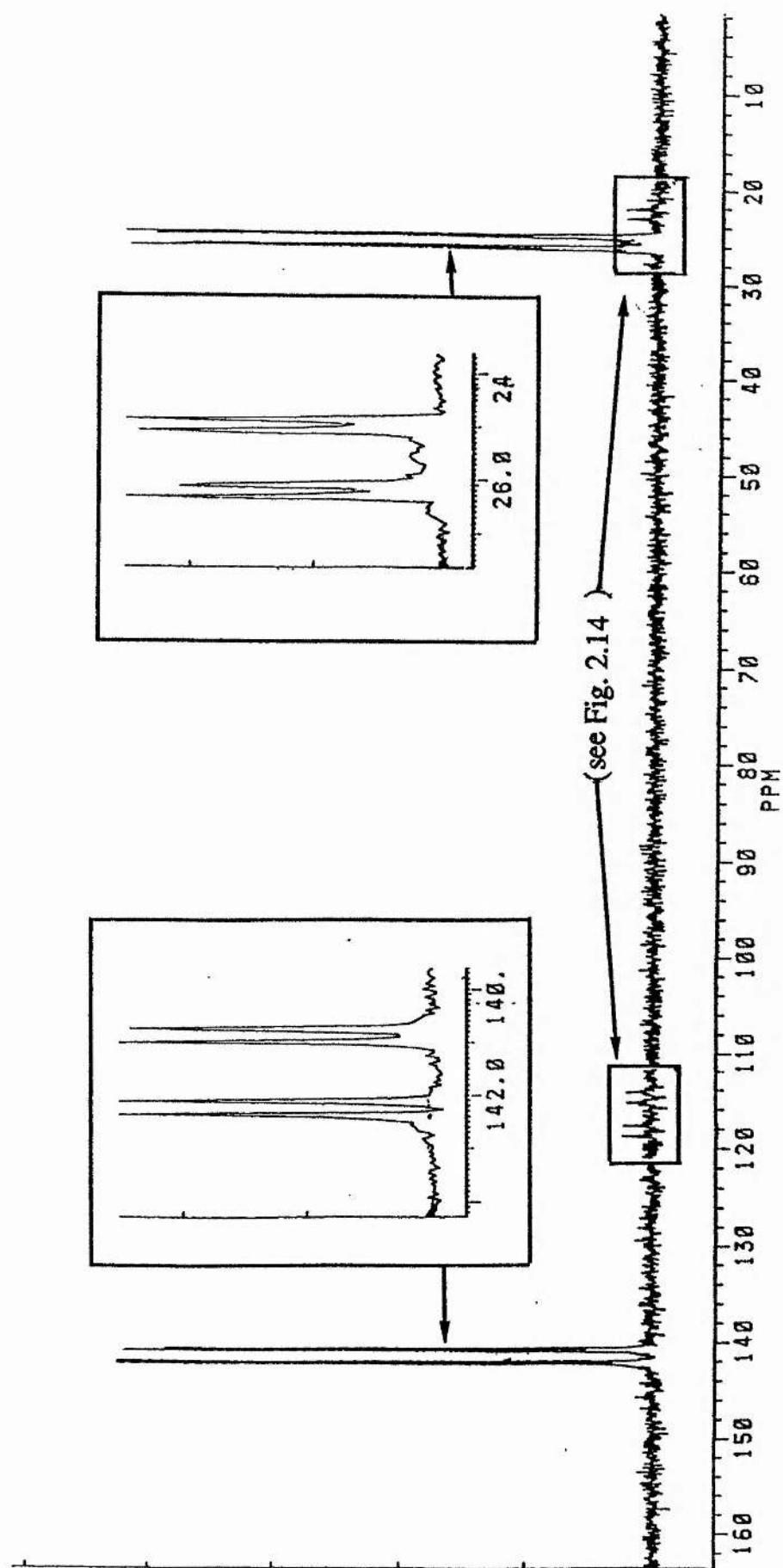


Fig. 2.12 ^{31}P n.m.r. spectrum (300 MHz) of $[\text{Rh}(\text{PPh}_3)(\text{MeHC}=\text{CHO}_2\text{PPh}_2)\text{Cl}]$

$(\text{CD}_2\text{Cl}_2, -25^\circ\text{C})$

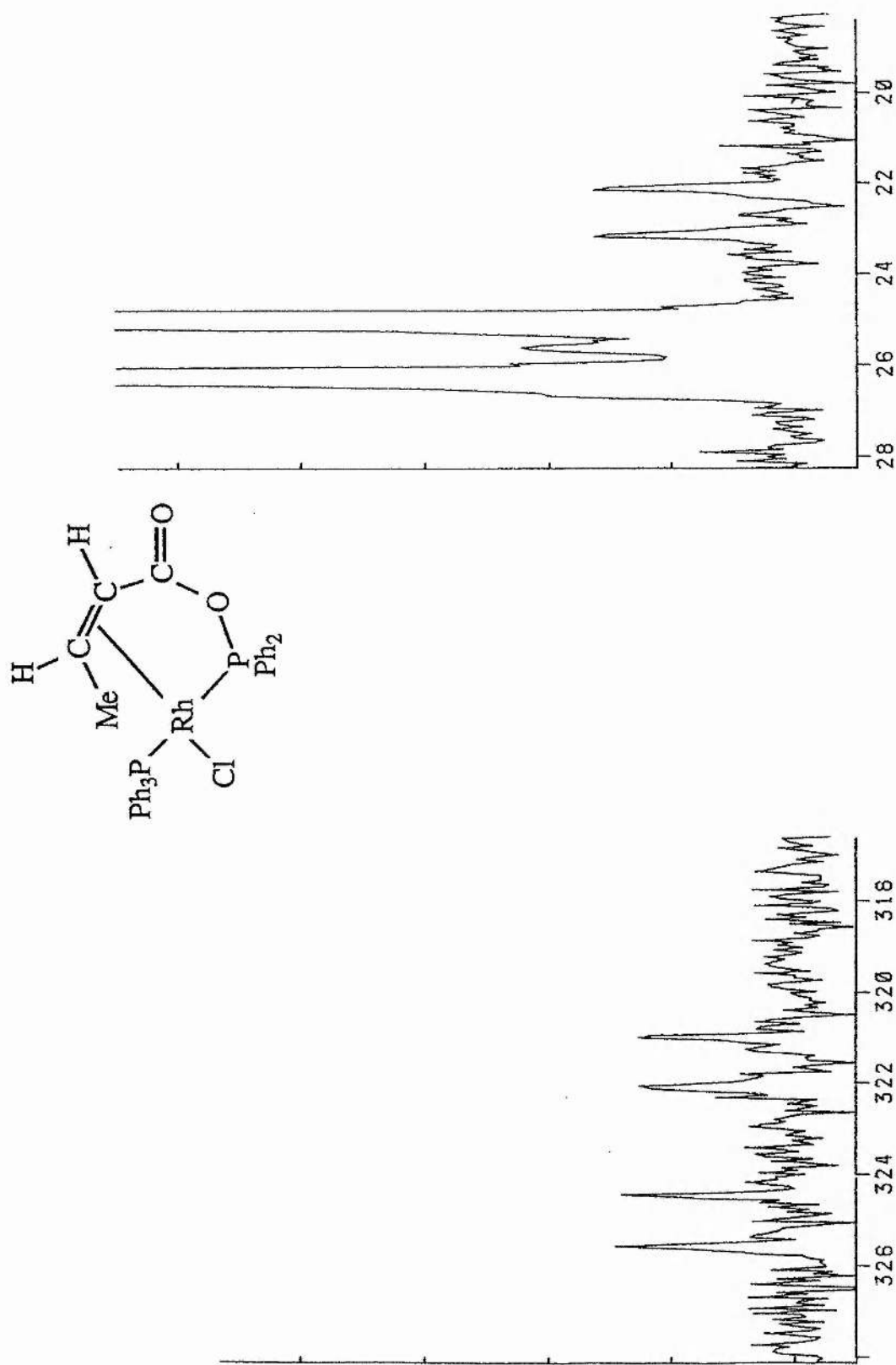


Fig. 2.14 ³¹P n.m.r. spectrum (300 MHz) of [Trans - Rh(PPh₃)(MeHC=CHO₂PPh₂)Cl] (CD₂Cl₂, -25°C)

Thus the slope of the graph is

$$\Delta H/R$$

and the intercept is

$$- \Delta S/R$$

The resulting values are $\Delta G^{\circ}_{298} = 5.3 \text{ KJmol}^{-1}$, $\Delta H^{\circ}_{298} = 3.7 \text{ KJmol}^{-1}$ and $\Delta S^{\circ}_{298} = -5.3 \text{ Jmol}^{-1}\text{K}^{-1}$.

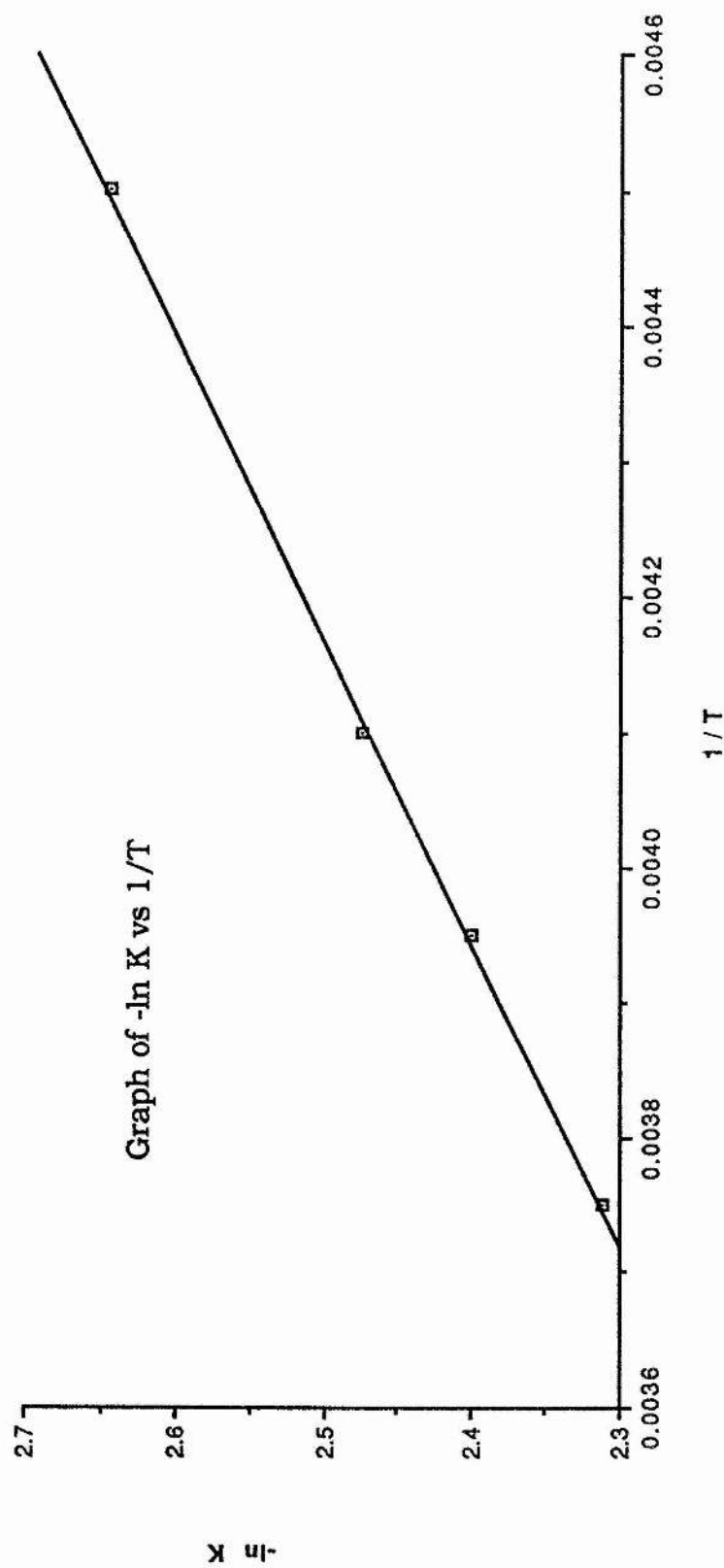
Furthermore if the ratio of the coupling constants, $J(\text{PP}_{cis}) / J(\text{PP}_{trans})$ (1:14), is compared to the ratio of the relative concentrations present at room temperature, *cis* / *trans* (8.5:1) (see Table 2.1), then a low coupling constant ratio would be expected if $J(\text{PP}_{cis})$ and $J(\text{PP}_{trans})$ have opposite signs. This change in sign therefore explains the appearance of the room temperature spectrum.

Table 2.1	% amount in sol ⁿ	Ratio	J _{pp} (Hz)	Ratio
<i>cis</i> [RhCl(PPh ₃)(CAA)]	88	8.5	30	1
Complex 2	12	1	424	14

It thus appears that the fluxionality of the [RhCl(PPh₃)(Ph₂O₂CCH=CHMe)] complex arises from the close potential energy of the *cis* and *trans* forms which in turn is largely determined by steric factors. This is supported by the complex

[RhCl(PPh₃)(Ph₂PO₂CCH=CHCH=CHMe)], which has a similar structure to that of [RhCl(PPh₃)(CAA)] with bonding of the mixed anhydride through the phosphorus atom and the 2 double bonds, and gives a sharp ³¹P spectrum at room temperature⁽¹²⁰⁾. This suggests that the slightly greater steric bulk of the mixed anhydride derived from hexa-2,4- dienoic acid reduces the stereochemical non rigidity of the complex. In order to further test this conclusion the study was extended to investigate the replacement of the chloride ligand in [RhCl(PPh₃)(Ph₂PO₂CCH=CHMe)] with the bulkier anion, O₂CCH=CHMe⁻. The new bulk of the O₂CCH=CHMe⁻ should, by increasing the non-bonded interactions ensure that the *trans* isomer is disfavoured and the fluxionality quenched (see Section 2.5).

The intimate mechanism for the *cis* - *trans* isomerisation is not identifiable directly from the n.m.r. spectra but it may involve decomplexation of the double bond as shown in Figure 2.18. This seems particularly likely since the complex [RhCl(PPh₃)₂(Ph₂PO₂CCH=CMe₂)], containing a mixed anhydride ligand only slightly more sterically congested than Ph₂PO₂CCH=CHMe, exhibits only monodentate coordination of the mixed anhydride, the ligand being bound via the phosphorus alone^(118,119).



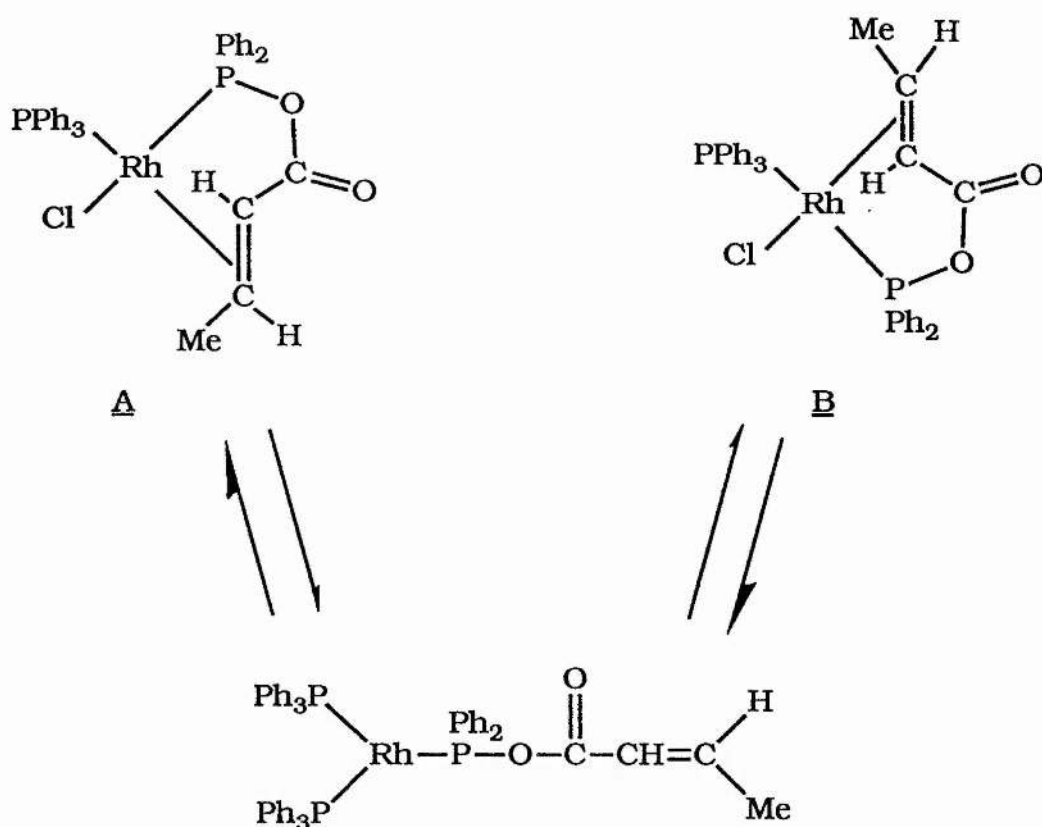


Fig 2.18

2.5 Reaction of Chloro-0-diphenylphosphino-E-but-2-enoate triphenylphosphinerhodium (1) and $[\text{K}^+][\text{O}_2\text{CCH}=\text{CHMe}]$

This reaction was carried out at room temperature and under dinitrogen, a sample of the purified acid salt being added to a mole equivalent of the isolated CAA complex in tetrahydrofuran. The colour of the resultant solution changed slightly from orange to yellow/orange and a microcrystalline solid was obtained by careful addition of cold petroleum (40-60°) to the filtered reaction solution, which had been concentrated to approximately 5-10cm³.

Alternatively the same microcrystalline solid can be isolated by standing the filtered and concentrated reaction solution at -3°C over several days. The compound analyses as $[\text{Rh}(\text{O}_2\text{CCH}=\text{CHMe})(\text{PPh}_3)(\text{Ph}_2\text{PO}_2\text{CCH}=\text{CHMe})]$ and the infra-red, proton and ^{31}P n.m.r. spectra all indicate that the fast exchange observed at room temperature for the chloro complex does not occur. The spectral broadening has been removed and the theoretically expected spectra are obtained at room temperature. The n.m.r. spectra are shown in figures 2.19 and 2.20. It is also noted that even at low temperature there is no evidence of the *trans* complex being present.

2.5.1 Infra-red Data

If this reaction has been successful it would be expected that the infra-red bands for the anhydride bound through the phosphorus atom and the double bond, namely the carbonyl band at 1740cm^{-1} , would be retained, where as the Rh-Cl band would disappear. In addition it would also be expected to observe new bands which correspond to the new butenoate ligand, the most diagnostically important of which are those for the OCO and C=C groups which will also occur in the 1800cm^{-1} - 1500cm^{-1} region. Transition metals and their carboxylate derivatives have been the subject of numerous studies in the past⁽¹³⁷⁻¹⁴⁵⁾ and have, themselves, been found to feature quite extensively in the area of homogeneous catalysis⁽¹⁴⁶⁻¹⁵¹⁾. Complexes of this type have been synthesised by a

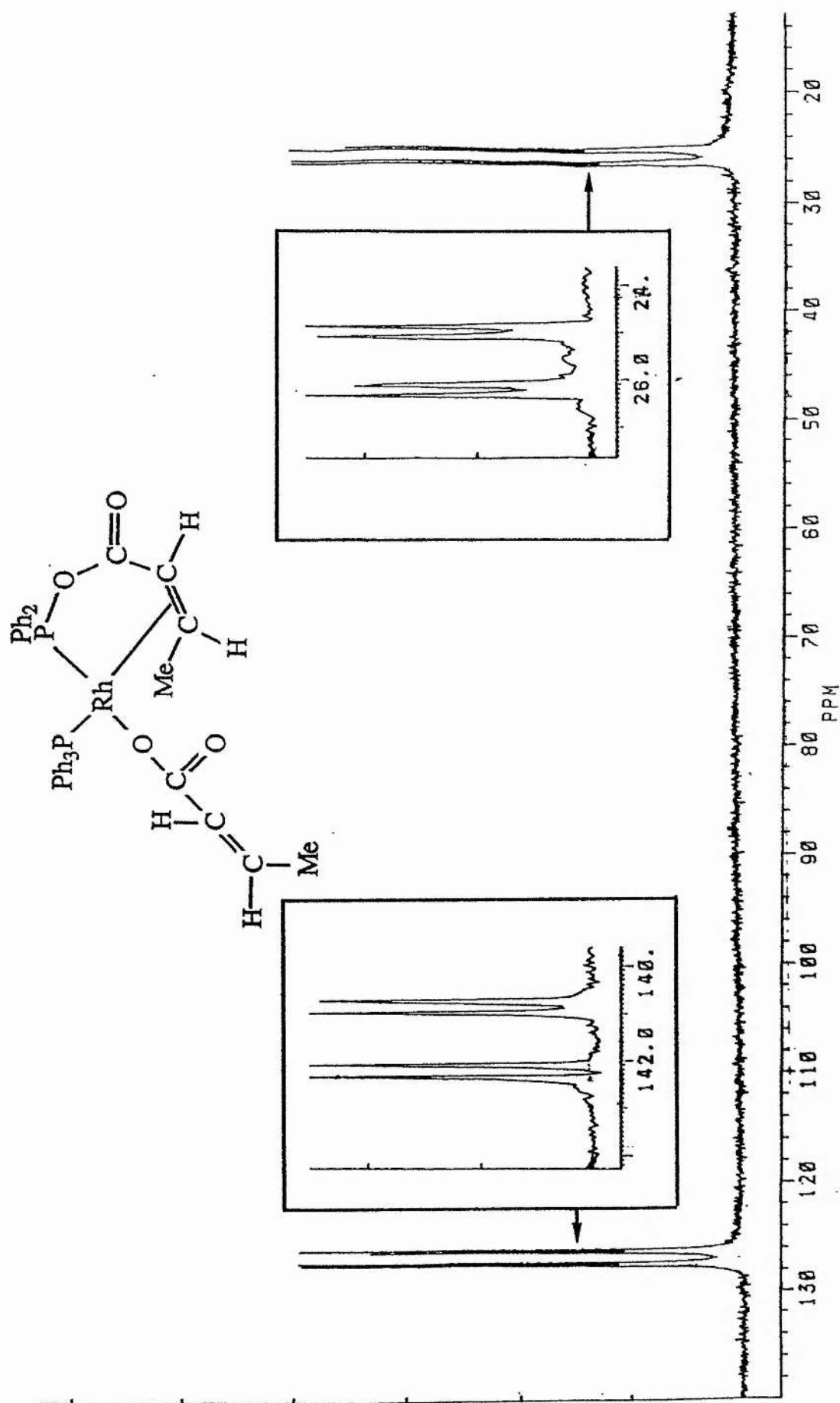


Fig. 2.19 ^{31}P n.m.r. spectrum (300 MHz) of [Cis - $\text{Rh}(\text{PPh}_3)(\text{MeHC}=\text{CHO}_2\text{PPh}_2)(\text{MeHC}=\text{CHO}_2)$] (CD_2Cl_2 , 25°C)

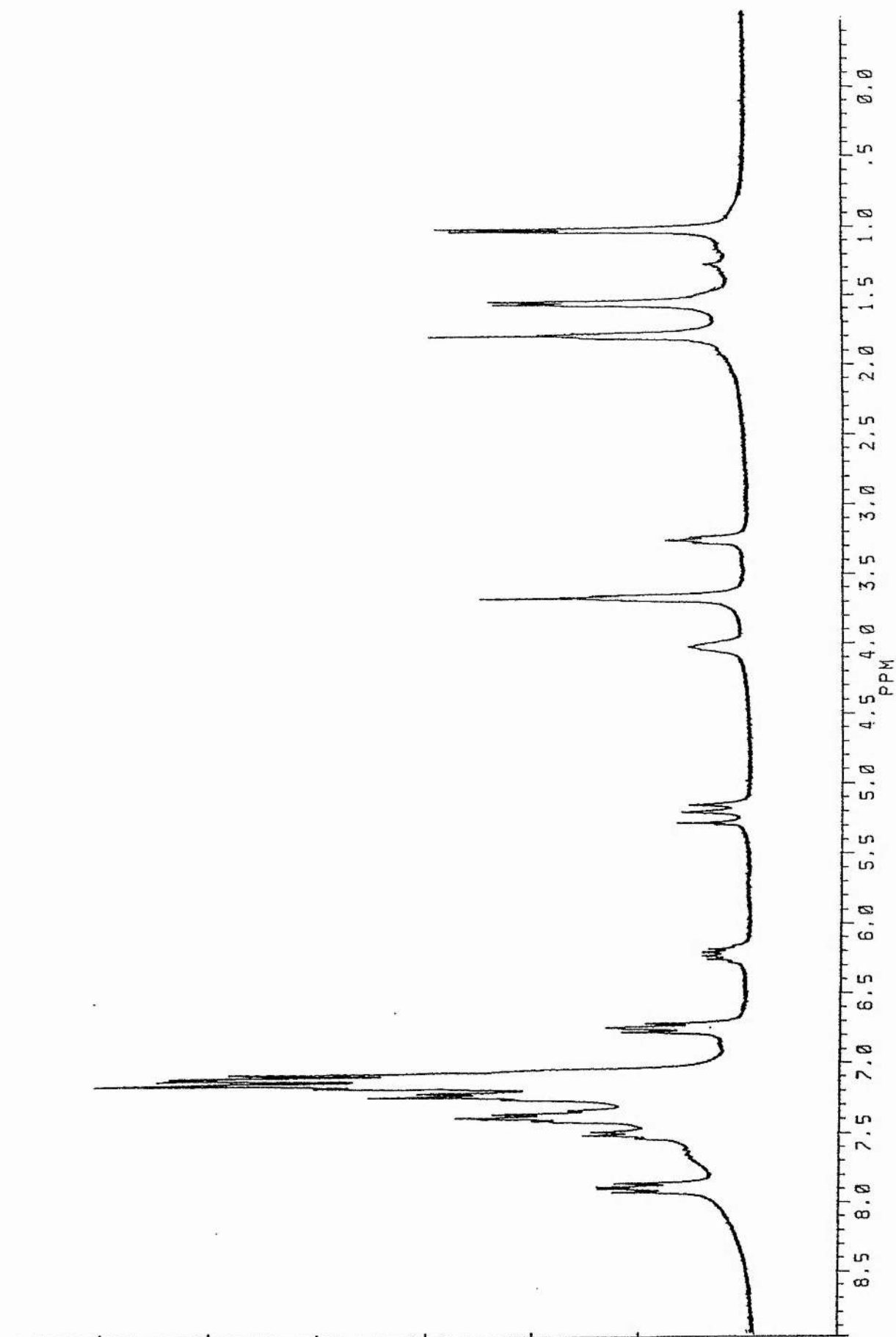
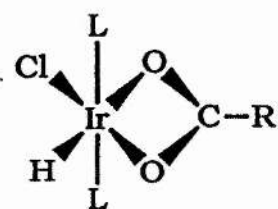
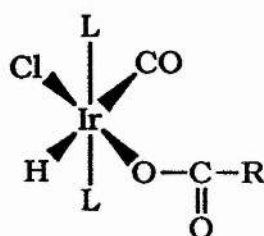


Fig. 2.20 ^1H n.m.r. spectrum (300 MHz) of $[\text{Rh}(\text{PPh}_3)_3](\text{MeHC}=\text{CHO}_2\text{CPh}_2)]$ (CD_2Cl_2 , -25°C)

variety of routes⁽¹⁴⁹⁾, the reaction of platinum metal halide-triphenylphosphine complexes and alkali metal carboxylates being an example of such a route. It has also been observed that the spectral properties of these complexes depend on the particular M-O, C-O and C-C bond strengths, OCO bond angle and the ionic radius of the metal ion present⁽¹⁵³⁾. A number of different coordination modes have been discovered for these carboxylate ligands, unidentate, bidentate and unidentate coordination which is supported by hydrogen bonding have all been observed and are shown in figure 2.21. The active infra-red vibrations associated with the carboxylate group are $\nu(\text{OCO})_{\text{symmetric}}$ and $\nu(\text{OCO})_{\text{antisymmetric}}$, with the values of $\nu(\text{OCO})_{\text{asym}}$ and $[\nu(\text{OCO})_{\text{asym}} - \nu(\text{OCO})_{\text{sym}}]$ found to correlate with the coordination mode present in a particular complex. The highest frequencies by far are recorded for the $\nu(\text{OCO})_{\text{asym}}$ of the unidentate carboxylate and consequently these produce the largest values of $[\nu(\text{OCO})_{\text{asym}} - \nu(\text{OCO})_{\text{sym}}]$ ⁽¹⁵³⁾.



Bidentate



Monodentate

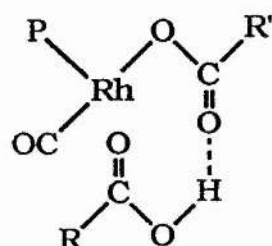
Monodentate with
Hydrogen bonding

Fig. 2.21

For rhodium complexes of the form $[\text{Rh}(\text{O}_2\text{CR})(\text{PPh}_3)_3]$ it has been shown that the asymmetric stretches ($\nu(\text{OCO})_{\text{asym}}$) of the carboxylates are generally found to centre approximately on 1600cm^{-1} ⁽¹⁴⁹⁾ (Table 2.2a) whilst the symmetric stretch ($\nu(\text{OCO})_{\text{sym}}$) is located at a sufficiently low frequency value to give a $\Delta\nu$ (i.e. $\nu_{\text{asym}} - \nu_{\text{sym}}$) of sufficient magnitude to indicate monodentate coordination. The actual frequency of the asymmetric vibration is found to vary slightly in these studies, dependent upon the electronic nature of the R group in addition to those factors already mentioned, Table 2.2b shows that the spread of the $\nu(\text{OCO})_{\text{asym}}$ bands for compounds containing strongly electron withdrawing groups centre 1670cm^{-1} ⁽¹⁴⁹⁾.

The infra-red spectrum of the product from the reaction of $[\text{RhCl}(\text{PPh}_3)(\text{Ph}_2\text{PO}_2\text{CCH}=\text{CHMe})]$ with $\text{MeCH}=\text{CHCO}_2^-$ indicates that the RhCl bond ($\approx 300\text{cm}^{-1}$) is absent but a high frequency carbonyl absorbance is present (1750cm^{-1}). This is assigned to be the carbonyl group of the bidentate anhydride, the absorption has been shifted slightly by coordination of this new ligand, the position in the chloride containing complex being 1740cm^{-1} . This indicates a slight alteration in the anhydrides ring environment upon the coordination of $\text{MeHC}=\text{CHCO}_2$, which is only to be expected as the complex will be slightly disrupted to accommodate the greater steric bulk. Also present in this region of the spectrum are absorptions at 1661cm^{-1} and 1535cm^{-1} . The band at 1661cm^{-1} is

assigned to the $\nu(\text{OCO})_{\text{asym}}$ for the monodentate $\text{O}_2\text{CCH}=\text{CHMe}$ ligand and although this is rather high compared with the values observed for the simple carboxylate (Table 2.2a), it is consistent with the electron withdrawing nature of the vinyl group. Conjugation of the $\text{C}=\text{O}$ with the $\text{C}=\text{C}$ cannot therefore be very important since this would be expected to weaken $\nu(\text{OCO})_{\text{asym}}$ but coordination does appear to lower $\nu(\text{C}=\text{C})$ from 1633cm^{-1} in the free anion to 1535cm^{-1} once the ligand is coordinated.

Table 2.2a I.R. Data On Rhodium Carboxylate Complexes			
Compound	$\nu_{\text{asym}}(\text{OCO})$	$\nu_{\text{sym}}(\text{OCO})$	$\Delta\nu(\nu_{\text{asym}}-\nu_{\text{sym}})$
$\text{Rh}(\text{OCOCH}_3)(\text{PPh}_3)_3$	1601	1370	231
$\text{Rh}(\text{OCOC}_2\text{H}_5)(\text{PPh}_3)_3$	1599	1379	230
$\text{Rh}(\text{OCOC}_5\text{H}_{11})(\text{PPh}_3)_3$	a	1383	---
$\text{Rh}(\text{OCOPh})(\text{PPh}_3)_3$	a	1389	---
$\text{Rh}(\text{OCOC}_3\text{H}_7)(\text{CO})(\text{PPh}_3)_2$	a	a	---
$\text{Rh}(\text{OCOCH}_3)(\text{CO})(\text{PPh}_3)_2$	1608	1377	231
$\text{Rh}(\text{OCOC}_2\text{H}_5)(\text{CO})(\text{PPh}_3)_2$	1607	1382	225
Table 2.2b I.R. Data With R Groups Of Increasing Electron Withdrawing Nature			
$\text{Rh}(\text{OCOCF}_3)(\text{PPh}_3)_2$	1673	1418	255
$\text{Rh}(\text{OCOC}_2\text{F}_5)(\text{PPh}_3)_2$	1685	a	---

a = band obscured

Unfortunately $\Delta\nu(\nu(\text{OCO})_{\text{asym}}-\nu(\text{OCO})_{\text{sym}})$ for this compound could not be calculated because the PPh_3 absorbances obscure the

region where $\nu(\text{OCO})_{\text{sym}}$ is located. The infra-red data however can clearly be seen to support the conclusion that the structure of this product is as shown in Figure 2.22. Furthermore the $\nu(\text{OCO})_{\text{asym}}$ is clearly at a high enough frequency to indicate monodentate coordination of the $\text{MeHC}=\text{CHCO}_2^-$ ligand.

2.5.2 ^1H n.m.r. Data

This data further supports the conclusions drawn from the infra-red spectrum which point toward the structure drawn in Figure 2.22 being correct. The spectrum contains evidence of both the bidentate anhydride and monodentate butenoate. The resonances from the anhydride are found in almost the exact same positions as in the chlorine containing starting material ($\delta 4.09$; $\delta 3.30$ and $\delta 1.6$ ppm) but, as with the infra-red data, show slight shifts due to slight structural changes induced in the bidentate ring to make room for the larger bulk of the butenoate anion. The resonances assigned to the monodentate $\text{MeHC}=\text{CHCO}_2^-$ are found at $\delta 6.22$ ppm, $\delta 5.19$ ppm and $\delta 1.15$ ppm. These positions are shifted from those of the free crotonic acid, namely $\delta 7.08$ ppm, $\delta 5.90$ ppm and $\delta 1.92$ ppm. These shifts can also be explained by a reduction in the bond order of $\text{C}=\text{C}$ due to the electron migration away from the double bond. If the bond order drops, the double bond moves toward becoming a pseudo single bond which will produce the

produce the observed shift to higher field for the C=C substituents.

2.5.3 ^{31}P n.m.r. Data

This spectrum, as already stated, exhibits the theoretically expected resonances for a rhodium complex which contains two different phosphorus containing, rhodium bound ligands. The mixed anhydride ligand is clearly bidentate as the resonance from the P atom is shifted to low field (127 ppm), the second P atom resonates in the characteristic area for a coordinated triphenylphosphine ligand. The two effects of coordinating the MeHC=CHCO_2 anion in the ^{31}P spectrum are that the phosphorus environment of the anhydride exhibits a small change due to structural changes to accommodate the more bulky anion ligand and that this extra bulk quenches the fluxionality as suggested in section 2.4.

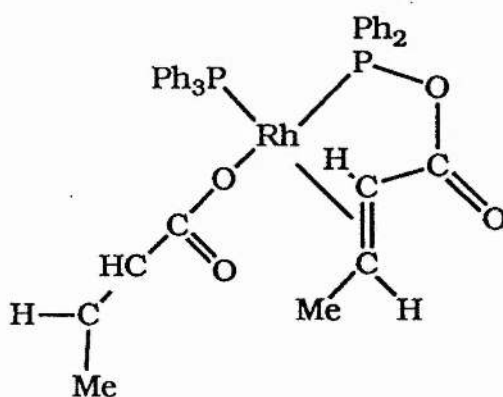


Fig. 2.22

2.6 Reaction of Wilkinson's Catalyst and the Anhydride Derived from Acrylic Acid

In order to study further the effect of steric bulk upon the coordination mode of the mixed anhydrides the reaction of $[\text{RhCl}(\text{PPh}_3)_3]$ and $\text{Ph}_2\text{PO}_2\text{CCH}=\text{CH}_2$, the anhydride derived from acrylic acid, was attempted.

As already stated, the AAA ligand is insufficiently stable to be isolated, so it was prepared by the "in-situ" method and reacted with a stoichiometric quantity of Wilkinson's Catalyst in tetrahydrofuran at ice temperatures. The reaction was monitored at 10 minute intervals by ^{31}P n.m.r. spectroscopy.

2.6.1 Spectral Data from AAA/Wilkinson's Catalyst Reaction

The ^{31}P n.m.r. spectrum obtained after 10 minutes is shown in figure 2.23 and contains a doublet of doublets at 114 ppm and a doublet of doublets at 27 ppm. The ^{31}P data is summarized in table 2.7 and by following the same arguments used in section 2.3 in assigning the spectral characteristics of the CAA complex, the major species present is concluded to be $[\text{Rh}(\text{Ph}_2\text{PO}_2\text{CCH}=\text{CH}_2)\text{Cl}(\text{PPh}_3)]$. The high value of J_{pp} , however, suggests that the major isomer of this compound has mutually *trans* phosphorus atoms. The other phosphorus containing species present are Wilkinson's Catalyst, assigned by the doublet of triplets at 47 ppm and the doublet of doublets at 29.5 ppm and $[\text{Rh}(\text{Ph}_2\text{POPPh}_2)(\text{PPh}_3)\text{Cl}]$, denoted by the multiplets of 107 ppm, 80 ppm and 25 ppm (the resonance at 25

ppm is largely obscured). The production and structure of the latter of these complexes will be discussed in chapter 3. It suffices at this point to state that it is the major complex formed if a 1:2 mole ratio of metal : anhydride rather than a 1:1 mole ratio is used. It has not proved possible to isolate $[\text{Rh}(\text{AAA})\text{Cl}(\text{PPh}_3)]$ from these solutions partly because it is always contaminated with unreacted starting material but also because it appears to decay back to $[\text{RhCl}(\text{PPh}_3)_3]$ on standing (see Figure 2.24). Following the reaction by ^{31}P n.m.r. shows that the resonances from Wilkinson's Catalyst increase until finally it dominates the spectrum and those from $[\text{Rh}(\text{AAA})\text{Cl}(\text{PPh}_3)]$ show that it is only present as a minor product. Other species noted to be present in the final spectrum are $\text{Ph}_2\text{PP}(\text{O})\text{Ph}_2$ and $(\text{C}_6\text{H}_5)_3\text{P}^+(\text{CH}_2)_2\text{CO}_2^-$, the doublet at 36.5 ppm and -22.5 ppm and a singlet at 24.8 ppm respectively. These are both by products known to stem from the free AAA ligand. The initial formation of $[\text{Rh}(\text{AAA})\text{Cl}(\text{PPh}_3)]$ from $[\text{RhCl}(\text{PPh}_3)_3]$ and AAA followed by reversion to $[\text{RhCl}(\text{PPh}_3)_3]$ is surprising but suggests that the replacement of PPh_3 by AAA is reversible and rapid. AAA is removed by formation of $[\text{RhCl}(\text{Ph}_2\text{POPPH}_2)(\text{PPh}_3)]$, $\text{Ph}_2\text{PP}(\text{O})\text{Ph}_2$ and $(\text{Ph}_3)_3\text{P}^+(\text{CH}_2)_2\text{CO}_2^-$, as it has been shown that when in excess PPh_3 will react on a small scale with AAA to produce this zwitterion (see section 2.6.4). Thus the equilibrium is displaced back toward $[\text{RhCl}(\text{PPh}_3)_3]$. The build up of an initial high concentration of $[\text{Rh}(\text{AAA})\text{Cl}(\text{PPh}_3)]$

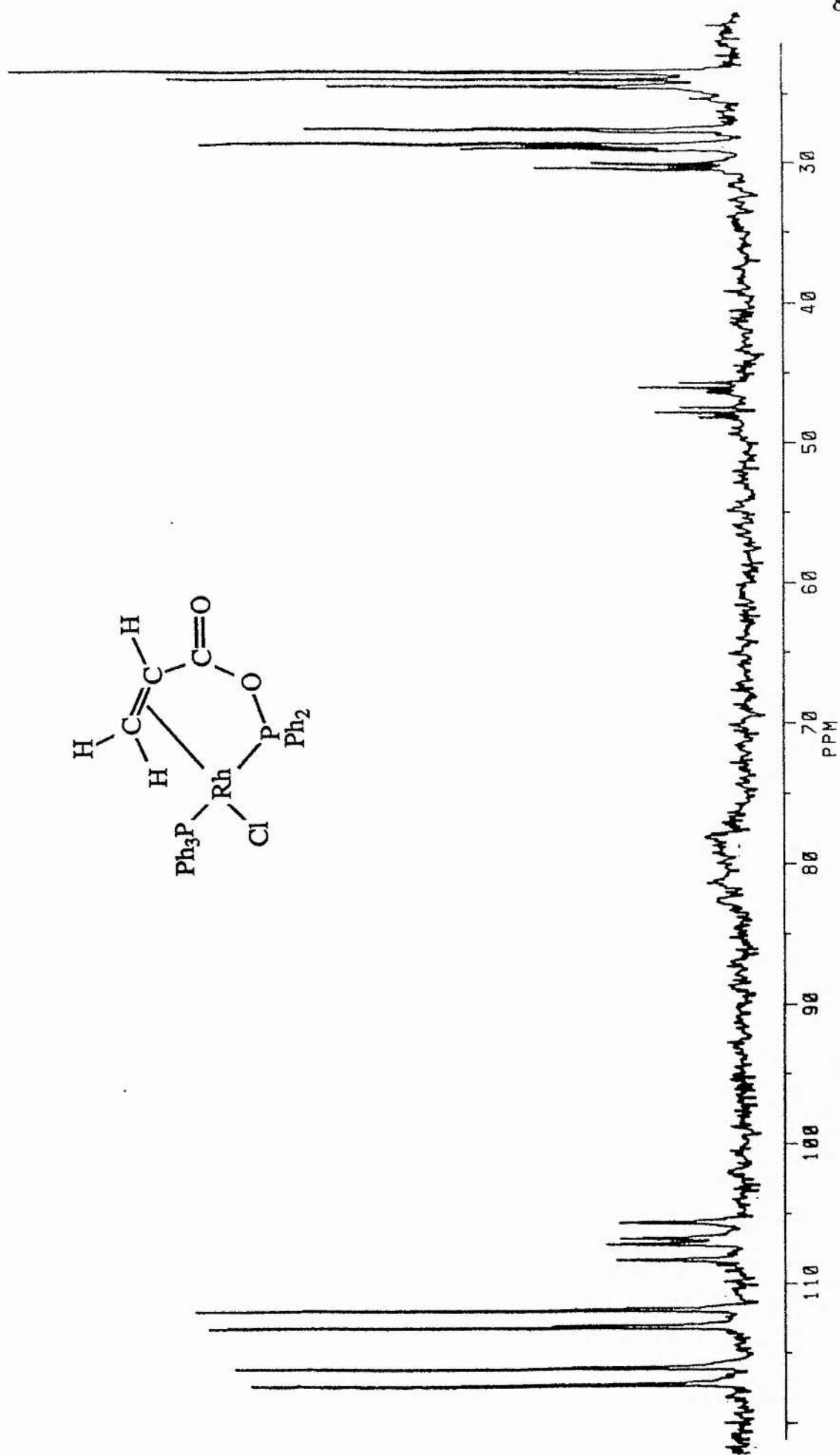


Fig. 2.23 ^{31}P n.m.r. spectrum (300 MHz) of $[\text{Rh}(\text{PPh}_3)(\text{H}_2\text{C}=\text{CHO}_2\text{PPh}_2)\text{Cl}]$

(CD_2Cl_2 , -50°C)

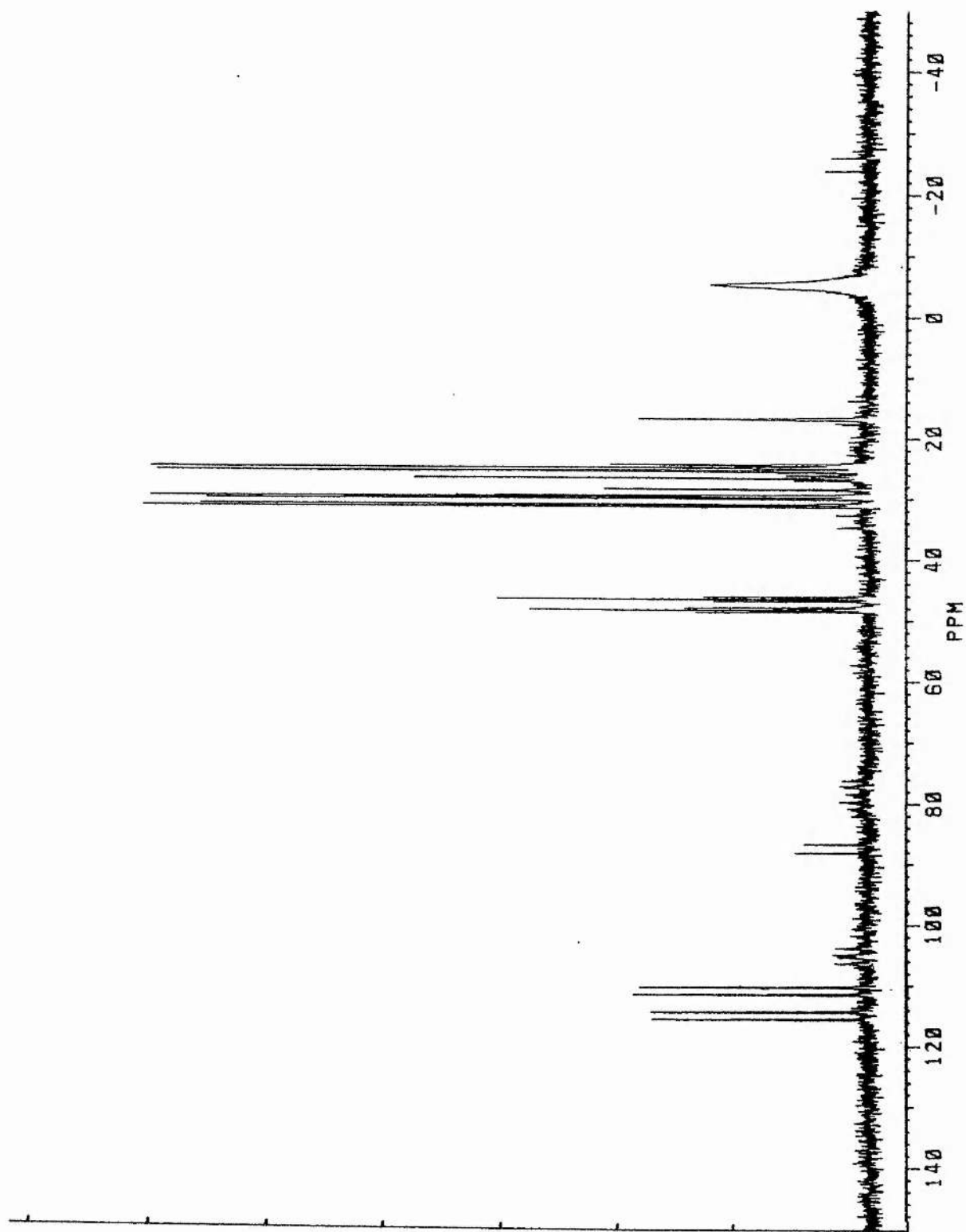


Fig. 2.24 ^{31}P n.m.r. spectrum (300 MHz) of $[\text{RhCl}(\text{Ph}_2\text{PO}_2\text{CCH}=\text{CH}_2)(\text{PPh}_3)]$ after 1 hour

$(\text{CD}_2\text{Cl}_2, -50^\circ\text{C})$

suggests that the reaction of $[\text{RhCl}(\text{PPh}_3)_3]$ with AAA is significantly faster than those that remove AAA. Consistent with this explanation for the appearance and disappearance of $[\text{Rh}(\text{AAA})\text{Cl}(\text{PPh}_3)]$ are spectra taken after prolonged periods. These show that not all the $[\text{RhCl}(\text{AAA})(\text{PPh}_3)]$ disappears, presumably because there is insufficient PPh_3 liberated both to recoordinate to form $[\text{RhCl}(\text{PPh}_3)_3]$ and react with the AAA and $(^-\text{O}_2\text{CCHCH}_2)$ present (see Figure 2.25). $^-\text{O}_2\text{CCHCH}_2$ is thought to be released during the rearrangement to $[\text{RhCl}(\text{Ph}_2\text{POPPH}_2)(\text{PPh}_3)]$.

Products (1) \rightarrow (4) are found in the final ^{31}P spectrum with (1) and (3) present in the largest percentages. The spectral data for the red crystals isolated upon allowing the Wilkinson's Catalyst/AAA reaction solution to stand at -3°C for several days are given in Table 2.3 and contrasted with that of Wilkinson's Catalyst^(154,155) showing that they are identical.

A solid sample though an impure one, of the target bidentate AAA complex can be obtained if the reaction volume is reduced after ≈ 2 -5 minutes and the resulting solution shot into a large volume of petrol which has been cooled (0°C), degassed and placed under dinitrogen. This sample allowed infra-red, proton n.m.r. and mass spectrometry studies to be carried out. Microanalysis results were not obtainable due to the poor purity of the sample. These results summarized in Tables 2.6, 7 and 8, show the presence of the anhydride bound through the phosphorus and

Fig. 2.25

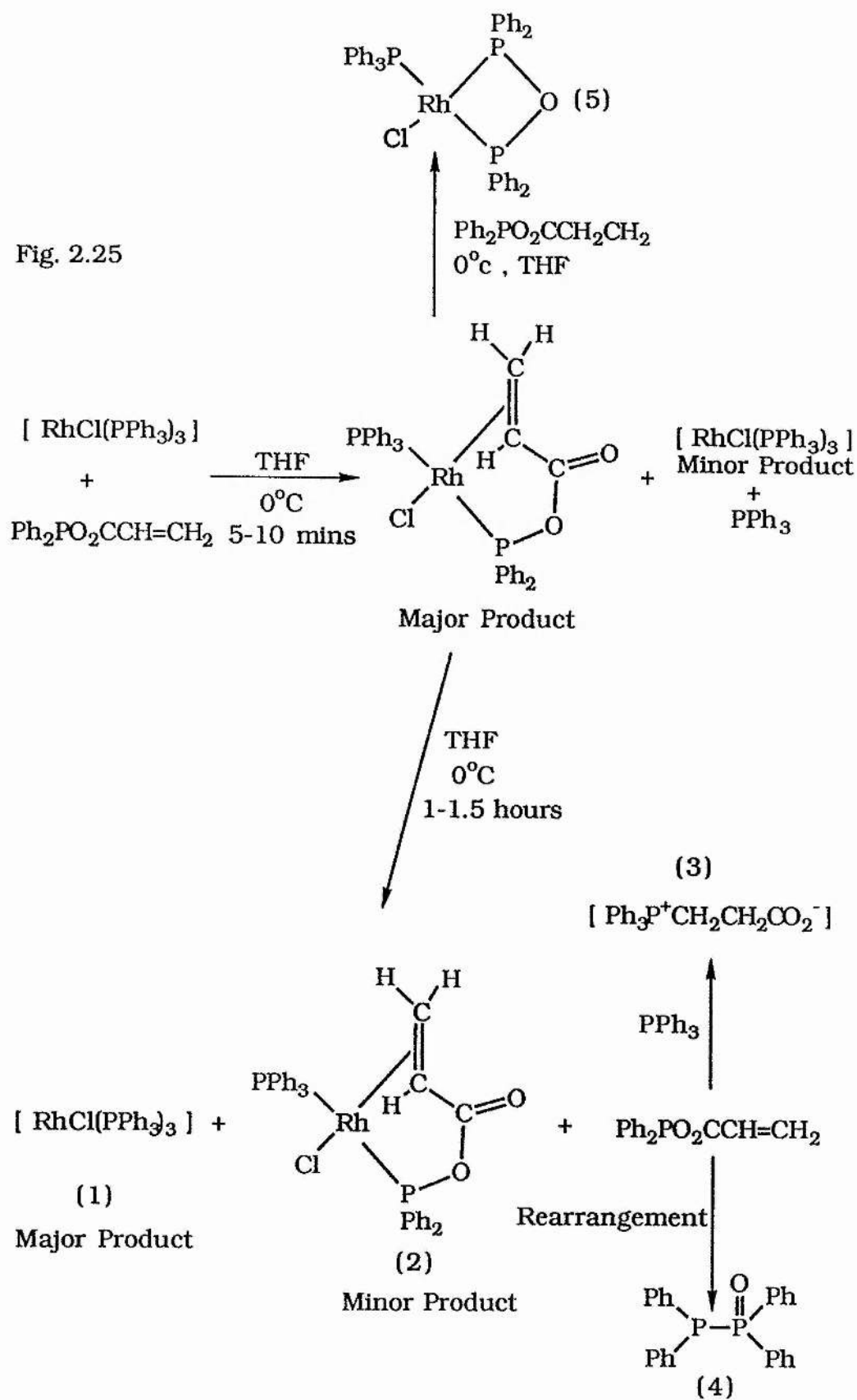
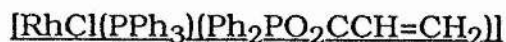


Table 2.3		Spectroscopic Data For [RhCl(PPh ₃) ₃] And WCEST			
Complex	I.R. (cm ⁻¹)	¹ H	³¹ P	F.A.B. (m/z)	
Wilkinson's Catalyst ([Rh(PPh ₃) ₃ Cl])	ν (C=C) = 1550 ν (C-H) = 735 ν (C-H) = 690 ν (Rh-Cl) = 292 No major peaks above 1600	Only ¹ H resonances are those of phenyl groups between δ 6.8 and δ 8.0	Pa 48.4 Pb 31.7 Pb 31.7 J _{Rh-Pa} 190.9 J _{Rh-Pb} 143.0 J _{Rh-Pc} 143.0 J _{Pa-Pb} 39.2 J _{Pa-Pc} 39.5 J _{Pb-Pc} 39.5	[Rh(PPh ₃) ₃] ⁺ 889 [Rh(PPh ₃) ₂] ⁺ 627 [Rh(PPh ₃) (PPh ₂)] ⁺ 889	
WCEST (Red crystals isolated from Wilkinson's Catalyst/AAA 1:1 mole reaction)	ν (C=C) = 1550 ν (C-H) = 735 ν (C-H) = 690 ν (Rh-Cl) = 292 No major peaks above 1600	Only ¹ H resonances are those of phenyl groups between δ 6.8 and δ 8.0	Pa 48.7 Pb 31.7 Pb 31.7 J _{Rh-Pa} 190.2 J _{Rh-Pb} 143.5 J _{Rh-Pc} 143.5 J _{Pa-Pb} 39.6 J _{Pa-Pc} 39.7 J _{Pb-Pc} 39.7	[Rh(PPh ₃) ₃] ⁺ 889 [Rh(PPh ₃) ₂] ⁺ 627 [Rh(PPh ₃) (PPh ₂)] ⁺ 889	

double bond.

2.6.2 Spectroscopic Properties of



As already indicated, the ^{31}P n.m.r. spectrum shows that the AAA ligand is bound through the phosphorus atom and the double bond and that the complex is stereochemically rigid, with the two phosphorus atoms mutually *trans* ($J_{\text{pp}} \approx 400$ Hz). No trace of the *cis* complex is observed and the close similarity of the shifts and coupling constants for *trans* $[\text{Rh}(\text{AAA})\text{Cl}(\text{PPh}_3)]$ and for the minor product in $[\text{Rh}(\text{CAA})\text{Cl}(\text{PPh}_3)]$ lends support to the assignment of the latter as *trans* $[\text{RhCl}(\text{CAA})(\text{PPh}_3)]$.

A final conclusion that can be drawn here is that the Δ_{R} for a *cis* anhydride complex is of the order of 40 ppm and for a *trans* complex is in the region of 15 ppm.

2.6.3 The Reaction of the Mixed Anhydrides with Triphenylphosphine

No reaction between the displaced triphenylphosphine and the free anhydride ligand had been observed prior to this study. However the work already reported in this area had all been concerned with mixed anhydride ligands containing highly substituted alkene species. This statement was confirmed when a reaction between

PPh_3 and $\text{Ph}_2\text{PO}_2\text{CCH}=\text{CMe}_2$ (DAA) was attempted employing the same reaction conditions used for the metal reactions reported in this chapter and found to produce no reaction. Figure 2.26 displays the result of this attempted reaction, the ^{31}P n.m.r. spectrum indicating only two compounds, namely the PPh_3 and $\text{Ph}_2\text{PO}_2\text{CCH}=\text{CMe}_2$. However CAA and AAA were found to react with PPh_3 under these conditions (0°C and in THF solutions), Figure 2.27 shows the products obtained from the reaction of PPh_3 and AAA. The main products are found to be the zwitterion $\text{PPh}_3^+\text{CH}_2\text{CH}_2\text{CO}_2^-$ (24.8 ppm) and $\text{Ph}_2\text{POPPh}_2$ (37 ppm and 22 ppm). There is also an unidentified peak at 16 ppm, which is thought to result from the further reaction of the Ph_2P unit displaced in the production of the zwitterion. There are several pieces of evidence which support the assignment of the zwitterion structure to the 24.8 ppm peak;

1) The ^{31}P n.m.r. results refer to samples run in CD_2Cl_2 , the literature quoted value is 23 ppm⁽¹⁵⁶⁾ in deuteromethanol a similar sample of this product gave a peak at 23.2 ppm in deuteromethanol.

2) The room temperature reaction of PPh_3 and acrylic acid is found to produce the same product as the AAA/ PPh_3 reaction, the ^{31}P n.m.r. of which (Figure 2.28) contains two major species. The first of these is $\text{Ph}_2\text{P(O)PPh}_2$ (doublets at 37.2 and -22.9 ppm) and the latter is in an identical position to the product of the AAA/ PPh_3 reaction (24.8 ppm). A similar reaction by Tsivunin, Zhegalina

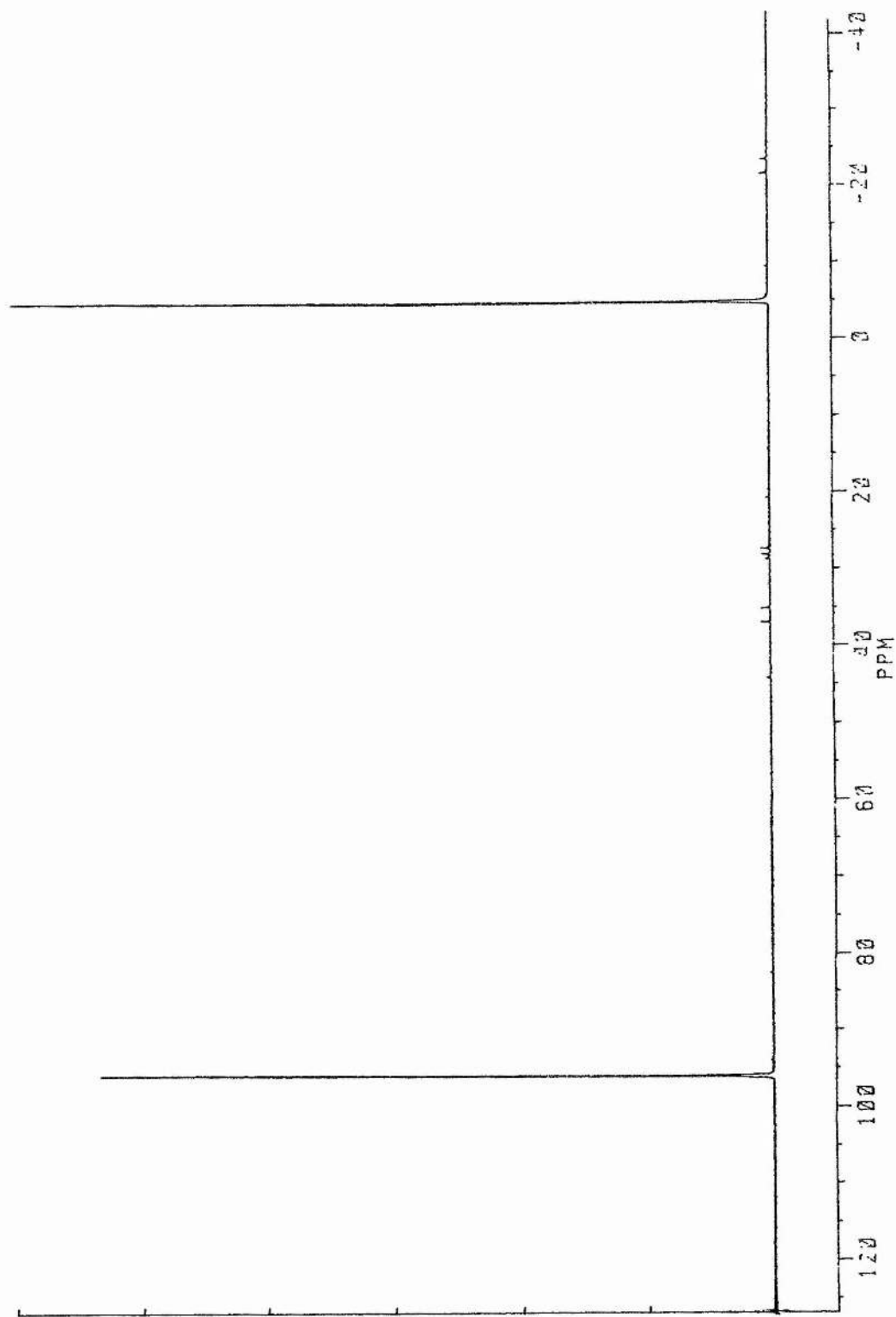


Fig. 2.26 ^{31}P n.m.r. spectrum (300MHz) of the products from reaction of $\text{HOOCCH}=\text{CMe}_2$ and PPh_3 (CD_2Cl_2 , 25°C)

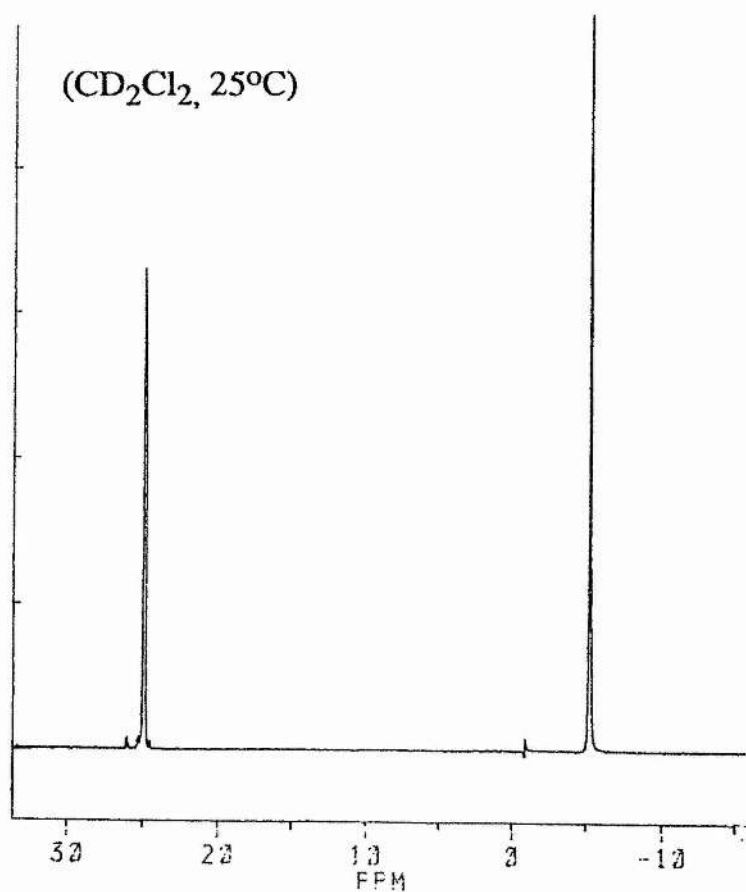


Fig. 2.27 ³¹P n.m.r. spectrum (300MHz) of the products from reaction of HOOCCH=CH₂ and PPh₃

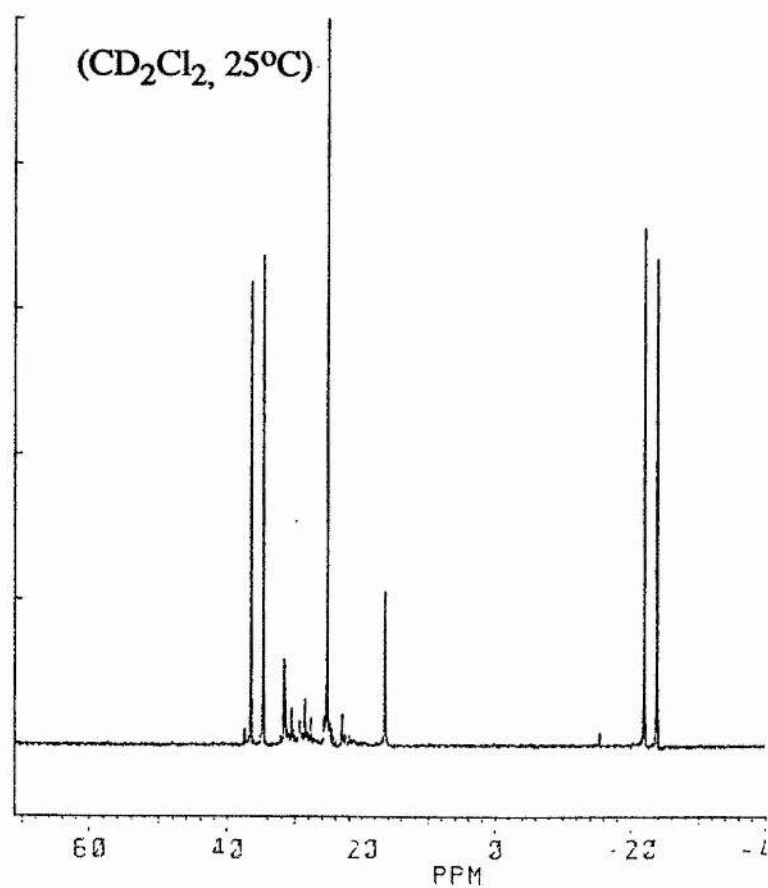


Fig. 2.28 ³¹P n.m.r. spectrum (300MHz) of the products from reaction of Ph₂PO₂CH=CH₂ and PPh₃

and Krutskii has been shown to produce similar zwitterions using, $\text{CH}_2=\text{CHCO}_2\text{H}$ and , $\text{CH}_2=\text{CMeCO}_2\text{H}$ as the parent acids⁽¹⁵⁷⁾.

3) The proton spectrum (Figure 2.29) of this compound contains two non- aromatic resonances at 3.4 and 2.7 ppm which are in a 1:1 ratio. This is consistent with the zwitterion formula quoted above. Furthermore although the proton n.m.r. spectrum for this compound has not been reported the resonances are found to be in similar position to those reported for compounds of the form $\text{PPh}_3^+\text{CHR}(\text{CH}_2)_n\text{CO}_2^-$, where $\text{R} = \text{H}$ and $n = 2$. The resonances are quoted as $\delta 1.72\text{-}2.2$ (m,2H), $\delta 2.7$ (t,2H) and $\delta 3.2\text{-}3.5$ (m,2H).

4) During the metal reactions with both rhodium (Chapter3) and ruthenium (Chapter 5) there is spectral evidence for the coordination of a $\text{PPh}_3\text{CH}_2\text{CH}_2\text{CO}_2^-$ zwitterion. This is supported in the ruthenium case by the F.A.B. mass spectral data results which display peaks consistent with the loss of a zwitterion fragment (m/z 334). Coordination of this zwitterion has been observed with tin as the metal centre⁽¹⁵⁸⁾. This work states that although there has been some controversy over the structure of the zwitterion, the possible structures being,

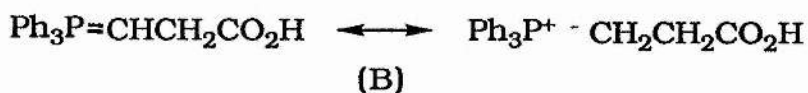
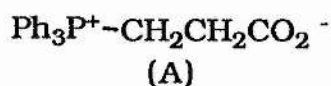


Fig. 2.30

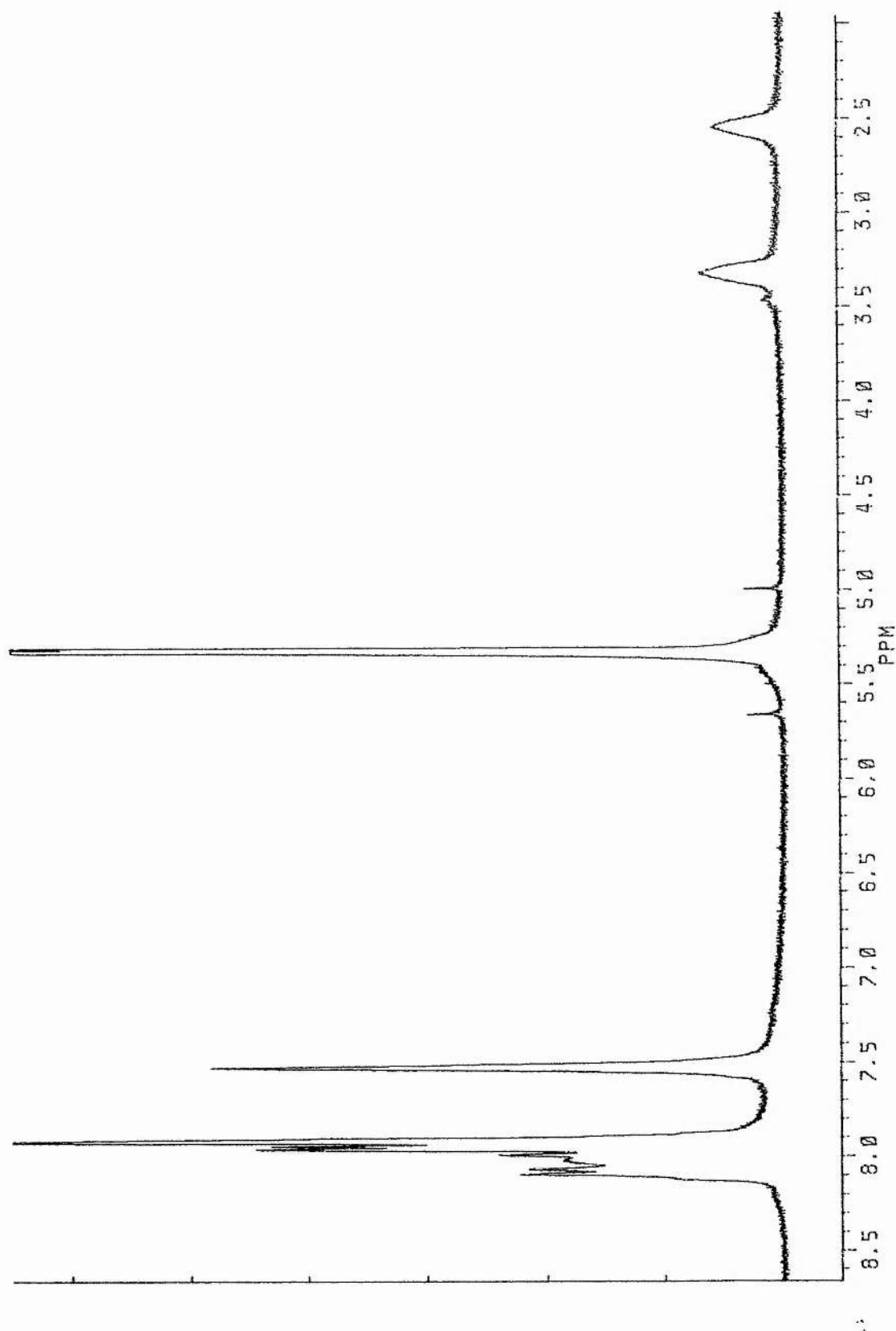


Fig. 2.29 ¹H n.m.r. spectrum (300MHz) of the ³¹P δ24.8 ppm product from reaction of Ph₂POCCH=CH₂ and PPh₃

their results indicate that the correct form is structure A leading to the formation of tin oxygen bonds. This work has also provided infrared data on the $\nu(\text{OCO})_{\text{asym}}$ bands of these compounds. Data which proved to be identical to that of the AAA/PPh_3 product.

Similar results have been obtained with the CAA ligand and in the reaction of the crotonic acid and PPh_3 , the ^{31}P resonance of the resultant zwitterion, $\text{PPh}_3\text{CH}^+(\text{CH}_3)\text{CH}_2\text{CO}_2^-$, being located at 30.1 ppm. This compound has also been discovered to act as a ligand in the ruthenium work reported in chapter 5.

2.7 Structural Trends of the Bidentate Anhydride Complexes of Wilkinson's Catalyst and Computer Studies on the Crotonic and Acrylic Acid Derivatives

From the results described in the previous sections the geometry of the complex appears to depend on the steric bulk around the double bond (Table 2.4). If structural preference depends upon the steric interaction of the ligands it, in turn, depends upon the non-bonded distances at areas A, B, A' and B' shown in Figure 2.31. The interactions at areas A and A' will dominate the choice of structure due to the far greater bulk of the triphenylphosphine ligand compared to that of the chlorine.

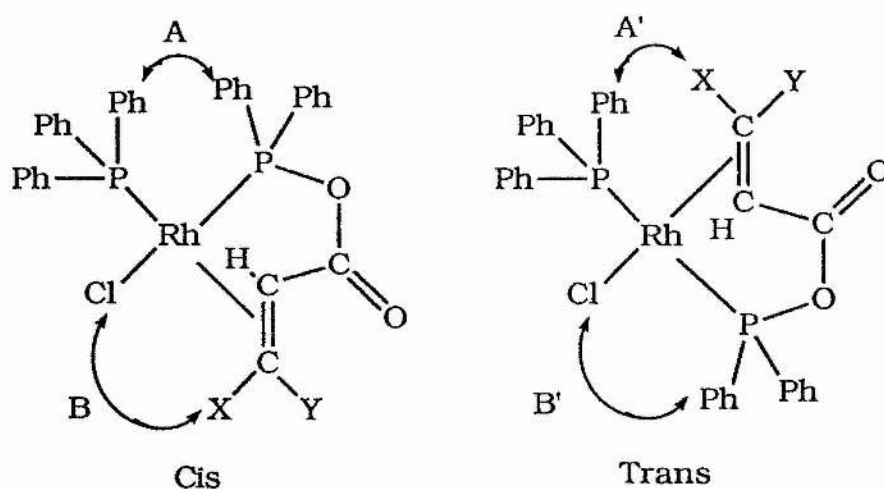


Fig. 2.31

Table 2.4	Structural Trends In The Bidentate Anhydride / Wilkinson's Catalyst Complexes	
Substitution Of Double Bonds	Coordination Geometry	
Trisubstituted or Greater	Monodentate anhydride coordinate	
Disubstituted where the substituents are of greater steric bulk than a methyl group	Bidentate anhydride coordination to produce a <i>cis</i> complex	
Disubstitution where one substituent is a methyl group	Bidentate anhydride coordination to produce a mixture of <i>cis</i> and <i>trans</i> complexes	
Monosubstituted	Bidentate anhydride binding to produce a <i>trans</i> complex	

For the Case of a Methyl or Larger Substituent

It has been shown during this chapter that the preferred conformer for this complex is the *cis* isomer, so it can be concluded that the steric interactions at areas A and A' favour this structure. This choice of structure hinges on the observation, from the crystal data on the CAA complex, that the methyl substituent points toward the chlorine ligand in the *cis* case or the triphenylphosphine in the *trans* case. In the *cis* structure the steric strain can be reduced by:

- i) free rotation around the P-Metal bond of the triphenyl phosphine ligand enabling it to assume the minimum energetic position.
- ii) bending the phenyl groups of the anhydride away from the triphenylphosphine.

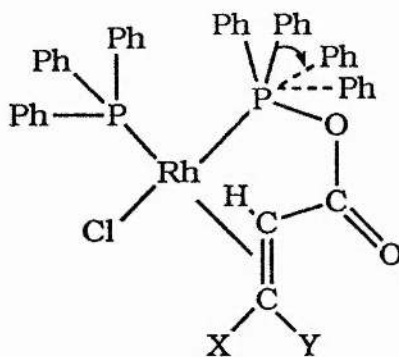


Fig. 2.32

The *trans* isomer can do less to relieve the interaction at A' as the methyl substituent remains rigidly fixed pointing toward the PPh_3 . Thus the *cis* conformer will be energetically more favourable for a substituent of the steric bulk of a methyl group or larger.

For Hydrogen Substituents

The small amount of *trans* isomer present in solutions of $[\text{RhCl}(\text{PPh}_3)(\text{Ph}_2\text{PO}_2\text{CCHCHMe})]$ shows that the arguments used above breakdown as the steric bulk of the monosubstituent is reduced below that of a methyl group. For the mixed anhydride of acrylic acid there is no substituent of large bulk on the double bond pointing toward the PPh_3 group in the *trans* isomer and the steric interactions are minimised by having the phenyl rings of the PPh_2 moiety away from those of the PPh_3 .

2.7.1 Chem-X Computer Study⁽¹⁵⁹⁾

The above reasoning was confirmed by a Chem-X computer study which used as its data the x-ray data set collected on the CAA complex and calculated the non-bonded interactions between the ligand species. The initial calculations carried out on the *cis* form of the CAA complex showed complete agreement between the calculated Chem-X values and those already documented by the x-ray crystallographic solution⁽¹²⁰⁾. Thus having been shown to provide reliable calculated values for the non-bonded interactions, the *trans* CAA isomer and the *cis* and *trans* isomers of the AAA complex were constructed and the non-bonded interactions calculated. These results are summarized in Table 2.5. Study of them immediately

supports the initial assumption that the areas A and A' are the most congested and thus will dictate isomeric selection.

2.7.2 AAA Complex Conclusions

From these observations it can be concluded that the *trans* isomer

Table 2.5	Non -bonded Interactions					
Complex	Ph ^a -Ph ^b	Ph ^a -Me	Ph ^a -H ^c	Cl-Me	Cl-H ^c	Cl-P
cis [RhCl(PPh ₃)(CAA)]	2.379	---	---	2.658	---	---
cis [RhCl(PPh ₃)(AAA)]	2.379	---	---	---	3.440	---
trans [RhCl(PPh ₃)(CAA)]	----	2.350	---	---	----	2.787
trans [RhCl(PPh ₃)(AAA)]	----	----	2.350	---	----	2.787

^a Hydrogen atom on the closest phenyl group of PPh₃

^b Hydrogen atom on the closest phenyl group of PPh₂ moiety

^c Alkene hydrogen substituent

will be the favoured conformer as although the double bond's substituent is closer to the PPh₃ when *trans* than to the chlorine when *cis*, the determining factor for structural preference, namely the overall closest approach, has been increased from 2.379Å to 2.517Å.

2.7.3 CAA Complex Conclusions

The CAA results for the CAA complex are not so well defined. It is clear from initial inspection of the interligand distances that

there is a case for the *cis* conformer being the preferred isomer. However there is only a small difference (0.03\AA) between the closest approaches of the *cis* and *trans* isomers when compared to the AAA case where the difference in closest approaches is 0.138\AA (a value approximately five times greater). Thus it would only require a small energy input to push the complex from *cis* to *trans*, energy which could be supplied at room temperature. The energy barrier for the similar transition of the AAA complex will be far greater and so no fluxionality would be expected.

This result also shows that a small (0.1\AA) increase in the CAA closest approach would be required to ensure that the *cis* isomer is the sole product in the solution. It can easily be concluded that a ligand of the relative bulk of the 2-butenic acid anion will be able to match if not exceed such an increase upon complexation and so completely discourage *trans* formation.

2.8 Reaction of Wilkinson's Catalyst and the Anhydride Derived from Vinylacetic Acid

The reaction was attempted for two reasons, firstly to try and suppress the triphenylphosphine exchange reaction observed with the AAA ligand to obtain a π coordinated monosubstituted mono olefin and secondly to extend the data on Wilkinson's Catalyst/Anhydride complexes to add further weight to the sterically based theory of structural choice.

In situ ^{31}P n.m.r. studies of $\text{Ph}_2\text{PO}_2\text{CCH}_2\text{CH}=\text{CH}_2$ showed

that, as with AAA it was over 97% pure. It too was found to rearrange to tetraphenyldiphosphine monoxide over a period of days as already observed with the acrylic acid anhydride.

A reaction with Wilkinson's Catalyst (molar ratio 1:1) carried out using the *in-situ* method developed for the acrylic acid anhydride led to the isolation of crystals found to contain, not the vinylacetic anhydride bound through the phosphorus atom and double bond as expected, but the crotonic acid anhydride bound in this fashion. Thus it is shown that upon coordination to the rhodium centre, the vinylacetic ligand (known as VAA from this point) undergoes a metal promoted double bond migration resulting in the isolation of crystalline $[\text{Rh}(\text{Ph}_2\text{PO}_2\text{CCH}=\text{CHMe})(\text{PPh}_3)\text{Cl}]$ as shown in Figure 2.28. Also found present in the crystalline product is a quantity of the $[\text{Rh}(\text{Ph}_2\text{POPPh}_2)\text{Cl}(\text{PPh}_3)]$ containing the 4 membered RhPOP ring, the formation of which will be discussed in chapter 3. Here it is a byproduct contaminating the major product and so can easily be removed by washing with cold tetrahydrofuran.

Similar double bond migrations have been noted for phosphorus containing compounds of similar structure by J. Hartwell and co-workers. They have shown ligands of the form $\text{Ph}_2\text{P}(\text{CH}_2)_n\text{CR}=\text{CR}'\text{R}''$ to be stable compounds which when complexed with $\text{Rh}_2\text{Cl}_2(\text{CO})_4$ are found to produce complexes of the form $[\text{RhCl}(\text{CO})(\text{Ph}_2\text{P}(\text{CH}_2)_n\text{CR}=\text{CR}'\text{R}'')_2]$ where the phosphorus containing ligand is bound through the phosphorus and the double

bond⁽¹⁶⁰⁾. Those of interest here are those of the general formula $\text{RhCl}(\text{CO})(\text{Ph}_2\text{P}(\text{CH}_2)_n\text{CH}=\text{CH}_2)_2$ where $n = 0, 1, 2$ and 3 . The last in the sequence, where $n=3$, is found upon refluxing in methanol or

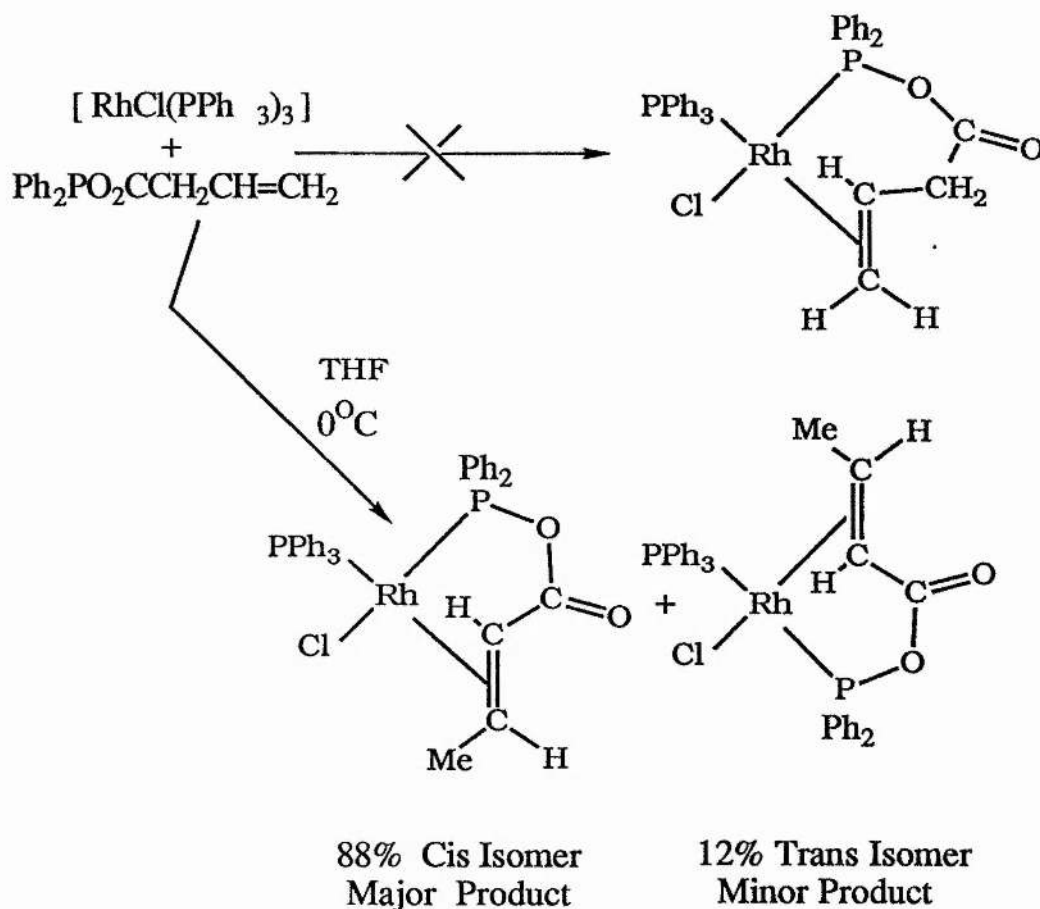


Fig. 2.33

benzene for about 5 hours to isomerize to $[\text{RhCl}(\text{CO})\text{Ph}_2\text{P}(\text{CH}_2)_2\text{CH}=\text{CHMe}]$ in which the olefin has a *cis* configuration. However the nearest analogue to the vinylacetic mixed anhydride, where $n=2$, only produced a mixture of compounds even after refluxing for 88 hours. (A point worthy of note is that the VAA isomerisation occurs at low temperature (0°C) whilst previously these types of isomerizations have involved harsh

conditions.) Other such isomerisms have also been found in the preparation of tetracarbonyl [diphenyl-2-(prop-cis-1-enyl)molybdenum(0)]^(90,91) and in the preparation of $[\text{Rh}(\eta^6\text{-C}_6\text{H}_5\text{BPh}_3)(\eta^2\text{-PPh}_2(\text{CH}_2\text{CH}_2\text{CH}=\text{CHCH}_3))]$ ⁽¹⁶¹⁾ (see chapter 1).

2.8.1 Mechanism of Double Bond Migration

Such isomerisations are proposed to proceed via a π allyl-hydride intermediate. An example of such a mechanism which is perhaps most easily shown is that of dienetricarbonyl complexes. In many attempts at the production and isolation of such complexes, involving the use of iron pentacarbonyl and high temperatures, rearrangement of the diene was found to be extensive. The mechanism proposed and more recently modified by Nelson and Sloan to account for the reaction being kinetically rather than thermodynamically controlled suggest the reaction goes via the mechanism shown in Figure 2.34^(162,163), the π allyl metal hydride intermediate formed with the loss of carbon monoxide. Other related examples have been reported by Casey and Cyr, an example being their study of 3-ethyl-1-pentene and its 3-deutero analog⁽¹⁶⁴⁾. Thus it is thought likely that the isomerism of VAA takes place via a similar mechanism (Figure 2.35). The observation that this isomerisation occurs at low temperature may therefore suggest that the presence of the carboxylate (CO_2) creates an electronic situation which favours the formation of the π allyl hydride intermediate.

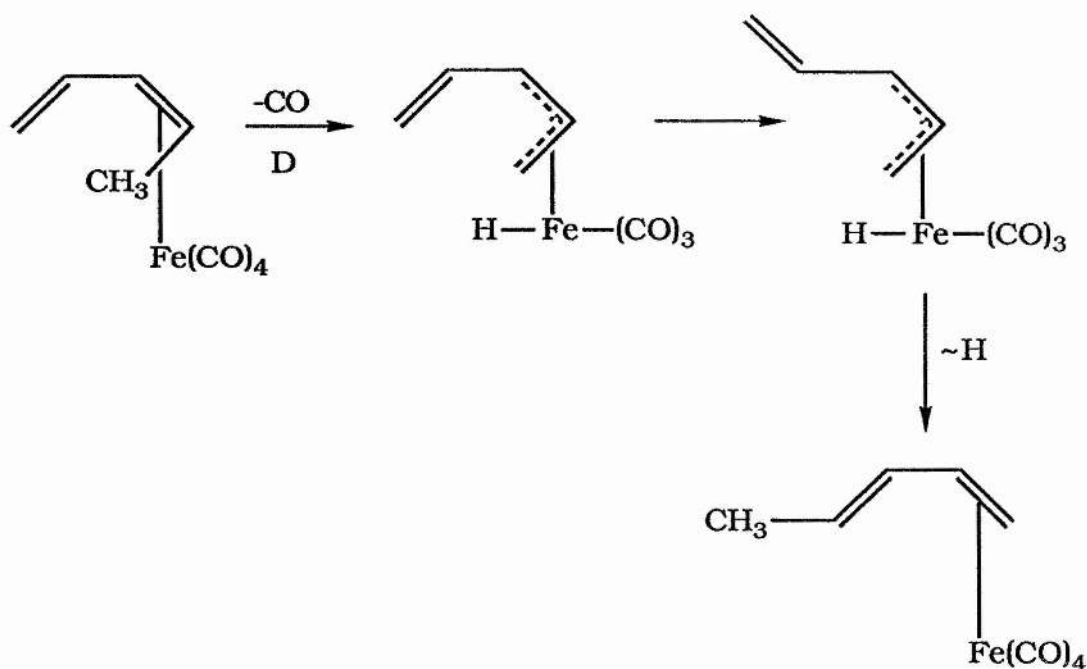


Fig. 2.34

2.9 Catalytic Studies Involving $[\text{RhCl}(\text{CAA})(\text{PPh}_3)]$

The double bond migration observed upon complexation of $\text{Ph}_2\text{PO}_2\text{CH}_2\text{CH}=\text{CH}_2$ suggested possible catalytic activity of the $[\text{RhCl}(\text{CAA})(\text{PPh}_3)]$ complex. Thus catalytic reactions were attempted at room temperature and ambient pressure using the title complex as the catalyst with vinylacetic acid, oleic acid and hexa-4-enoic acid. The reactions were carried out using the following procedure. The complex was dissolved in tetrahydrofuran, along with a ten fold excess of the acidic substrate and a quantity of potassium hydroxide as co-catalyst. These solutions were stirred at room temperature and ambient pressure for varying time periods, after which the reaction solutions were evaporated to dryness and worked up using the procedure outlined in the experimental section and studied using ^1H n.m.r. techniques.

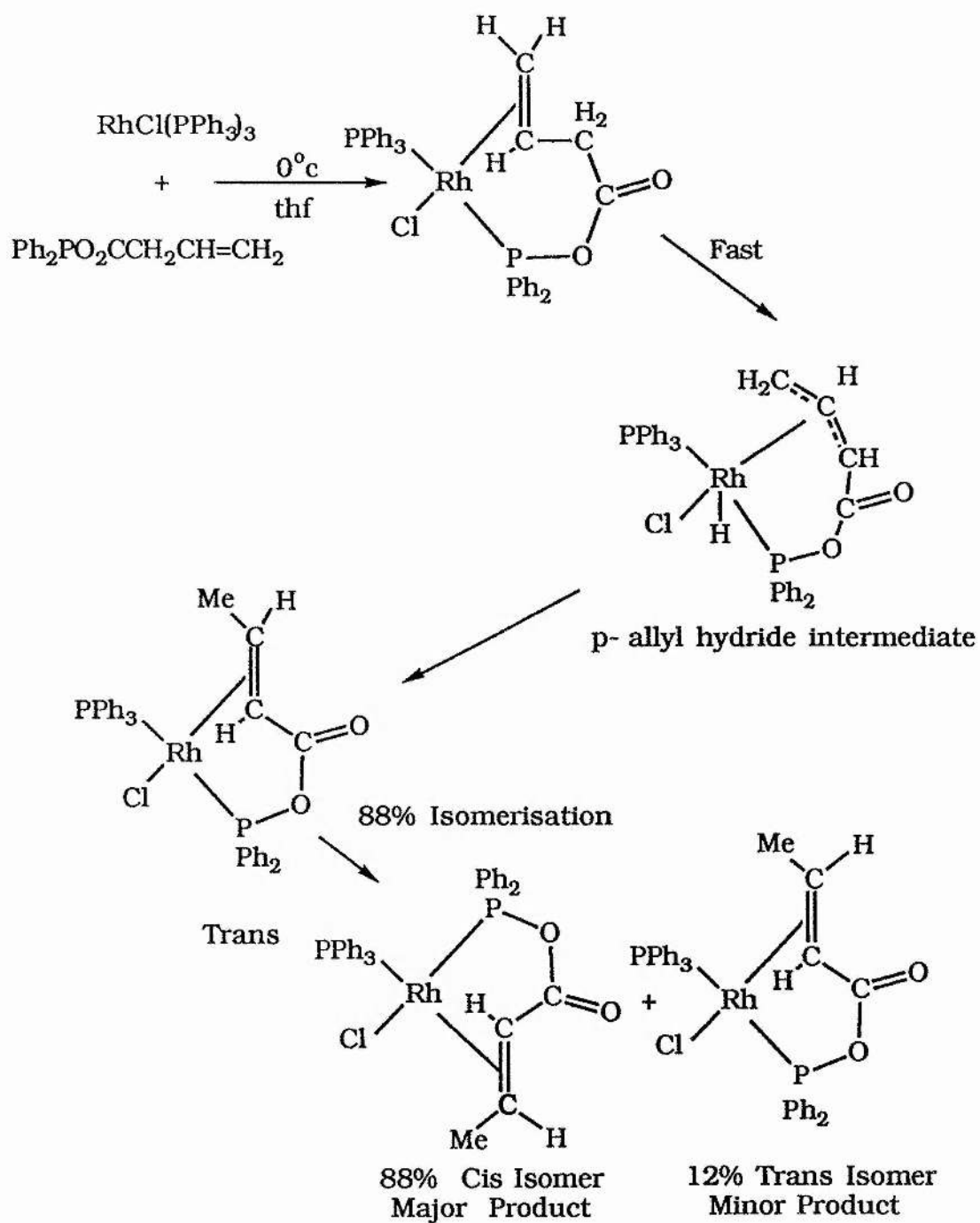


Fig. 2.35

2.9.1 Results Of Catalytic Studies

These reactions were observed to produce a quantity of crotonic acid ; however over the varying time periods used the relative quantity of the crotonic acid observed in the product is approximately 10% of the total product. This amount of crotonic acid would be expected from a stoichiometric rather than a catalytic reaction. Thus it was concluded that at ambient temperatures and pressures reactions of $[\text{RhCl}(\text{CAA})(\text{PPh}_3)]$ and the acids listed above (all of which contain a double bond in the three position) are stoichiometric rather than catalytic.

Table 2.6	I.R. Spectral Data for The Mixed Anhydrides And The Related Metal Complexes	I.R.			
		$\nu(\text{C=O})$	$\nu(\text{C=C})$	$\nu(\text{P-O})$	$\nu(\text{Rh-Cl})$
MeCHCHCO ₂ PPh ₂		1705sst	1645s	736s	
CH ₂ CHCO ₂ PPh ₂		Not Obtainable			
CH ₂ CHCH ₂ CO ₂ PPh ₂		Not Obtainable			
RhCl(PPh ₃)(Ph ₂ PO ₂ CCH=CHMe)		1744	-----		282
(cis) RhCl(PPh ₃)(Ph ₂ PO ₂ CCH=CHMe)		.	.	.	"
(trans)RhCl(PPh ₃)(Ph ₂ PO ₂ CCH=CHMe)		.	"	.	"
(trans)RhCl(PPh ₃)(Ph ₂ PO ₂ CCH=CH ₂)		1740	-----		290
(cis) RhCl(L ₁)(L ₂)(O ₂ CCH=CHMe) ^f		1744, 1661	1535		282

^f L₁ = PPh₃ L₂ = (Ph₂PO₂CCH=CHMe)

Table 2.7		³¹ P Spectral Data for The Mixed Anhydrides And The Related Metal Complexes					
Compound		Chemical Shift (ppm)		Coupling Constants(Hz)			
		Pa	Pb	RhPa	RhPb	PaPb	
MeCHCHCO ₂ PPh ₂		98.9s	-----	-----	-----	-----	
CH ₂ CHCO ₂ PPh ₂		100.1s	-----	-----	-----	-----	
CH ₂ CHCH ₂ CO ₂ PPh ₂		100.5s	-----	-----	-----	-----	
RhCl(PPh ₃)(Ph ₂ PO ₂ CCH=CHMe)		140br	25.5d	-----	147	-----	
(cis) RhCl(PPh ₃)(Ph ₂ PO ₂ CCH=CHMe)*		142dd	25.6dd	164	153	30	
(trans)RhCl(PPh ₃)(Ph ₂ PO ₂ CCH=CHMe)*		116.5dd	24.3dd	133	122	424	
(trans)RhCl(PPh ₃)(Ph ₂ PO ₂ CCH=CH ₂)		116dd	27.5dd	130	113.5	437	
(cis) RhCl(L ₁)(L ₂)(O ₂ CCH=CHMe) ^f		127dd	25.9dd	145	145	27	

All spectra run in CD₂Cl₂ * Low Temperature Spectra

^f L₁ = PPh₃ L₂ = (Ph₂PO₂CCH=CHMe)

Table 2.8		¹ H n.m.r. Data for The Mixed Anhydrides And Related Complexes (CD ₂ Cl ₂ , 25°C)	
Compound		Chemical Shift (ppm)	
		dMe	dH
Me ^a CH ^b CH ^c CO ₂ PPh ₂		^a 1.92d	^b 7.1m, ^c 6.0m
CH ₂ CHCO ₂ PPh ₂		Not Obtained	
CH ₂ CHCH ₂ CO ₂ PPh ₂		Not Obtained	
RhCl(PPh ₃)(Ph ₂ PO ₂ CCH ^c =CH ^b Me ^a)		^a 1.69m	^b 4.75m, ^c 4.07m
(cis) RhCl(PPh ₃)(Ph ₂ PO ₂ CCH ^c =CH ^b Me ^a) *		^a 1.92d	^b 4.98m, ^c 4.37m
(trans)RhCl(PPh ₃)(Ph ₂ PO ₂ CCH ^f =CH ^b Me ^a) *		^a 1.76d	^b 4.98dddq, ^c 4.37dd
(trans)RhCl(PPh ₃)(Ph ₂ PO ₂ CCH ^b =CH ₂ ^a)		-----	^a 4.01m, ^b 4.51m
(cis) RhCl(L ₁)(Ph ₂ PO ₂ CCH ^f =CH ^c Me ^d) ^f (O ₂ CCH ^c =CH ^b Me ^a)		^a 1.6d, ^d 1.15 d	^b 4.09m, ^c 3.30m, ^e 6.22m, ^f 5.19m

* Low Temperature Spectra ^f L₁ = PPh₃

2.10 Experimental

Mixed Anhydride of Acrylic Acid ($\text{Ph}_2\text{PO}_2\text{CCH}=\text{CH}_2$)

1 molar solutions of $\text{H}_2\text{C}=\text{CHCO}_2\text{H}$, Ph_2PCl and Et_3N using tetrahydrofuran as an dilutant are prepared under dinitrogen. Equivalent amounts of these molar solutions are added, under dinitrogen, to a cooled solution of (0°C) tetrahydrofuran or diethyl ether (20ml). The immediate production of the white precipitate $([\text{HEt}_3\text{N}^+][\text{Cl}^-])$ is observed and the solution is stirred for a further 5 minutes before being filtered. No attempt was made to concentrate this solution as it increases the rate at which the compound converts to tetraphenyldiphosphoxane ($\text{Ph}_2\text{PP}(\text{O})\text{Ph}_2$). Compound identification was by spectroscopic means.

Mixed Anhydride of Vinyl Acetic Acid ($\text{Ph}_2\text{PO}_2\text{CCH}_2\text{CH}=\text{CH}_2$)

A 1 molar solution solution of $\text{H}_2\text{C}=\text{CHCH}_2\text{CCO}_2\text{H}$ is prepared and replaces the 1 molar acid solution in the method described for the production of $\text{Ph}_2\text{PO}_2\text{CCH}=\text{CH}_2$. Again no concentration was attempted as this increased the conversion, also shown by $\text{Ph}_2\text{PO}_2\text{CCH}=\text{CH}_2$, to $\text{Ph}_2\text{PP}(\text{O})\text{Ph}_2$. As a result this compound has only been spectroscopically identified as in the case of $\text{Ph}_2\text{PO}_2\text{CCH}=\text{CH}_2$.

[RhCl(PPh₃)(Ph₂PO₂CCHCHMe)]

Method 1

To a cooled solution (0°C) of RhCl(PPh₃)₃ (0.50g, 0.54 mmol) in tetrahydrofuran (50 cm³) a cooled (-10°C) solution of Ph₂PO₂CCH=CHMe (0.18g, 0.65 mmol) in tetrahydrofuran was added. On addition a slow reaction occurred and the solution gradually became orange. The solution was stirred for 30-40 minutes then filtered and the volume reduced to approximately 6 cm³, at which point an orange/yellow material began to precipitate. It was further concentrated to about 2 cm³ before slowly adding 20 cm³ of cooled (-5°C) petroleum ether (40-60°C). The resulting suspension was allowed to settle overnight at -30°C before filtration. The product was washed (3 × 10 cm³) with cooled petroleum ether (-40°C) and dried under vacuum. Orange crystals suitable for crystallographic analysis were obtained from dichloromethane and diethyl ether. Yield 0.29g (80%).

Theoretical [RhCl(PPh₃)(Ph₂PO₂CCHCHMe)] C, 60.9%; H, 4.5%;

Found [RhCl(PPh₃)(Ph₂PO₂CCHCHMe)] C, 60.8%; H, 4.4%;

Method 2

To a cooled (0°C) solution of RhCl(PPh₃)₃ (0.5g, 0.54

mmol) a similarly cooled tetrahydrofuran solution of $\text{Ph}_2\text{PO}_2\text{CCH}_2\text{CHCH}_2$ (0.14g, 0.3 mmol) is added with constant stirring, the $\text{Ph}_2\text{PO}_2\text{CCH}_2\text{CH}=\text{CH}_2$ having been produced by the same prereaction of 1 molar solutions as described in the synthesis of $[\text{RhCl}(\text{PPh}_3)(\text{Ph}_2\text{PO}_2\text{CCH}=\text{CH}_2)]$. The volume is reduced to approximately 5 ml and careful addition of petrol produces orange microcrystalline solid. Crystals can be obtained from dichloromethane and ether or concentrated tetrahydrofuran solutions. The microcrystalline solid contains some $[\text{RhCl}(\text{Ph}_2\text{POPPH}_2)]$ which can either be removed by recrystallization or washing with cooled (0°C) tetrahydrofuran. Yield 0.28g (77%).

$[\text{RhCl}(\text{PPh}_3)(\text{Ph}_2\text{PO}_2\text{CCH}_2\text{CHCH}_2)]$

A cooled solution (0°C) of $\text{RhCl}(\text{PPh}_3)_3$ (0.50g, 0.54 mmol) was added to a cooled solution (0°C) of $\text{Ph}_2\text{PO}_2\text{CCH}=\text{CH}_2$ in tetrahydrofuran (0.14g, 0.54 mmol), the $\text{Ph}_2\text{PO}_2\text{CCH}=\text{CH}_2$ having been preformed at 0°C in tetrahydrofuran from 1 molar solutions of acrylic acid (0.04g, 0.54 mmol), chlorodiphenyl phosphine (0.12g, 0.54 mmol) and triethylamine (0.054g, 0.54 mmol) under dinitrogen. After a reaction period of 5-10 minutes the volume of the filtered reaction solution is reduced to approximately 5 ml and the solution shot into a large volume of cold petroleum spirit (40 to 60°C) producing a yellow solid which contained

$[\text{RhCl}(\text{PPh}_3)(\text{Ph}_2\text{PO}_2\text{CCH}=\text{CH}_2)]$ as its major product. This complex is contaminated with $\text{RhCl}(\text{PPh}_3)_3$ and $\text{Ph}_3\text{P}^+\text{CH}_2\text{CH}_2\text{CO}_2^-$ but was identified by spectroscopic studies.

$\text{K}^+\text{MeHC}=\text{CHCO}_2^-$

To a stirring room temperature solution of $\text{MeHC}=\text{CHCO}_2\text{H}$ (10g, 0.12 mol) in tetrahydrofuran an equimolar amount of KOH was added (6.5g, 0.12 mol). The immediate generation of heat is noted and the solution is allowed to stir for approximately 24 hours, at the end of which a white solid has separated. This solid, the $\text{K}^+\text{O}_2\text{CC}=\text{CHMe}$, is filtered off and dried under vacuum. Yield 12.4g (85.5%).

$\text{Ph}_3\text{P}^+\text{CH}_2\text{CH}_2\text{CO}_2^-$

Method 1

To a cooled solution (0°C) THF solution of $\text{Ph}_2\text{PO}_2\text{CCH}=\text{CH}_2$ a mole equivalent of PPh_3 is added and stirred constantly at 0°C for half an hour. The product along with $\text{PPh}_2\text{OPPh}_2$ appears as a white precipitate upon the concentration of the reaction solution and can be purified upon removal of the supernatant, by recrystallisation from THF or dichloromethane solutions.

Method 2

To a room temperature solution of acrylic acid a mole equivalent of PPh_3 was added with constant stirring. After the reaction solution was concentrated and the white precipitate collected. This precipitate contained both PPh_3 and $\text{P}^+\text{Ph}_3\text{CH}_2\text{CH}_2\text{CO}_2^-$, the PPh_3 could be removed with exhaustive washing with diethyl ether.



Method 1

As above but with $\text{Ph}_2\text{PO}_2\text{CCH}=\text{CHMe}$ as the parent anhydride.

Method 2

As above but with crotonic acid as the parent acid.

This compound, however, has not been obtained in a pure state.



To a precooled (0°C) tetrahydrofuran solution of $[\text{Rh}(\text{PPh}_3)\text{Cl}(\text{Ph}_2\text{PO}_2\text{CCH}=\text{CHMe})]$ (0.5g, 0.7 mmol) a 10 fold excess of $\text{K}^+\text{O}_2\text{CC}=\text{CHMe}$ (0.9g, 7 mmol) was added. The solution was stirred for half an hour and a fine white precipitate of KCl is evolved over this period. The solution is then left to stand for approximately 10 minutes until the white precipitate has settled. It is then filtered through celite and the resultant solutions volume reduced to approximately 5 mls. A yellow solid is obtained on addition of

petroleum spirit (40-60°C) to this solution. Crystals were obtained upon recrystallization from dichloromethane and diethyl ether, and are found to retain a mole of tetrahydrofuran of crystallisation. Yield 0.46g, 85%.

Theoretical $[\text{Rh}(\text{PPh}_3)(\text{Ph}_2\text{PO}_2\text{CCHCHMe})(\text{O}_2\text{CCHCHMe})].\text{thf}$

C 63.65%; H 5.47%

Found $[\text{Rh}(\text{PPh}_3)(\text{Ph}_2\text{PO}_2\text{CCHCHMe})(\text{O}_2\text{CCHCHMe})].\text{thf}$

C 64.07%; H 5.29%.

Attempted Catalytic Reactions With Vinylacetic , Oleic and Hexa-4-enoic acids

A quantity of $[\text{RhCl}(\text{CAA})(\text{PPh}_3)]$ was dissolved in tetrahydrofuran (approx 20 ml) and to the resulting solution a 10 fold excess of the acidic substrate and a 5 fold excess quantity of potassium hydroxide were added. The solution was stirred at room temperature and ambient pressure for the required time period after which it was evaporated to dryness. The resulting solid was then dissolved in a quantity of dichloromethane and extracted using water (50 mls) and concentrated hydrochloric acid (5 mls). The dichloromethane fraction containing the organic acids was collected and evaporated to dryness and the resultant mixtures studied by proton n.m.r.

CHAPTER 3

Rearrangements of the Mixed Anhydrides Ligands

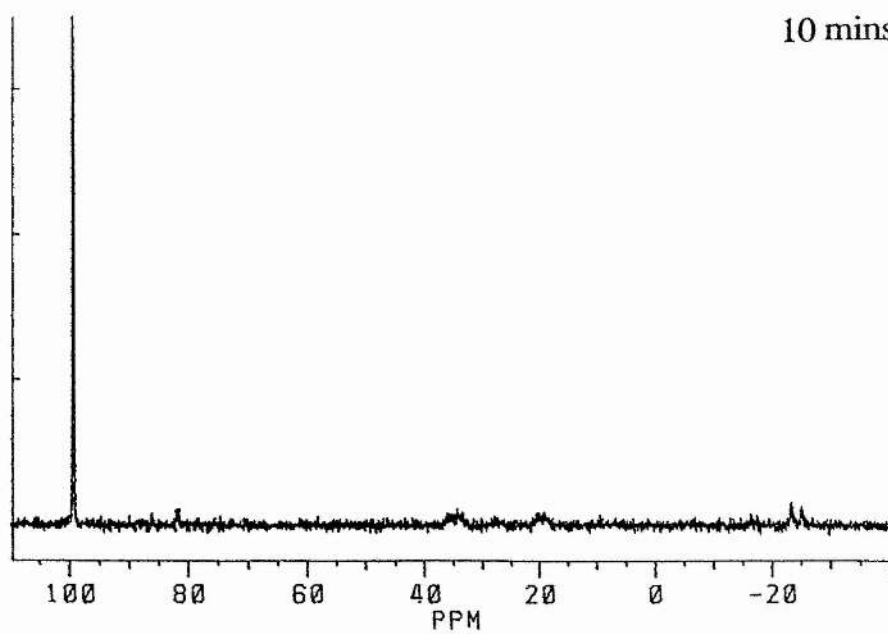
In chapter 2 the initial reactions between Wilkinson's Catalyst and the mixed anhydride were reported and the arguments supporting the conclusions made on the mode of anhydride coordination were discussed. The mixed anhydrides of acrylic acid and vinylacetic acid were also commented upon as they exhibited a rearrangement to tetraphenyldiphosphine monoxide. A similar rearrangement had previously been observed for $\text{Ph}_2\text{PO}_2\text{CCH}=\text{CHCH}=\text{CHMe}$ but not recognised as such⁽¹¹⁹⁾. Further study into the nature of this rearrangement and the subsequent metal reactions are now reported.

3.1 Investigation into the Rearrangement to $\text{Ph}_2\text{PP}(\text{O})\text{Ph}_2$

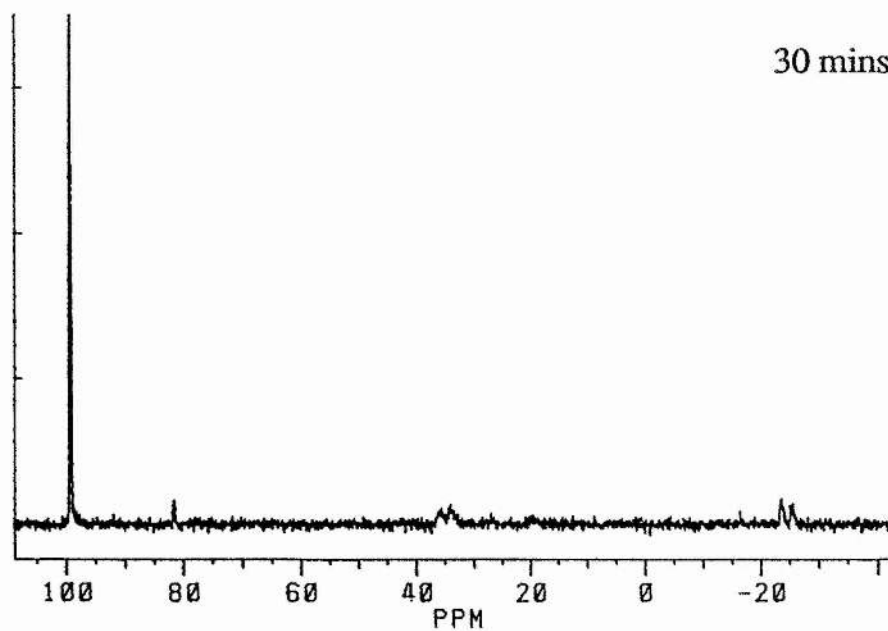
As reported attempts to isolate $\text{Ph}_2\text{PO}_2\text{CCH}=\text{CH}_2$ and $\text{Ph}_2\text{PO}_2\text{CCH}_2\text{CH}=\text{CH}_2$ were frustrated by a facile rearrangement of these ligands in solution to give $\text{Ph}_2\text{PP}(\text{O})\text{Ph}_2$, the spectral data for which is summarised in Table 3.1 (165,172). ^{31}P n.m.r. studies showed that very little rearrangement occurs in dilute solution at 0°C over a 24 hour period (Figures 3.1-3.3). However, attempts to isolate these mixed anhydrides by concentration of their tetrahydrofuran solutions resulted in the isolation of $\text{Ph}_2\text{PP}(\text{O})\text{Ph}_2$. The mechanism of this rearrangement is unknown but further low

10 mins

117

 $(\text{CD}_2\text{Cl}_2, -5^\circ\text{C})$ 

30 mins



60 mins

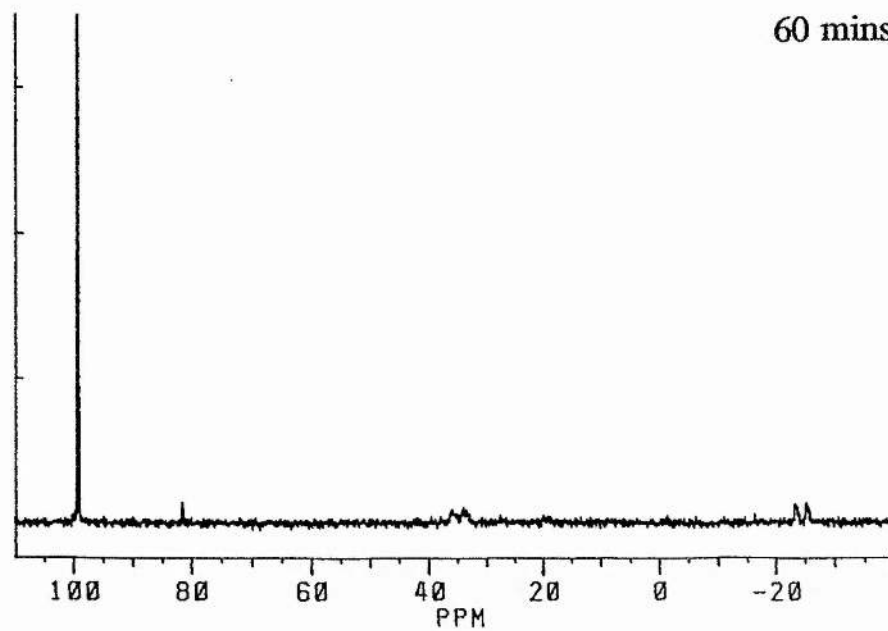
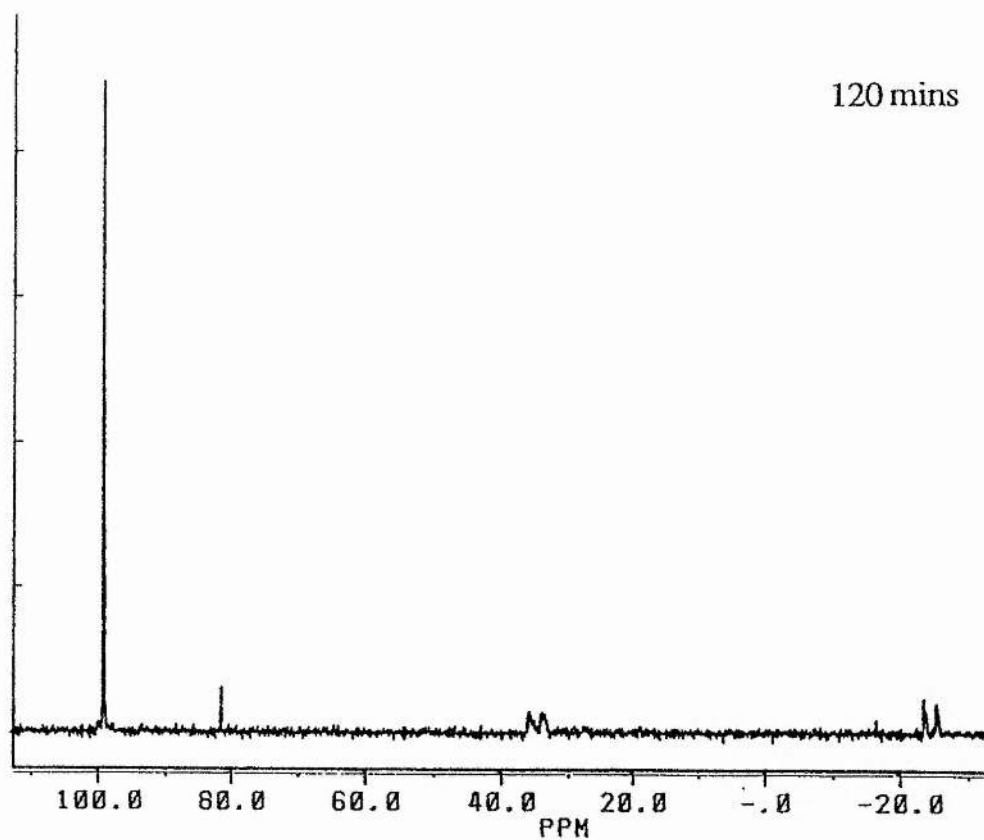


Fig. 3.1 Change in the ^{31}P n.m.r. spectrum (300 MHz) of $\text{Ph}_2\text{PCO}_2\text{CH}=\text{CH}_2$ over the duration of a day

120 mins

 $(\text{CD}_2\text{Cl}_2, -5^\circ\text{C})$

24 hours

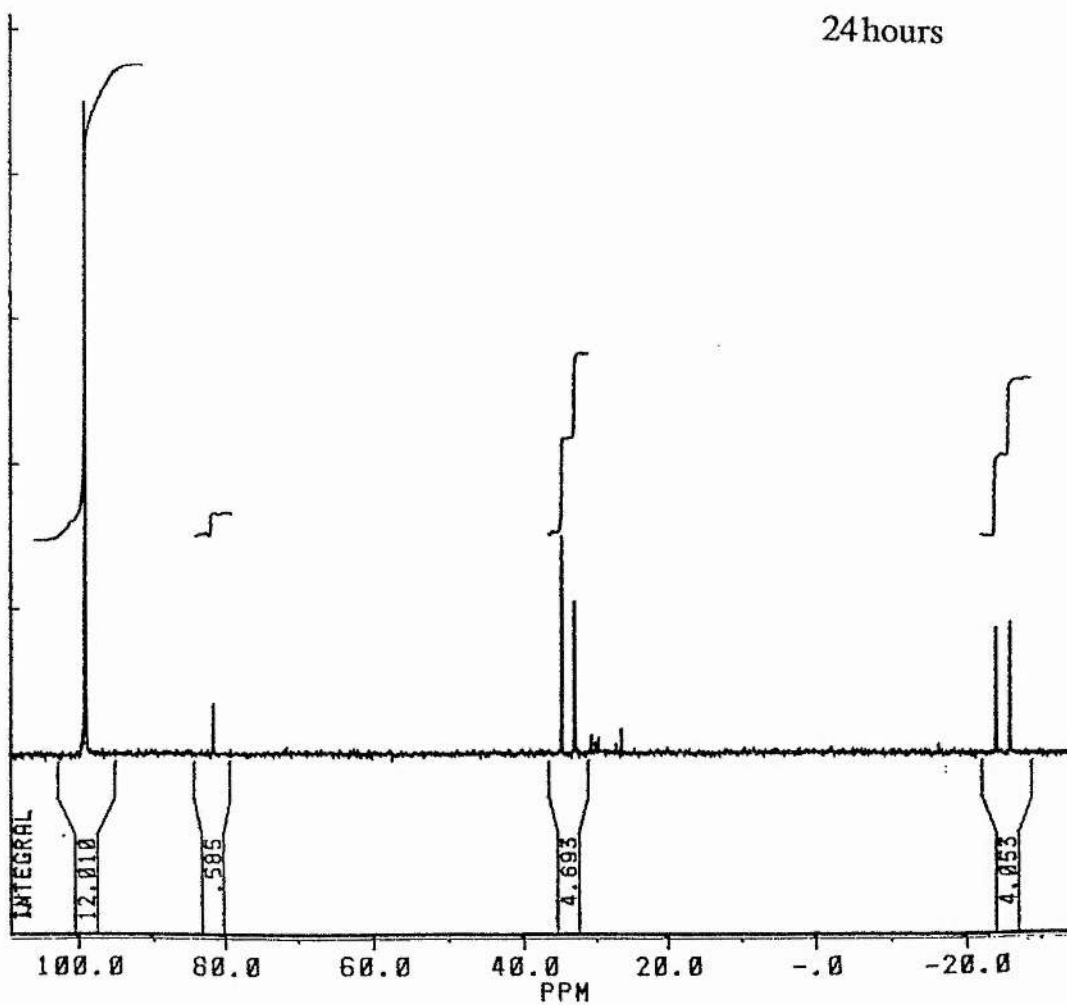


Fig. 3.2 Change in the ^{31}P n.m.r. spectrum (300 MHz) of $\text{Ph}_2\text{PCO}_2\text{CH}=\text{CH}_2$ over the duration of a day

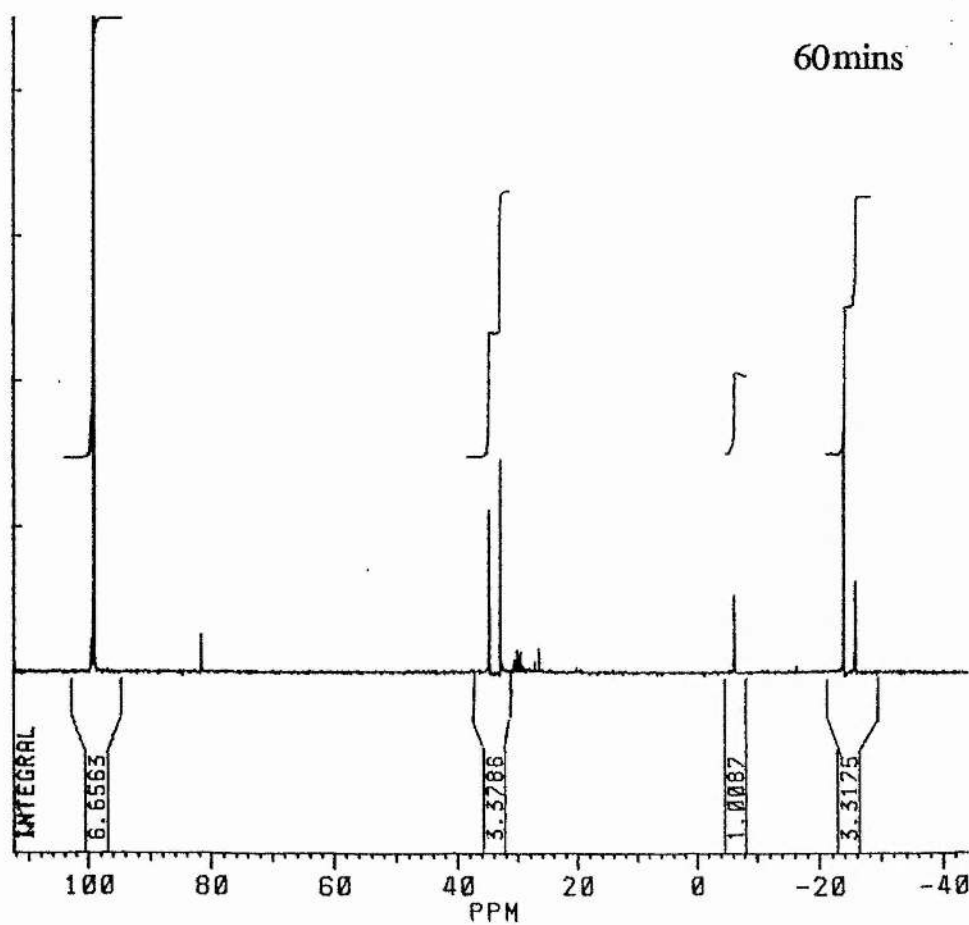
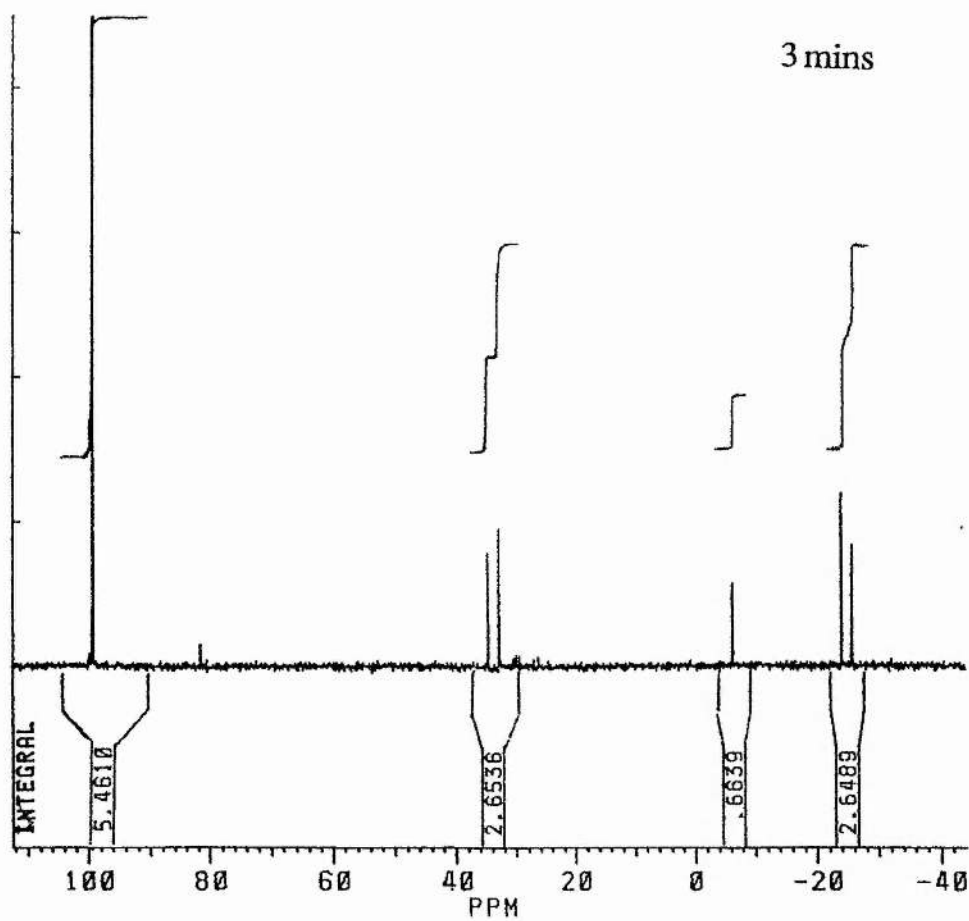


Fig. 3.3 Change in the ^{31}P n.m.r. spectrum (300 MHz) of $\text{Ph}_2\text{PCO}_2\text{CH}=\text{CH}_2$ on addition of PPh_3 (CD_2Cl_2 , -50°C)

temperature ^{31}P n.m.r. studies proved that this rearrangement is unaffected by NEt_3 , Ph_2PCl and PPh_3 (Figure 3.3). Thus although the mechanism is unknown, it is plausible that it occurs via a disproportionate reaction (See Figure 3.4).

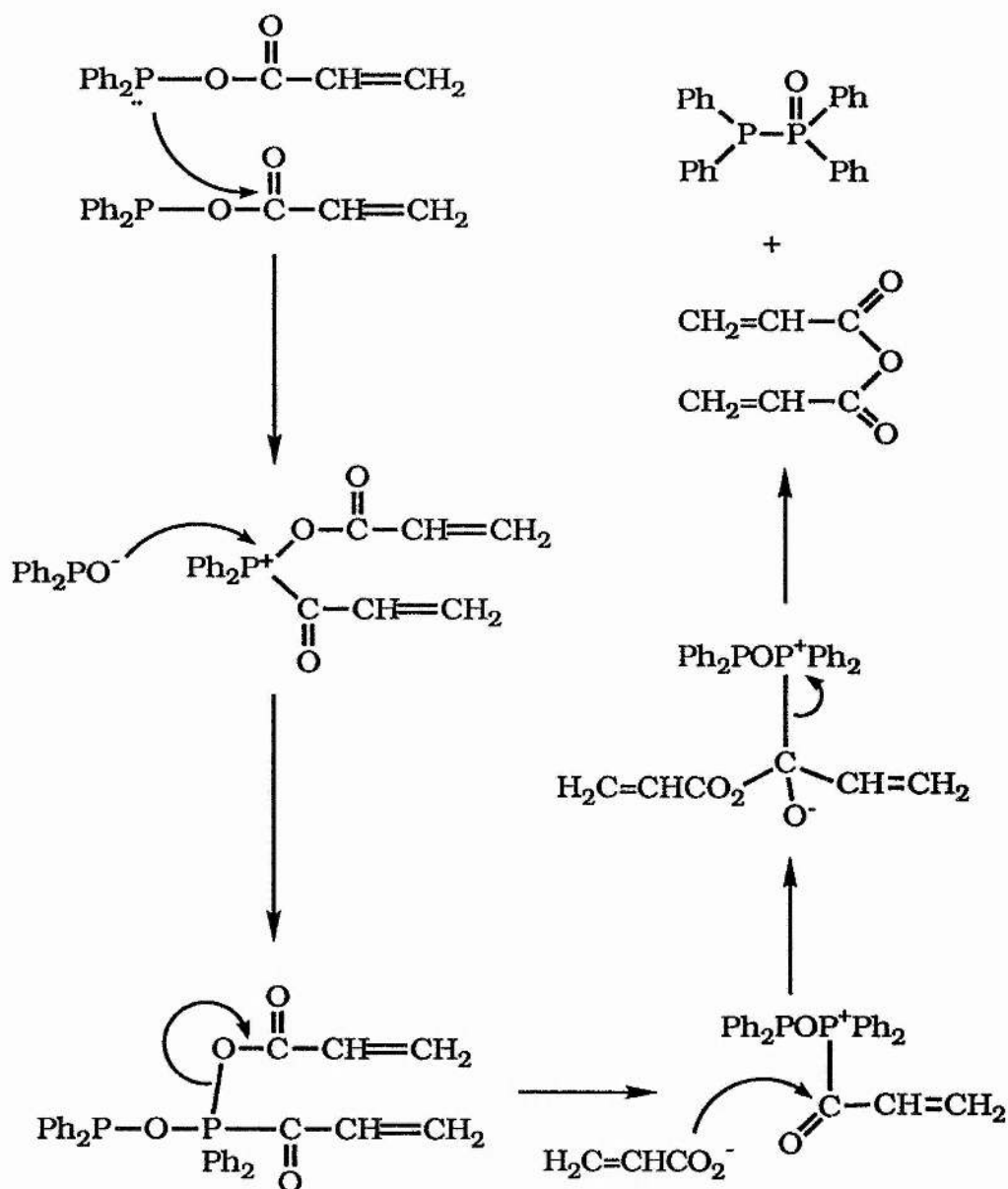


Fig. 3.4

Proposed Rearrangement Mechanism

This type of rearrangement does not occur for mixed anhydrides with more than one substituent on the double bond suggesting that steric factors may play an important role in determining the stability of the mixed anhydrides. $\text{Ph}_2\text{PP}(\text{O})\text{Ph}_2$ has previously been prepared from chlorodiphenylphosphine and oxidised to $\text{Ph}_2\text{P}(\text{O})\text{P}(\text{O})\text{Ph}_2$ by McKechnie, Payne and Sim (173).

3.2 The 2:1 Mole Ratio Reaction of $\text{Ph}_2\text{PO}_2\text{CCH}=\text{CH}_2$ and Wilkinsons Catalyst

In Chapter 2 it was reported that the first product obtained from the 1:1 reaction of AAA and $[\text{RhCl}(\text{PPh}_3)_3]$ was $[\text{RhCl}(\text{PPh}_3)(\text{Ph}_2\text{PO}_2\text{CCH}=\text{CH}_2)]$. Furthermore the binding of the AAA ligand was proved to be via the phosphorus atom and the double bond. However, by employing a 2:1 mole ratio in favour of the mixed anhydride and following the experimental procedure described in Chapter 2 for the 1:1 mole reaction, yellow/orange crystals were isolated from the filtered and concentrated reaction solution upon standing at -3°C for several days. The ^{31}P and ^1H n.m.r. spectra were obtained (Figures 3.5 and 3.6) but were initially uninterpretable. However, careful recrystallisation from THF or THF/diethyl ether solutions afforded crystals of x-ray quality. The x-ray structure solution proved that the isolated product is not a complex involving coordination of the AAA ligand but was $[\text{RhCl}(\text{PPh}_3)(\text{Ph}_2\text{POPPH}_2)]\cdot\text{thf}$, tetraphenyldiphosphoxanetriphenyl phosphinechlororhodium (1)(174). This is one of the few examples of

a complex containing a chelate tetraphenyl disphosphoxane ligand and the first such platinum metal complex recorded (from this point tetraphenyldiphosphoxane will be abbreviated to tdp). The acquisition of the crystal structure solution led to the retrospective interpretation of the spectral data.

3.2.1 Spectral Data of $[\text{RhCl}(\text{PPh}_3)(\text{Ph}_2\text{POPPh}_2)]\cdot\text{thf}$

^{31}P n.m.r. Data

This spectrum contains 3 resonances at 106.5, 81.2 and 25.1 ppm (Figure 3.5). Unfortunately, the crystal structure of the isoelectronic $[\text{RhCl}(\text{Ph}_2\text{PCH}_2\text{PPh}_2)(\text{PPh}_3)]$ has not been reported, although a similar value for J_{pp} between the RhPXP phosphorus atoms (where $\text{X} = \text{O}$ or CH_2) in complexes with similar structures suggests that this complex may have similar P-P interactions to those already documented⁽¹⁷⁵⁾. The spectral profile for P_B (as denoted in Figure 3.7) takes the form of a doublet of doublets of doublets.

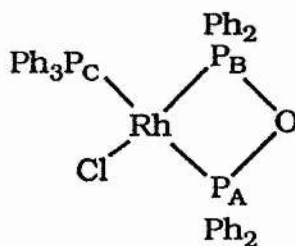


Fig. 3.7

This profile is due to a coupling between P_B and the rhodium, a ring *cis* coupling to P_A and a *cis* coupling of different size to P_C . P_A is assigned to the resonance at 80 ppm which is a doublet of triplets. This profile differs from P_B because by chance the P_A exhibits two couplings of similar size (the ring *cis* coupling and the Rh-P coupling). The third resonance, that of the triphenylphosphine is similar to that for P_B as all the couplings are of differing sizes.

^1H n.m.r. Data

The proton n.m.r. spectrum (Figure 3.6) provides little information as, apart from those resonances associated with the THF of crystallisation, all the information is held in a multiplet between 6.8 ppm and 8.0 ppm too complex to interpret.

Infra-red Data

This has little information above 1500 cm^{-1} due to the loss of the vinylic backbone. The important peaks present below 1500 cm^{-1} include that at 290 cm^{-1} which is assigned to the rhodium-chlorine absorbance. The $\nu(\text{P-O})_{\text{asym}}$ band of the Rh-P-O-P ring is located at 800 cm^{-1} its position being a good indication of chelate coordination. Previously reported work, mainly on group 6 metals, showed that the $\nu(\text{P-O})_{\text{asym}}$ band position indicates the mode of tpdp coordination, those of monodentate tpdp are found in the

1100cm⁻¹ region whilst those of bridging and chelate tdpd ligands are found typically in the 860-890 and 760-800 cm⁻¹ regions respectively (176).

3.3 Formation of the Tdpd Complexes

3.3.1 Proposed Mechanism for the Metal Promoted Rearrangement of Ph₂PO₂CCH=CH₂

The metal promoted rearrangement which results in the creation of the tdpd complex [RhCl(PPh₃)(Ph₂POPPH₂)] is vastly different from those previously reported to result in chelate tdpd complexes. These literature reported methods are dealt with in Chapter 6. In an attempt to understand the mechanism by which this rearrangement occurs, the reaction was followed by low temperature ³¹P n.m.r.

The first step in this process was to add only a single mole equivalent of the mixed anhydride to Wilkinson's Catalyst in tetrahydrofuran at 0°C. This is the reaction first described in Chapter 2 and is observed to have the same result, namely the formation of the rhodium complex which contains a mixed anhydride ligand bound to the rhodium via the phosphorus atom and the double bond (see Figure 3.8 for ³¹P spectrum).

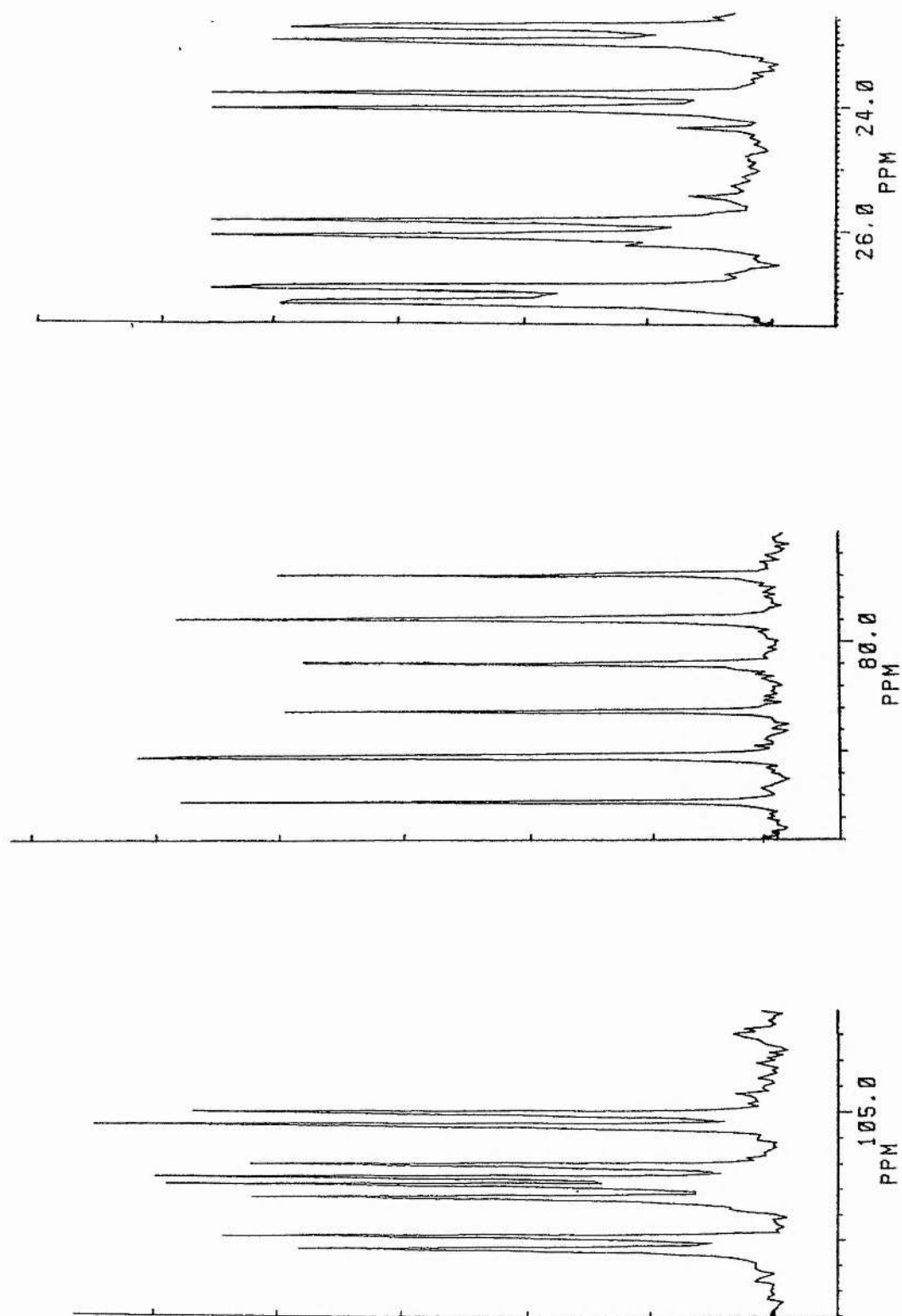
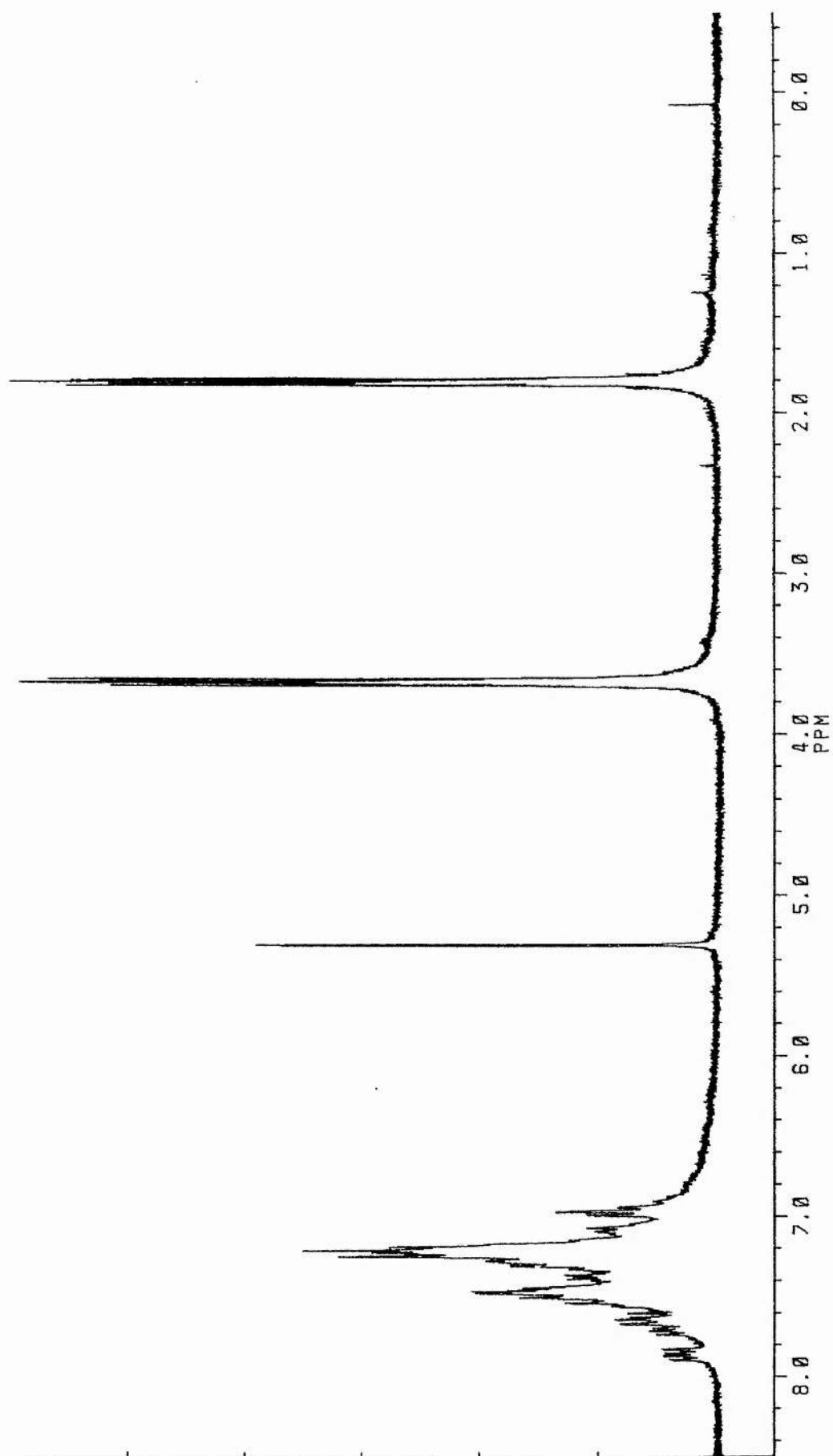


Fig. 3.5 ^{31}P n.m.r. spectrum (300 MHz) of $[\text{RhCl}(\text{PPh}_3)_3]$ (CD_2Cl_2 , 25°C)

(CD₂Cl₂, 25°C)Fig. 3.6 ^1H n.m.r. spectrum (300 MHz) of $[\text{RhCl}(\text{PPh}_3)(\text{Ph}_2\text{POPPh}_2)]$

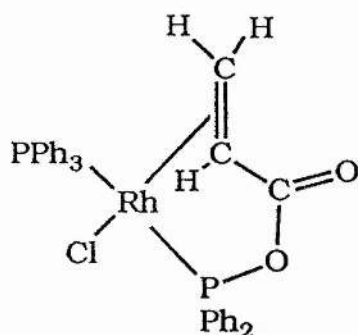


Fig. 3.9

A second mole of the anhydride was then added. The resonances allocated to the chelate product shown in Figure 3.9 were immediately replaced by a resonance at 109 ppm (figure 3.10) which is assigned to complex (b) in Figure 3.11. A five coordinate species in which all the triphenylphosphine species have been displaced.

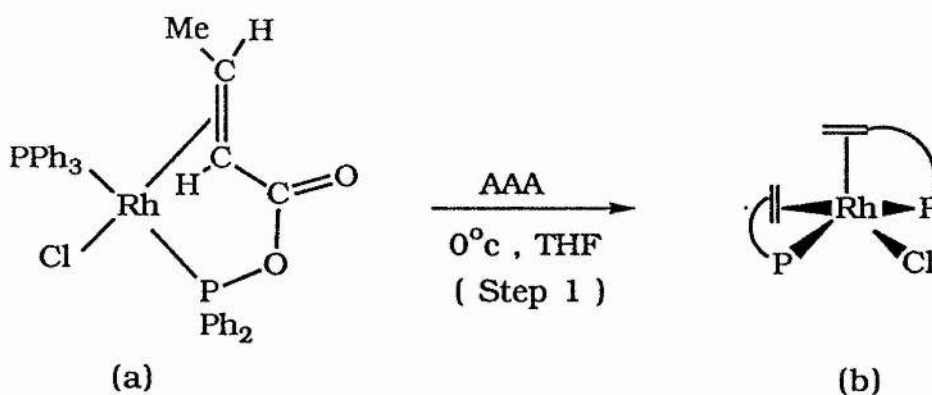


Fig. 3.11

Strong evidence to support this assignment is contained in Chapter 4 in which the isolation and subsequent characterisation of this five coordinate species is reported and shown to have the ^{31}P n.m.r. spectrum

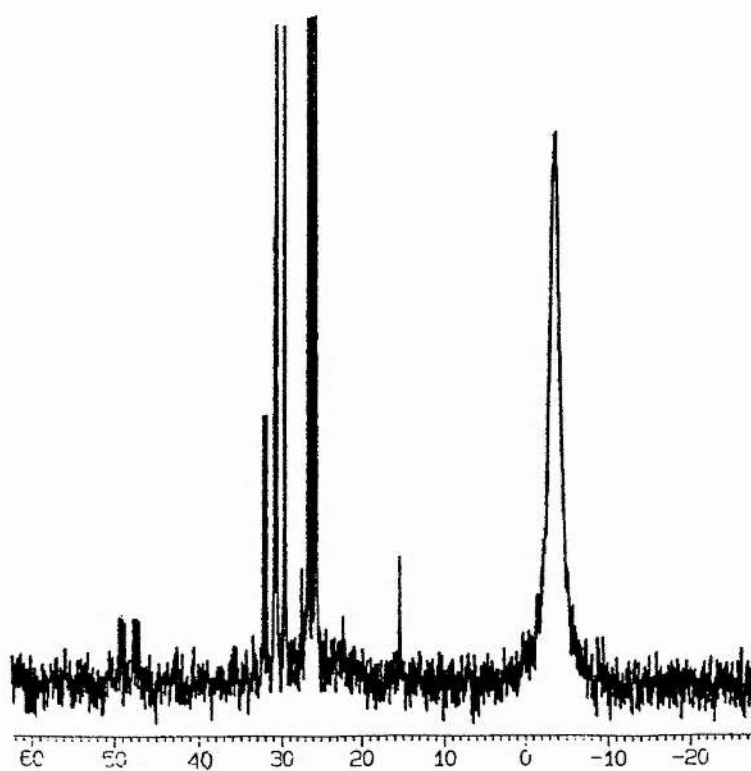
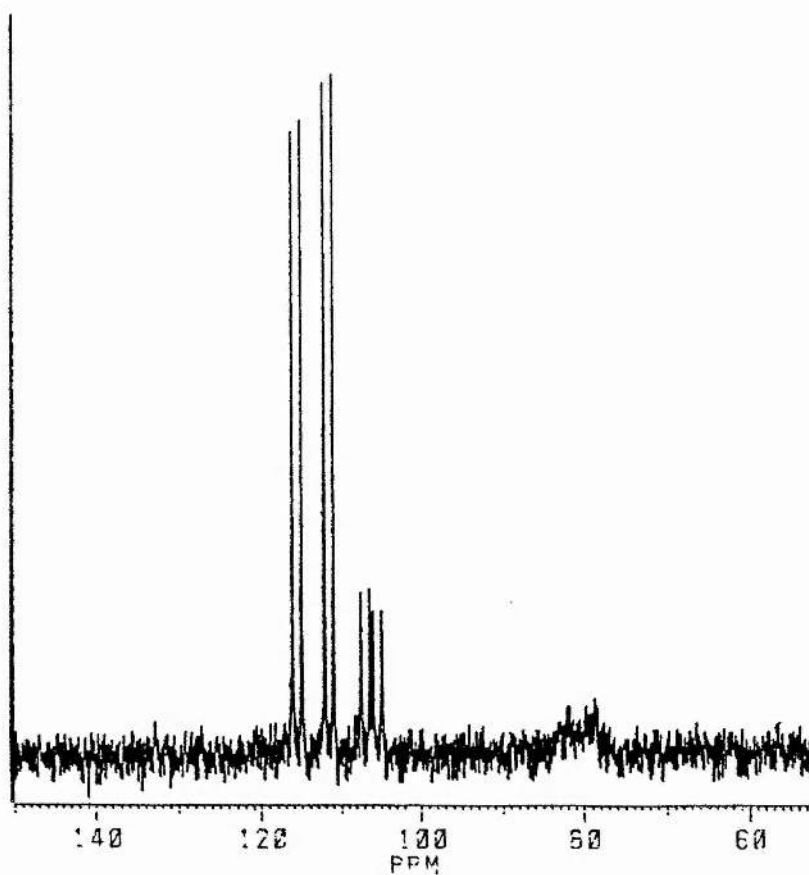
$(\text{CD}_2\text{Cl}_2, -10^\circ\text{C})$ 

Fig. 3.8 $[\text{RhCl}(\text{PPh}_3)_3] + 1 \text{ mole of } \text{Ph}_2\text{PO}_2\text{CCH}=\text{CH}_2$

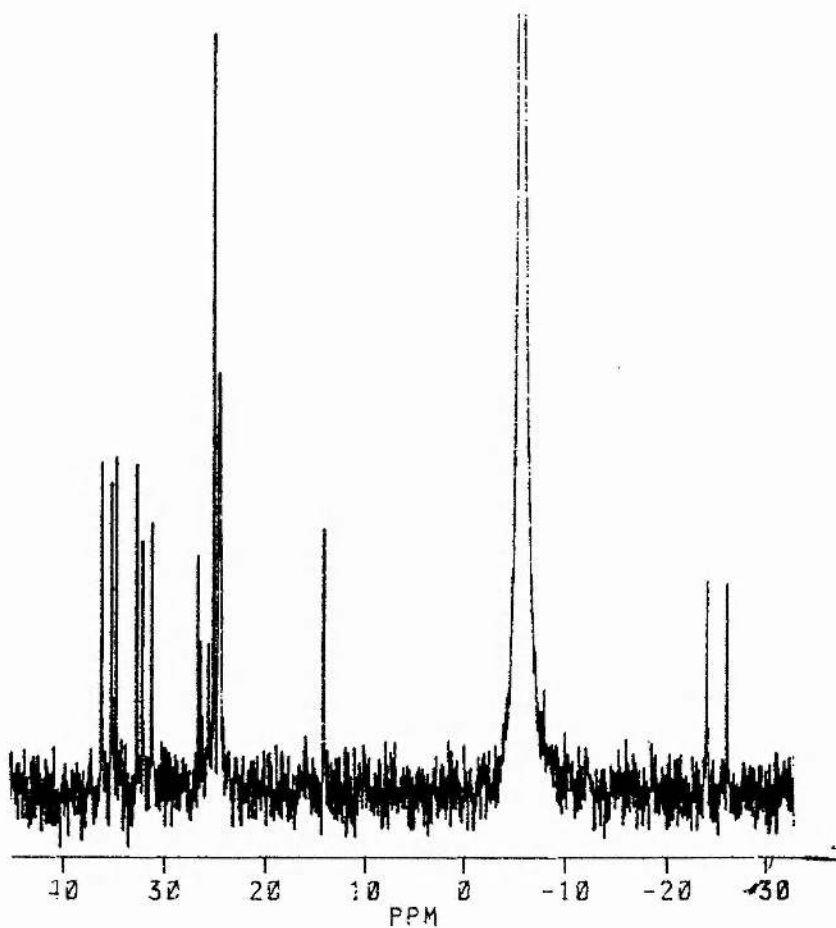
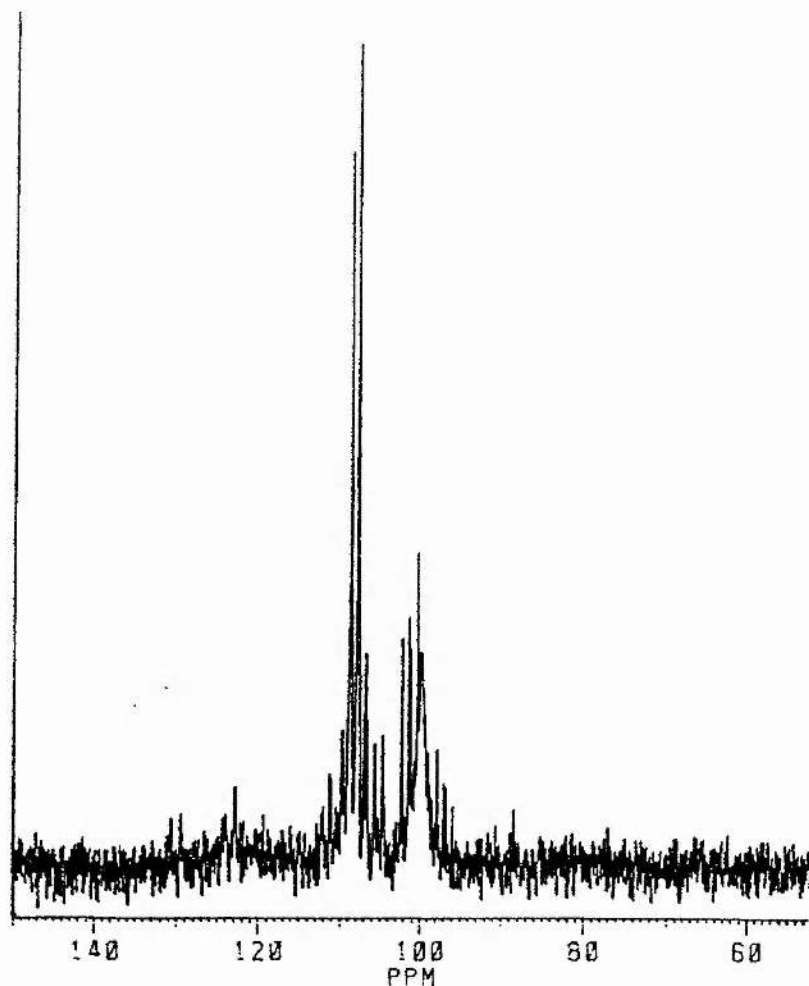
$(\text{CD}_2\text{Cl}_2, -10^\circ\text{C})$ 

Fig. 3.10 Spectrum upon addition of a second mole of $\text{Ph}_2\text{PO}_2\text{CCH}=\text{CH}_2$

described above. From this point the rearrangement is noted to proceed via two other intermediates (see Figures 3.12 and 3.13) and although not enough information is available to assign structures to these intermediates, the reaction of an isolated sample of the five coordinate complex (b) with an excess of PPh_3 (described in Chapter 4) was also found to result in the formation of $[\text{RhCl}(\text{PPh}_3)(\text{Ph}_2\text{POPPh}_2)]$. This suggests that the mechanism involves a recoordination of PPh_3 which entails at least one of the coordinated AAA ligands becoming a monodentate ligand bound through the phosphorus atom only.

3.3.2 Reaction of Wilkinson's Catalyst and Tetraphenyldiphosphine Monoxide

A second possible explanation for the isolation of this chelate tpdp complex is that the AAA ligand rearranges to $\text{Ph}_2\text{PP}(\text{O})\text{Ph}_2$ prior to complexation with the metal centre. Although the major weight of evidence lies against this scenario, the above reaction was attempted employing the same conditions used in the 1:2 mole reaction of Wilkinson's Catalyst and AAA. A mole equivalent of $\text{Ph}_2\text{PP}(\text{O})\text{Ph}_2$ was added to a precooled (0°) tetrahydrofuran solution of Wilkinson's Catalyst and stirred for an hour, after which the solution was filtered and concentrated. Yellow crystals were obtained from the concentrated reaction solution after standing at -3°C for approximately a day. Analysis of these crystals showed that

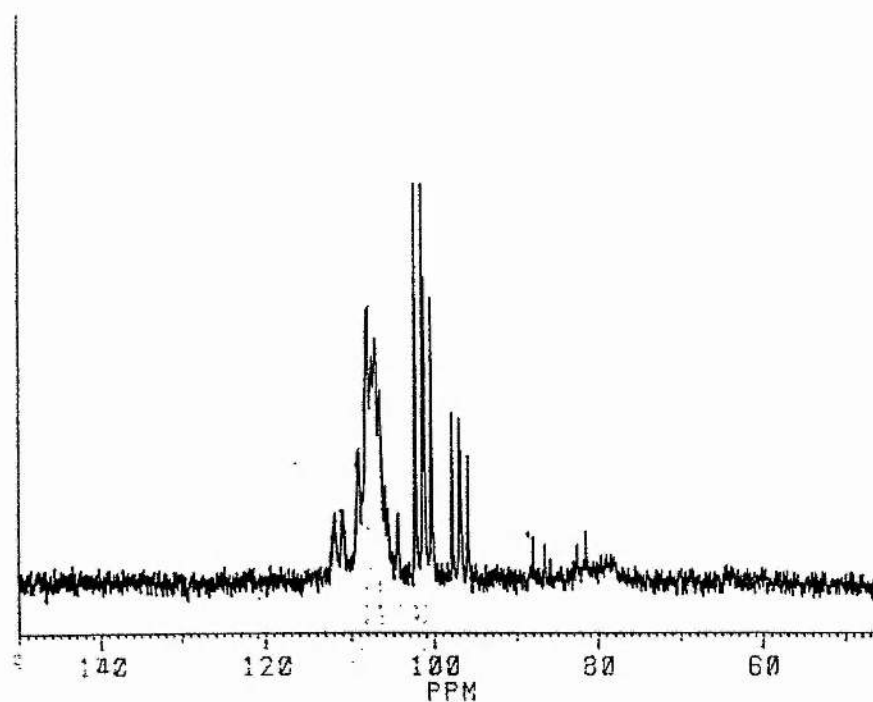
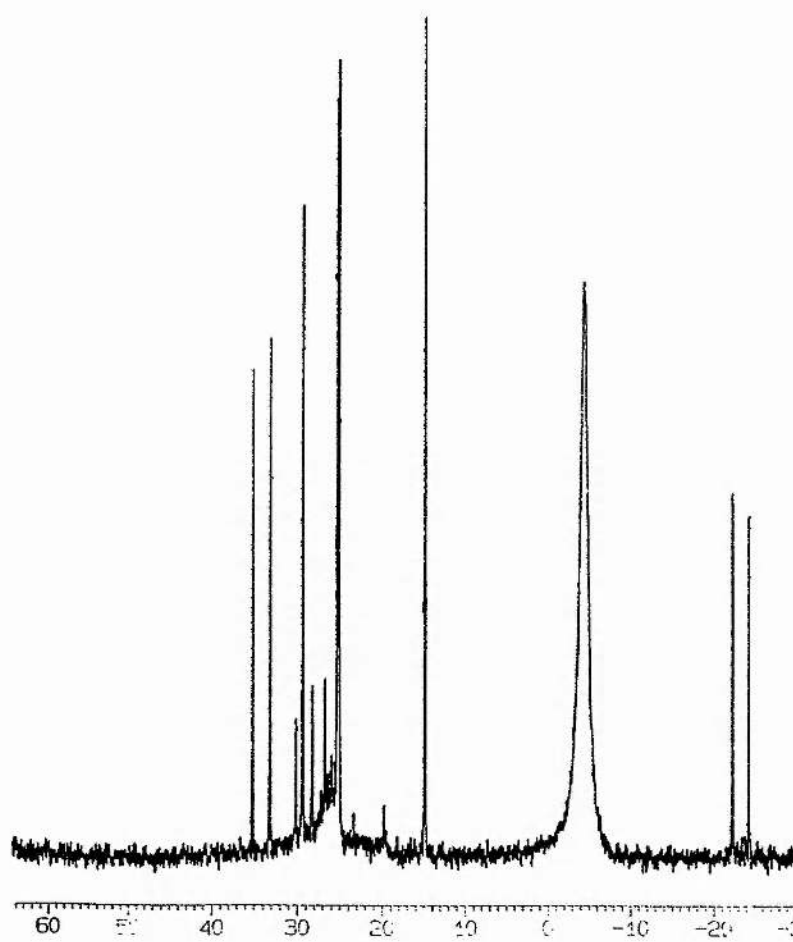
 $(\text{CD}_2\text{Cl}_2, -10^\circ\text{C})$ 

Fig. 3.12 Spectrum after 2 hours

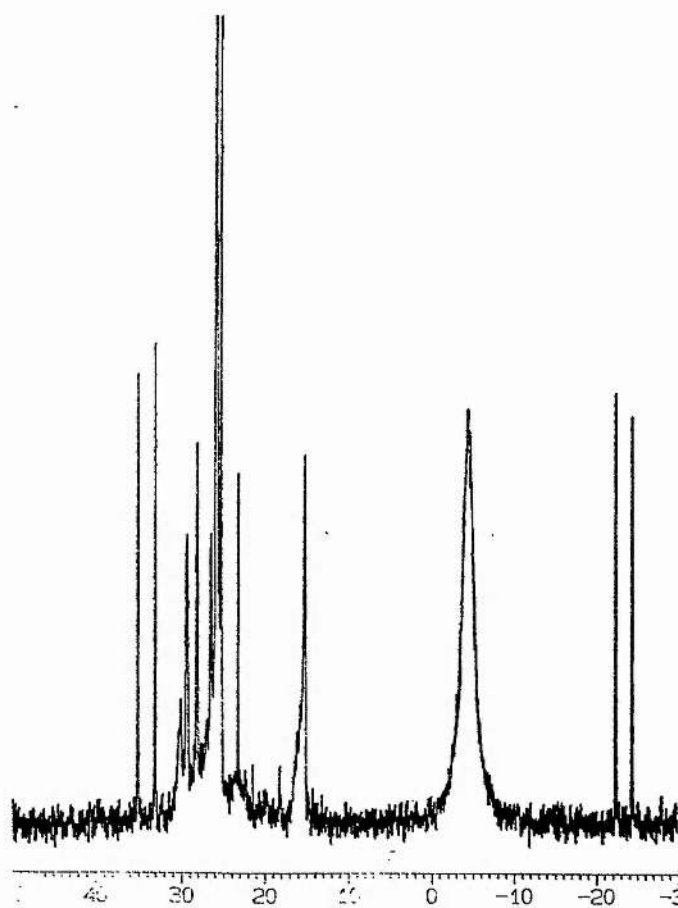
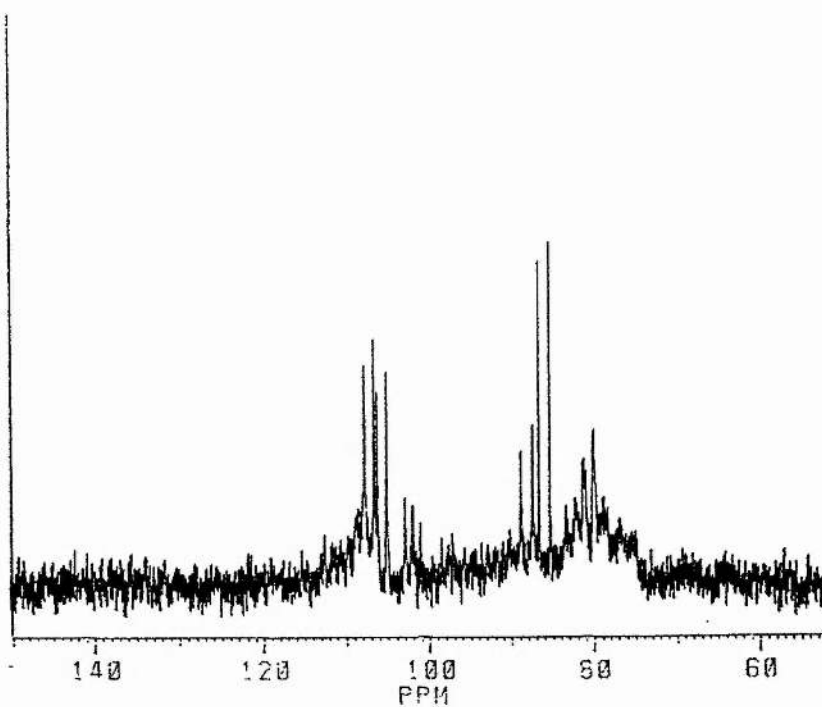
$(\text{CD}_2\text{Cl}_2, -10^\circ\text{C})$ 

Fig. 3.13 Spectrum after 2 days

there were two products present, neither of which were $[\text{RhCl}(\text{tpdp})(\text{PPh}_3)]$. Thus this experiment proved that the AAA ligand does not rearrange prior to coordinating to the metal centre.

The resultant complexes have not been fully characterized although analysis by infra red and F.A.B. mass spectrum techniques suggest that the major product may be that shown in Figure 3.14.

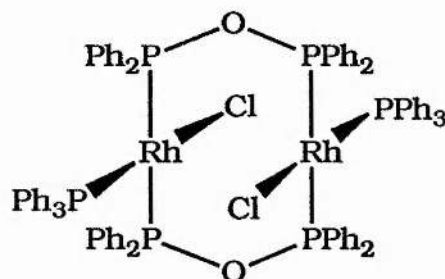


Fig. 3.14

Infra-red Data

This complex has an absorbance at 280 cm^{-1} which is assigned to the Rh-Cl band. Also present is the $\nu(\text{P-O})_{\text{asym}}$ at 900 cm^{-1} which is indicative of a bridging tpdp ligand.

F.A.B. Mass Spectrum

This indicates the molecular ion peak to be $[(\text{Rh}(\text{tpdp})(\text{PPh}_3)(\text{Cl}))_2]$, the full fragmentation pattern is shown in Table 3.4.

^{31}P n.m.r. Data

The ^{31}P n.m.r. data is not yet fully understood. It is found to contain a doublet at 83.3 ppm and a singlet at 28 ppm, the intensity of which is half that of doublet. The resonances are broad indicating the possibility of unresolved coupling. However all attempts to resolve this coupling has proved unsuccessful and this requires further study.

3.4 Reaction of $[\text{RhCl}(\text{PPh}_3)(\text{tpdp})]$ and TlPF_6

The reaction of a quantity of isolated $[\text{RhCl}(\text{PPh}_3)(\text{tpdp})]$ with TlPF_6 when stirred at room temperature results in a slight colour change of the solution to deeper orange and in the appearance of a fine white precipitate of thallium chloride. After approximately fifteen minutes stirring the fine white precipitate was allowed to settle over a further fifteen minute period and the solution filtered through hiflo celite. Yellow needle like crystals were obtained upon allowing a concentrated dichloromethane solution to stand at -3°C for several days. Upon analysis, the crystals proved to be $[\text{Rh}(\text{PPh}_3)_2(\text{Ph}_2\text{POPPh}_2)][\text{PF}_6]$, a second chelate tdpd complex (see Figure 3.15).

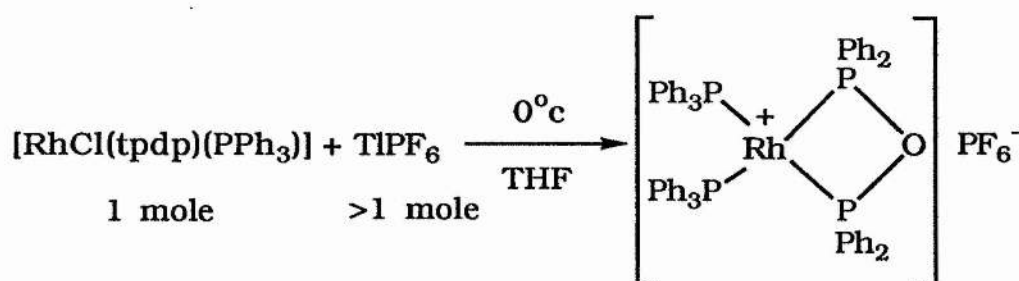
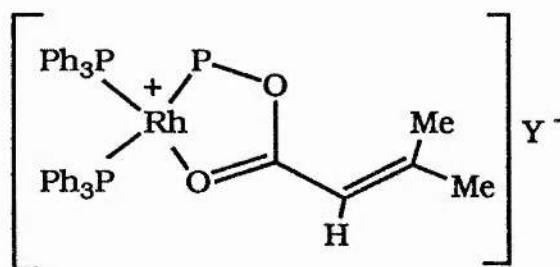


Fig. 3.15

The yields achieved for this reaction all prove to be less than 50%. Similar observations have previously been made in the study of the reaction of $[\text{RhCl}(\text{PPh}_3)(\text{Ph}_2\text{PO}_2\text{CCHCHMe})]$ and mole equivalents of TiPF_6 and AgSbF_6 (120). In this case the product is that shown in Figure 3.16, an example where the mixed anhydride ligand is bound not through the phosphorus atom and double bond but through the phosphorus and carbonyl oxygen atom.



where Y is the counter ion

Fig. 3.16

Thus it would appear that both these reactions proceed via a mechanism in which dechlorination of the initial complex leads to a scavenging of a triphenylphosphine ligand from a second molecule of the starting material and so leads to the formation of a new bis(triphenylphosphine) complex from the triphenylphosphine acceptor and decomposition of the donor. $[\text{Rh}(\text{PPh}_3)_3(\text{tpdp})]^+$ is found as a minor by-product in many of the reactions mentioned to date, for example the 2:1 mole reaction of anhydride and Wilkinson's Catalyst, the 1:1 mole reaction of the VAA and Wilkinson's Catalyst and the reaction of $[\text{RhCl}(\text{PPh}_3)_3]$ and tetraphenyldiphosphine monoxide discussed in Section 3.3.2.

However, in these cases the compound formed is thought to be $[\text{Rh}(\text{PPh}_3)_2(\text{Ph}_2\text{POPPh}_2)]\text{Cl}$, the displaced chlorine atom fulfilling the role of counter ion.

3.4.1 Spectroscopic Data of $[\text{Rh}(\text{PPh}_3)_2(\text{Ph}_2\text{POPPh}_2)]\text{PF}_6$ and $[\text{Rh}(\text{PPh}_3)_2(\text{Ph}_2\text{POPPh}_2)]\text{Cl}$

^1H n.m.r. Data

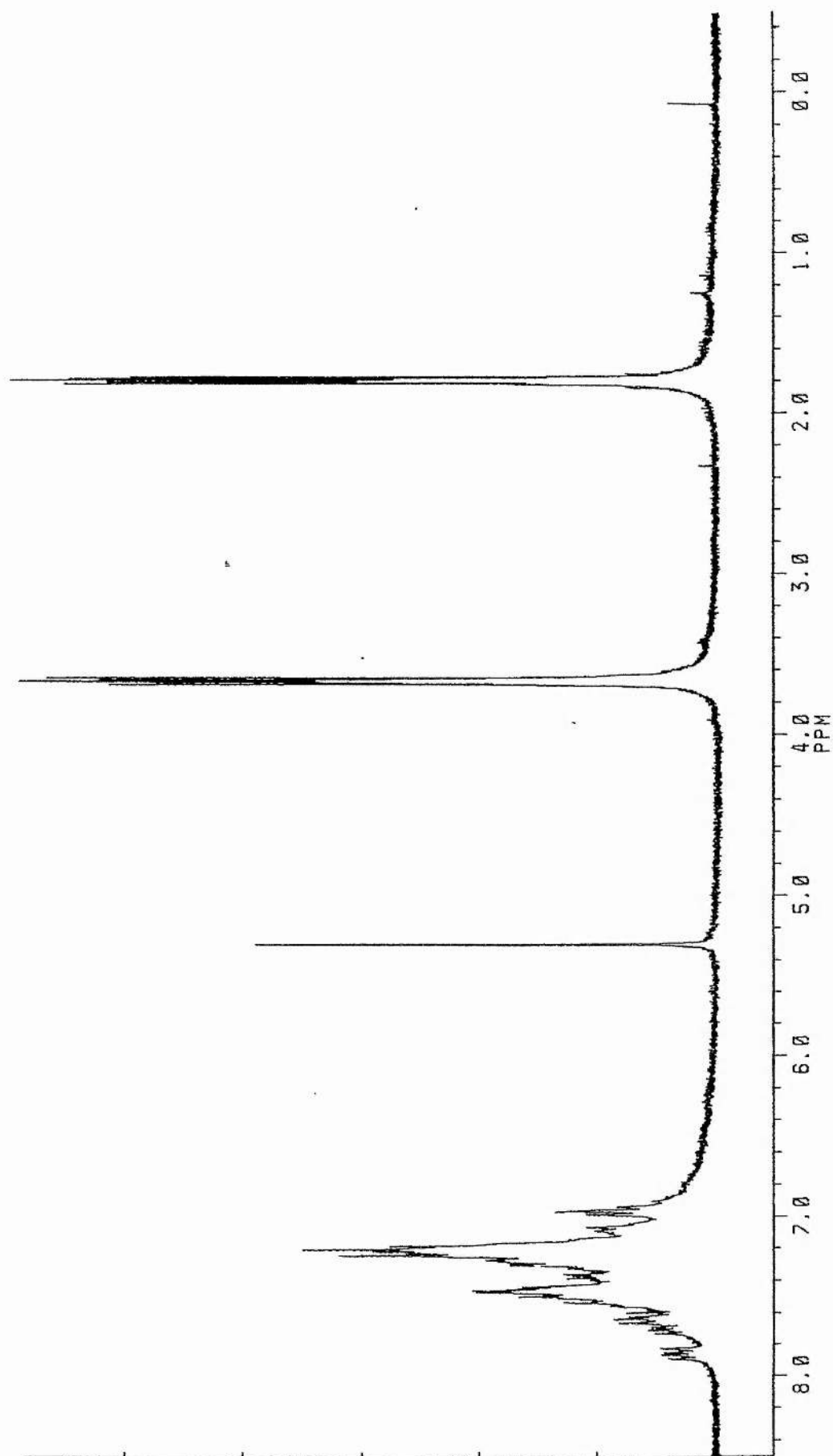
The proton n.m.r. (Figure 3.17) displays peaks in the phenyl region along with those assigned to THF, (the latter are present if crystals are grown from THF). No other information is contained in this spectrum.

Infra-red Data

This also shows no vinyl proton absorbances. Also missing is the Rh-Cl band indicating that chloride abstraction has taken place. The most important feature present is the $\nu(\text{P-O})$ bands, the $\nu(\text{P-O})_{\text{asym}}$ position shows that there is still a P-O-P ligand present and its position (830 cm^{-1}) indicates that it is bound in a chelate fashion.

^{31}P n.m.r.

This spectrum shown in Figures 3.18 and 3.19 can be

 $(\text{CD}_2\text{Cl}_2, 25^\circ\text{C})$ Fig. 3.17 ^1H n.m.r. spectrum (300 MHz) of $[\text{RhCl}(\text{PPh}_3)(\text{Ph}_2\text{POPPh}_2)]$

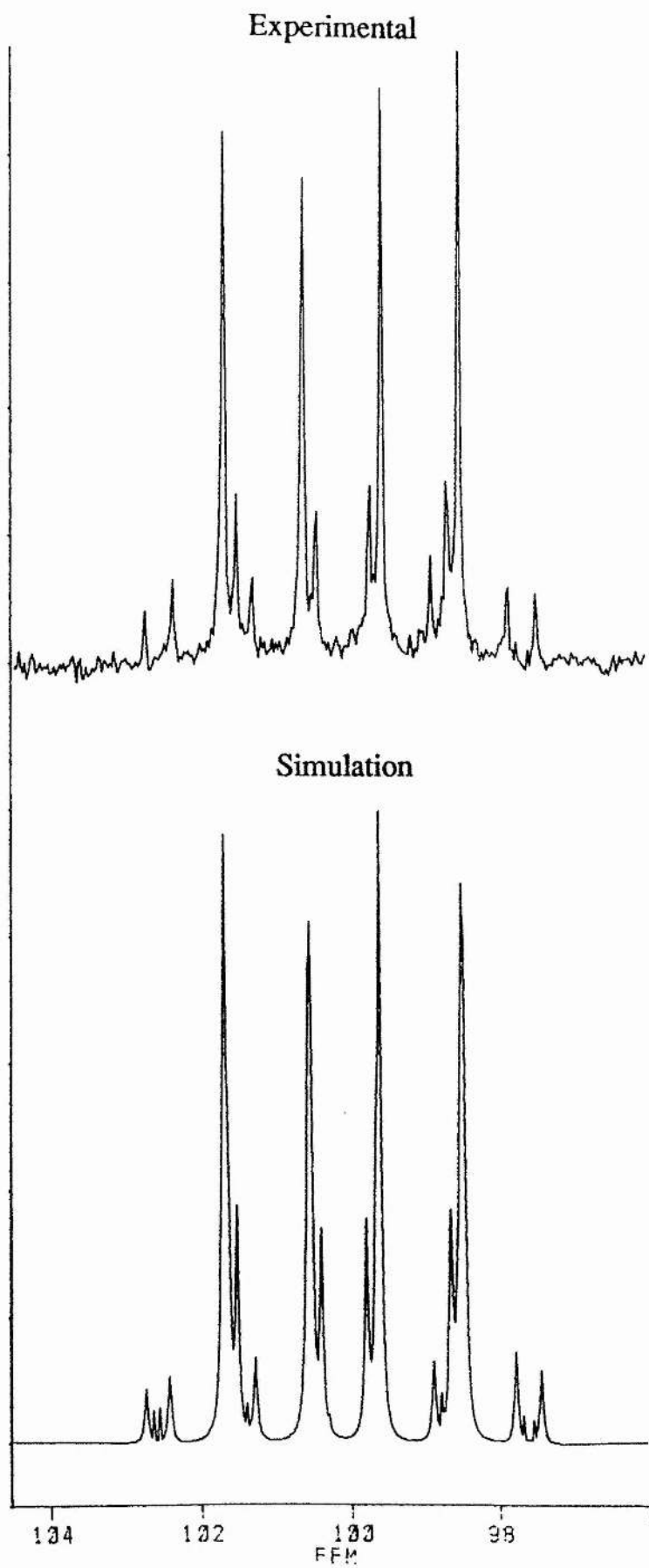


Fig. 3.18 ^{31}P n.m.r. spectrum (300 MHz) of $[\text{Rh}(\text{Ph}_2\text{POPPh}_2)(\text{PPh}_3)_2][\text{PF}_6]$ Part A (CD_2Cl_2 , 25°C)

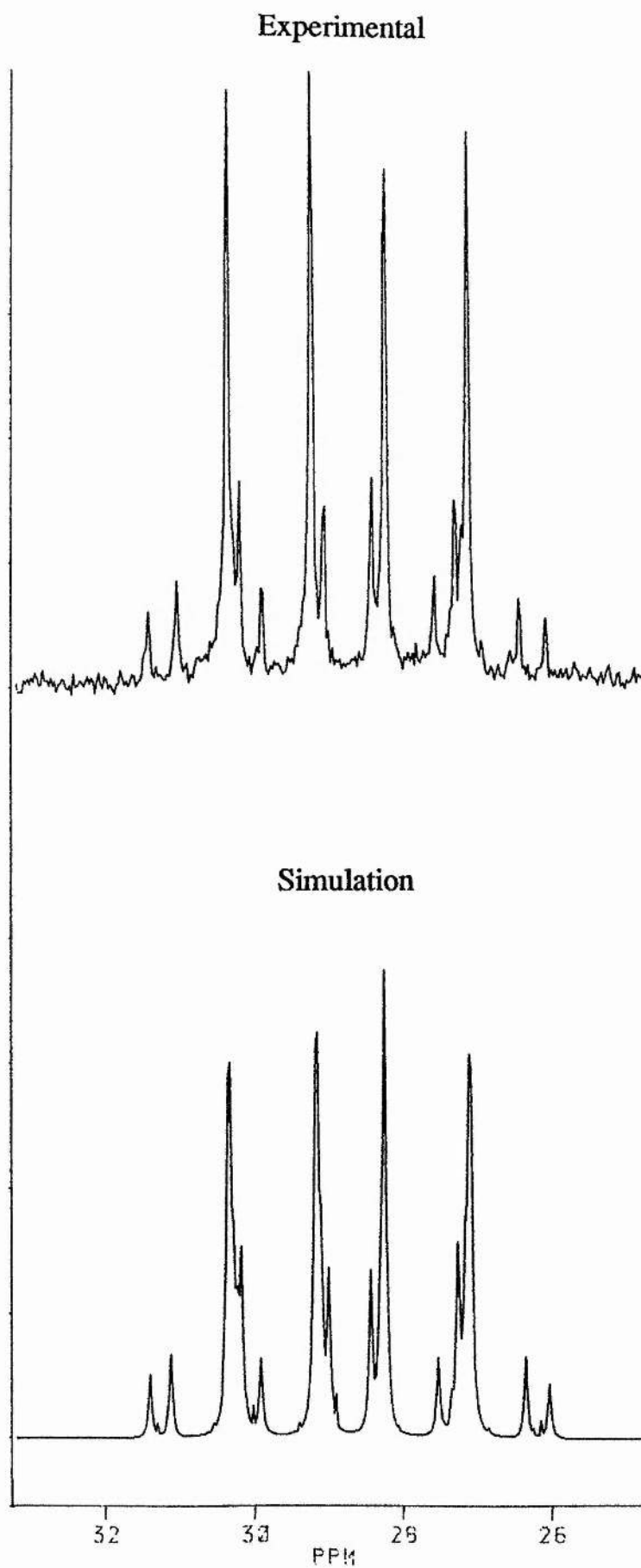


Fig. 3.19 ^{31}P n.m.r. spectrum (300 MHz) of $[\text{Rh}(\text{Ph}_2\text{POPPh}_2)(\text{PPh}_3)_2][\text{PF}_6]$ Part B (CD_2Cl_2 , 25°C)

interpreted in terms of an AA'XX' spin system with resonances at 98.4 and 26.3 ppm. The couplings are summarised in Table 3.3.

F.A.B. Mass Spectral Data

This adds further weight to the spectrometrically derived conclusions. The molecular ion peak occurs at m/z 1013 corresponding to $[\text{Rh}(\text{PPh}_3)_2(\text{Ph}_2\text{POPPh}_2)]^+$. The full fragmentation pattern is shown in Table 3.5.

3.5 Reaction of $[\text{RhCl}(\text{PPh}_3)_3]$, $\text{Ph}_2\text{PO}_2\text{CCHCH}_2$ and TiPF_6

Following a similar procedure to that outlined in Section 3.4 $[\text{RhCl}(\text{PPh}_3)_3]$ and $\text{Ph}_2\text{PO}_2\text{CCH}=\text{CH}_2$ were mixed in THF at ice temperatures and the resulting solution was filtered into an ice cold flask containing just under a mole equivalent of TiPF_6 . A fine white precipitate appeared almost immediately. However the reaction was allowed to proceed for fifteen minutes with constant stirring followed by a further fifteen minutes without stirring during which time the precipitate settled. A bright orange precipitate could be obtained by careful addition of petroleum spirit (40°-60°C). This precipitate was found to contain two products, the minor of which was identified as $[\text{Rh}(\text{PPh}_3)_3(\text{Ph}_2\text{POPPh}_2)][\text{PF}_6]$. The major product could be purified by extraction with diethylether and analysed to be $[\text{Rh}(\text{PPh}_3)_3(\text{O}_2\text{CCH}_2\text{CH}_2\text{PPh}_3)][\text{PF}_6]$.

3.5.1 Spectroscopic Data for



The room temperature spectrum of this complex contains four resonances a doublet of triplets at 51.3 ppm, a doublet of doublets at 34.8 ppm, a singlet at 22.8 ppm and a multiplet at -144.167 ppm. The last of these is the typical resonance exhibited by a PF_6^- anion; the other resonances are indicative of a structure shown in Figure 3.20.

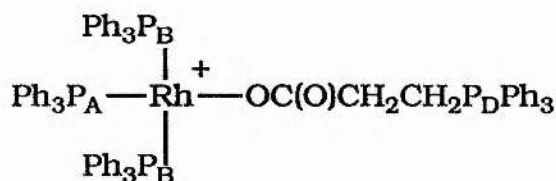


Fig. 3.20

The P_A species gives rise to a doublet of triplets and P_B to a doublet of doublets as observed in all such complexes which have square planar structures in which the coordinated triphenylphosphine ligands are in a T formation (cf. $[\text{RhCl}(\text{PPh}_3)_3]$). The singlet arises from the coordinated zwitterion which is formed from the reaction of the acrylic acid anhydride and triphenylphosphine (see chapter 2) and is coordinated upon dechlorination of the rhodium complex.

^1H n.m.r. Data

Disregarding the phenyl region the only observed

resonances are those of the retained THF and those of the methylene groups of the coordinated zwitterion. These are located at δ 1.67 ppm and δ 1.0 ppm (ratio 1:1) and so support the structure assignment shown in Figure 3.21. The methylene resonances exhibit high field shifts upon coordination, the free ligand values of the zwitterion resonances are located at 3.72 ppm and 2.72 ppm.

Infra-red Data

The infra-red spectrum contains an absorption at ν (1620 cm^{-1}) which is assigned to the $\nu(\text{OC})_{\text{asym}}$ of the zwitterion. This is in the region expected for such carboxyl group coordination as discussed in Chapter 2, and is also the region in which tin complexes of the zwitterion exhibit their $\nu(\text{OCO})$ absorbances. The $\nu(\text{Rh-Cl})$ absorbance is noted to be absent showing that the chloride ligand has been substituted.

F.A.B. m.s.

The highest observed peak is at m/z 961. This peak is not the molecular ion peak but corresponds to a fragment of the form $[\text{Rh}^+(\text{PPh}_3)_3(\text{O}_2\text{CCHCH}_2)]$ in which the PPh_3 unit of the zwitterion has been lost during the bombardment of the sample. The full

fragmentation pattern is listed in Table 3.6.

3.6 Spectroscopic Properties of $[\text{Rh}(\text{PPh}_3)_3(\text{thf})][\text{PF}_6]$ and $[\text{Rh}(\text{PPh}_3)_3(\text{O}_2\text{CCH}=\text{CH}_2)]$

Other possibilities for the complex formed by the reaction are $[\text{Rh}^+(\text{PPh}_3)_3\text{thf}]$ and $[\text{Rh}(\text{PPh}_3)_3(\text{O}_2\text{CCH}=\text{CH}_2)]$. Thus to support the conclusions made in Section 3.5 these complexes were synthesised and their spectroscopic properties studied.

3.6.1 Reaction of $[\text{RhCl}(\text{PPh}_3)_3]$ and TiPF_6 in THF

The formation of a solvent coordinated complex has precedence in the isolation of a complex containing coordinated acetone via a similar reaction to that proposed here⁽¹²⁰⁾. This acetone complex was subsequently used in the synthesis of cationic mixed anhydride complexes (see Figure 3.16) in which the anhydride coordination is via the phosphorus atom and the oxygen atom of the carbonyl group.

The reaction conditions applied were those used in the anhydride reaction described in Section 3.5. An isolated sample of $[\text{RhCl}(\text{PPh}_3)_3]$ was dissolved in a large volume of precooled (0°C) tetrahydrofuran. To this cooled solution slightly less than a mole equivalent of TiPF_6 was added and the resulting suspension stirred at 0°C for approximately 1 hour. After this period the volume was

reduced to approximately 20 mls and the fine white precipitate which appeared during the reaction allowed to settle. The resulting solution was filtered through hiflo celite and further concentrated. A bright orange precipitate was produced upon addition of cold diethyl ether, the resultant solid proved to be indefinitely stable if stored under dinitrogen.

3.6.2 Spectral Data On $[\text{Rh}(\text{PPh}_3)_3(\text{thf})][\text{PF}_6]$

^{31}P n.m.r. Data

The room temperature ^{31}P spectrum (Figure 3.22) proved that the complex produced by this reaction is not that produced in Section 3.5. This profile takes the form of a very broad doublet and a singlet. The broadness of the spectrum indicates the presence of unresolved coupling and also prevents the assignment of a structure to the room temperature form. The low temperature limiting spectrum (Figure 3.23) resolves the coupling, showing three main resonances. This result indicates that the complex is fluxional, this fluxionality being a result of a weak interaction between the rhodium cation $[(\text{PPh}_3)_3\text{Rh}]^+$ and the THF moiety.

The first step of the reaction is dechlorination as shown in Figure 3.24. Slightly less than a mole of TlPF_6 was used to prevent problems with excess thallium by-products during work up of the products.

Fig. 3.22

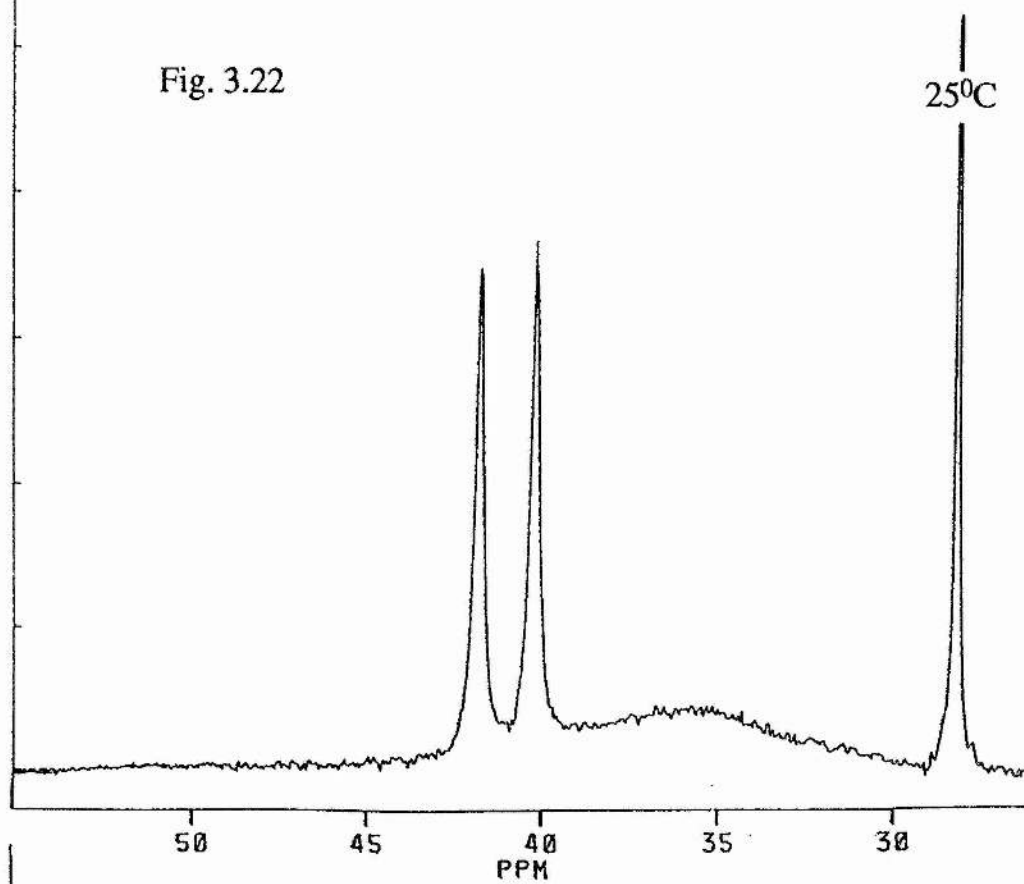
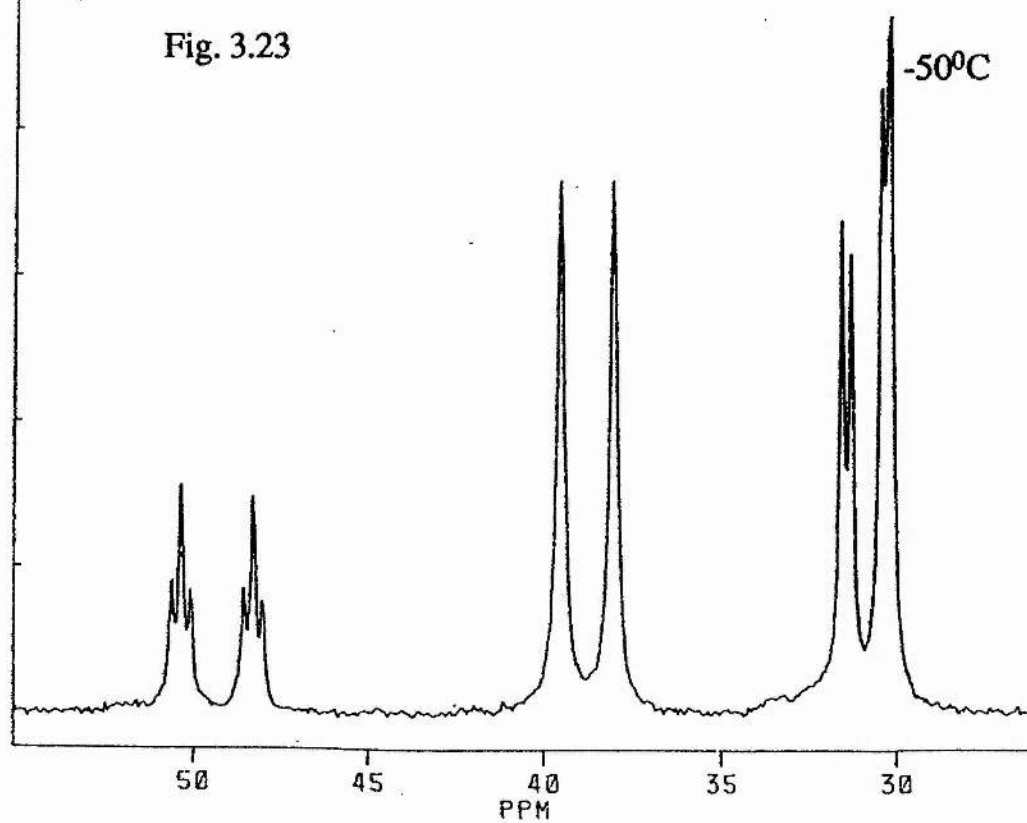


Fig. 3.23



31P n.m.r. spectrum (300 MHz) of $[\text{Rh}(\text{PPh}_3)_3(\text{thf})][\text{PF}_6]$ Part B (CD₂Cl₂)

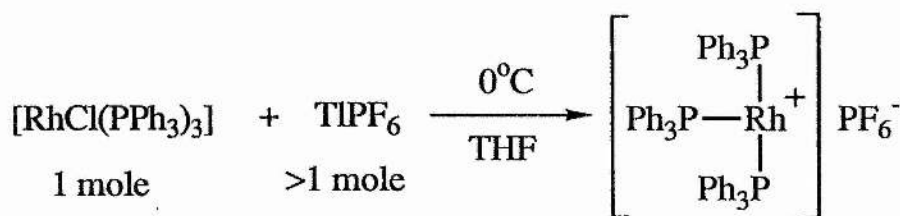


Fig. 3.24

(A)

This cationic species goes on to react with the THF solvent to produce the complex shown in Figure 3.25.

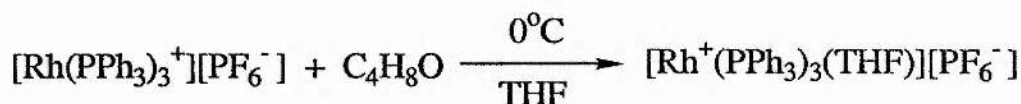


Fig. 3.25

(B)

Complex B gives rise to two of the resonances present in the low temperature limiting spectrum, these being the doublet of triplets at 49.3 ppm and the doublet of doublets at 30.8 ppm. This is the expected spectrum for such $[\text{RhP}_3\text{X}]$ species which are known to be square planar and possesses the structure shown in Figure 3.26a and c. However, the weak interaction between the THF and the rhodium results in this complex readily losing the THF species to reform the cationic species $[\text{Rh}(\text{PPh}_3)_3]^+$ (Figure 3.26b). The loss of the THF ligand leaves the rhodium centre bound to three PPh_3 ligands, a structure which will take up the sterically least hindered Y shaped structure. In this structure the phosphorus species are all in similar environments, resulting in the doublet at 38.8 ppm displaying only the Rh-P coupling. Thus the weak interaction is thought to result in the fast exchange process shown in Figure 3.26 when the solution is at room temperature which results in the

broadness of the ^{31}P n.m.r. spectra, an exchange process which is quenched at low temperature.

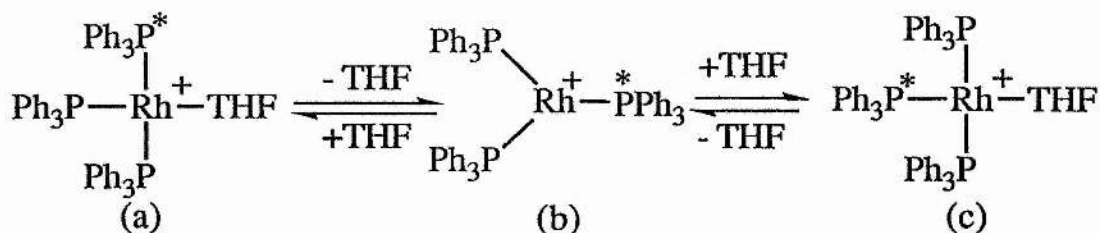


Fig. 3.26

An exchange which has also been observed in the study of $[\text{Rh}(\text{PPh}_3)_3]^+$ salts⁽¹⁷⁷⁾.

^1H n.m.r. Data

The proton n.m.r. contains information in a broad phenyl region. The only other resonances observed are the THF resonances at 3.67 ppm and 1.8 ppm.

Infra-red Data

No information is displayed outside the fingerprint region other than that which is assigned to the phenyl species supporting the structure assignment above. Also noted is the absence of the $\nu(\text{Rh}-\text{Cl})$ absorbance indicating that the $[\text{Rh}(\text{PPh}_3)\text{Cl}]$ starting material has indeed been dechlorinated. Also absent is the absorbance at 1620 cm^{-1} observed for the product discussed in Section 3.6.

Thus the conclusion from this experiment is that the product isolated in section 3.5 is not $[\text{Rh}(\text{PPh}_3)_3(\text{thf})][\text{PF}_6]$.

3.6.3 Reaction of $[\text{RhCl}(\text{PPh}_3)_3]$, TiPF_6 and $\text{K}^+ \text{O}_2\text{CCH}=\text{CH}_2$

This experiment also closely applied the same conditions used in Section 3.5 in the production of $[\text{Rh}(\text{O}_2\text{CCH}_2\text{CH}_2\text{PPh}_3)(\text{PPh}_3)_3][\text{PF}_6]$. The $[\text{RhCl}(\text{PPh}_3)_3]$ and TiPF_6 were reacted as in 3.6.1. and the product was then filtered into a precooled flask containing a mole equivalent of $\text{K}^+ \text{O}_2\text{CCH}=\text{CH}_2$. Upon addition of the metal containing solution to this flask a fine white precipitate was observed (KPF_6). The reaction was allowed to proceed for approximately 1 hour after which the reaction mixture was filtered and concentrated. A precipitate could then be obtained upon the addition of petroleum spirit. The filtered precipitate was then washed with diethyl ether.

3.6.4 Spectral Data for $[\text{Rh}(\text{PPh}_3)_3(\text{O}_2\text{CCHCH}_2)]$

^{31}P n.m.r. Data

The room temperature ^{31}P n.m.r. spectrum contained two resonances, a doublet of triplets at 51.2 ppm and a doublet of doublets at 33.2 ppm. This is consistent with the structure being

that shown in Figure 3.27. The PF_6 resonances were also noted to be absent.

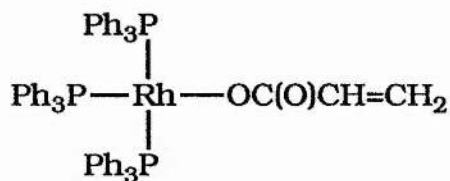


Fig 3.27

It is also noted that these resonances are shifted slightly down field from those of the starting material. This is similar to the observations made in the case of the $[\text{Rh}(\text{PPh}_3)_3(\text{O}_2\text{CCH}_2\text{CH}_2\text{PPh}_3)][\text{PF}_6]$ and supports the conclusion that the product discussed in Section 3.5 is coordinated via an oxygen atom of a carboxyl group.

Infra-red Data

This also exhibits no $\nu(\text{Rh}-\text{Cl})$ absorbance and a $\nu(\text{OC})$ absorbance in this case located at 1625 cm^{-1} . This latter band is very broad and is thought also to contain the $\nu(\text{C}=\text{C})$ absorbance which appears in this region in the free ligand.

^1H n.m.r. Data

This definitely proves that this complex is not that isolated in Section 3.5 because all the proton data occurs in the region

around $\delta 7$ ppm. There is no evidence for any proton resonances outside this area suggesting that the protons of the acrylic anion are subject to small upfield shifts upon coordination to the metal centre.

Thus this experiment leads to two conclusions. (1) This complex is not that isolated in Section 3.5 (2) but it can be concluded that both complexes have replaced the chlorine species with a new ligand coordinated via a carboxylato group.

Table 3.1	Spectral Data for Tetraphenyldiphosphoxane (CD ₂ Cl ₂ , 25°C)			
Compound	¹ H	³¹ P		IR
		δ (PPM)	J (Hz)	
Ph ₂ P ^a P ^b (O)Ph ₂	All Resonances are in the phenyl region between δ 6.8 and δ 8.0	Pa 37.2d	227.2	ν (P-C) = 1430
		Pb -22.9d		1120 1105 ν (P=O) = 1170

Table 3.2		I.R and ¹ H n.m.r. Data for Rhodium Complexes of Rearranged Mixed Anhydrides				
Complex	I.R. (cm ⁻¹)			¹ H Chemical Shift (ppm)*		
	v(P-O)asym	v(Rh-Cl)	v(OCO)asym	a	b	
[Rh(Ph ₂ POPPh ₂)(PPh ₃)Cl]	800	290	----	All resonances in the phenyl region		
[Rh(Ph ₂ POPPh ₂)(PPh ₃) ₂][PF ₆]	830	----	----	All resonances in the phenyl region		
[Rh(PPh ₃) ₃ (O ₂ CH ₂ ^a CH ₂ ^b PPh ₃)]][PF ₆]	----	----	1620	1.00	1.67	
[Rh(PPh ₃) ₃ (OC ₄ H ₈ ^{a,b})]][PF ₆]	----	----	----	1.80	3.67	
[Rh(PPh ₃) ₃ (O ₂ CH=CH ₂)]	----	----	1625	All resonances in the phenyl region		

* 25°C , CD_2Cl_2

Table 3.3 ^{31}P n.m.r. Data for Rhodium Complexes of Rearranged Mixed Anhydrides (25°C , CD_2Cl_2)

Complex	^{31}P n.m.r. Data for Rhodium Complexes of Rearranged Mixed Anhydrides (25°C , CD_2Cl_2)	Chemical Shifts				Coupling Constants (Hz)									
		Pa	Pb	Pc	Pd	RhPa	RhPb	RhPc	RhPd	PaPb	PaPc	PaPd	PbPc	PbPd	PcPd
$[\text{Rh}(\text{Ph}_2\text{P}^a\text{OPP}^b\text{h}_2)(\text{P}^c\text{Ph}_3)\text{Cl}]$		106.5ddd	81.2ddd	25.1ddd	—	170	125	132	—	122	30	—	382	—	—
$[\text{Rh}^+(\text{Ph}_2\text{P}^a\text{OP}^b\text{Ph}_2)(\text{P}^c\text{Ph}_3)_2]^\dagger$		100.2	100.15	28.56	28.5	135	130	138	140	117	-45	271	292	-25	25
$[\text{Rh}^+(\text{P}^{a,b}\text{Ph}_3)_3(\text{O}_2\text{CH}_2\text{CH}_2\text{P}^c\text{Ph}_3)]^\dagger$		51.3dt	34.8dt	22.2s	—	177	152	—	—	42	—	—	—	—	—
$[\text{Rh}(\text{P}^{a,b}\text{Ph}_3)_3(\text{OC}_4\text{H}_9)][\text{PF}_6]$		49.3dt	30.8dt	—	—	245	133	—	—	31	—	—	—	—	—
$[\text{Rh}(\text{P}^a\text{Ph}_3)_3][\text{PF}_6]^*$		38.8dt	—	—	—	179	—	—	—	—	—	—	—	—	—
$[\text{Rh}(\text{P}^{a,b}\text{Ph}_3)_3(\text{O}_2\text{CH}=\text{CH}_2)]$		51.1dt	33.2dd	—	—	190	146	147	—	40	—	—	—	—	—

* -30°C $^\dagger [\text{PF}_6]$ counter ion

Table 3.4F.A.B. m.s. Fragmentation Pattern of $[\text{Rh}_2\text{Cl}_2(\text{PPh}_3)_2(\text{Ph}_2\text{POPPh}_2)_2]$

	m/z
$[\text{Rh}_2(\text{PPh}_3)_2\text{Cl}_2(\text{Ph}_2\text{POPPh}_2)_2]^+$	1075
$[\text{Rh}_2\text{Cl}_2(\text{Ph}_2\text{POPPh}_2)_2]^+$	1049
$[\text{Rh}_2\text{Cl}(\text{Ph}_2\text{POPPh}_2)_2]^+$	1013
$[\text{Rh}_2(\text{PPh}_3)\text{Cl}(\text{Ph}_2\text{POPPh}_2)]^+$	889
$[\text{Rh}(\text{PPh}_3)(\text{Ph}_2\text{POPPh}_2)]^+$	751
$[\text{Rh}_2\text{Cl}(\text{Ph}_2\text{POPPh}_2)]^+$	627

Table 3.5F.A.B. m.s. Fragmentation Pattern of $[\text{Rh}(\text{PPh}_3)_2(\text{Ph}_2\text{POPPh}_2)][\text{PF}_6]$

	m/z
$[\text{Rh}(\text{PPh}_3)_2(\text{Ph}_2\text{POPPh}_2)]^+$	1013
$[\text{Rh}(\text{PPh}_3)(\text{PPh}_2)_3]^+$	766

$[\text{Rh}(\text{PPh}_3)(\text{Ph}_2\text{POPPh}_2)]^+$	751
$[\text{Rh}(\text{PPh}_3)_2]^+$	627
$[\text{Rh}(\text{PPh}_3)(\text{Ph}_2\text{PO})]^+$	350

Table 3.6F.A.B. m.s. Fragmentation Pattern of $[\text{Rh}(\text{PPh}_3)_3(\text{O}_2\text{CCH}_2\text{CH}_2\text{PPh}_3)]\text{PF}_6$

	m/z
$[\text{Rh}(\text{PPh}_3)_3(\text{O}_2\text{CCH}_2\text{CH}_2)]^+$	961
$[\text{Rh}(\text{PPh}_3)_3]^+$	889
$[\text{Rh}(\text{PPh}_3)(\text{PPh}_2)_2(\text{O})]^+$	751
$[\text{Rh}(\text{PPh}_2)(\text{PPh}(\text{OCO}))]^+$	718
$[\text{Rh}(\text{PPh}_3)_2]^+$	627
$[\text{Rh}(\text{PPh}_3)(\text{PPh}_2)(\text{OC})]^+$	593
$[\text{Rh}(\text{PPh}_3)(\text{PPh}_2)(\text{O})]^+$	566
$[\text{Rh}(\text{PPh}_3)(\text{PPh}_2)]^+$	550
$[\text{Rh}(\text{PPh}_3)(\text{OC})]^+$	393
$[\text{Rh}(\text{PPh}_3)]^+$	365

3.7 Experimental

Mixed Anhydrides of Acrylic and Vinylacetic Acids

These were produced using the methods detailed in Section 2.10

$\text{Ph}_2\text{P(O)PPh}_2$

Produced via the literature methods⁽¹⁷³⁾

$[\text{RhCl}(\text{PPh}_3)(\text{Ph}_2\text{POPPh}_2)]$

To a cooled (0°C) solution of $[\text{RhCl}(\text{PPh}_3)_3]$ (0.5g, 0.54 mmol) a similarly cooled tetrahydrofuran solution of $\text{Ph}_2\text{PO}_2\text{CCH}=\text{CH}_2$ (0.28g, 1.08 mmol) was introduced using the in-situ method developed in chapter 2. The reaction was allowed to proceed for approximately 1-2 hours, with a colour change to orange noted, then filtered and the volume reduced to approximately 10 cm^3 . Crystals were obtained on standing for several days at -30°C and needed no further purification. Yield 0.3g (78%).

Theoretical $[\text{RhCl}(\text{PPh}_3)(\text{Ph}_2\text{POPPh}_2)]\cdot\text{thf} = \text{C } 64.3\%; \text{H } 5.0\%$

Found $[\text{RhCl}(\text{PPh}_3)(\text{Ph}_2\text{POPPh}_2)]\cdot\text{thf} = \text{C } 64.3\%; \text{H } 5.0\%$

$[\text{Rh}(\text{PPh}_3)_2(\text{Ph}_2\text{POPPh}_2)][\text{PF}_6]$

To an isolated sample of $[\text{RhCl}(\text{PPh}_3)(\text{Ph}_2\text{POPPh}_2)]$ (0.2g, 0.25 mmol) in tetrahydrofuran at 0°C slightly less than a mole equivalent of TiPF_6 was added and the reaction allowed to proceed with stirring for 15 minutes. During this time a fine white precipitate

appeared. After a further 15 minute period without stirring to allow the precipitate to settle, the solution was filtered through hiflo celite and the volume reduced. A yellow precipitate could be obtained by careful addition of petroleum ether. Yellow needle like crystals could be produced by careful recrystallisation from a dichloromethane solution. Yield 0.1g (40%)

Theoretical $[\text{Rh}(\text{PPh}_3)_2(\text{Ph}_2\text{POPPh}_2)][\text{PF}_6].\text{thf} = \text{C } 62.5\%; \text{H } 4.8\%$

Found $[\text{Rh}(\text{PPh}_3)_2(\text{Ph}_2\text{POPPh}_2)][\text{PF}_6].\text{thf} = \text{C } 62.5\%; \text{H } 4.8\%$

$[\text{Rh}(\text{PPh}_3)_3(\text{PPh}_3\text{CH}_2\text{CH}_2\text{CO}_2)]$

This method followed that described for the production of $[\text{RhCl}(\text{PPh}_3)(\text{Ph}_2\text{POPPh}_2)]$, but in addition slightly less than a mole equivalent of TiPF_6 was added after time periods varying from 1 hour to 1 day to the initial reaction solution. The fine white precipitate was allowed to settle, the solution filtered and its volume reduced to about 10 cm³. Bright orange crystallites were obtained after standing for approximately 1 day and needed no further purification. Yield 0.33g (64%).

Theoretical $[\text{Rh}(\text{PPh}_3)_3(\text{PPh}_3\text{CH}_2\text{CH}_2\text{CO}_2)][\text{PF}_6].\text{thf} \quad \text{C } 65.8\%; \text{H } 5.0\%$

Found $[\text{Rh}(\text{PPh}_3)_3(\text{PPh}_3\text{CH}_2\text{CH}_2\text{CO}_2)][\text{PF}_6].\text{thf} \quad \text{C } 66.0\%; \text{H } 4.7\%$

$[\text{Rh}(\text{PPh}_3)_3(\text{thf})][\text{PF}_6]$

To a cooled (0°C) solution of $[\text{RhCl}(\text{PPh}_3)_3]$ (0.3g, 0.32 mmol) slightly less than a mole equivalent of TiPF_6 was added and the

solution stirred for 15 minutes. The fine white precipitate was then allowed to settle over a further fifteen minutes, after which the solution filtered and its volume reduced to about 10 cm³. A bright orange precipitate was obtained upon careful addition of petroleum spirit(40-60°). The complex was then identified by spectroscopic methods.

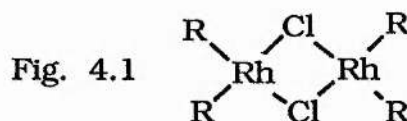
[Rh(PPh₃)₃ (O₂CCH=CH₂)]

Under similar conditions to those used in the production of [Rh(PPh₃)₃ (PPh₃CH₂CH₂CO₂)] just under a mole equivalent of TlPF₆ was added a [Rh(PPh₃)₃ Cl] solution with the appearance of a white precipitate. The resultant solution was then filtered into a precooled flask containing a mole equivalent of K⁺ CO₂CH=CH₂. Upon addition of the metal containing solution a fine white precipitate was observed (KPF₆). The reaction was then allowed to proceed for one hour after which it was filtered and concentrated. A precipitate could then be obtained upon the addition of petroleum spirit, and was washed exhaustively with diethyl ether. The complexes were then identified by spectroscopic techniques.

CHAPTER 4

Reactions of Mixed Anhydrides and Rhodium Chlorine Bridged Dimers

With the discovery that the AAA complex $[\text{RhCl}(\text{AAA})\text{PPh}_3]$ reacted with PPh_3 to reform Wilkinson's Catalyst (see Chapter 2), attention was directed toward metal starting materials which did not contain triphenylphosphine. Consequently rhodium chlorine bridged dimers, the general form of which is shown in Figure 4.1, were chosen, as similar work with the higher substituted anhydrides had resulted in chelate binding of the mixed anhydride, *via* the phosphorus atom and the double bond, without exception (117,131).



4.1 General Method for the Anhydride/Dimer Reactions

The general method employed for the reactions between the mixed anhydrides and the rhodium dimers was as follows. The mixed anhydride was added via the in-situ method to a suspension or solution of the rhodium dimer (1 mole of anhydride per mole of Rh) at 0°C under a dinitrogen atmosphere. This produced a very slight colour change, the solution being more yellow after addition and also resulted in the complete dissolution of the metal complex in the case of $[(\text{RhCl}(\text{C}_8\text{H}_{14})_2)_2]$. The reaction was allowed to

proceed for about an hour after which time the reaction solution was concentrated to approximately half its volume. From this solution, by careful addition of petroleum ether (40-60°), an orange precipitate was isolated and washed exhaustively with cold diethyl ether. The spectroscopic properties of these compounds, summarised in Tables 4.1-4.3, indicate firstly that the anhydrides are bound through the phosphorus atom and the double bond and secondly that the complexes are chlorine bridged dimers.

4.2 Spectroscopic Details of Anhydride/Dimer Complexes

4.2.1 Infra-red Data

The chelate nature of the anhydride coordination is indicated by the shift of the carbonyl band to the 1740 cm^{-1} region and the disappearance of the $\nu(\text{C}=\text{C})$ band upon coordination (see Chapter 2). The presence of the chlorine bridge is confirmed by the existence of a rhodium-chloride stretch in the region of 280 cm^{-1} .

4.2.2 ^{31}P n.m.r. Spectrum

A) CAA Dimer

With the dimeric complexes of the highly substituted mixed anhydrides there is no indication of more than one isomer of the product. However the ^{31}P spectrum of the dimeric CAA complex, which had been isolated prior to the commencement of this study, does not contain a single doublet, rather it displays two doublets, at 132.2 ppm and 131.9 ppm (119,131) (see Figure 4.2). It

was concluded that these arose from two different isomers of the product.

The appearance, for the CAA complex, of two isomers indicates that as a result of reducing the steric bulk of the alkene substituents the preferred conformer changes. This is an exact analogy to the Wilkinson's Catalyst/mixed anhydride complexes discussed in Chapter 2, a mixture of isomers being obtained from the complex containing CAA. In the series of anhydride complexes derived from Wilkinson's Catalyst, the CAA complex was also discovered to exist in two isomers (*cis* and *trans*). However with an anhydride containing a less sterically hindered alkene moiety the resultant complex was found to exist in the *trans* form only. This trend was found to be mirrored in the dimeric systems, as the AAA dimer was found in only one of the isomeric forms.

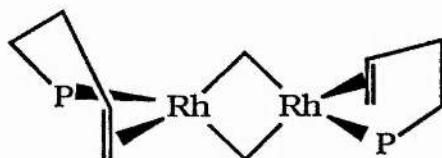


Fig. 4.3

Isomer A

Isomer A is the preferred isomer for the dimeric complexes of mixed anhydrides containing highly substituted alkene species, no second isomer being detected by ^{31}P n.m.r. even when the solutions are cooled or warmed⁽¹¹⁹⁾. When the CAA dimeric complex was first isolated one isomer was assigned as A (Figure 4.3) and it was thought that the other might be a mixture of isomers B and C (Figure 4.4).

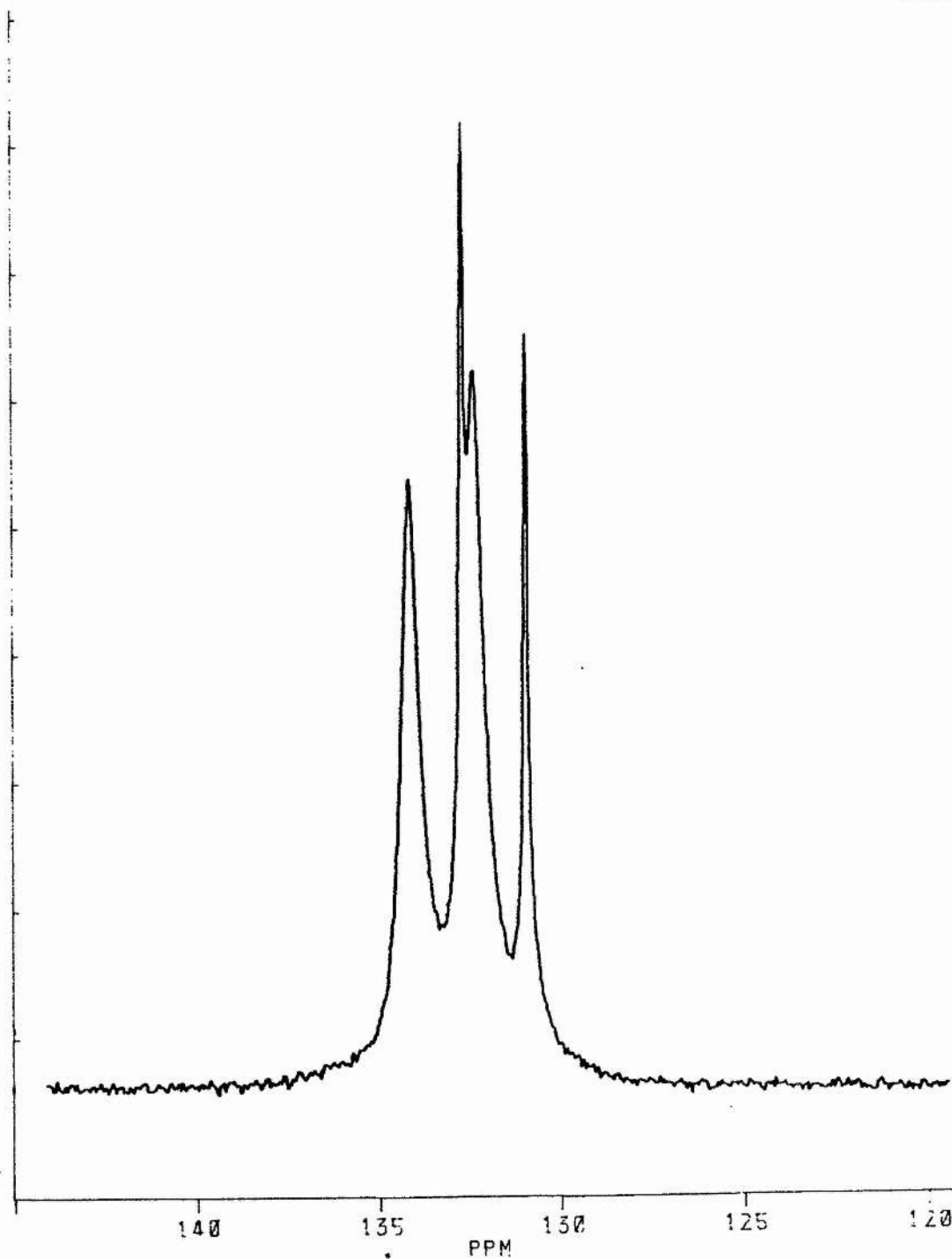
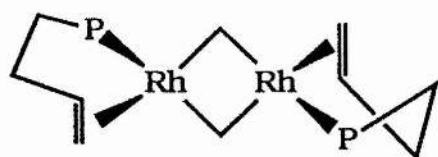
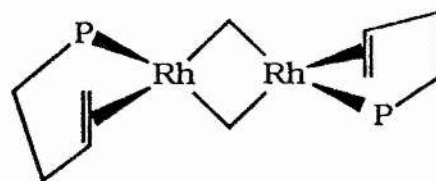


Fig. 4.2 ^{31}P n.m.r. spectrum of $[(\text{RhCl}(\text{Ph}_2\text{PO}_2\text{CCH}=\text{CHMe}))_2]$
(CD_2Cl_2 , 25°C)



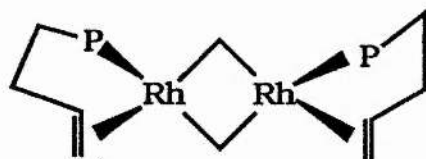
Isomer B



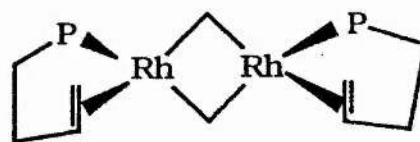
Isomer C

Fig. 4.4

These are still *trans* isomers, but they differ in the relative face of the alkene presented to the metal. However only one doublet will be observed for B and C because they are enantiomorphs and thus contain phosphorus nuclei which are magnetically indistinguishable⁽¹⁷⁸⁾. However in the light of the Wilkinson's Catalyst studies an alternative explanation must now be considered, namely that, as the Wilkinson's catalyst series is observed to move from *cis* \rightarrow *trans* so the dimeric series may move from *trans* \rightarrow *cis*. There will be, as with the *trans* case, three possible *cis* isomers, the most favoured being those equivalent to *trans* isomer A (Figure 4.5), thus the actual isomeric change may be from *trans* A \rightarrow *cis* B and *cis* C.



Cis B



Cis C

Fig. 4.5

In the Wilkinson's Catalyst/CAA example the *trans* isomer was found to be the minor isomer, in the dimeric case it will be impossible to decide the relative percentages present until a crystal

structure has been obtained. This is because it is impracticable to assign the observed doublets to either of the isomeric possibilities by ^{31}P n.m.r. alone owing to the purely empirical nature of the Δ_R contribution.

B) AAA Dimer

Although ^{31}P n.m.r. studies show that only one isomer of $[\text{Rh}(\text{AAA})\text{Cl}]_2$ is present in solution two other products are also observed (Figure 4.6a). The reasoning behind the assignments of these complexes is dealt with in later sections, it will suffice here to assign the broad doublet at 109.2 ppm to the complex $[\text{RhCl}(\text{Ph}_2\text{PO}_2\text{CCH}=\text{CH}_2)_2]$ (Figure 4.20) and the doublet of doublets at 136.5 ppm and apparent doublet of triplets at 131.8 ppm (the second set of resonances are obscured by the main $[\text{Rh}_2\text{Cl}_2(\text{AAA})_2]$ doublet) as $[\text{Rh}_2\text{Cl}_2(\text{Ph}_2\text{PO}_2\text{CCH}=\text{CH}_2)_2(\text{Ph}_2\text{POPPh}_2)]$, a complex containing two bidentate AAA ligands and a $\text{Ph}_2\text{POPPh}_2$ bridge (Figure 4.11). A very approximate calculation of the relative percentage gives values of $[\text{Rh}_2\text{Cl}_2(\text{AAA})_2]=71\%$, $[\text{RhCl}(\text{AAA})_2]=20\%$ and $[\text{Rh}_2\text{Cl}_2(\text{AAA})_2(\text{tpdp})]=9\%$. A pure sample of $[\text{Rh}_2\text{Cl}_2(\text{AAA})_2]$ (Figure 4.6b) could be obtained by the method described in Section 4.7.

C) VAA Dimer

The reaction of VAA and the rhodium dimer also produces

a result different from that obtained with $[\text{RhCl}(\text{PPh}_3)_3]$. With $[\text{RhCl}(\text{PPh}_3)_3]$ the VAA ligand was found to undergo a metal promoted double bond migration so that the isolated product contained the CAA not the VAA ligand. The product of the VAA/dimer reaction exhibits the correct shifts for phosphorus, double bond binding but in this case coordination is through the double bond in the original VAA position with no migration observed. Again no real assignment to the stereochemistry of the product can be made although it may be one of the four structures shown in figure 4.7. It is noted however, that the larger chain between the phosphorus atom and the double bond will lead to greater flexibility and possible fluxionality. Once again only one isomer is observed, although the ^{31}P resonances do exhibit some broadening.

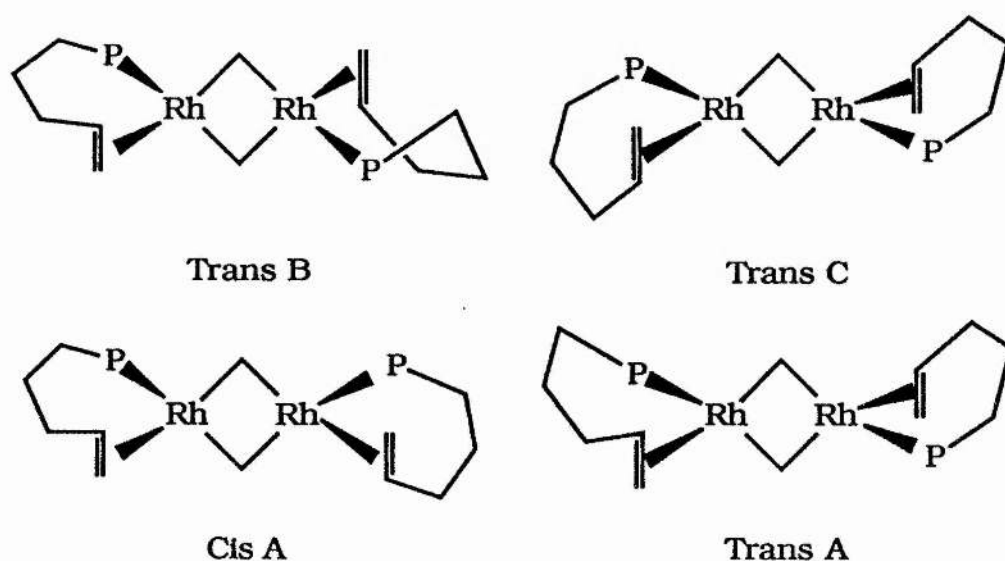
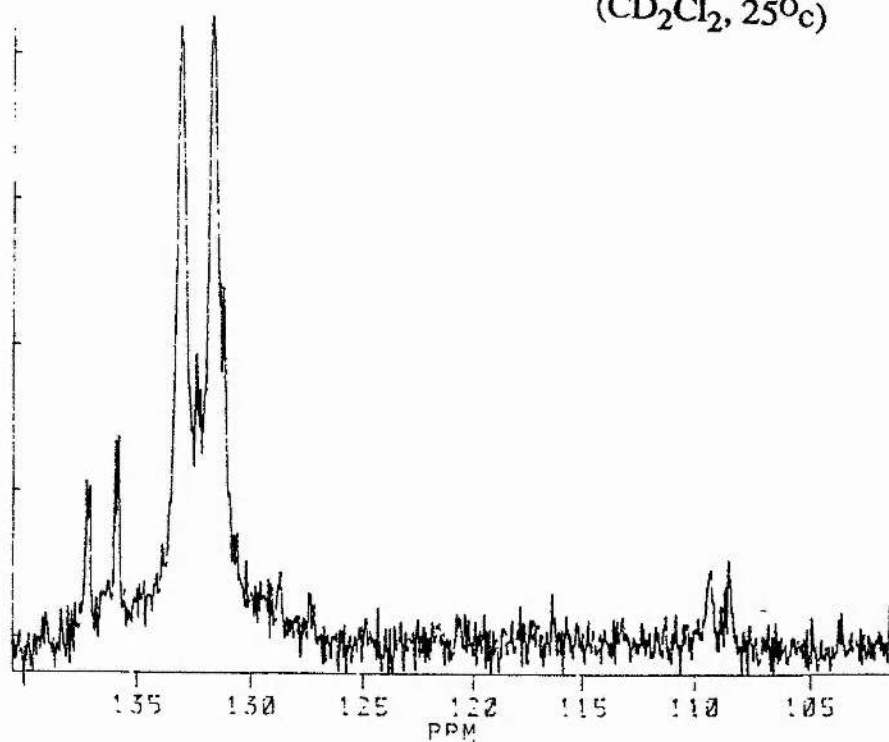


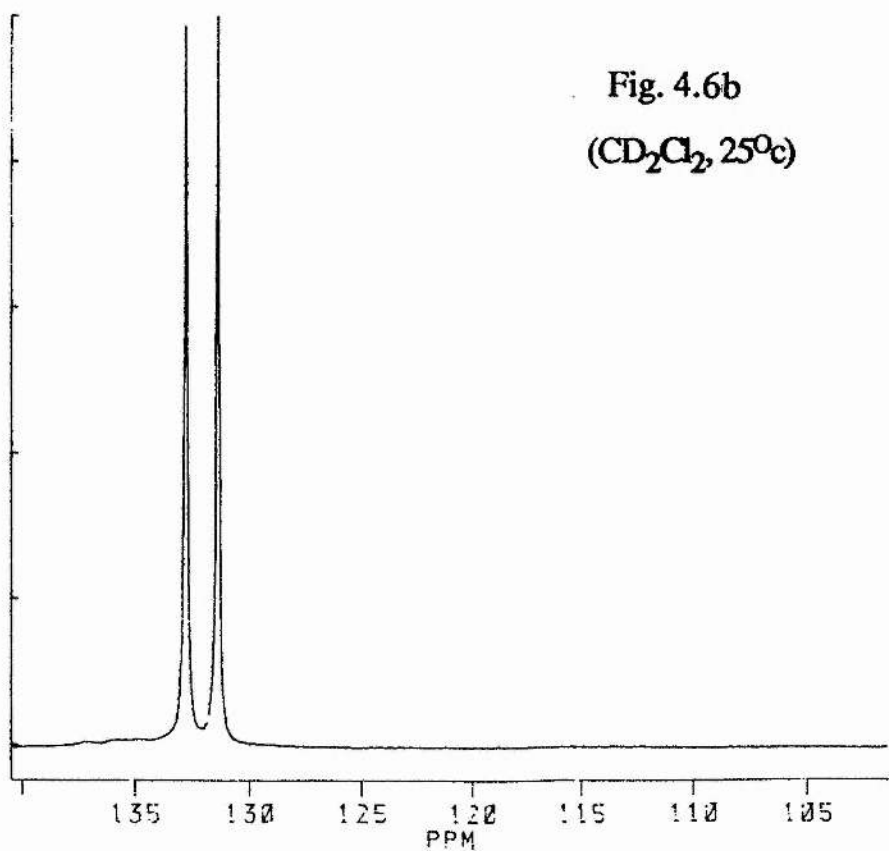
Fig. 4.7

Fig. 4.6a

(CD₂Cl₂, 25°C)

³¹P n.m.r. spectrum of [(RhCl(Ph₂PO₂CCH=CH₂))₂] reaction solution

Fig. 4.6b

(CD₂Cl₂, 25°C)

³¹P n.m.r. spectrum of [(RhCl(Ph₂PO₂CCH=CH₂))₂] purified

Almost certainly, the lack of double bond isomerisation observed with the dimeric VAA complex arises because the metal is insufficiently electron rich to promote the required formation of the hydrido-allyl intermediate. Most dimers of this kind have not been reported to act as alkene isomerization catalysts.

4.2.3 Summary of ^{31}P n.m.r. Conclusions

A pictorial summary of the information obtained from the ^{31}P n.m.r. information from the cyclooctene/rhodium dimer reactions is shown in Figures 4.8 and 4.9.

4.2.4 ^1H n.m.r. Studies of Rhodium Cyclooctene Derived Anhydride Dimers

The proton n.m.r. spectra of these dimers all confirm the presence of the ligands bound through the phosphorus atom and the double bond. The spectral data, summarized in Table 4.2, shows the correct shifts to higher field for the vinylic protons associated with π coordination of the double bond to the metal. For all the complexes these are observed in the region $\delta 2.5\text{--}2.7$ ppm. The resonance from the methyl hydrogen atoms in $[(\text{RhCl}(\text{CAA}))_2]$ also shifts up field on coordination but only by 0.5 ppm. For the VAA complex, the methylene protons give a broad resonance at $\delta 5.6$ ppm. For all the possible structures, Hd and He should be non equivalent unless there is some fluxionality (e.g. rotation about the

alkene-Rh bond).

4.3 Effects of Altering The Mole Ratio Of the AAA/Octene Dimer Reaction And Spectral Evidence for



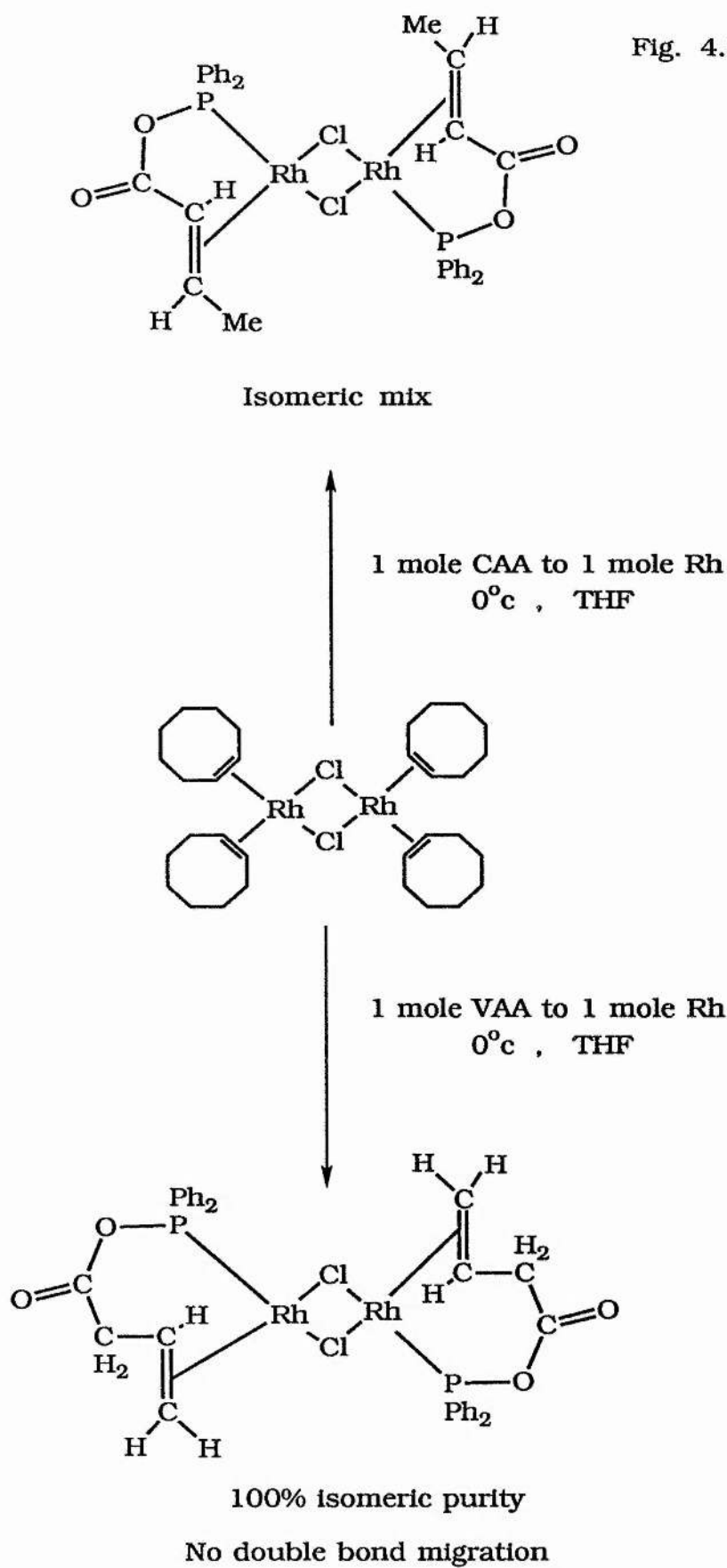
As shown in Section 4.2.3 the 1:1 AAA/Octene dimer reaction gives rise to three products. It was found that by altering the molar ratio of anhydride to metal used in the reaction, the relative yields of these products could be changed.

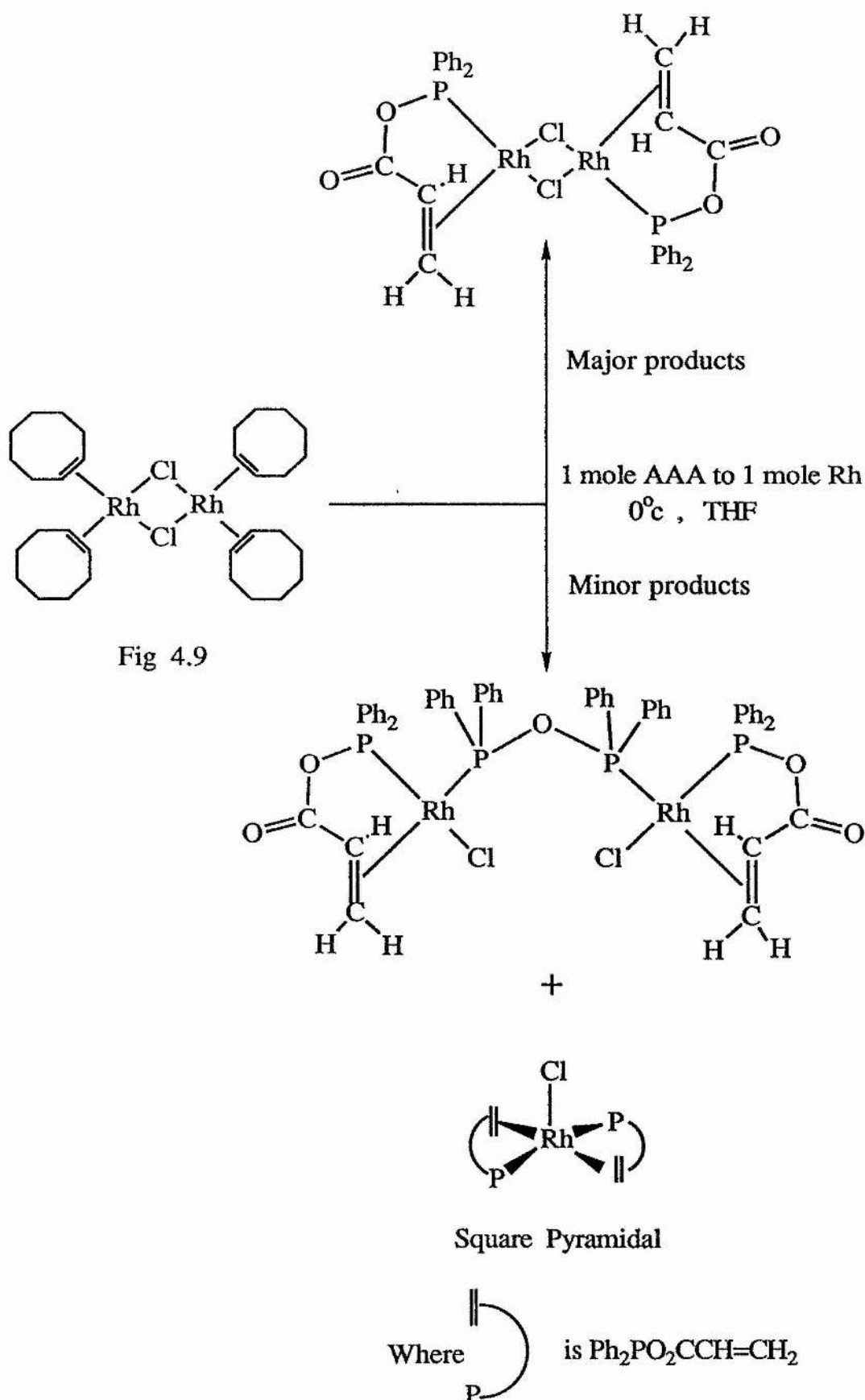
If 2 moles of AAA were added per mole of rhodium and the reaction procedure then followed as before. The only differences noted were a more drastic colour change to bright yellow upon addition of the AAA ligand and the appearance of a fine white precipitate during the reaction which was removed by filtration. Bright yellow crystallites could then be obtained by allowing the concentrated reaction solution to stand at -3°C for 2-3 days. These bright yellow crystallites, which analysed as $[\text{Rh}_2\text{Cl}_2(\text{AAA})_2(\text{Ph}_2\text{POPPh}_2)]\cdot\text{thf}$, were found to be relatively stable in air for short periods of time and indefinitely stable if stored at 0°C and under dinitrogen.

Infra-red Data

The carbonyl band of these yellow crystals is located at 1740 cm^{-1} suggesting that there is a bidentate anhydride ligand.

Fig. 4.8





The $\nu(\text{C}=\text{C})$ band is also missing which is consistent with this conclusion. Other features present are the Rh-Cl band at 280 cm^{-1} and a band at 855 cm^{-1} unobserved in any previous anhydride/dimer product. This novel band is assigned to be the $\nu(\text{P}-\text{O}-\text{P})_{\text{asym}}$ of a $\text{Ph}_2\text{POPPh}_2$ (tpdp) ligand. From work already published the typical position for both the $\nu(\text{P}-\text{O}-\text{P})_{\text{asym}}$ and $\nu(\text{P}-\text{O}-\text{P})_{\text{sym}}$ bands of a chelate tpdp ligand is in the region of 760 cm^{-1} (176). This higher position is the typical region for $\nu(\text{P}-\text{O}-\text{P})_{\text{asym}}$ of a bridging tpdp ligand as, for example, in $[(\text{CO})_5\text{W}(\text{R}_2\text{POPR}_2)\text{W}(\text{CO})_5]$ (179).

^1H n.m.r. Data

The majority of the information of the proton spectrum is contained in the phenyl region which is too complex to interpret accurately. However it also contains resonances from a AAA ligand bound through the phosphorus atom and the double bond at $\delta 3.41$ ppm (H_a) and 3.0 ppm (both H_c and H_b).

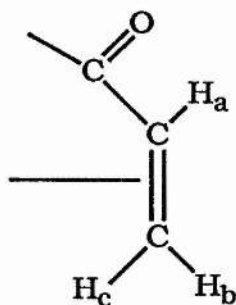


Fig. 4.10

The F.A.B. mass spectrum of the crystallites proved to be very informative. The results of this analysis are listed in Table 4.4 and show that the molecular ion is $[(\text{RhCl}(\text{Ph}_2\text{POCCH}=\text{CH}_2))_2(\text{Ph}_2\text{POPPh}_2)]$. Thus the structure, in broad terms, suggested by the IR, ^1H n.m.r. and F.A.B. studies is a dimeric complex containing two chelate anhydride ligands and a bridging tpdp ligand as shown in Figure 4.11.

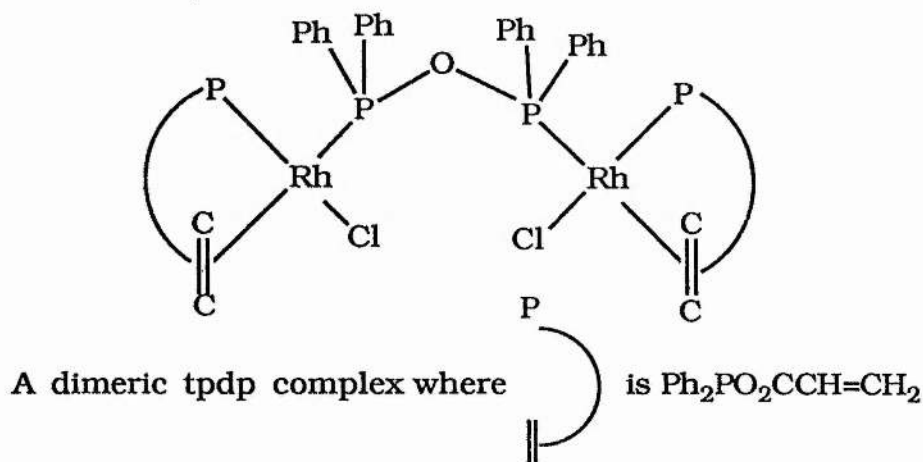


Fig. 4.11

where the phenyl groups have been missed out for simplicity.

^{31}P n.m.r. Data

The ^{31}P n.m.r. spectrum proves to be second order consisting of a doublet of doublets at 136.5 ppm and an apparent doublet of triplets at 131.8 ppm (see Figure 4.12a). The spectrum was simulated using the P.A.N.I.C. simulation program⁽¹⁸⁰⁾ (Figure 4.12b) and found to fit the structure if both of the anhydride ligands

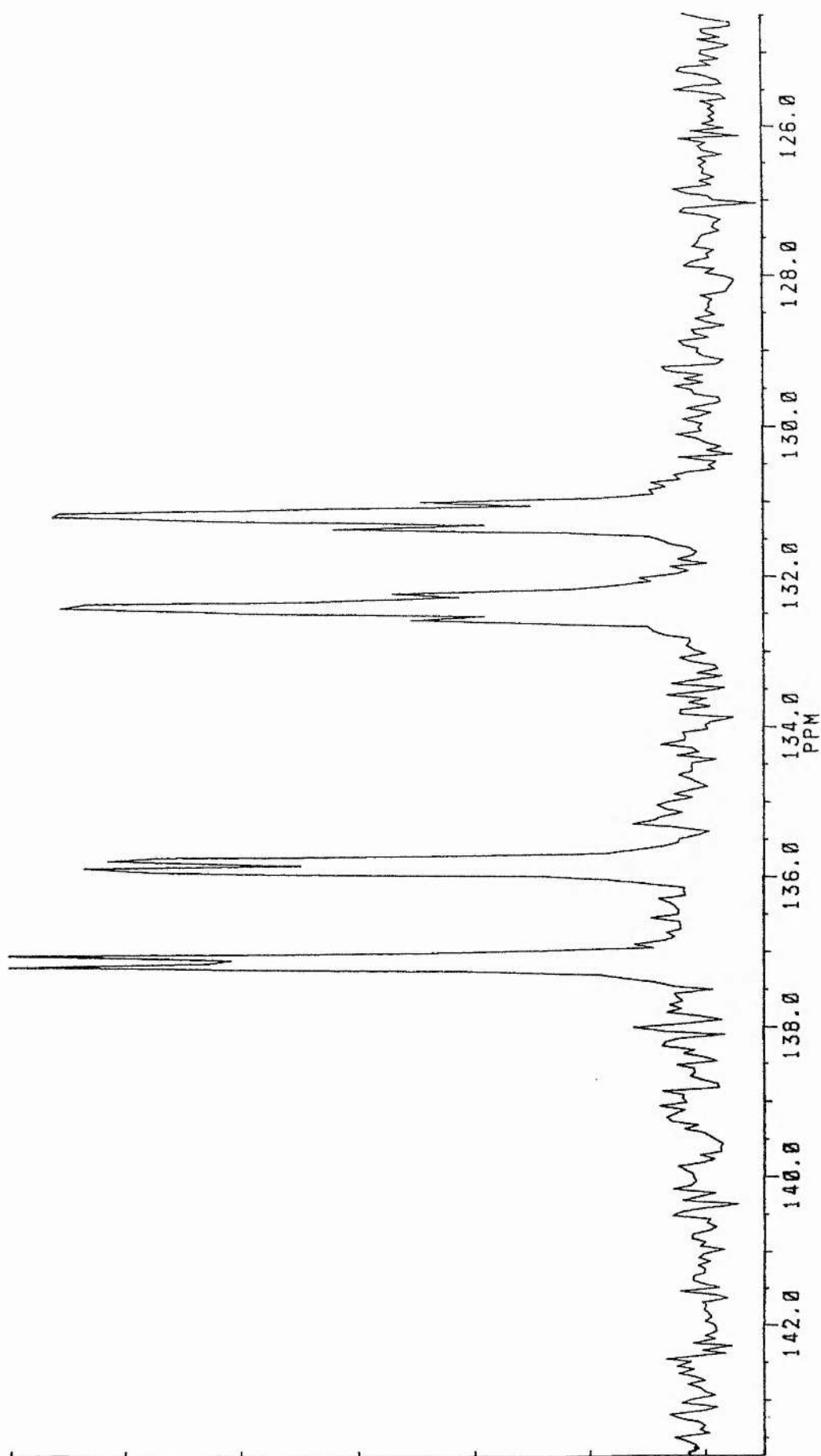


Fig. 4.12a ^{31}P n.m.r. spectrum (300 MHz) of $[\text{Rh}_2(\text{H}_2\text{C}=\text{CHO}_2\text{PPh}_2)_2\text{Cl}_2(\text{Ph}_2\text{POPPPh}_2)]$

$(\text{CD}_2\text{Cl}_2, 25^\circ\text{C})$

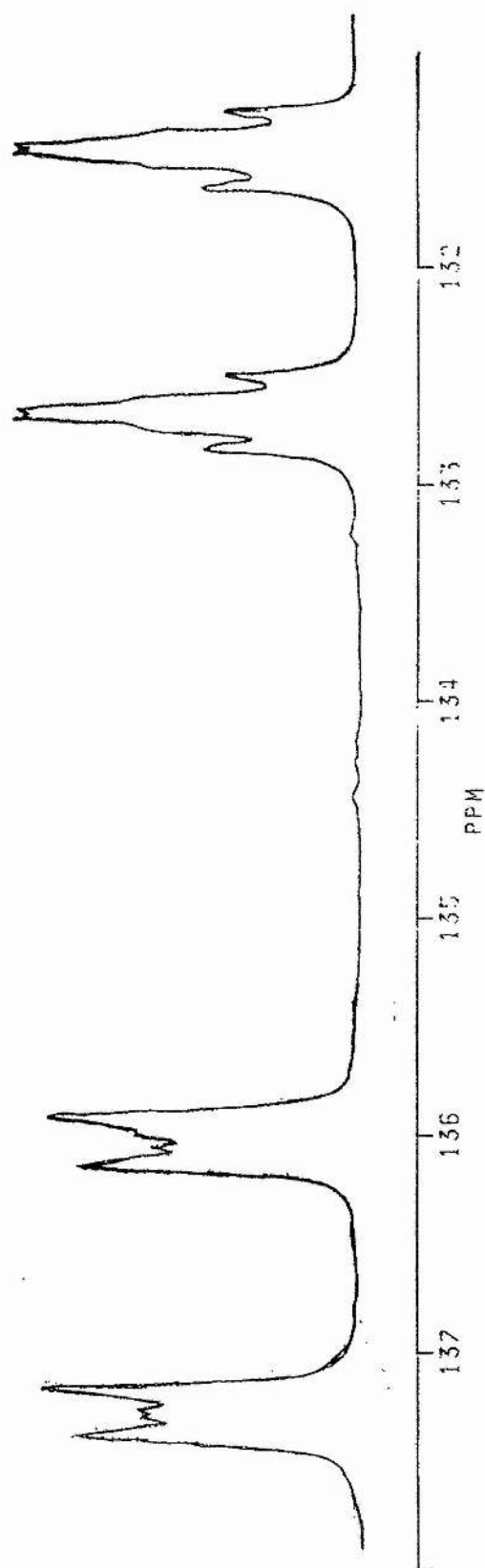


Fig 4.12b P.A.N.I.C. Simulation of ^{31}P n.m.r. spectrum of $[\text{Rh}_2\text{Cl}_2(\text{Ph}_2\text{POPPPh}_2)(\text{Ph}_2\text{PO}_2\text{CCHCH}_2)_2]$

are bound *cis* to the tpdp species. The coupling constants found to provide the simulation solution are summarized in Table 4.3 along with the ^{31}P information for all these complexes. The final structure for this compound is therefore concluded to be that in Figure 4.11, with the phosphorus atoms of both metal centres bound *cis* to the tpdp phosphorus atoms. Although the ^{31}P n.m.r. simulation requires that both phosphorus atoms of the tpdp ligand have identical chemical shifts and that the two phosphorus atoms of the mixed anhydrides also have identical chemical shifts which seems highly unlikely, it is the only simple explanation of the spectroscopic properties. The *cis* / *trans* isomer (Figure 4.13), the complex in which one anhydride is bound *cis* to the tpdp and the second *trans* may be present in very small amounts, as two doublets are observed at 121.1 ppm and 116.7 ppm.

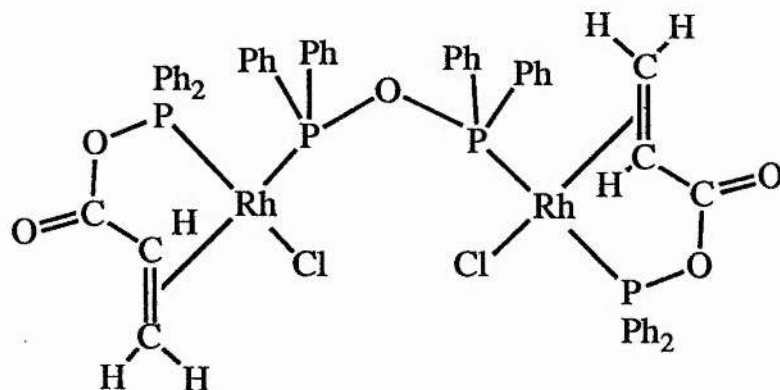


Fig. 4.13

The resonance are too small, however, to distinguish the smaller coupling.

Thus analysis of the yellow crystallites had identified one of the "secondary complexes", the other was discovered to be the

fine white precipitate which dropped out of solution during the metal/anhydride reaction. The observations and conclusions which lead to the identification of this complex are contained in Section 4.4.

4.4 Reaction of AAA with Tetrakis(ethylene)di- μ -chlororhodium ($[\text{Rh}_2\text{Cl}_2(\text{CH}_2=\text{CH}_2)_4]$) And Spectral Evidence For $[\text{RhCl}(\text{Ph}_2\text{PO}_2\text{CCHCH}_2)_2]$

The method used in this reaction is the same as that used in the reactions of AAA and the octene dimer $[\text{Rh}_2\text{Cl}_2(\text{C}_8\text{H}_{14})_4]$ (as described in Sections 4.1 to 4.3). The reaction discussed here is a 1:1 mole reaction (1 mole AAA added to 1 mole rhodium). In this system a far larger quantity of precipitate is produced than in the comparable octene dimer reaction. The precipitate was filtered off and washed with cold tetrahydrofuran whilst the filtrate was worked up as before and found to produce the tpdp bridged product, also in greater yield. The colour of the precipitate upon washing varied from colourless to very pale yellow/orange. Analysis led to it being assigned the formula $[\text{RhCl}(\text{Ph}_2\text{PO}_2\text{CCHCH}_2)_2]$, a five coordinate complex containing two AAA ligands bound through the phosphorus atom and the double bond.

Infra-red Data Of $[\text{RhCl}(\text{Ph}_2\text{PO}_2\text{CCHCH}_2)_2]$

The carbonyl band is located in the 1750 cm^{-1} region

indicating phosphorus and double bond coordination but two distinct peaks are present rather than the single entities exhibited by the previous bidentate anhydride complexes. This is attributed to there being two bound anhydrides. The presence is also noted of a Rh-Cl band at 280 cm^{-1} showing that the complex still contains a chlorine ligand and supporting the assignment of a five coordinate structure. This conclusion is also supported by the complexes' lack of conductivity in CH_2Cl_2 which ruled out the alternative ionic structure (Figure 4.14)

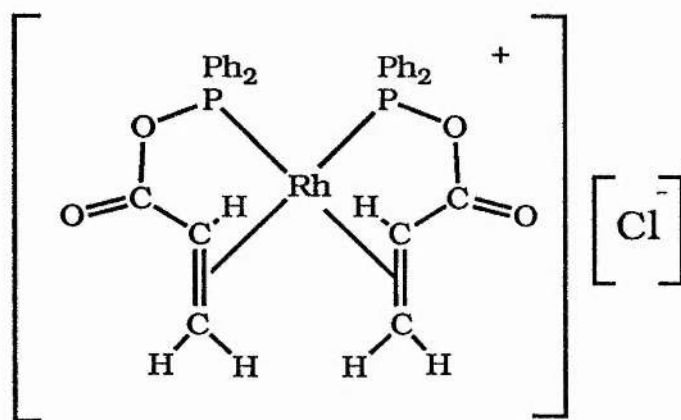


Fig. 4.14

^1H n.m.r. Data of $[\text{RhCl}(\text{Ph}_2\text{PO}_2\text{CCH}=\text{CH}_2)_2]$

At low temperature all the peaks assigned to the vinylic protons are found in the 2.5-3.9 ppm region, the region associated with π bonding. The presence of two slightly dissimilar π bound anhydrides is indicated by the two anhydride ligands giving rise to separate vinylic resonances (see Table 4.2).

F.A.B. Mass Spectrum of $[\text{RhCl}(\text{Ph}_2\text{PO}_2\text{CCHCH}_2)_2]$

The F.A.B. mass spectrum study on this compound showed that the sample used was still slightly contaminated with the bridged tpdp complex but that the molecular ion $[\text{RhCl}(\text{Ph}_2\text{PO}_2\text{CCHCH}_2)_2]$ and its fragments are present (see Table 4.5).

^{31}P n.m.r. Data of $[\text{RhCl}(\text{Ph}_2\text{PO}_2\text{CCHCH}_2)_2]$

The room temperature ^{31}P n.m.r. data consists of a broad doublet positioned at 109.2 ppm. This resonance indicates the presence of phosphorus atom and double bond coordination whilst exhibiting no evidence for the presence of a monodentate species. Figure 4.15 shows the room temperature spectrum of the complex. The observed peaks show an uncharacteristic broadness suggesting that they contain some unresolved coupling. Cooling of the solution to -25°C (Figure 4.16) resolves the coupling and displays the low temperature limiting ^{31}P spectrum. Figure 4.17a is an expansion of the $\delta 110$ ppm region clearly showing the presence of smaller satellite peaks either side of the main apparent doublet of doublets (located at 110.0 ppm). Figure 4.17b shows the P.A.N.I.C. simulation obtained with the parameters shown in Table 4.3.

In proton n.m.r. spectroscopy many spectra, such as 1-amino-3,6 dimethyl-2-nitrobenzene, are found to give rise to AB type spectra (Figure 4.18)⁽¹⁸¹⁾.

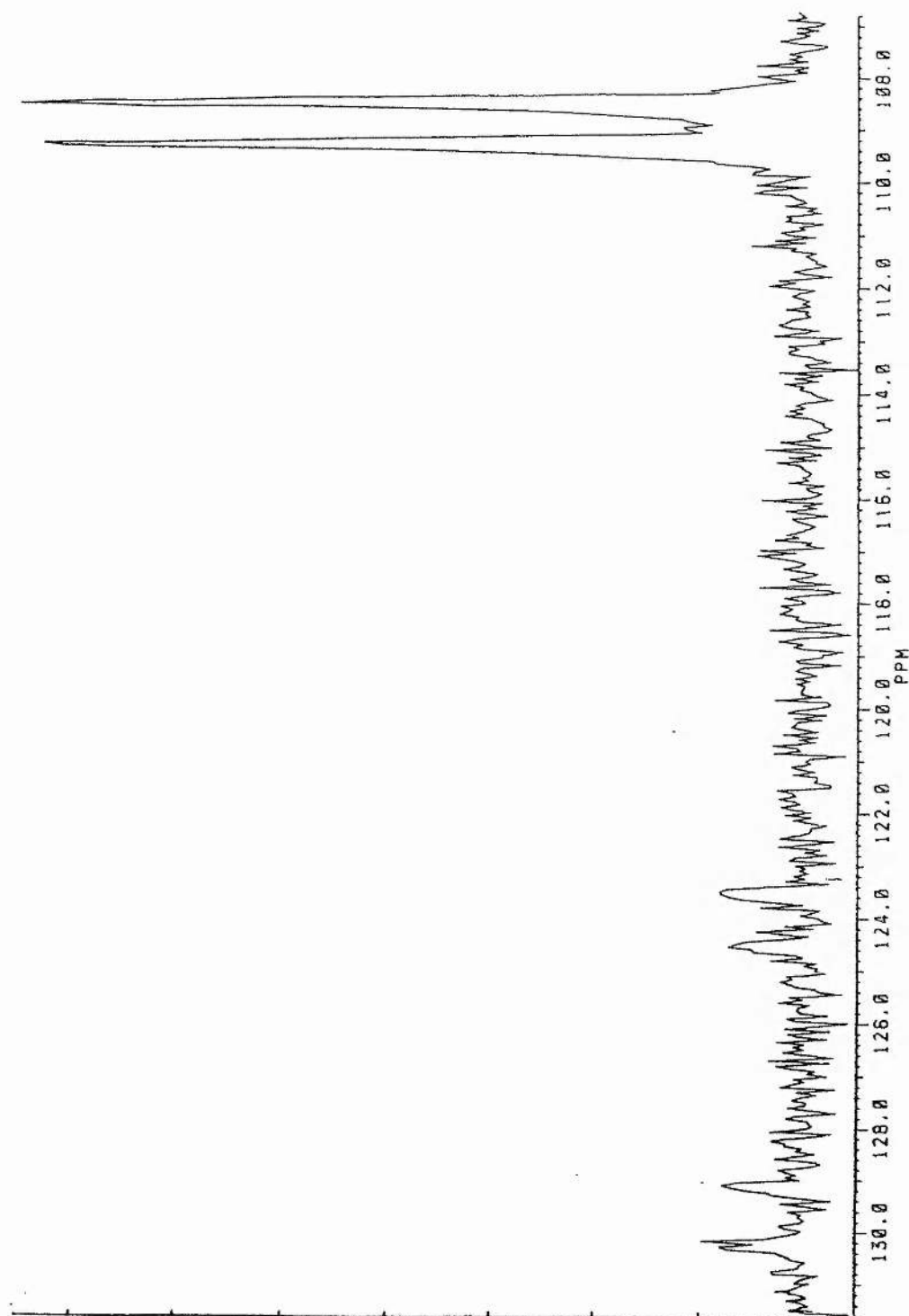


Fig. 4.15 ^{31}P n.m.r. spectrum (300 MHz) of $[\text{Rh}(\text{H}_2\text{C}=\text{CHO}_2\text{PPh}_2)_2\text{Cl}]$

$(\text{CD}_2\text{Cl}_2, 25^\circ\text{C})$

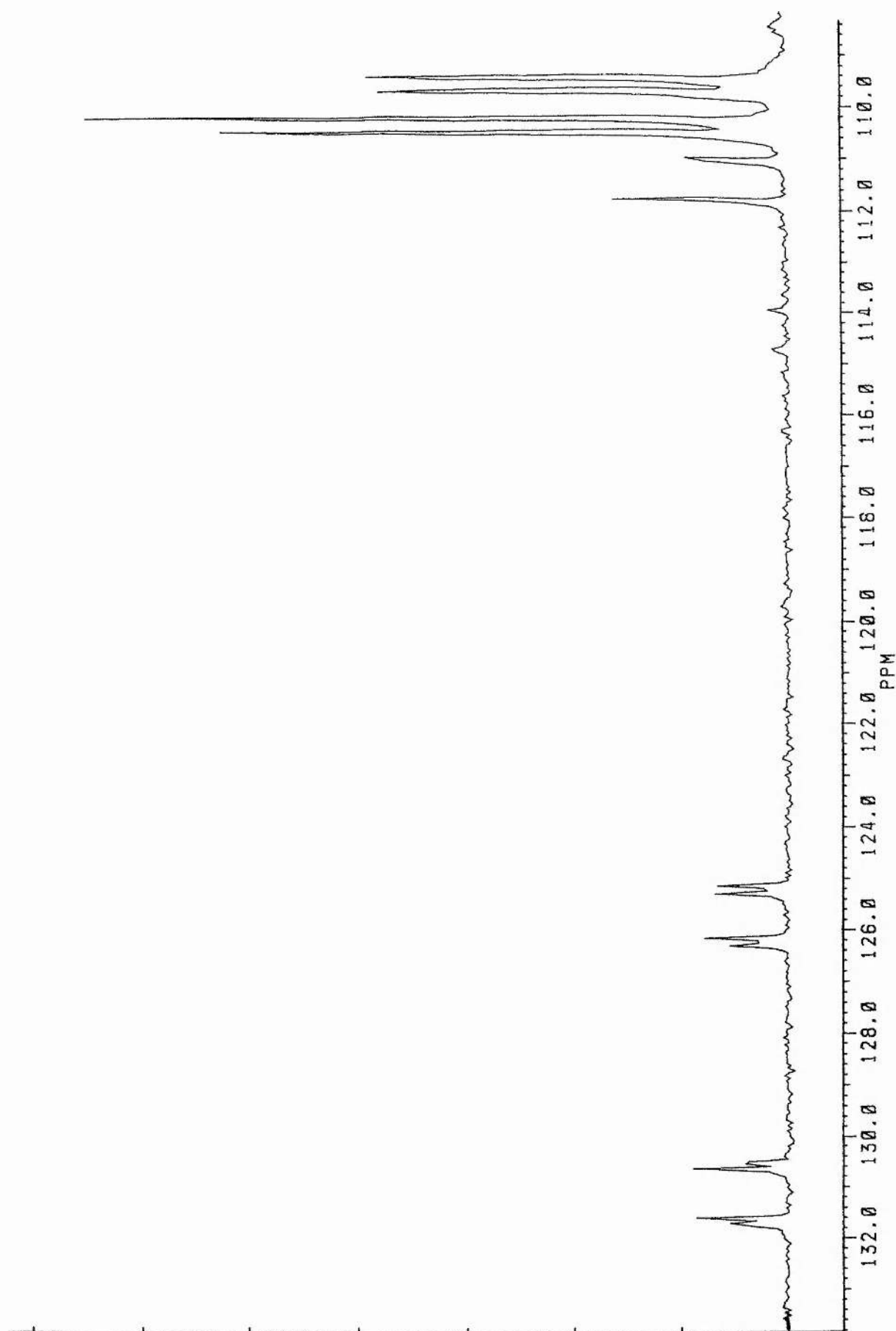
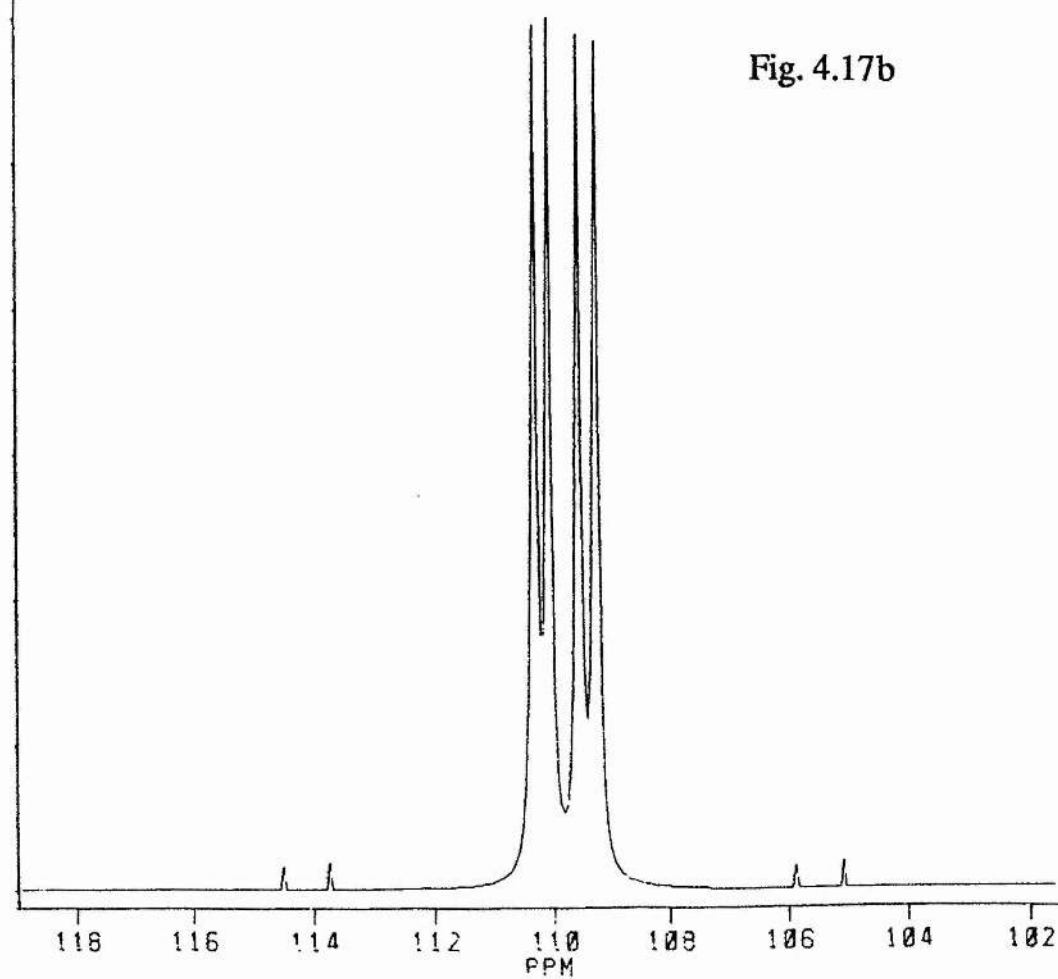
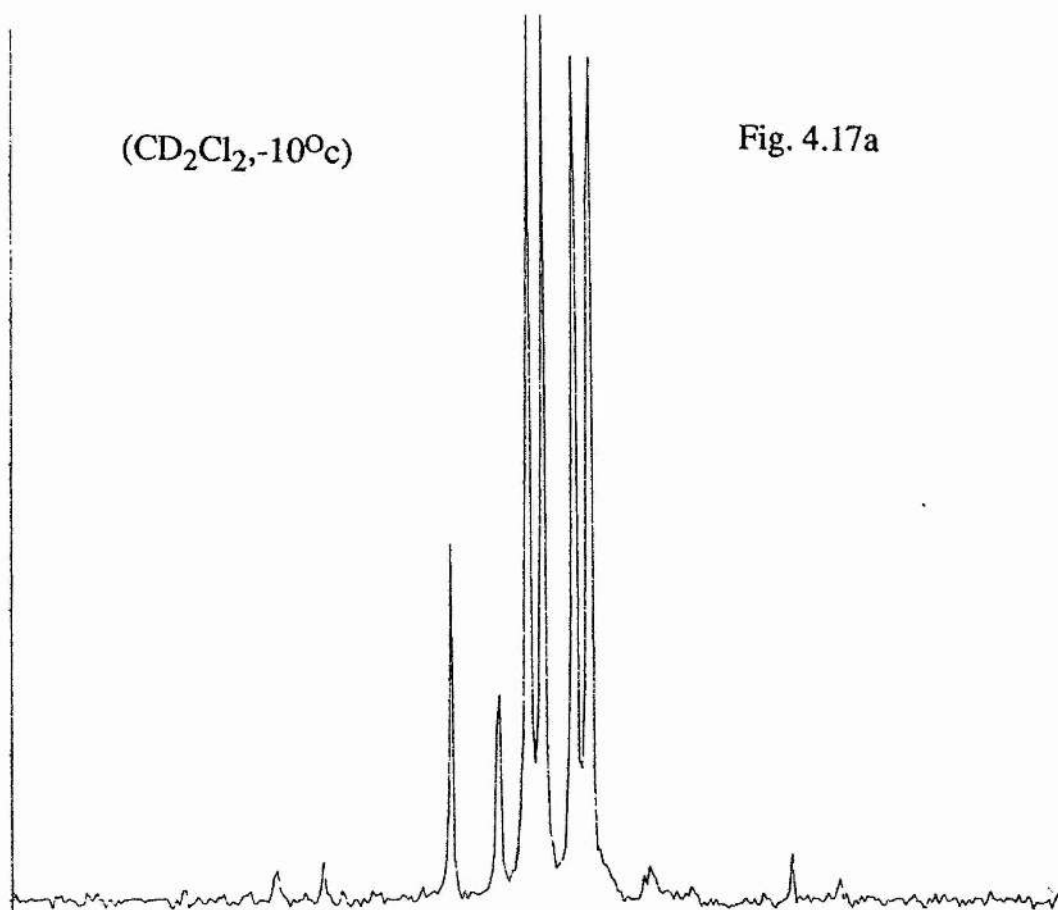


Fig. 4.16 ^{31}P n.m.r. spectrum (300 MHz) of $[\text{Rh}(\text{H}_2\text{C}=\text{CHO}_2\text{PPh}_2)_2\text{Cl}]$

$(\text{CD}_2\text{Cl}_2, -100^\circ\text{C})$



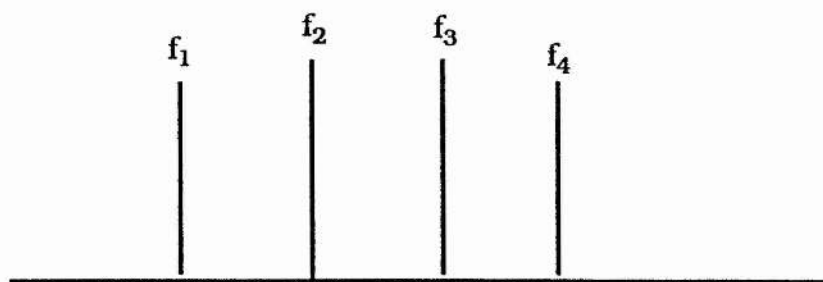
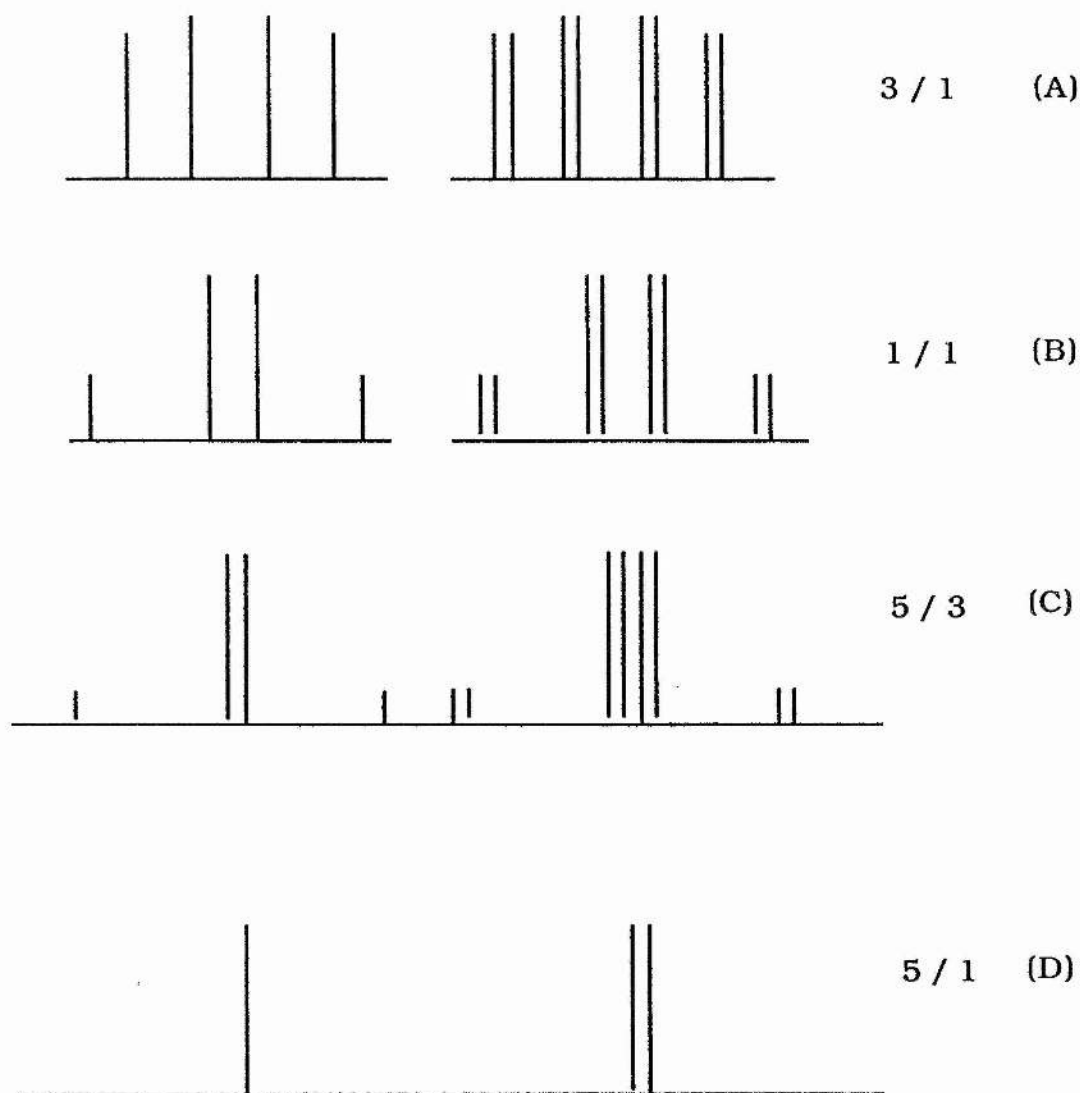


Fig. 4.18

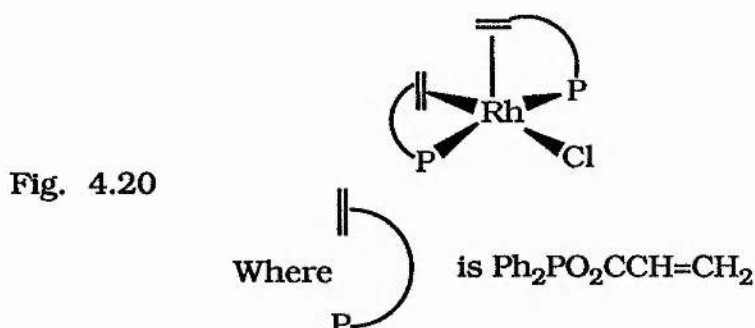
Further study of AB systems leads to the conclusion that the AB profile exhibited is determined by the ratio $J/\delta V_0$, where J is the size of the coupling constant and δV_0 is the difference in the chemical shifts for the complex (mathematically $\delta V_0 = \sqrt{(f_2 - f_3)(f_1 - f_4)}$)⁽¹⁸¹⁾. Thus if a series of compounds of varying $J/\delta V_0$ are studied by ^1H n.m.r. techniques, the profiles are found to vary as shown in Figure 4.19⁽¹⁸¹⁾. The only difference between the proton spectra and those adjacent to them which relate to the phosphorus/rhodium complexes is that the profiles are further complicated by the presence of a second coupling, which in this case is a rhodium/ phosphorus coupling. (A) is essentially the case described in chapter 2, that of phosphorus atoms in markedly different environments, where as in (D) both phosphorus atoms exist in the same environment. (B) and (C) are situations which lie between the two first order situations above and give rise to second order spectra. The experimental situation for $[\text{RhCl}(\text{Ph}_2\text{PO}_2\text{CCH}=\text{CH}_2)_2]$ is found to be close to situation (C), the couplings

Fig. 4.19

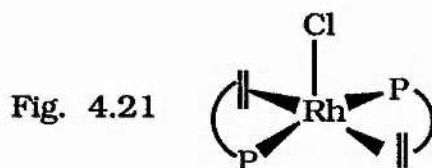
 J / dV_0 

calculated during the simulation give a $J/\delta V_0$ ratio of $8/3$. Thus a ratio of this size indicates that the phosphorus atoms are in similar but not identical environments whilst the value of J_{pp} (512 Hz) suggests that the phosphorus atoms are almost mutually *trans*. This can only be achieved in a square pyramidal structure (figure 4.20). The low temperature limiting spectrum contains two other species, one a single doublet at 111.5 ppm which only appears at low

temperature and the second comprising of two resonances a doublet of doublets at 131.8 ppm and at 127.5 ppm. The resonances of this second species are also observed at room temperature although



all the minor couplings are lost at this temperature. Since the doublet at $\delta 111.5$ disappears on warming the sample to room temperature it seems likely that it arises from an isomer of $[\text{RhCl}(\text{Ph}_2\text{PO}_2\text{CCH}=\text{CH}_2)_2]$ in which both phosphorus atoms are equivalent (Figure 4.21) and that under conditions where fluxionality is observed it exchanges with the major isomer.



The other species (the doublets of doublets at 131.1 and 127.5 ppm) clearly contain two mutually *cis* phosphorus atoms ($J_{\text{pp}}=17.7$ Hz) but its failure to exchange with the other species may mean that it is not an isomer of $[\text{RhCl}(\text{Ph}_2\text{POCCHCH}_2)_2]$. However its failure to coalesce could be due to the greater chemical shift difference of the resonances, the greater this difference the higher the temperature required for the resonances to coalesce. There is, in fact,

insufficient evidence to assign a structure to this complex.

4.4.1 Summary of Results Obtained By Altering The Mole Ratios And Dimeric Substrate In the Anhydride/Dimer Reactions

This is a summary of the reactions discussed in sections 4.3 and 4.4 and are an extension to those summarized in section 4.2.3.

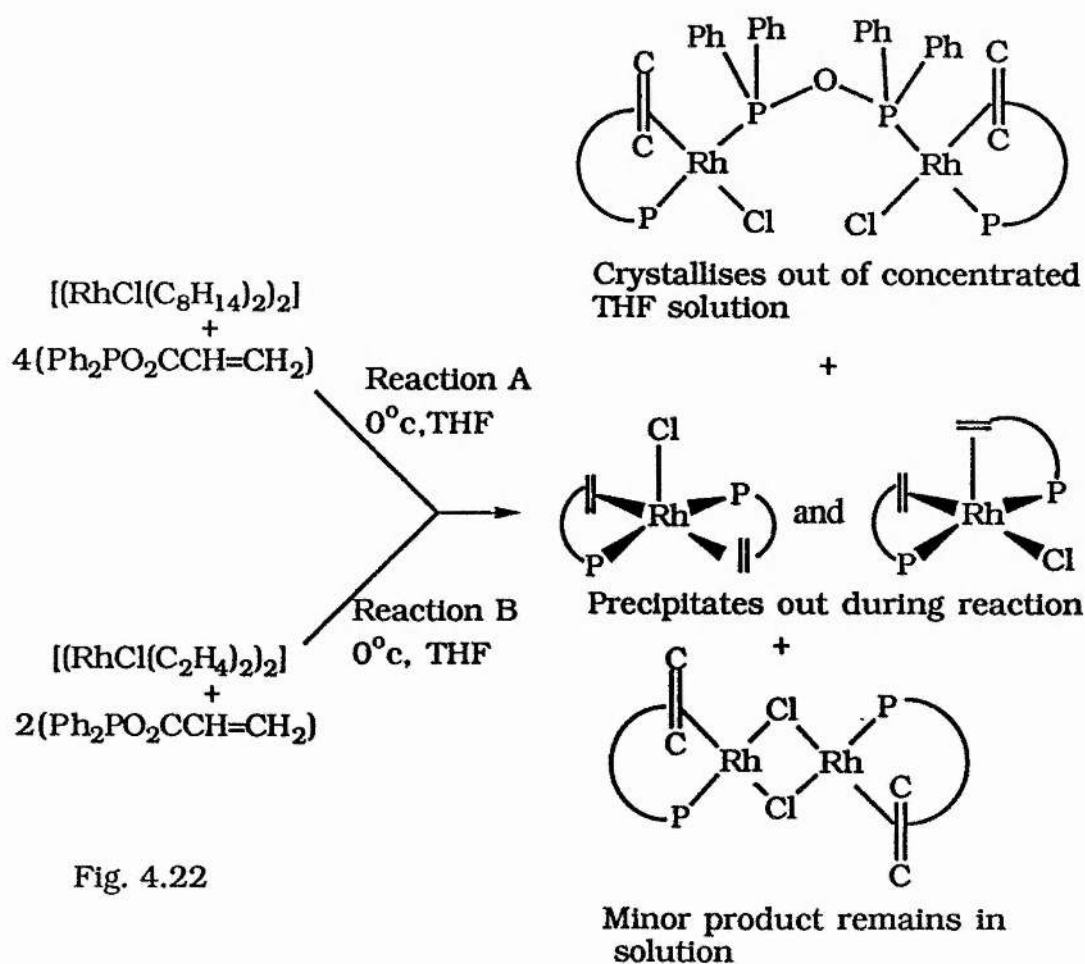


Fig. 4.22

4.5 Reactions of $[\text{RhCl}(\text{Ph}_2\text{PO}_2\text{CCH}=\text{CH}_2)_2]$

4.5.1 Reaction of $[\text{RhCl}(\text{Ph}_2\text{PO}_2\text{CCH}=\text{CH}_2)_2]$ With Triphenylphosphine

In section 3.3 where the mechanism that leads to the creation and isolation of the chelate tdpdp product is discussed, the initial supposition made is that two anhydride units are substituted on to the rhodium in the initial stages of the process. Thus the reaction of $[\text{RhCl}(\text{Ph}_2\text{PO}_2\text{CCH}=\text{CH}_2)_2]$ and PPh_3 utilizing the same conditions used in the 1:2 mole reaction of $[\text{RhCl}(\text{PPh}_3)_3]$ and $\text{Ph}_2\text{PO}_2\text{CCH}=\text{CH}_2$ was carried out to test this argument. An isolated sample of $[\text{RhCl}(\text{Ph}_2\text{PO}_2\text{CCH}=\text{CH}_2)_2]$ was dissolved in dichloromethane or THF and cooled to 0°C , to this solution three mole equivalents of triphenylphosphine were added and the solution stirred for approximately 1 hour. The solution was evaporated to dryness, redissolved in tetrahydrofuran, filtered then concentrated and allowed to stand at 0°C for several days. No crystals were isolated but the ^{31}P n.m.r. (Figure 4.23) showed the compounds present were $[\text{RhCl}(\text{PPh}_3)(\text{Ph}_2\text{POPPH}_2)]$, PPh_3 and the by-product ammonium inner salt $\text{Ph}_3\text{P}^+\text{CH}_2\text{CH}_2\text{CO}_2^-$. Thus this shows that the addition of triphenylphosphine will cause a metal promoted rearrangement to occur and confirming the mechanism suggested in Chapter 3.

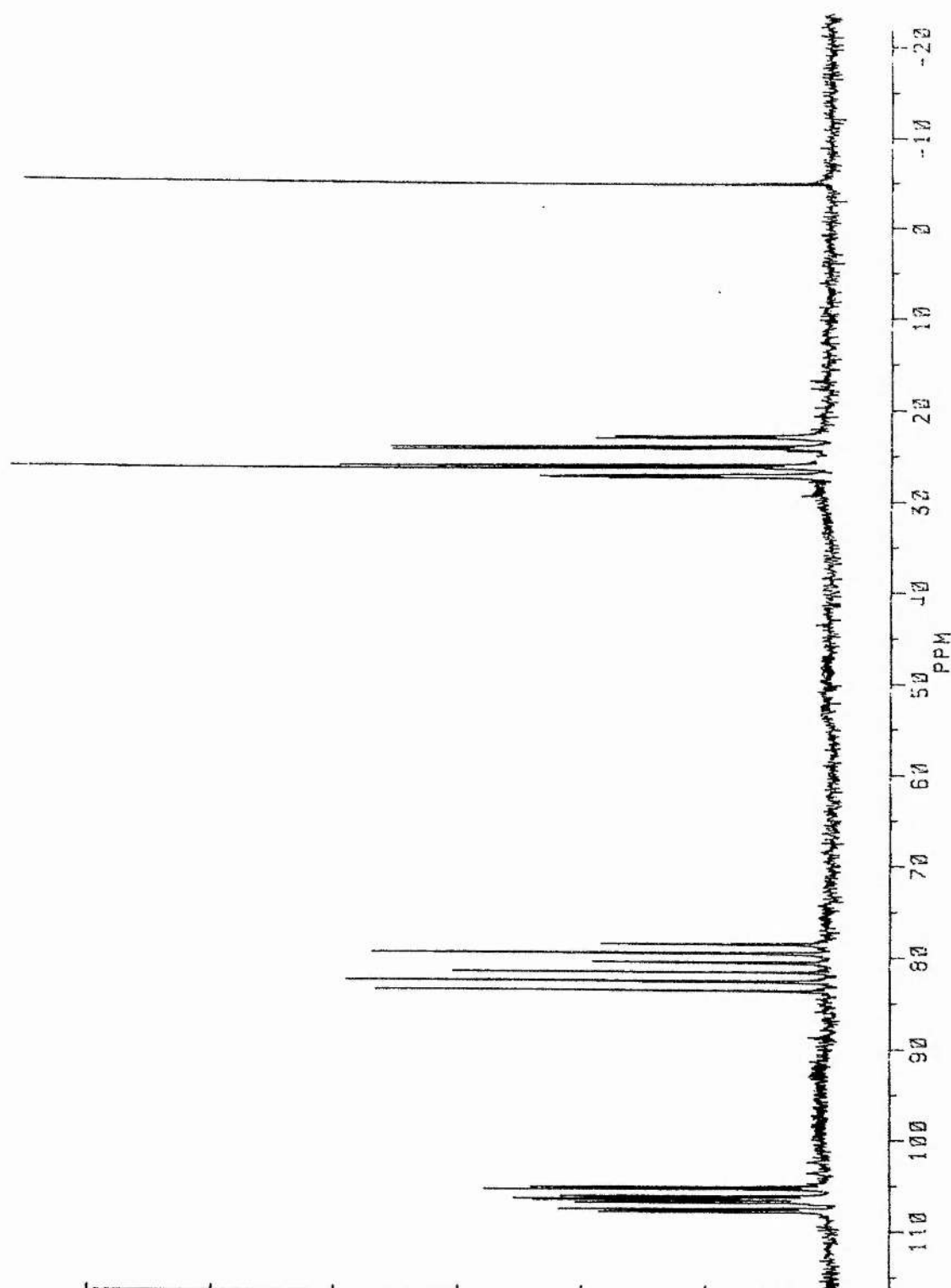
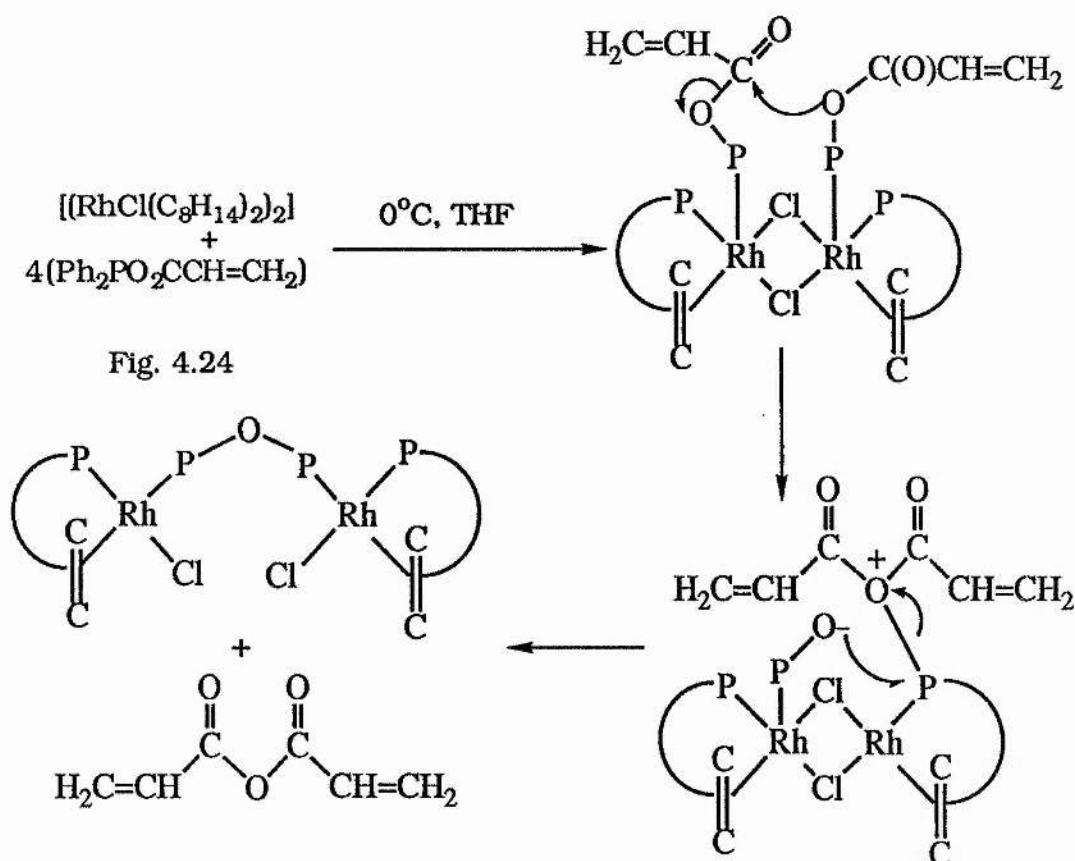


Fig 4.23 ^{31}P n.m.r. spectrum (300 MHz) of the products from the reaction of $[\text{RhCl}(\text{Ph}_2\text{PO}_2\text{CCHCH}_2)_2]$ and PPh_3

4.5.2 Mechanism To Produce $[\text{Rh}_2\text{Cl}_2(\text{Ph}_2\text{PO}_2\text{CCH}=\text{CH}_2)_2]$
 $(\text{Ph}_2\text{POPPh}_2)]$ And Reactions of
 $[\text{RhCl}(\text{Ph}_2\text{PO}_2\text{CCH}=\text{CH}_2)_2]$ With KPF_6 and TlPF_6

It is possible that a similar metal promoted rearrangement pathway as suggested for the formation of $[\text{Rh}(\text{PPh}_3)(\text{Ph}_2\text{POPPh}_2)\text{Cl}]$ in Chapter 3 may be responsible for the formation of $[\text{Rh}_2\text{Cl}_2(\text{Ph}_2\text{PO}_2\text{CCH}=\text{CH}_2)_2(\text{Ph}_2\text{POPPh}_2)]$. The difference in this case is that the two metal centres are held in close proximity by the chlorine bridges resulting in a rearrangement not between the ligands bound to the same metal centre but rather across the dimer (see Figure 4.24).



However no evidence for these intermediates has been provided from the ^{31}P n.m.r. experimentation. Small amounts of the dimeric tdpd bridged complexes are obtained from the reaction of $[\text{RhCl}(\text{Ph}_2\text{PO}_2\text{CCH}=\text{CH}_2)_2]$ and MPF_6 ($\text{M} = \text{K}$ or Tl), suggesting that alternative mechanistic pathways are possible but there is not sufficient evidence to speculate upon them.

Table 4.1		I. R. Spectral Data for The Mixed Anhydrides				
Complex		IR (cm ⁻¹)				v(P-O)sym*v(P-O)sym*
		v(C=O)	v(C=C)	v(Rh-Cl)	v(P-O)asym	
$[(\text{RhCl}(\text{Ph}_2\text{PO}_2\text{CCH}^c=\text{CH}_2^{a,b}))_2]$		1750s	-----	300w	-----	-----
$[(\text{RhCl}(\text{Ph}_2\text{PO}_2\text{CCH}_2^{e,f}\text{CH}^c=\text{CH}_2^{a,b}))_2]$		1755s	-----	395w	-----	-----
$[(\text{RhCl}(\text{Ph}_2\text{PO}_2\text{CCH}^c=\text{CH}_2^{a,b}))_2(\text{tpdp})]$		1740s	-----	280w	855s	770w
$[\text{RhCl}(\text{Ph}_2\text{PO}_2\text{CCH}^c=\text{CH}_2^{a,b})_2]$		1740s, 1760s	-----	280w	-----	-----

* From the tpdp group

Table 4.2 ^1H Spectral Data for The Mixed Anhydrides		$(\text{CD}_2\text{Cl}_2, 25^\circ\text{C})$	
Complex		^1H (ppm)	
$[\text{RhCl}(\text{Ph}_2\text{PO}_2\text{CCH}^c=\text{CH}_2^{a,b})_2]$		a,b 3.0m	c 3.7m
$[\text{RhCl}(\text{Ph}_2\text{PO}_2\text{CCH}_2^{e,f}\text{CH}^c=\text{CH}_2^{a,b})_2]$		a 3.1m	b 3.2m c 2.7m d,e 5.6m
$[\text{RhCl}(\text{Ph}_2\text{PO}_2\text{CCH}^c=\text{CH}_2^{a,b})_2(\text{tpdp})]$		a,b 3.0m	c 3.41m
$[\text{RhCl}(\text{Ph}_2\text{PO}_2\text{CCH}^c=\text{CH}_2^{a,b})_2]^*$		a 3.1m	b 3.4m c 3.9m
$[\text{RhCl}(\text{Ph}_2\text{PO}_2\text{CCH}^c=\text{CH}_2^{a,b})_2]^f$		a 3.1, 3.2m	b 3.45, 3.55m c 3.7, 3.9m

* room temperature f -25°C

Table 4.3		³¹ P Spectral Data for the Rhodium Mixed Anhydride Dimers (CD ₂ Cl ₂ , 25°C)									
Complex		Chemical Shifts		Coupling Constants(Hz)							
		Pa	Pb	RhPa	RhPb	RhPc	RhPd	PaPb	PaPc	PaPd	PbPc PbPd PcPd
[RhCl(Ph ₂ P ^a O ₂ CCH=CH ₂)) ₂]		132.4d	-----	172.4	—	—	—	—	—	—	—
[RhCl(Ph ₂ P ^a O ₂ CH ₂ CH=CH ₂)) ₂]		149.3d	-----	196.3	—	—	—	—	—	—	—
[RhCl(Ph ₂ P ^a O ₂ CCH=CH ₂)) ₂ (Ph ₂ P ^b OP ^b Ph ₂)]		131.8dt	136.5dd	148.6	148.6	155.0	155.0	0.0	28.0	-10.6	50 215.0
[RhCl(Ph ₂ P ^a O ₂ CCH=CH ₂)) ₂ (Ph ₂ P ^b OP ^b Ph ₂)]		121.1d	116.8d	120.8	116.1	@	—	—	—	—	—
[RhCl(Ph ₂ P ^{a,b} O ₂ CCH=CH ₂)) ₂] ^f		109.2d	-----	97.2	—	—	—	—	—	—	—
[RhCl(Ph ₂ P ^{a,b} O ₂ CCH=CH ₂)) ₂] [*]		110.8	109.2	103.6	85.6	512.6	—	—	—	—	—
[RhCl(Ph ₂ P ^{a,b} O ₂ CCH=CH ₂)) ₂] [*]		115.5d	-----	95.9	—	—	—	—	—	—	—

^f room temperature ^{*} - 25°C @ not observed

Table 4.4

F.A.B. m.s. Fragmentation Pattern of
 $[\text{Rh}_2\text{Cl}_2(\text{Ph}_2\text{POPPh}_2)(\text{Ph}_2\text{PO}_2\text{CCHCH}_2)_2]$

	m/z
$[\text{Rh}_2\text{Cl}_2(\text{Ph}_2\text{POPPh}_2)(\text{Ph}_2\text{PO}_2\text{CCHCH}_2)_2]^+$	1175
$[\text{Rh}_2\text{Cl}_2(\text{Ph}_2\text{POPPh}_2)(\text{Ph}_2\text{PO}_2\text{CCHCH}_2)]^+$	1140
$[\text{Rh}_2\text{Cl}_2(\text{Ph}_2\text{POPPh}_2)(\text{Ph}_2\text{PO}_2\text{CCHCH}_2)]^+$	919
$[\text{Rh}(\text{Ph}_2\text{POPPh}_2)(\text{Ph}_2\text{PO}_2\text{CCHCH}_2)]^+$	745
$[\text{RhCl}(\text{Ph}_2\text{PO})]^+$	339

Table 4.5F.A.B. m.s. Fragmentation Pattern of $[\text{RhCl}(\text{Ph}_2\text{PO}_2\text{CCHCH}_2)_2]$

	m/z
$[\text{RhCl}(\text{Ph}_2\text{PO}_2\text{CCHCH}_2)_2]^+$	650
$[\text{Rh}(\text{Ph}_2\text{PO}_2\text{CCHCH}_2)_2]^+$	615
$[\text{Rh}(\text{Ph}_2\text{PO}_2\text{CCHCH}_2)(\text{PPh}_2\text{O})]^+$	560
$[\text{Rh}(\text{PPh}_2)(\text{Ph}_2\text{PO})]^+$	489
$[\text{Rh}(\text{PPh})(\text{Ph}_2\text{POC})]^+$	460

Section 4.6 Experimental

$[\text{Rh}_2\text{Cl}_2(\text{Ph}_2\text{PO}_2\text{CCH}=\text{CHMe})_2]$ ⁽¹³¹⁾

Prepared following literature method

$[\text{Rh}_2\text{Cl}_2(\text{Ph}_2\text{PO}_2\text{CCH}=\text{CH}_2)_2]$

To a suspension of $[(\text{RhCl}(\text{C}_8\text{H}_{14}))_2]$ (0.3g = 0.42 mmol) in tetrahydrofuran (20 cm³) a sample of $\text{Ph}_2\text{PO}_2\text{CCH}=\text{CH}_2$ (0.2g, 0.85 mmol) was added using the "in situ" method. Upon addition the starting material dissolved and a slight colour change was noted, the solutions becoming more yellow signalling an immediate reaction. The reaction solution was reduced in volume to approximately 5 cm³, a bright orange precipitate was produced upon careful addition of petroleum spirit (40-60°). This precipitate was found to be contaminated with $[\text{RhCl}(\text{Ph}_2\text{PO}_2\text{CCH}=\text{CH}_2)_2]$ and $[(\text{Rh}_2\text{Cl}_2(\text{Ph}_2\text{POPPh}_2)(\text{Ph}_2\text{PO}_2\text{CCH}=\text{CH}_2)_2)]$. It could be purified by dissolving in cold THF and allowing this solution, once filtered, to stand at -3°C for several days to remove the $[\text{Rh}_2\text{Cl}_2(\text{AAA})_2(\text{Ph}_2\text{POPPh}_2)]$ by recrystallisation. A pure sample of the complex can be obtained by filtering a second time followed by careful addition of petroleum spirit (40-60°). Yield 0.26g (55%)

$[\text{Rh}_2\text{Cl}_2(\text{Ph}_2\text{PO}_2\text{CCH}_2\text{CH}=\text{CH}_2)_2]$

Prepared as above, but using $\text{Ph}_2\text{PO}_2\text{CCH}_2\text{CH}=\text{CH}_2$ (0.23g, 0.85

mmol). In this case the product was not contaminated with $[(\text{RhCl}(\text{Ph}_2\text{PO}_2\text{CCH}_2\text{CH}=\text{CH}_2)_2)]$ and $[(\text{Rh}_2\text{Cl}_2(\text{Ph}_2\text{PO}_2\text{CCH}_2\text{CH}=\text{CH}_2)_2(\text{Ph}_2\text{POPPH}_2)]$ and was washed exhaustively with diethylether. Yield 0.3g (60%)

Theoretical $[(\text{RhCl}(\text{Ph}_2\text{PO}_2\text{CCH}_2\text{CHCH}_2)_2)]\cdot\text{thf}$ C = 48.6%; H = 4.3%

Found $[(\text{RhCl}(\text{Ph}_2\text{PO}_2\text{CCH}_2\text{CHCH}_2)_2)]\cdot\text{thf}$ C = 48.8%; H = 3.9%

$[\text{RhCl}(\text{Ph}_2\text{PO}_2\text{CCH}=\text{CH}_2)_2]$

Method 1

This followed the method described for $[(\text{RhCl}(\text{Ph}_2\text{PO}_2\text{CCH}=\text{CH}_2)_2)]$ but used 2 mol equivalents of $\text{Ph}_2\text{PO}_2\text{CCH}=\text{CH}_2$ (0.4g, 1.7 mmol). Shortly after the addition a white precipitate appeared. When no further precipitation was evident, the solution was filtered and the white precipitate washed with cold tetrahydrofuran.

Theoretical $[\text{RhCl}(\text{Ph}_2\text{PO}_2\text{CCHCH}_2)_2]\cdot\text{thf}$ C = 55.4%; H = 4.0%

Found $[\text{RhCl}(\text{Ph}_2\text{PO}_2\text{CCHCH}_2)_2]\cdot\text{thf}$ C = 55.8%; H = 4.4%

Method 2

As method 1 but using $[(\text{RhCl}(\text{C}_2\text{H}_4)_2)_2]$ (0.3g, 0.8 mmol) and $\text{Ph}_2\text{PO}_2\text{CCH}=\text{CH}_2$ (0.39g, 1.6 mmol). Yield 0.13g (50%)

$[\text{Rh}_2\text{Cl}_2(\text{Ph}_2\text{PO}_2\text{CCHCH}_2)_2(\text{Ph}_2\text{POPPh}_2)]$

The method followed was that detailed for $[\text{RhCl}(\text{Ph}_2\text{PO}_2\text{CCH}=\text{CH}_2)_2]$ but isolation of this complex was achieved by removing the $[\text{RhCl}(\text{Ph}_2\text{PO}_2\text{CCH}=\text{CH}_2)_2]$ precipitate and concentrating the filtrate obtained to approximately 6 cm³. After standing for several days at -3°C bright yellow crystallites were formed. These were collected and dried *in vacuo*. The crystals contained one mole of tetrahydrofuran as a solvent of crystallization.

Theoretical $[\text{Rh}_2\text{Cl}_2(\text{Ph}_2\text{PO}_2\text{CCHCH}_2)_2(\text{Ph}_2\text{POPPh}_2)].\text{thf}$ C = 55.8%;

H = 4.4%

Found $[\text{Rh}_2\text{Cl}_2(\text{Ph}_2\text{PO}_2\text{CCHCH}_2)_2(\text{Ph}_2\text{POPPh}_2)].\text{thf}$ C = 55.9%;

H = 4.7%.

$[\text{Rh}(\text{PPh}_3)\text{Cl}(\text{Ph}_2\text{POPPh}_2)]$

A quantity of $[\text{RhCl}(\text{Ph}_2\text{PO}_2\text{CCHCH}_2)_2]$ (0.4g, 0.6 mmol) was dissolved in dichloromethane or tetrahydrofuran (25 ml) and treated with 3 mole equivalents of triphenylphosphine (0.48g, 1.8 mmol). After stirring at 0°C for 1 hour, the solution was filtered and

allowed to stand at -3°C for several days. The resultant solution was studied by n.m.r. spectroscopy.

CHAPTER 5

The Reaction of Selected Mixed Anhydrides and $[\text{Ru}(\text{PPh}_3)_4\text{Cl}_2]$

The results detailed in Chapters 2,3 and 4 dealt with the chemistry resulting from the reaction of the mixed anhydrides with rhodium reagents. This chapter details further investigations into the analogous ruthenium chemistry, reporting studies into the coordination of varying mixed anhydrides and $[\text{Ru}(\text{PPh}_3)_4\text{Cl}_2]$.

5.1 Introduction

In recent years several reactions of mixed anhydrides derived from diphenylphosphinous acid and allylic alcohols have been attempted with $[\text{RuCl}_2(\text{PPh}_3)_4]$. The reaction of two equivalents of $\text{Ph}_2\text{PO}_2\text{CCH}=\text{CMe}_2$ (derived from dimethylacrylic acid) and $[\text{RuCl}_2(\text{PPh}_3)_4]$ produced $[\text{RuCl}_2(\text{Ph}_2\text{PO}_2\text{CCH}=\text{CMe}_2)_2]$, and a similar product was isolated from the same reaction with $\text{Ph}_2\text{PO}_2\text{CCMe}=\text{CHPh}$ (derived from α -methylcinnamic acid)⁽¹⁸²⁾. Both these species were concluded to be complexes in which the mixed anhydride ligands were bound in a chelate manner through the phosphorus atom and the oxygen atom of the carbonyl group (Figure 5.1). In contrast the 1:2 mode reaction of $\text{Ph}_2\text{POCH}_2\text{CH}=\text{CMe}_2$ (derived from 3 methyl-2-buten-1-ol), following the same method resulted in what was thought to be a five coordinate complex, $[\text{RuCl}_2(\text{Ph}_2\text{POCH}_2\text{CH}=\text{CMe}_2)(\text{PPh}_3)_2]$, in

which

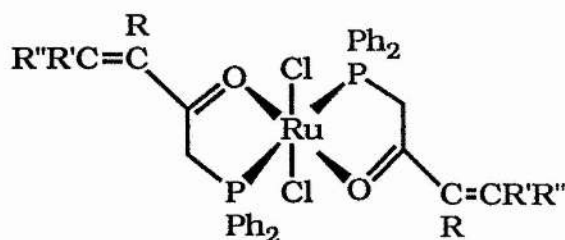


Fig. 5.1

the mixed anhydride is bound through the phosphorus atom only (Figure 5.2). The same reaction with the AAA ligand produces a 6 coordinate tdpdp containing complex (section 5.6)⁽¹⁸²⁾.

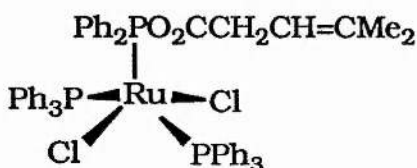


Fig. 5.2

5.2 The 1:1 mole Reaction of $\text{Ph}_2\text{PO}_2\text{CCH}=\text{CMe}_2$ and $[\text{RuCl}_2(\text{PPh}_3)_4]$

One mole equivalent of $\text{Ph}_2\text{PO}_2\text{CCH}=\text{CMe}_2$ (DAA) was added to a room temperature dichloromethane or THF solution of $[\text{RuCl}_2(\text{PPh}_3)_4]$. A slight colour change was noted, the initial brown/black solution acquiring an orange tinge. A brown precipitate was obtained by careful addition of petroleum spirit (40-60°). This precipitate was found to contain several species but could be extracted with cold tetrahydrofuran, the resultant product of which analysed as $[\text{RuCl}_2(\text{PPh}_3)_2(\text{DAA})]$.

^{31}P n.m.r. Data

The initial impure precipitate contained PPh_3 , PPh_3O , $\text{RuCl}_2(\text{PPh}_3)_4$ and the product complex. However further purification isolated the product complex containing a coordinated DAA ligand. The exact binding mode is difficult to elucidate solely on the basis of the ^{31}P n.m.r. studies since the chemical shift of the phosphorus atom (153.3 ppm) lies between that expected for compounds exhibiting binding through the phosphorus atom and the double bond (c.a. 130 ppm) and binding through the phosphorus and oxygen atoms (c.a. 170 ppm). Nevertheless it seems probable that the complex is a 6 coordinate species of the form $[\text{RuCl}_2(\text{PPh}_3)_2(\text{Ph}_2\text{PO}_2\text{CCH}=\text{CMe}_2)]$ and containing a DAA ligand bound in a bidentate manner.

Infra-red Data

There is no high value carbonyl peak in this spectrum, indicating coordination of the mixed anhydrides is via the oxygen atom of the carbonyl group rather than the $\text{C}=\text{C}$ species.

The only observed feature above 1600cm^{-1} is a weak band at 1637 cm^{-1} assigned to be the $\nu(\text{C}=\text{O})$ of the DAA ligand, its value being consistent with those complexes shown to contain bidentate mixed anhydride ligands bound via the phosphorus atom and oxygen of the carbonyl group (see the examples in Section 5.1 and $[\text{Rh}(\text{DAA})(\text{PPh}_3)_2][\text{Cl}]$ Chapters 1 and 3). The disruption of the π electron density caused by coordination weakens the bond and thus

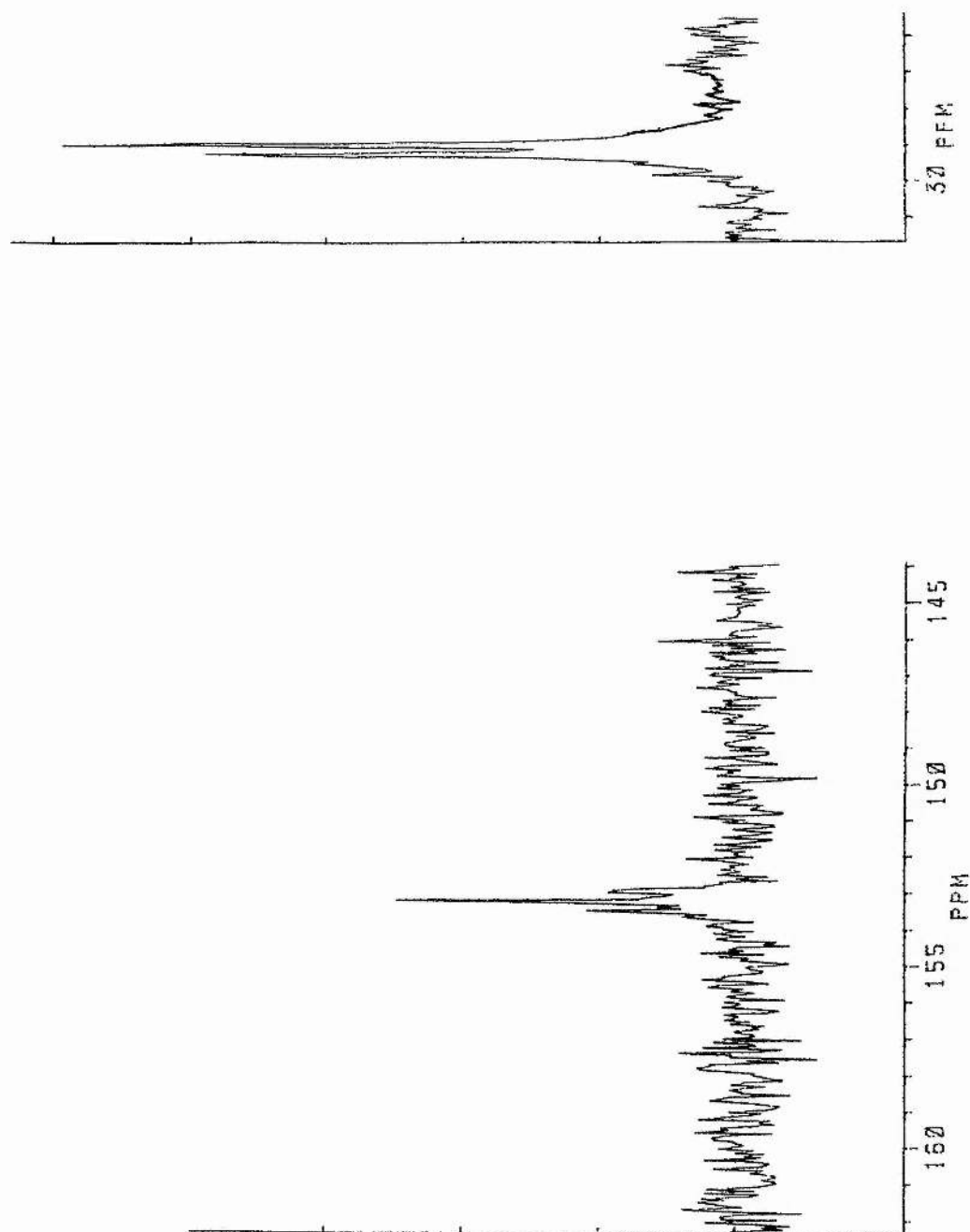


Fig. 5.3 ^{31}P n.m.r. spectrum (300MHz) of $[\text{RuCl}_2(\text{Ph}_2\text{PO}_2\text{CCH}=\text{CH}=\text{CMe}_2)(\text{PPh}_3)_2]$ (CD_2Cl_2 , 25°C)

lowers its frequency. This band is broad and is thought also to contain the $\nu(\text{C}=\text{C})$ resonance which will be in a similar position to that of the free ligand but will be quite weak because there will be much less intensity borrowing from $\nu(\text{C}=\text{O})$ than in complexes where the carbonyl group is not coordinated. A Ru-Cl band is also present at 340 cm^{-1} .

^1H n.m.r. Data

The resonances at $\delta 5.75\text{ ppm}$, $\delta 2.2\text{ ppm}$ and $\delta 1.9\text{ ppm}$ were assigned to the vinylic protons of the DAA ligand, which are consistent with coordination of the anhydride via the phosphorus and oxygen atoms as they are in similar position to those of the free ligand. The complex is therefore concluded to have the structure shown in Figure 5.4.

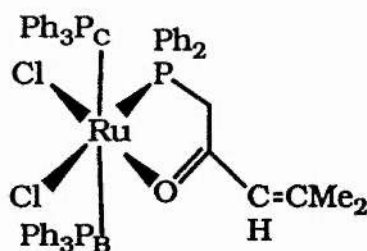


Fig. 5.4

The large *trans* coupling that would normally be expected between P_B and P_C is not observed because these phosphorus atoms exist in equivalent environments.

5.3 The Reaction of $\text{Ph}_2\text{PO}_2\text{CCH}=\text{CHMe}$ and $\text{Ph}_2\text{PO}_2\text{CCH}=\text{CH}_2$ with $[\text{RuCl}_2(\text{PPh}_3)_4]$

The method used in these experiments was virtually identical to that used in the DAA experiment described in Section 5.2. The only difference between the two methods was that only cooled (0°C) THF solutions were employed in the CAA and AAA cases. In the CAA case two products were isolated. However in the AAA case two products were observed but only one was isolated.

5.3.1 Product 1

In both cases product 1 is observed in the ^{31}P n.m.r. spectra and found to exhibit similar ^{31}P n.m.r. spectra to that of the DAA product. These profiles take the form of a triplet in the 150 ppm region and a doublet in the 29 ppm region observed to be twice the intensity of the 150 ppm resonance (see Table 5.3). In the CAA case this product takes the form of red/purple crystallites. However it proved impossible to obtain this product without contamination with product 2 or in sufficient yield to obtain further accurate spectral data. In the AAA case product 1 has not, as yet, been isolated. Both product 1 complexes have therefore been assigned similar structures to that shown in Figure 5.4, the resultant formulae being $[\text{RuCl}_2(\text{PPh}_3)_2(\text{Ph}_2\text{PO}_2\text{CCH}=\text{CHMe})]$ and $[\text{RuCl}_2(\text{PPh}_3)_2(\text{Ph}_2\text{PO}_2\text{CCH}=\text{CH}_2)]$ respectively.

5.3.2 Product 2

Both the CAA and AAA products took the form of yellow precipitates and appeared upon allowing the concentrated reaction to stand at -3°C for several days. Analysis of the spectral data has led to the conclusions that the compounds have similar structures and are fluxional at room temperature (see Tables 5.2, 5.3).

^1H n.m.r. Data

Apart from the phenyl region the only resonances observed in the low temperature limiting spectrum were those of the retained THF ($\delta 3.6$ ppm and $\delta 1.8$ ppm) and two resonances one at $\delta 1.55$ ppm and one at $\delta 1.20$ ppm. The latter are broad and the couplings cannot be established even in the low temperature (-30°C) spectrum.

^{31}P n.m.r. Data

At room temperature the ^{31}P n.m.r. spectrum of the AAA complex contains a very broad resonance at 112.0 ppm, a triplet at 52.7 ppm and a singlet at 24.7 ppm (see Figure 5.5). The low temperature limiting spectrum displays all the coupling exhibited by the complex. This spectrum (Figure 5.6) contains (in the AAA case) a singlet at 23.0 ppm, a doublet of doublets at 115.5 ppm, a triplet at 110.8 ppm and a doublet of doublets at 51.6 ppm. Similar spectra have been obtained in the CAA case (see Table 5.3).

F.A.B. Mass Spectrum Data

The highest observed species in the AAA case is m/z 1101. Furthermore the isotopic patterns also suggests the presence of two chlorine groups in many of the fragments (Table 5.4 has a full list of fragments).

Infra-red Data

No high value carbonyl group is observed. The absorbance at 1550 cm^{-1} is assigned to be the $\nu(\text{OCO})_{\text{asym}}$ of the carbonyl group. These spectra also contain two $\nu(\text{Ru-Cl})$ absorbances. The only major difference in the two spectra lies in the area around 800 cm^{-1} . The AAA contains peaks at 825 cm^{-1} and 750 cm^{-1} , the corresponding peaks in the CAA case are located at 770 cm^{-1} and 755 cm^{-1} .

5.3.3 Structural Conclusions

At this point no definite structural assignment has been made. The data, however, does suggest that both complexes involve the coordination of a ligand of the form $\text{Ph}_3\text{PCHXCH}_2\text{CO}_2$, where $\text{X} = \text{CH}_3$ for the CAA case and H for the AAA case. This ligand is formed by the reaction of the relevant mixed anhydride and triphenylphosphine. Furthermore it appears to be the ability of the anhydride concerned to take part in this reaction that determines the relative quantities of the two products formed. This reaction is

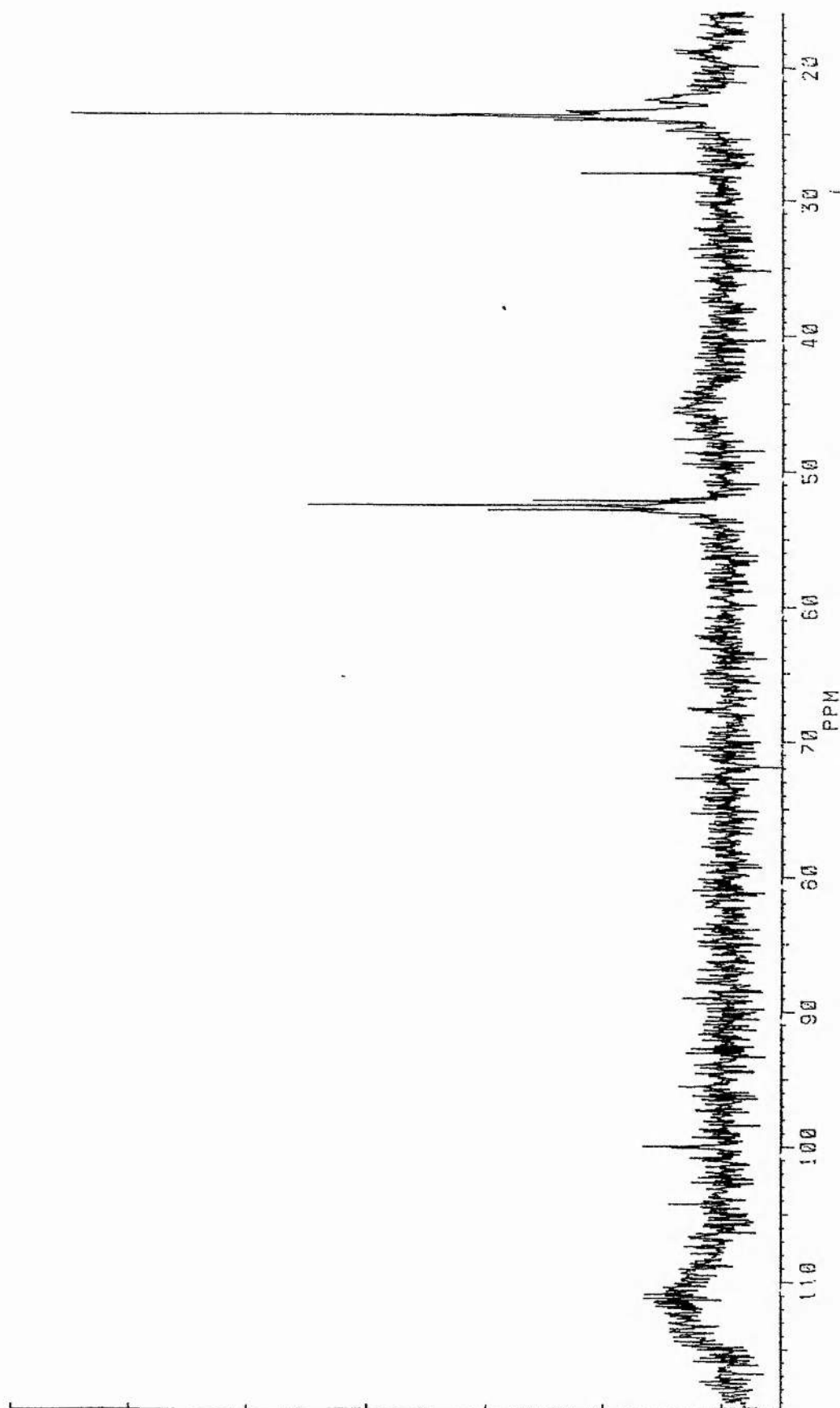


Fig. 5.5 ^{31}P n.m.r. spectrum (300MHz) of Product 2 of the $[\text{RuCl}_2(\text{PPh}_3)_4] + \text{Ph}_2\text{POCCH}=\text{CH}_2$ reaction (CD_2Cl_2 , 25°C)

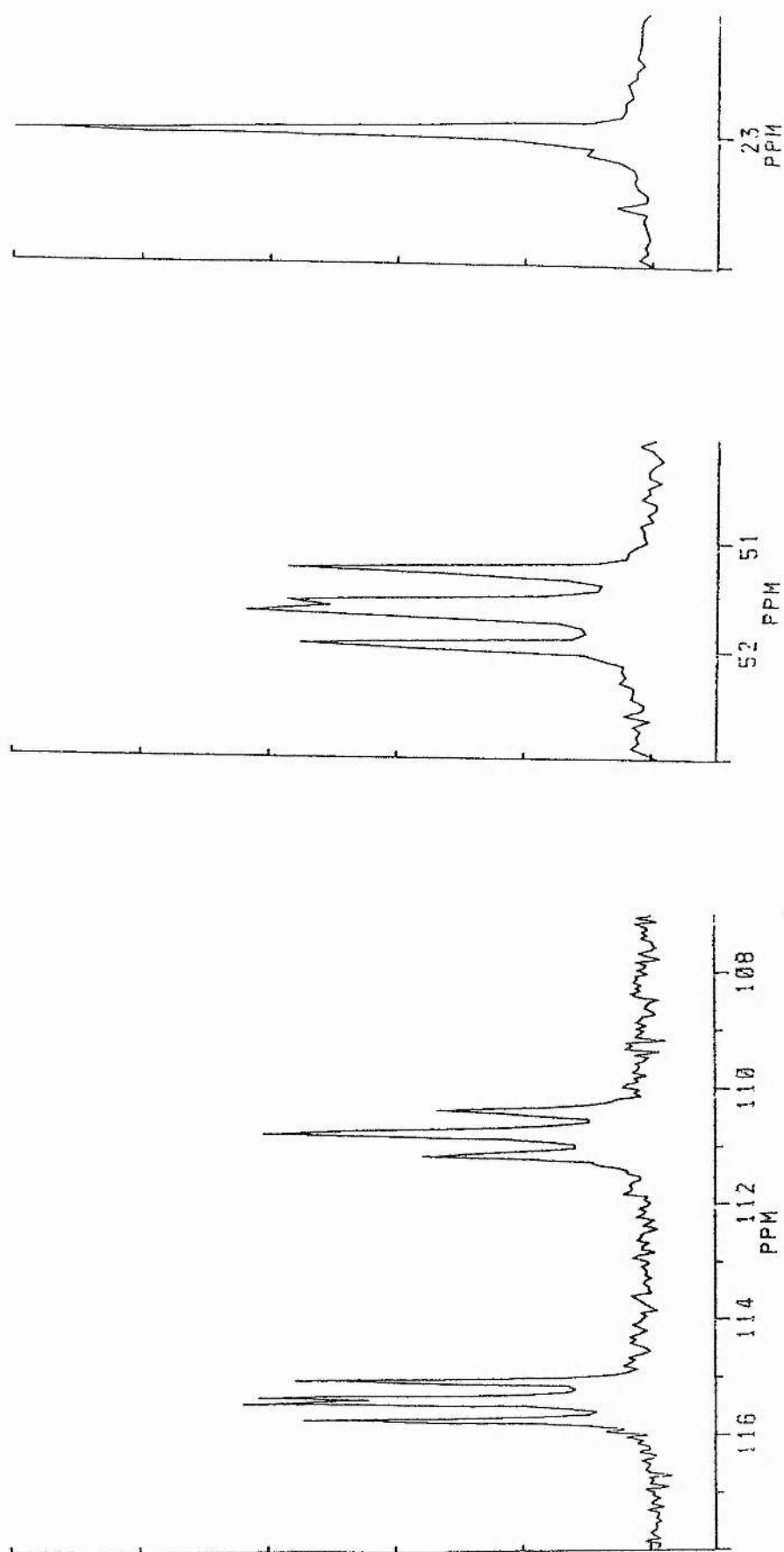


Fig. 5.6 ^{31}P n.m.r. spectrum (300MHz) of Product 2 of the $[\text{RuCl}_2(\text{PPh}_3)_4] + \text{Ph}_2\text{POCCH}=\text{CH}_2$ reaction (CD_2Cl_2 , -25°C)

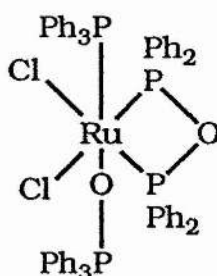
less favoured in the CAA case and as a result the relative quantity of product 2 is less. The evidence for this zwitterion ligand coordination to the complex comes mainly from the F.A.B. and n.m.r. spectra. The F.A.B. spectrum of the AAA product 2 is found to contain evidence for the loss of zwitterion fragments and contains a peak of m/z 334 which corresponds to the zwitterion itself (see Table 5.4). In the AAA case the proton n.m.r. spectrum contains two proton resonances at δ 1.55 ppm and δ 1.20 ppm. This is analogous to the rhodium complex discussed in Section 3.5 which was concluded to contain an oxygen bound zwitterion. The CAA complex also contain zwitterion peaks exhibiting similar high field shifts and as a result is also thought to contain an oxygen bound, CAA derived, zwitterion ligand. This conclusion is supported by the ^{31}P n.m.r. spectrum which exhibits singlets which are assigned to the uncoordinated phosphorus atom of the zwitterion. Furthermore the triphenylphosphine ligand's chemical shift (\approx 52 ppm) is analogous to that in the rhodium complex $[\text{Rh}(\text{PPh}_3)_3(\text{O}_2\text{CCH}_2\text{CH}_2\text{PPh}_3)][\text{PF}_6]$ and suggests that this compound contains a PPh_3 ligand bound *trans* to the zwitterion. The low temperature limiting ^{31}P spectrum is observed to contain 4 resonances (see Table 5.3) one of which is the zwitterion singlet, the others all exhibit mutual coupling. The location of the ^{31}P n.m.r. resonances which haven't been discussed, namely those at 115.4 ppm and 110.8 ppm, are thought to be at too low a field value to be due to a monodentate phosphorus ligand. Rather some form of phosphorus containing ring is thought to be

present. A bidentate mixed anhydride coordinated via the phosphorus atom and the double bond is discounted because no high value carbonyl group is observed in the infra-red spectrum, whilst the same ligand only bound via the carbonyl oxygen atom rather than the double bond is unlikely because the phosphorus resonances are located at too high a field value to indicate this ≈ 150 ppm is the expected region for this form of coordination. A bidentate zwitterion coordinated via the phosphorus atom is also ruled out as no bond can exist between the metal and the phosphorus atom in this species. The above structures can also be discounted on the grounds that they could not explain the mutual phosphorus coupling observed. The coupling suggests that three phosphorus atoms are bound directly to the metal centre.

One possible way to explain this coupling is the coordination of a tdpd ligand. The 110 ppm region is the correct area for the resonances of such a ligand to be found (c.f. the rhodium complexes in Chapter 3 and a second ruthenium compound discussed in Section 5.5) and the assignment of a chelate tdpd ligand would also be supported by the infra-red bands in the 800 cm^{-1} region. These bands may be assigned to the $\nu(\text{P-O-P})_{\text{asym}}$ and $\nu(\text{P-O-P})_{\text{sym}}$ bands of such a chelate ligand. The slight difference in the position of the $\nu(\text{P-O})_{\text{asym}}$ band may be explained by slight differences in the structure of the tdpd ligand to accommodate the steric bulk of the methyl substituent of the CAA zwitterion. Thus these facts combined with the information from the infra-red and F.A.B. results that two

chlorine ligands are present lead to the assignment of one possible structure shown in Figure 5.7.

In the F.A.B. spectrum, the highest observed fragment is at m/z 1101. This corresponds to a complex of the formula $[\text{RuCl}_2(\text{PPh}_3)(\text{Ph}_3\text{PCH}_2\text{CH}_2\text{CO}_2)_2]$, but such a complex has already been discounted. Such



where $\text{O}-\text{PPh}_3 = \text{PPh}_3\text{CHXCH}_2\text{CO}_2$

Fig. 5.7

a fragment, however, also supports the structure shown in Figure 5.7; the m/z 1101 fragment corresponding to the fragment $[\text{RuCl}(\text{PPh}_3)(\text{Ph}_2\text{POPPH}_2)(\text{OCH}_2\text{CH}_2\text{PPh}_3)]$ (i.e. loss of a chlorine ligand and oxygen atom from the species in Figure 5.7).

A further possibility is suggested by the low frequency of the $\nu(\text{OCO})_{\text{asym}}$ infra-red absorbance. This absorbance is observed to be at a lower frequency than the rhodium analogue suggesting, for reasons discussed in Section 2.5.1, bidentate binding of the zwitterion. This shift in the $\nu(\text{OCO})$ band may alternatively be due to the difference in the metal centre. If, however, the zwitterion is bidentate this could mean that the conclusions made about the

number of chlorine species may be incorrect. The most probable structures containing a bidentate zwitterion are shown in Figure 5.8. Figure 5.8(b) can be discounted as it cannot explain the ^{31}P n.m.r. coupling, thus a further possible structure for these product 2 complexes is Figure 5.8(a).

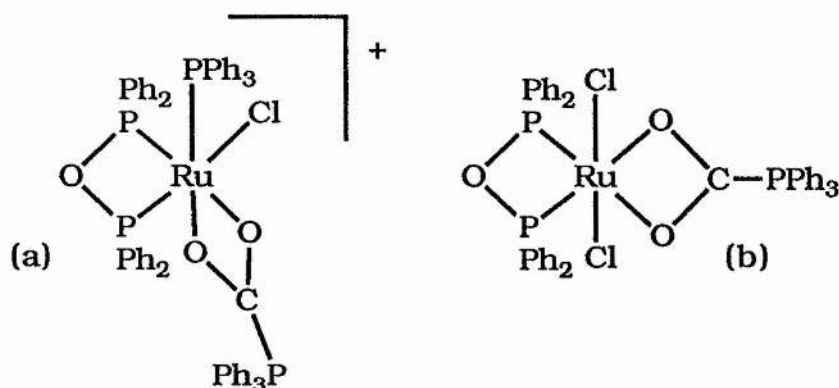


Fig. 5.8

It is also possible that the bidentate zwitterion is part of a dimeric structure. This would also explain the low value of the carbonyl group in the infra-red spectrum and may also explain the low solubility of the complex. A possible dimeric structure is shown in Figure 5.9.

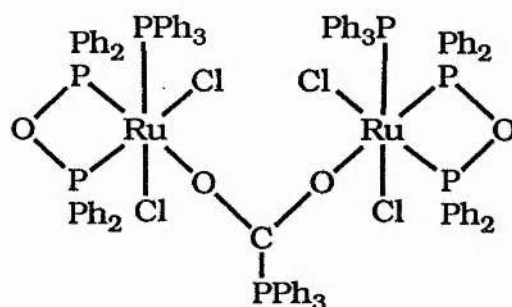


Fig. 5.9

This contains the bidentate zwitterion and the two chlorine ligands suggested by the infra-red spectrum. Similar coordination

to that shown in Figure 5.9 has been observed in tin complexes of the AAA zwitterion. Furthermore both structures shown in Figure 5.8a and 5.9 can produce the m/z 1101 fragment observed in the F.A.B. spectrum.

However, one point against the assignment of such a ligand is the size of the ^{31}P n.m.r. couplings. Normally the inter ring coupling of a tdpdp ligand is in the region of 90 Hz for a ruthenium complex. The coupling here is of the order of 40 Hz which leads to the conclusion that the ring may not be a tdpdp ring but a $\text{Ph}_2\text{POHOPPh}_2$ ring like those discussed in Chapter 6. Thus product 2 may possess a structure similar to those shown in Figures 5.7 - 5.9 but containing a $\text{Ph}_2\text{POHOPPh}_2$ ring. These compounds would be cationic which may explain the low solubility exhibited by product 2. Alternatively it is possible that rather than a $\text{Ph}_2\text{POHOPPh}_2$ ring the complexes may contain two Ph_2POH ligands as the resonances for such species are found in relatively low field positions in the ^{31}P n.m.r (e.g. in $[\text{Ru}(\text{tdpd})(\text{Ph}_2\text{POH})_2\text{Cl}_2]$ the Ph_2POH ligands are located at ≈ 80 ppm). These would give neutral species and the infrared spectra do contain peaks around 900 cm^{-1} which would be in the correct region for this type of ligand. However the absence of a resonance for the P-OH group in the proton n.m.r. disfavors this explanation. Thus no firm conclusion about the presence or otherwise of such a ligand can be made at this point because the spectral information is somewhat contradictory.

The fluxional process is not understood and is not likely to

be until the intimate structure has been determined. Crystals of x-ray quality have been grown from dichloromethane solutions and an x-ray structure is presently underway. This should resolve all the structural questions and may ultimately shed light on the fluxionality of the complex in Sections 5.3 and 5.4.

5.4 Discussion of the Coordination Exhibited by the Ruthenium Complexes

The coordination of the DAA ligand, through the phosphorus and oxygen atoms, is supported by previous work done on ligands of this type and similar coordination is also observed for the minor products of the CAA and AAA ligands. The isolation of the second complexes from both the CAA and AAA reactions have been attributed to properties of the metal reagent used. In the rhodium cases the only PPh_3 present in solution is that displaced from the rhodium centre upon coordination of the AAA ligand. Thus initially there is little free PPh_3 in solution to disrupt the coordination of the AAA ligand. In the ruthenium case a mole of triphenylphosphine is liberated immediately upon dissolving this reagent. This released PPh_3 is thus free to take part in the reaction already described in Chapter 2 for the CAA and AAA ligands and then coordinates to the metal centre. The ability of the mixed anhydride to coordinate appears to depend on the degree of substitution of the mixed anhydride's double bond. DAA does not react with

triphenylphosphine, thus the only product contains a coordinated mixed anhydride ligand. Both CAA and AAA react resulting in the formation of two products. AAA reacts more efficiently and so results in a greater quantity of product 2 in the AAA case. This effect is surpassed in the 1:2 mole reaction because the greater quantity of AAA added supplies enough ligand both to react with the metal reagent and with the free triphenyl phosphine. This may also explain the lower yields observed for this complex.

5.5 The 1.2 Mole Reaction of $\text{Ph}_2\text{PO}_2\text{CCH}=\text{CH}_2$ with $\text{RuCl}_2(\text{PPh}_3)_4$

The procedure used in this reaction was identical to that for the reaction with $[\text{RhCl}(\text{PPh}_3)_3]$ described in Section 3.2, Chapter 3. On stirring $[\text{RuCl}_2(\text{PPh}_3)_4]$ with two mole equivalents of $\text{Ph}_2\text{PO}_2\text{CCH}=\text{CH}_2$ in THF no colour change occurred, but the starting metal complex was noted to dissolve gradually. No crystals were isolated from this solution but a pale yellow solid could be isolated by the careful addition of petroleum ether (40-60°). The resultant complex could be purified by exhaustive washing with diethyl ether followed by extraction with THF and analysed to be $[\text{RuCl}_2(\text{Ph}_2\text{POPPH}_2)(\text{Ph}_2\text{PO}_2\text{CCH}=\text{CH}_2)(\text{PPh}_3)]$. The spectral data is discussed in the following sections.

Infra-red Data

The $\nu(\text{Ru-Cl})$ band is present (330 cm^{-1}) and absorbances at

830 cm^{-1} and 780 cm^{-1} are assigned to be the $\nu(\text{P-O-P})_{\text{asym}}$ and $\nu(\text{P-O-P})_{\text{sym}}$ bands of the tetraphenyldiphosphoxane ligand, their position indicating coordination of this ligand in the same manner as $[\text{RhCl}(\text{PPh}_3)(\text{Ph}_2\text{POPPh}_2)]$. Also present is a broad band at 1710 cm^{-1} which is due to the carbonyl group of an AAA ligand bound only through the phosphorus atom. This assignment is supported by an absorbance at 1580 cm^{-1} which is assigned to the $\nu(\text{C}=\text{C})$ of such a ligand.

^1H n.m.r. Data

All the protons in this complex are found to be located in the phenyl region of the proton spectrum. The acrylic acid parent acid's proton resonances are close to the phenyl region. It is thought that formation and coordination of the mixed anhydrides shifts these resonances up into the phenyl region.

^{31}P n.m.r. Data

The ^{31}P n.m.r. spectrum contains 4 resonances (see Figure 5.10) these are three doublets of doublets at 111.2 and 106.8 and 84.5 ppm and an apparent doublet of triplets at 18.7 ppm. The coupling information is summarised in Table 5.3 and indicate that all four phosphorus species are bound to the metal and each display mutual coupling to the other 3 phosphorus atoms present. Thus

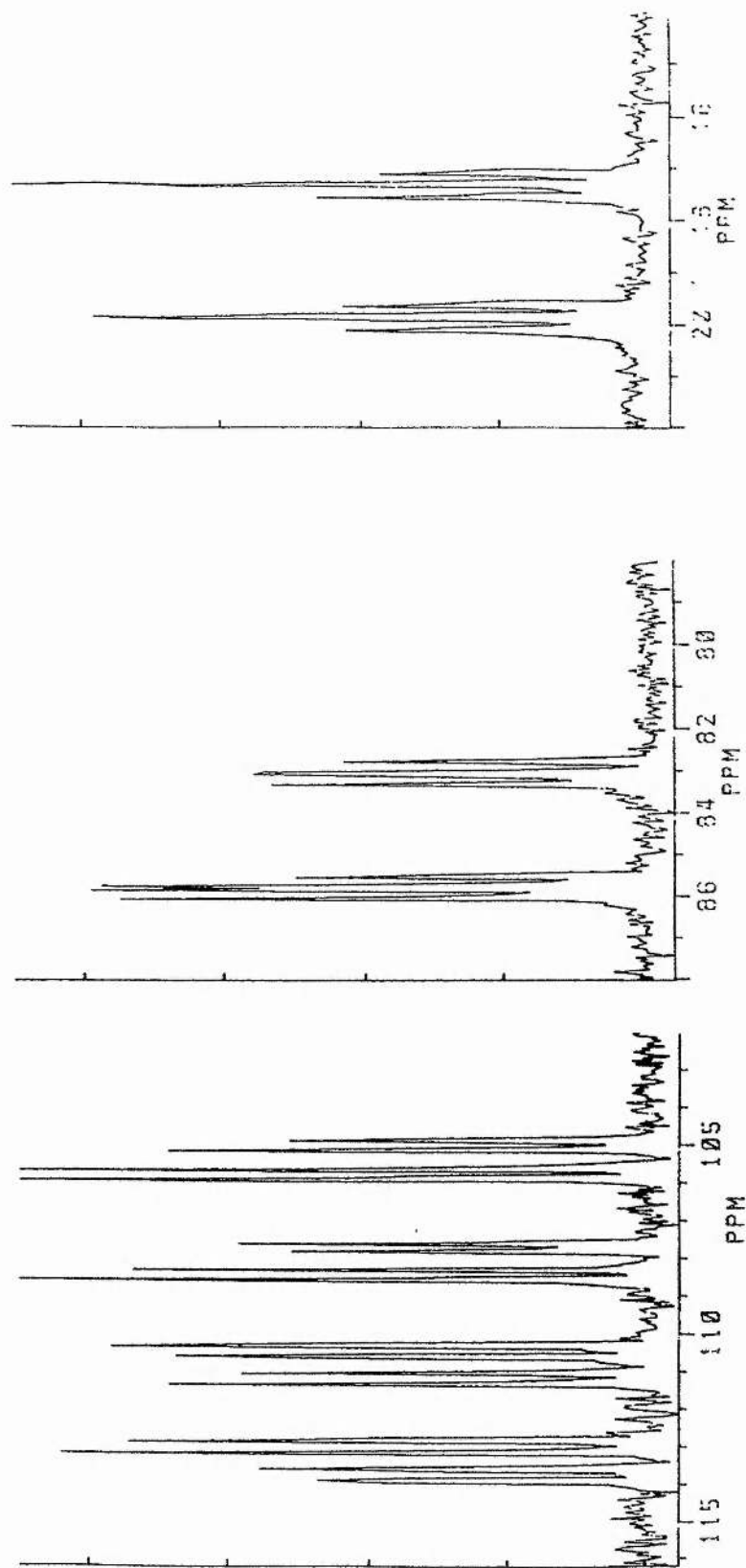


Fig. 5.10 ^{31}P n.m.r. spectrum (300MHz) of $[\text{RuCl}_2(\text{Ph}_2\text{POPPh}_2)(\text{Ph}_2\text{POCCH}=\text{CH}_2)(\text{PPh}_3)_2]$ (CD_2Cl_2 , 25°C)

first inspection signifies that the complex contains four phosphorus species in different environments. The two resonances above 100 ppm are assigned to a tpdp ring. This is further supported by the mutual coupling between these species being 90.0 Hz which when compared to the case of $[\text{RhCl}(\text{tpdp})(\text{PPh}_3)]$ (ring coupling 122 Hz) is the correct order of magnitude to indicate that ring formation has occurred. As regards the resonances at 18.7 ppm and 84.5 ppm, the first is in the typical position for a triphenylphosphine ligand bound to ruthenium and *trans* to a ligand of fairly high *trans* influence and the latter is assigned to the AAA ligand. Thus the overall structure is thought to be that in Figure 5.11.

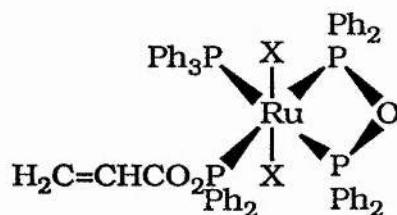


Fig. 5.11

F.A.B. Mass Spectrum

The highest observed species cannot be assigned to a complex with the above structure. The matrix used was nitrobenzyl alcohol (N.B.A.) and in F.A.B. studies it is possible for a solvent fragment to attach to a fragment of the test substance resulting in peaks of higher than expected m/z values. The major fragments from N.B.A. are m/z 136, 154, 289, 307, 460⁽¹⁸³⁾. The highest value fragment which is found not to be related to smaller m/z complex

fragments is 1076 which relates to $[\text{Ru}(\text{PPh}_3)(\text{tpdp})(\text{Ph}_2\text{PO}_2\text{CCHCH}_2)\text{Cl}_2]$, the full fragmentation pattern is shown in Table 5.5 and thus suggests the full complex structure is as in Figure 5.12

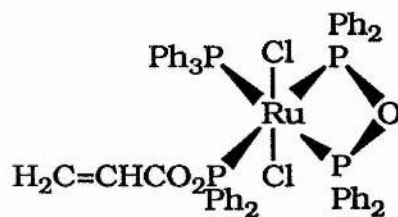


Fig. 5.12

Table 5.1		Spectral Data for the Zwitterion Ligands			(CD ₂ Cl ₂ , 25°C)	
Compound		¹ H (ppm)		³¹ P	IR	
		δH	δMe		ν(C=O)	
Ph ₃ PCH ₂ ^b CH ₂ ^a CO ₂		a 3.4, b 2.7	-----	24.7	1593, 1583	
Ph ₃ PCH ^c CH ₃ ^d CH ₂ ^{a,b} CO ₂		a 3.0, b 4.7, c 2.25	d 1.4	30.1	1588br	

Table 5.2 ^1H n.m.r. and I. R. Spectral Data for the Ruthenium Complexes		$(\text{CD}_2\text{Cl}_2, 25^\circ\text{C})$	
Complex		I.R. (cm^{-1})	
		$\nu(\text{C}=\text{O})$ $\nu(\text{C}=\text{C})$ $\nu(\text{Rh}-\text{Cl})$	$\nu(\text{P}-\text{O})_{\text{asym}}$ * $\nu(\text{P}-\text{O})_{\text{sym}}$ *
$[\text{RuCl}_2(\text{PPh}_3)_2(\text{Ph}_2\text{PO}_2\text{CCH}^{\text{f}}=\text{CMe}_2^{\text{a,b}})]$		1637s 1637 340w	-----
$[\text{RuCl}_2(\text{PPh}_3)_2(\text{Ph}_2\text{PO}_2\text{CCH}=\text{CHMe})]$		Not Observed	
$[\text{RuCl}_2(\text{PPh}_3)_2(\text{Ph}_2\text{PO}_2\text{CCH}=\text{CH}_2)]$		Not Observed	
CAA Product 2		1550s ----- 340,300	770 755
AAA Product 2		1550s ----- 335,290	825 750
$[\text{RuCl}_2(\text{PPh}_3)(\text{Ph}_2\text{PO}_2\text{CCH}=\text{CH}_2)(\text{Ph}_2\text{POPPH}_2)]$		1170br 1580br 330w	830 780
		^1H (ppm)	
		δMe	δH
		a 2.2, b 1.9	c 5.75
		Not Observed	
		Not Observed	
		0.5 2.85, 2.5, 1.6	
		-----	1.55, 1.20
		All protons in the phenyl region	

* From the tpdp group

Table 5.3		³¹ P Spectral Data for the Ruthenium Complexes				(CD ₂ Cl ₂ , 25°C)							
Complex		Chemical Shifts				Coupling Constants(Hz)							
		Pa	Pb	Pc	Pd	PaPb	PaPc	PaPd	PbPc	PbPd	PcPd		
[RuCl ₂ (PPh ₃) ₂ (Ph ₂ P ^a O ₂ CCH=CMe ₂)]		153.3t	29.3d	----	----	30.6	30.6	----	----	----	----		
[RuCl ₂ (PPh ₃) ₂ (Ph ₂ P ^a O ₂ CCH=CHMe)]		153.0t	29.2d	----	----	33.2	30.6	----	----	----	----		
[RuCl ₂ (PPh ₃) ₂ (Ph ₂ P ^a O ₂ CCH=CH ₂)]		153.3t	29.2d	----	----	32.6	30.6	----	----	----	----		
CAA Product 2 ^f		111.0m	53.8t	28.9s	----	----	43.8	----	43.8	----	----		
CAA Product 2 [*]		113.4dd	110.7dt	52.7t	28.7s	47.7	38.6	----	49.7	----	----		
AAA Product 2 ^f		112.0m	52.7t	23.9s	----	----	43.1	----	43.8	----	----		
AAA Product 2 [*]		115.4dd	110.8dt	51.6t	23.0s	46.1	38.6	----	47.3	----	----		
[(RhCl(PPh ₃) ₂ (Ph ₂ P ^a O ₂ CCH=CH ₂)(Ph ₂ P ^b OP ^b Ph ₂)]		111.2ddd	106.8ddd	84.5dt	18.7dt	89.9	35.1	305.4	329.3	28.2	31.6		

^f room temperature * - 25°C

Table 5.4

m/z values for AAA product 2 and their possible assignments

m/z

1101	[RuCl ₂ (PPh ₃)(Ph ₃ PCH ₂ CH ₂ CO ₂) ₂], [RuCl(PPh ₃)(Ph ₃ PCH ₂ CH ₂ CO)(Ph ₂ POPPh ₂)]
934	[Ru(Ph ₂ POPPh ₂)(PPh ₃)]
922	[Ru(Ph ₂ POPPh ₂)(PPh ₃)Cl ₂ (PCH ₂ CH ₂ CO ₂)]
795	[RuCl ₂ (PPh ₃)(Ph ₃ CH ₂ CH ₂ CO ₂)(OC)]
781	
767	[RuCl ₂ (PPh ₃)(Ph ₃ PCH ₂ CH ₂ CO ₂)], [RuCl ₂ (PPh ₃)(Ph ₃ PCH ₂ CH ₂ CO ₂)]
689	[RuCl ₂ (PPh ₃)(Ph ₂ PCHCH ₂ CO ₂)]
639	[Ru(PPh ₃)(Ph ₃ PCH ₂)]
587	
563	
460	
407	
363	
334	Ph ₃ PCH ₂ CH ₂ CO ₂

Table 5.5

	m/z
$[\text{Ru}(\text{tpdp})(\text{PPh}_3)(\text{Ph}_2\text{PO}_2\text{CC}=\text{CH}_2)\text{Cl}(\text{NBA})]^+$	1175
$[\text{Ru}(\text{tpdp})(\text{PPh}_3)(\text{PhPO}_2\text{CCH}=\text{CH})\text{Cl}(\text{NBA})]^+$	1115
$[\text{Ru}(\text{tpdp})(\text{PPh}_3)(\text{PhPO}_2\text{CCH}=\text{CH})\text{Cl}(\text{NBA})]^+$	1098
$[\text{Ru}(\text{tpdp})(\text{PPh}_3)(\text{Ph}_2\text{PO}_2\text{CCH}=\text{CH}_2)\text{Cl}_2]^+$	1075
$[\text{Ru}(\text{tpdp})(\text{PPh}_3)(\text{Ph}_2\text{POCC}=\text{C})\text{Cl}_2]^+$	1055
$[\text{Ru}(\text{tpdp})(\text{PPh}_3)(\text{Ph}_2\text{PO}_2\text{CC})\text{Cl}]^+$	1025
$[\text{Ru}(\text{tpdp})(\text{PPh}_3)(\text{PhPO}_2\text{CCH}=\text{CH})]^+$	927
$[\text{Ru}(\text{tpdp})(\text{PPh}_3)(\text{PPhO})]^+$	872
$[\text{Ru}(\text{tpdp})(\text{Ph}_2\text{POCC})(\text{Cl})]^+$	762
$[\text{Ru}(\text{tpdp})(\text{PPh}_2\text{O})\text{Cl}]^+$	724
$[\text{Ru}(\text{tpdp})(\text{PPh}_2\text{O})]^+$	689

5.6 Experimental

[Ru(PPh₃)₂Cl₂(Ph₂PO₂CCH=CMe₂)]

To a room temperature THF or dichloromethane (30cm³) solution of [RuCl₂(PPh₃)₄] (0.5g, 0.41 mmol) was added one mole equivalent of Ph₂PO₂CCH=CMe₂ (0.11g, 0.41 mmol). The solution was stirred constantly for one hour after which time the solution was filtered and concentrated. Upon careful addition of petroleum ether (40-60⁰) a black semi-crystalline solid was obtained and washed with cold tetrahydrofuran. Yield 0.28g (70.7%).

Theoretical [Ru(PPh₃)₂Cl₂(Ph₂PO₂CCH=CMe₂)] = C 64.9%; H 4.8%

Found [Ru(PPh₃)₂Cl₂(Ph₂PO₂CCH=CMe₂)] = C 64.7%; H 4.4%

Reactions of [RuCl₂(PPh₃)₄] with Ph₂PO₂CCH=CHMe and Ph₂PO₂CCH=CH₂

These followed the same method as that described above but the reactions were carried out at ice temperatures and in THF solutions only. The products appeared after standing at -30⁰c for several days.

[Ru(PPh₃)Cl₂(Ph₂PO₂CCH=CH₂)(Ph₂POPPH₂)]

This reaction followed the same procedure as that described for the 1:2 Wilkinson's Catalyst reaction in chapter 2. However in this experiment the metal containing starting material is [RuCl₂(PPh₃)₄]. No crystals were obtained; rather a fine yellow precipitate was

collected upon either standing for several days at -30°C or by careful addition of petroleum ether ($40-60^{\circ}$). This precipitate could be purified by extraction with diethyl ether. Yield 0.29g (49%)

Theoretical $[\text{Ru}(\text{PPh}_3)\text{Cl}_2(\text{Ph}_2\text{PO}_2\text{CCH}=\text{CH}_2)(\text{Ph}_2\text{POPPh}_2)].\text{thf}$

C 63.4%; H 5.0%

Found $[\text{Ru}(\text{PPh}_3)\text{Cl}_2(\text{Ph}_2\text{PO}_2\text{CCH}=\text{CH}_2)(\text{Ph}_2\text{POPPh}_2)].\text{thf}$

C 63.3%; H 4.9%

CHAPTER 6

The Reaction of Platinum Metals and Tetraphenyldiphosphine Monoxide

6.1 Introduction

6.1.1 Literature Routes to Complexes Containing Chelate Ph₂POPPh₂ Ligands

The first reported Ph₂POPPh₂ complex contained a bridging tdpd ligand was isolated from the reaction of [Mo(CO)₅(P(C₆H₅)₂Cl)] and [Mo(CO)₅(P(C₆H₅)₂)₂][HN(C₂H₅)₃] in the presence of triethylamine and was assigned the formula [Mo(CO)₅-((Ph₂)POP(Ph₂))-Mo(CO)₅]⁽¹⁸⁴⁾. Further examples of binuclear complexes possessing bridging tdpd ligands arose from the reaction of the monodentate complexes of the form [M(CO)₅(Ph₂POPPh₂)] (M= Cr, Mo or W), which readily displaced labile donor ligands on other metals to give bridged bimetallic products. For example, the reaction of [Mo(CO)₅(Ph₂POPPh₂)] and Cr(CO)₅.CH₃CN produced the complex shown in Figure 6.1⁽¹⁸⁵⁾.

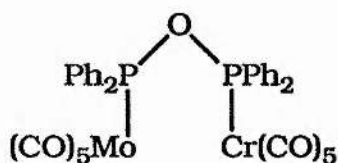


Fig. 6.1

A similar reaction, but with [Fe₂(CO)₉] yielded a yellow complex Mo(CO)₅-Ph₂POPPh₂-Fe(CO)₄ whose structure is analogous to that above ⁽¹⁸⁵⁾. This structure, confirmed by x-ray

crystallography, was shown to have a tdpd ligand bridging a six coordinate molybdenum centre and a five coordinate iron centre⁽¹⁸⁵⁾. Trinuclear complexes were also synthesized using a similar method, the reaction of two mole equivalents of $[\text{Mo}(\text{CO})_5(\text{Ph}_2\text{POPPh}_2)]$ with $(\text{PhCN})_2\text{PdCl}_2$ yielding the product in Figure 6.2 ⁽¹⁸⁵⁾.

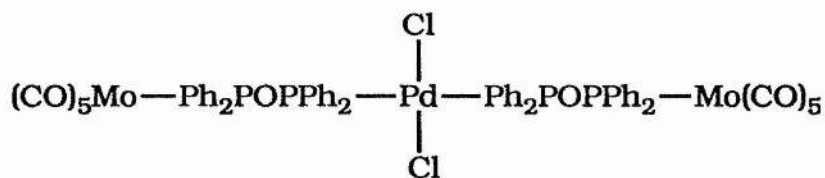
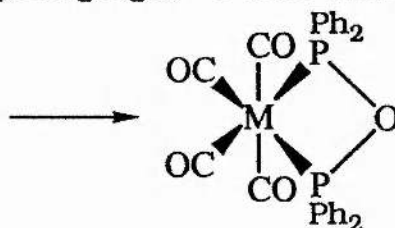
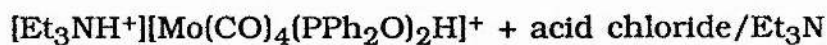


Fig. 6.2

Tdpd complexes have also been synthesized by using sulphonyl chlorides (RSO_2Cl). Zeiher, Mohyla, Lorenz and Hiller found that reaction of complexes of the form $[(\text{CO})_5\text{MP}(\text{C}_6\text{H}_5)_2\text{H}]$ ($\text{M} = \text{Cr}, \text{Mo}$ and W) in diethyl ether with sulphonyl chlorides gave rise to bridging tdpd complexes via the mechanism shown in Figures 6.3 and 6.4⁽¹⁸⁶⁾.

Due to the fact that all the complexes isolated up to this point had contained $\text{R}'\text{RPOPRR}'$ bridging ligands, it was thought that these ligands necessitated such a large angle at oxygen that chelation was prohibited. However, in recent years complexes containing chelate $\text{R}'\text{RPOPRR}'$ ligands have been isolated. The first examples of such compounds were isolated by Choi and Muttarties, who reported the isolation of Mo, W and Re complexes of $(\text{MeO})_2\text{POP}(\text{OMe})_2$ ⁽¹⁸⁷⁾ which contained a chelate tdpd ligand. Gray and Kraihanzel were

they prepared *cis* $[(\text{CO})_4\text{Mo}(\text{Ph}_2\text{POPPh}_2)]^{10}$ from the reaction of *cis* $[(\text{CO})_4\text{Mo}(\text{Ph}_2\text{PO})_2\text{H}^-]$ and acryl chlorides or chlorophosphines (Figure 6.5)⁽¹⁸⁸⁾.



(where the acid chloride = $2\text{CH}_3\text{C}(\text{O})\text{Cl}$, PCl_3 , $(\text{MeO})\text{P}(\text{O})\text{Cl}_2$).

Fig. 6.5

Wong extended this study with the isolation of the complexes of the form *cis* $[(\text{CO})_4\text{M}(\text{Ph}_2\text{POPPh}_2)]$ (where $\text{M} = \text{Cr}$, Mo and W) from the direct reaction of tetraphenyldiphosphine monoxide ($\text{Ph}_2\text{PP}(\text{O})\text{Ph}_2$) and metal carbonyls⁽¹⁸⁹⁾. The full reaction scheme developed by Wong is shown in Figure 6.6⁽¹⁹⁰⁾.

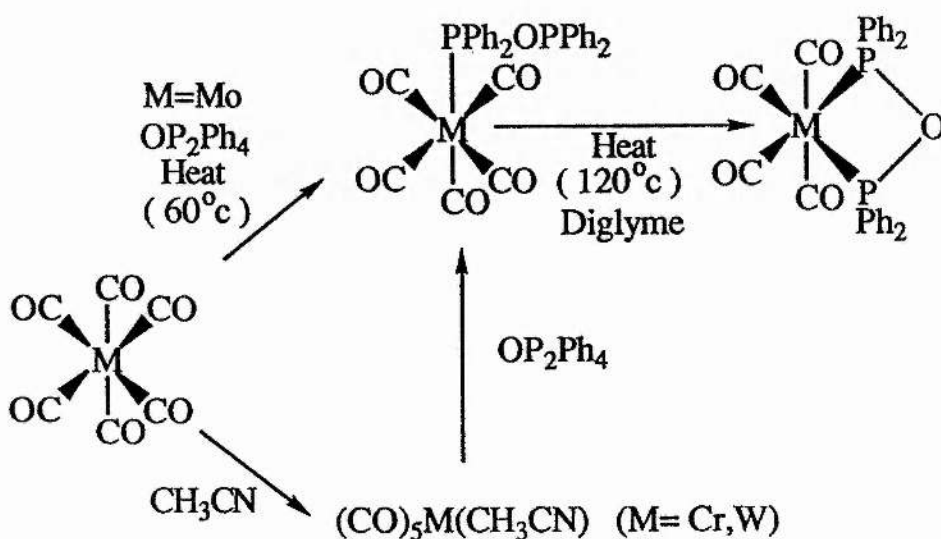


Fig. 6.6

6.1.2 Literature Examples of Complexes of Diphenyl- Phosphinous Acid and Secondary Phosphites

A number of transition metal complexes containing hydrogen bonded $[R_2POHOPR_2]^-$ ligands ($R = Ph, OMe, OEt$) have been synthesised (191,195). If the platinum metal complexes of these ligands are considered, the majority of the early studies were confined to the complexes of palladium (II) and platinum (II), for example, the complex shown in Figure 6.7⁽¹⁹⁶⁾.

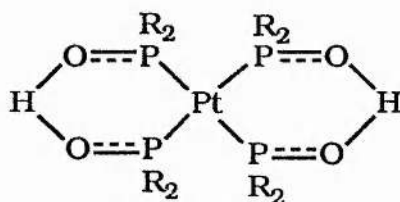


Fig. 6.7

Furthermore, it was found that the acidic protons could be removed to yield the anionic platinum complexes (Figure 6.8a) which could function as a chelating ligand, through the oxygen atoms, for a second transition metal ion (Figure 6.8b)⁽¹⁹⁶⁾. More recently $[R_2POHOPR_2]^-$ complexes of other platinum metals have been isolated. These include complexes of ruthenium, iridium and rhodium. $[(P(OMe)Ph_2)_2(P(OH)Ph_2)RuCl_3Ru((Ph_2PO)_3H_2)]$ for

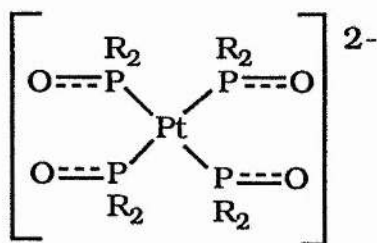
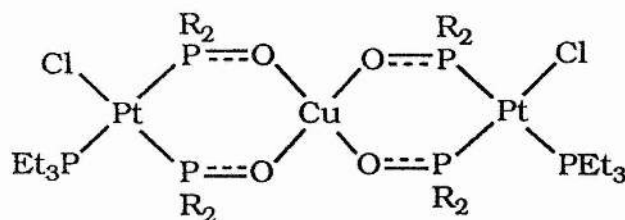


Fig. 6.8a



where R= OMe or OPh

Fig 6.8b

example was reported by T.A. Stephenson and co-workers in 1977⁽¹⁹⁷⁾. Stephenson isolated further ruthenium $[R_2POHOPR_2]^-$ complexes, which also contained chelate dimethyl dithiophosphinate ligands (Figure 6.9)

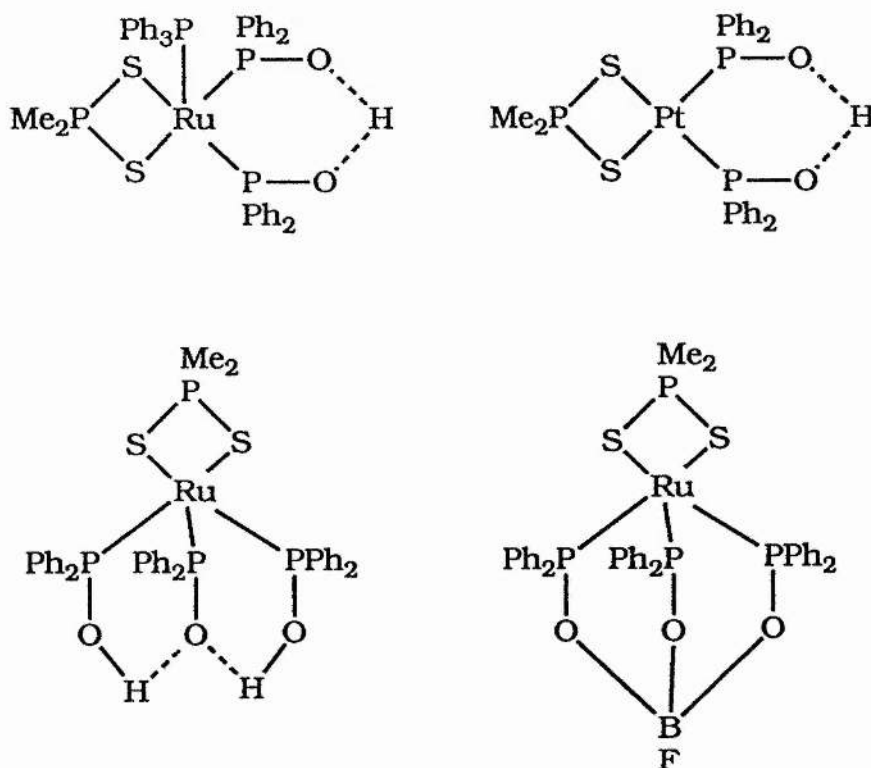


Fig. 6.9

from the reaction of *cis* $[Ru(S_2PMe_2)(PPh_3)_2]$ and varying quantities of PPh_2Cl in acetone to which $\approx 10\%$ water was added to

convert the free chlorodiphenylphosphine to $\text{PPh}_2(\text{O})\text{H}$ ⁽¹⁹⁸⁾.

A similar series of iridium complexes have also been obtained, examples of which are shown in Figures 6.10 a and b⁽¹⁹⁹⁾.

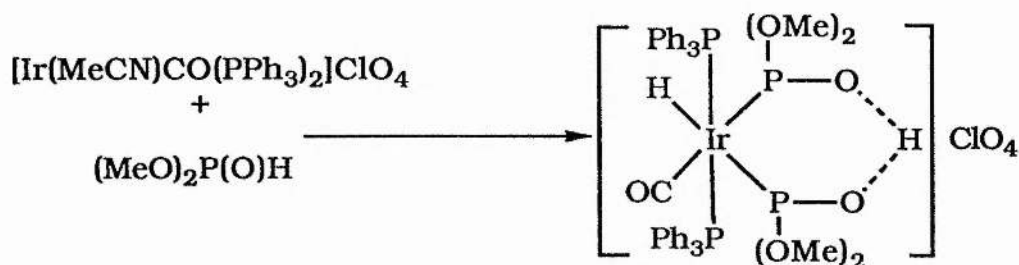
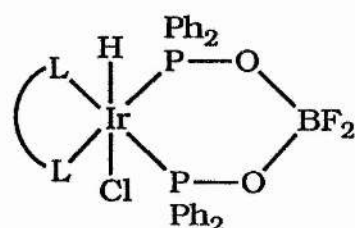
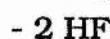
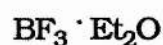
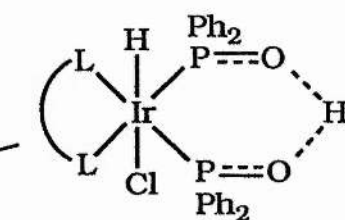
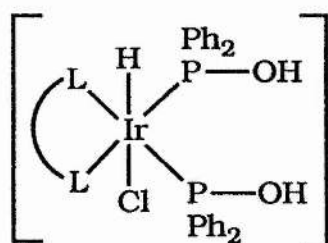
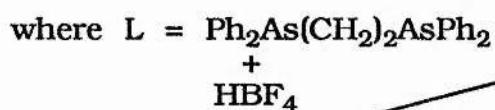
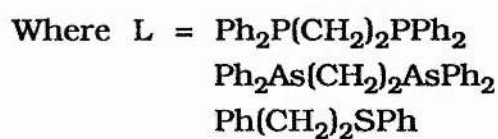
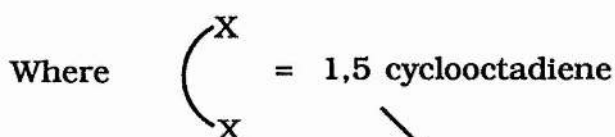
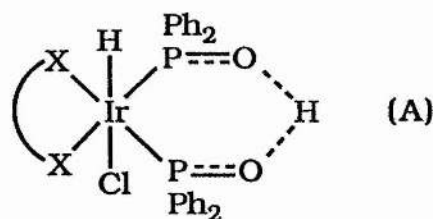
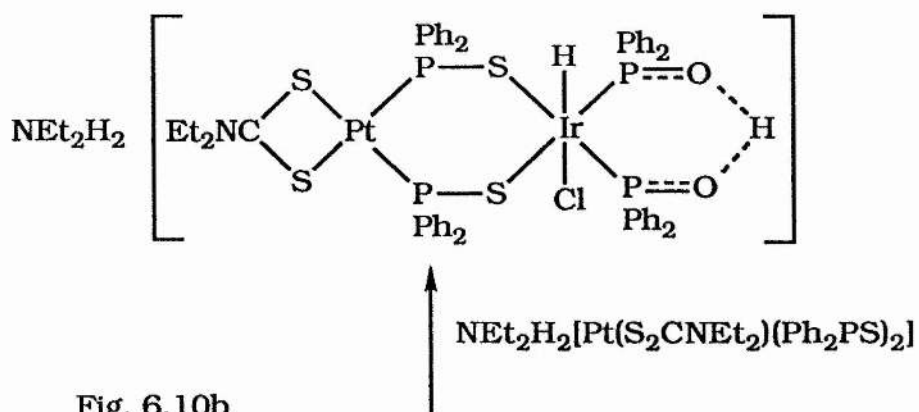


Fig. 6.10a

In the case shown in Figure 6.10b complex (A) was made from the treatment of $[(\text{IrCl}(\text{COD}))_2]$ (COD = cyclo octa-1,5-diene) with an excess of Ph_2PCl in aqueous methanol at ambient temperature⁽¹⁹⁹⁾.

In contrast related (diene) rhodium (I) compounds were found to react with various $\text{R}_2\text{P}(\text{O})\text{H}$ ligands, undergoing facile diene displacements to generate quite different species (Figure 6.11)⁽²⁰⁰⁾. The species X and Y were found not to undergo hydrolysis of the coordinated $\text{PPh}_2(\text{OMe})$ ligands. In the same work the $[\text{Rh}(\text{PPh}_2(\text{OEt}))_4]^+$ was also reported to result from the reaction of $[\text{RhL}_2(\text{C}_8\text{H}_{12})]\text{Z}$ (where $\text{Z} = \text{ClO}_4^-$ or BPh_4^- and $\text{L}_2 = \text{Ph}_2\text{AsCH}_2\text{CH}_2\text{AsPh}_2$, $\text{PhSCH}_2\text{CH}_2\text{SPh}$ or 2,2' bipyridyl) with $\text{PPh}_2(\text{OEt})$, whereas with the $[\text{Rh}(\text{Ph}_2\text{PCH}_2\text{CH}_2\text{PPh}_2)(\text{C}_8\text{H}_{12})]^+$ cation $[\text{Rh}(\text{Ph}_2\text{PCH}_2\text{CH}_2\text{PPh}_2)(\text{PPh}_2(\text{OEt}))_2][\text{BPh}_4]$ is the complex isolated (Figure 6.12). Furthermore, reaction of $[\text{RhL}_2(\text{diene})][\text{ClO}_4]$ (where L_2

= diphosphine or bis(phosphine)) with H_2 followed by addition of $P(OR)_2(O)H$ ($R = Me$ or Et) resulted in the unstable cations $[RhL_2(P(OR)_2OH)_2]^+$ (200). For other examples of related studies on rhodium and iridium see work by M. A. Bennett et al (201) and H. Werner et al (202).



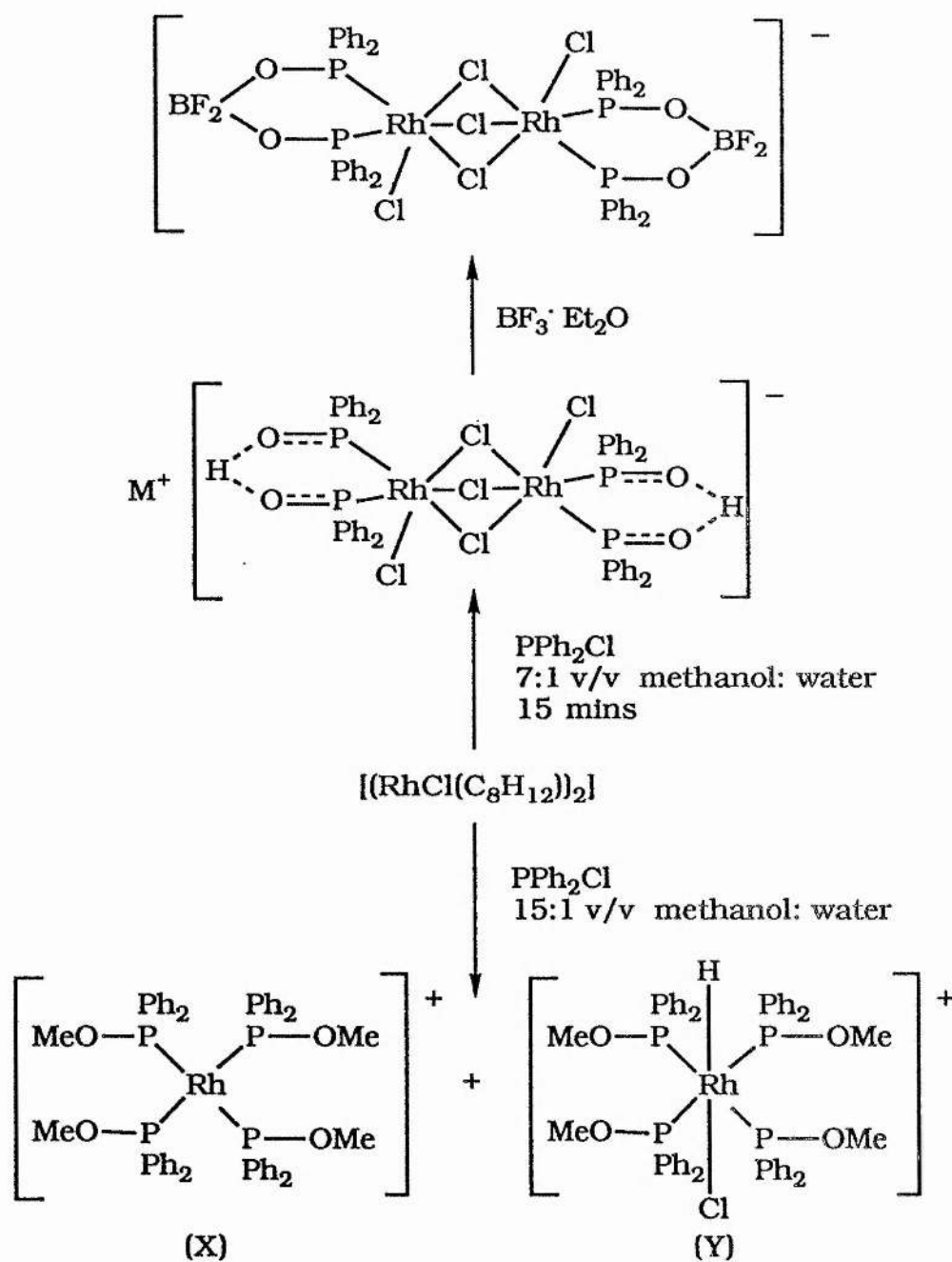


Fig. 6.11

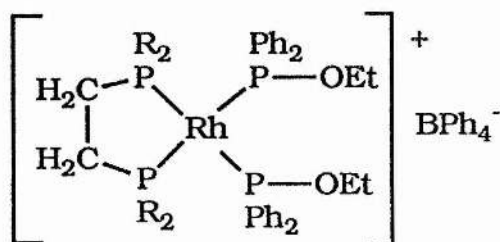


Fig. 6.12

6.2 Reflux Reactions of $\text{Ph}_2\text{PP}(\text{O})\text{Ph}_2$ and $[\text{RhCl}(\text{PPh}_3)_3]$.

$[\text{RuCl}_2(\text{PPh}_3)_4]$ and $[\text{OsCl}_2(\text{PPh}_3)_4]$

Chapter 3 detailed the formation of the first platinum metal complexes containing chelate tdpd ligands, and reported the low temperature reaction of $[\text{RhCl}(\text{PPh}_3)_3]$ and tetraphenyldiphosphine monoxide. This chapter details further reactions with the late transition metals and tetraphenyldiphosphine monoxide. The following reactions were carried out in the presence of small amounts of $[\text{NEt}_3\text{H}][\text{Cl}]$.

6.2.1 Reflux of $[\text{RhCl}(\text{PPh}_3)_3]$ and $\text{PhPP}(\text{O})\text{Ph}_2$ In Tetrahydrofuran

Wilkinson's Catalyst was refluxed with one mole equivalent of $\text{Ph}_2\text{PP}(\text{O})\text{Ph}_2$ in tetrahydrofuran for a period of 4 hours. Orange crystallites were produced from the cooled, filtered and concentrated reaction solution upon standing at -3°C for several days. Analysis of these crystallites proved them to be a mixture of several complexes. The major product isolated by further recrystallisation proved to be $[\text{RhCl}(\text{PPh}_3)(\text{Ph}_2\text{POPPh}_2)]$, the complex described in Chapter 3 containing a chelate tdpd ligand. However, repeating the reaction with an excess of $\text{Ph}_2\text{POPPh}_2$ following the same procedure resulted in the isolation of a small batch of pale yellow crystals. Again, analysis proved that several

complexes were present, two of which were suggested by ^{31}P nmr and F.A.B. mass spectral data to be $[\text{Rh}(\text{PPh}_3)_2(\text{tpdp})][\text{Cl}]$ and $[\text{Rh}(\text{tpdp})(\text{Ph}_2\text{POH})_2]$. The x-ray structure of a third complex was obtained, proving this complex to be $[\text{RhCl}_2(\text{Ph}_2\text{PO})_3\text{H}][\text{HNEt}_3]$. This complex is shown to be a hydrogen bonded ion pair, the structure of which is detailed in Chapter 7 (see Figure 7.7).

6.2.2 Reflux of $[\text{RuCl}_2(\text{PPh}_3)_4]$ and $\text{Ph}_2\text{PP}(\text{O})\text{Ph}_2$ in Tetrahydrofuran

Following the method described in Section 6.2.1 $[\text{RuCl}_2(\text{PPh}_3)_4]$ was refluxed in tetrahydrofuran with a mole equivalent of $\text{Ph}_2\text{PP}(\text{O})\text{Ph}_2$. No crystals were isolated from this reaction solution upon standing at -3°C . However a pale yellow precipitate could be isolated from the reaction solution upon careful addition of petroleum ether. This complex analysed to be $[\text{Ru}(\text{PPh}_2\text{OH})_2(\text{Ph}_2\text{POPPh}_2)\text{Cl}_2]$.

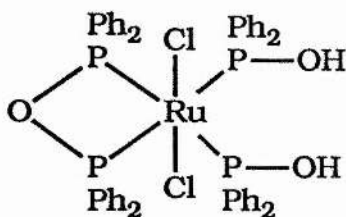


Fig. 6.13

Infra-red Data

The $\nu(\text{Ru}-\text{Cl})$ absorption was located at 280 cm^{-1} . The

presence of a chelating tdpd ligand is confirmed by the position of the $\nu(\text{P-O-P})_{\text{asym}}$ bond at 780 cm^{-1} . Also present is a second $\nu(\text{P-O-P})$ peak at 863 cm^{-1} indicating the presence of the Ph_2POH ligand. For example, the $\nu(\text{P-O})$ band in $[\text{IrHCl}(\text{Ph}_2\text{AsC}_2\text{H}_4\text{AsPh}_2)(\text{Ph}_2\text{OH})_2][\text{BF}_4]$ is located at 885 cm^{-1} whilst $\text{Ph}_2\text{POHOPPh}_2$ absorbances are found in the region of 1000 cm^{-1} (203). Also present are broad bands corresponding to the absorbances of the OH groups. These indicate the presence of both intermolecular hydrogen bonding (broad band at $\approx 3200\text{ cm}^{-1}$) and intramolecular hydrogen bonding (broad band at $\approx 1680\text{ cm}^{-1}$). The symmetrical nature of the intramolecular hydrogen bonding between the oxygen atoms of the Ph_2POH groups results in the OH absorbance being located not in the 3200 cm^{-1} region but in the $1700\text{-}1600\text{ cm}^{-1}$ region(204).

^{31}P nmr Data

The ^{31}P n.m.r. spectrum of this complex exhibits a AA'XX' spin system with resonances at 114.4 and 84.6 ppm (Figures 6.14a and b). The 114.4 resonance is in the typical position for a chelate tdpd in a ruthenium complex as shown in Chapter 5 with $[\text{RuCl}_2(\text{PPh}_3)(\text{AAA})(\text{tdpd})]$. The 84.6 ppm resonance is also in a typical position for a Ph_2PO ligand as shown in the literature values of such ligands. The couplings, summarized in Table 6.2, include 2 large *trans* couplings and 3 *cis* couplings of similar size indicating a basic structure of the form shown in Figure 6.16. The fourth *cis*

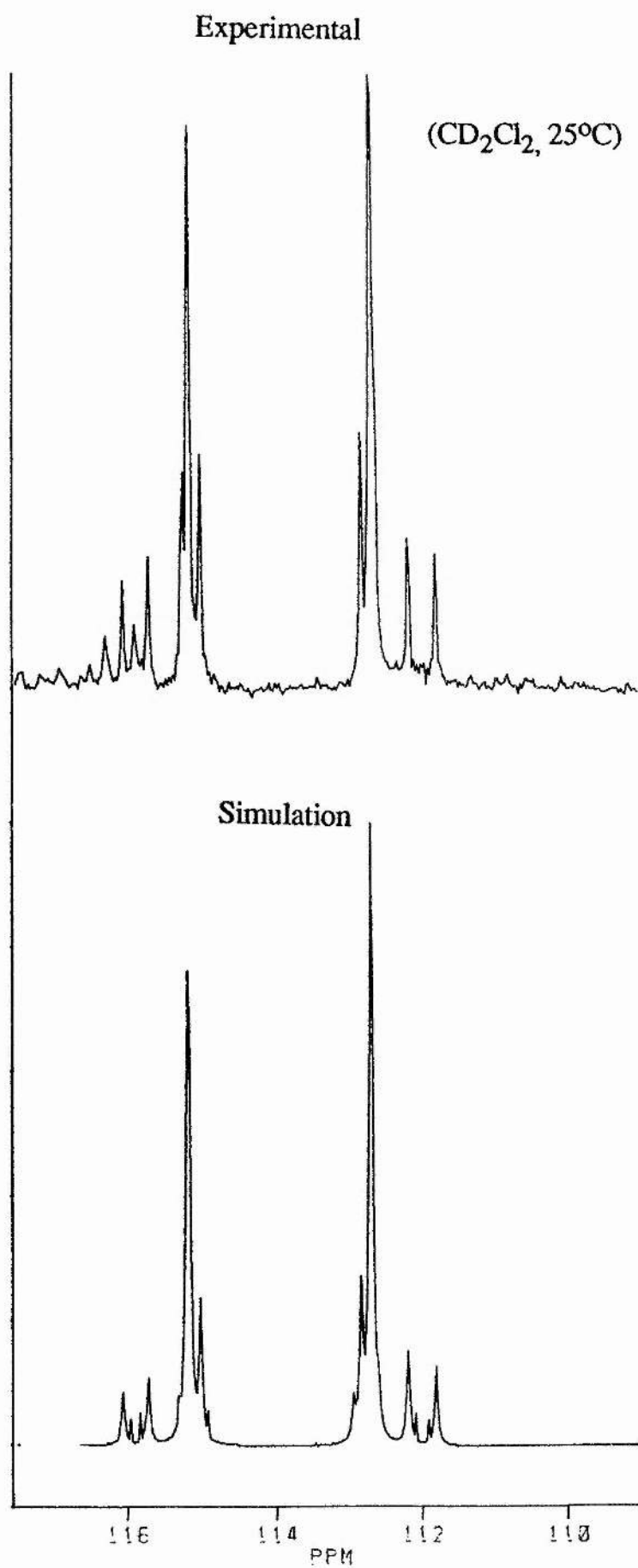


Fig. 6.14a ³¹P n.m.r. spectrum (300MHz) of [RuCl₂(Ph₂POPPh₂)(Ph₂POH)₂] Part A

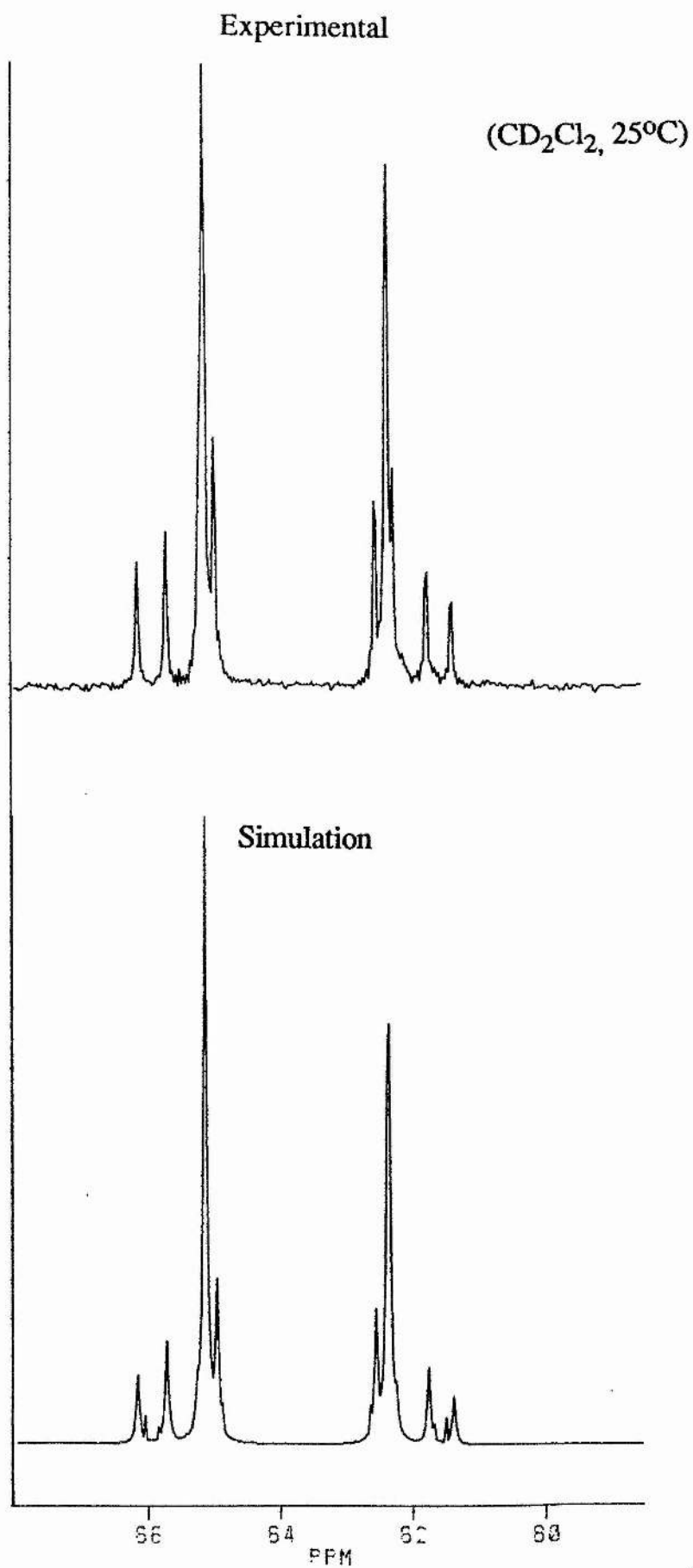


Fig. 6.14b ³¹P n.m.r. spectrum (300MHz) of [RuCl₂(Ph₂POPPPh₂)(Ph₂POH)₂] Part B

coupling is large in size which is consistent with its assignment as the J_{pp} of the POP ring.

^1H nmr Data

Most of the proton data is contained in the phenyl region (Figure 6.15). The only features observed outside this region are the resonances relating to the retained THF and a broad singlet at 5.85 ppm. This is assigned to be the resonance of the PPh_2OH group, which supports the conclusion that the complex under study contains two Ph_2POH ligands rather than a hydrogen bonded RuPOHOP ring, as the resonances of the latter are found in the region of 11-10 ppm, whilst that of $[\text{IrHCl}(\text{Ph}_2\text{AsC}_2\text{H}_4\text{AsPh}_2)(\text{Ph}_2\text{OH})_2][\text{BF}_4]$ is located at 4.1 ppm⁽²⁰³⁾.

6.2.3 Reflux of $[\text{OsCl}_2(\text{PPh}_3)_4]$ and $\text{Ph}_2\text{PP}(\text{O})\text{Ph}_2$ in Tetrahydrofuran

Following the same method described in Section 6.2.1 the title reaction was carried out and resulted in the isolation of a bright yellow complex which analysed to be $[\text{OsCl}_2(\text{Ph}_2\text{POPPh}_2)(\text{PPh}_2\text{OH})_2]$ (Figure 6.16).

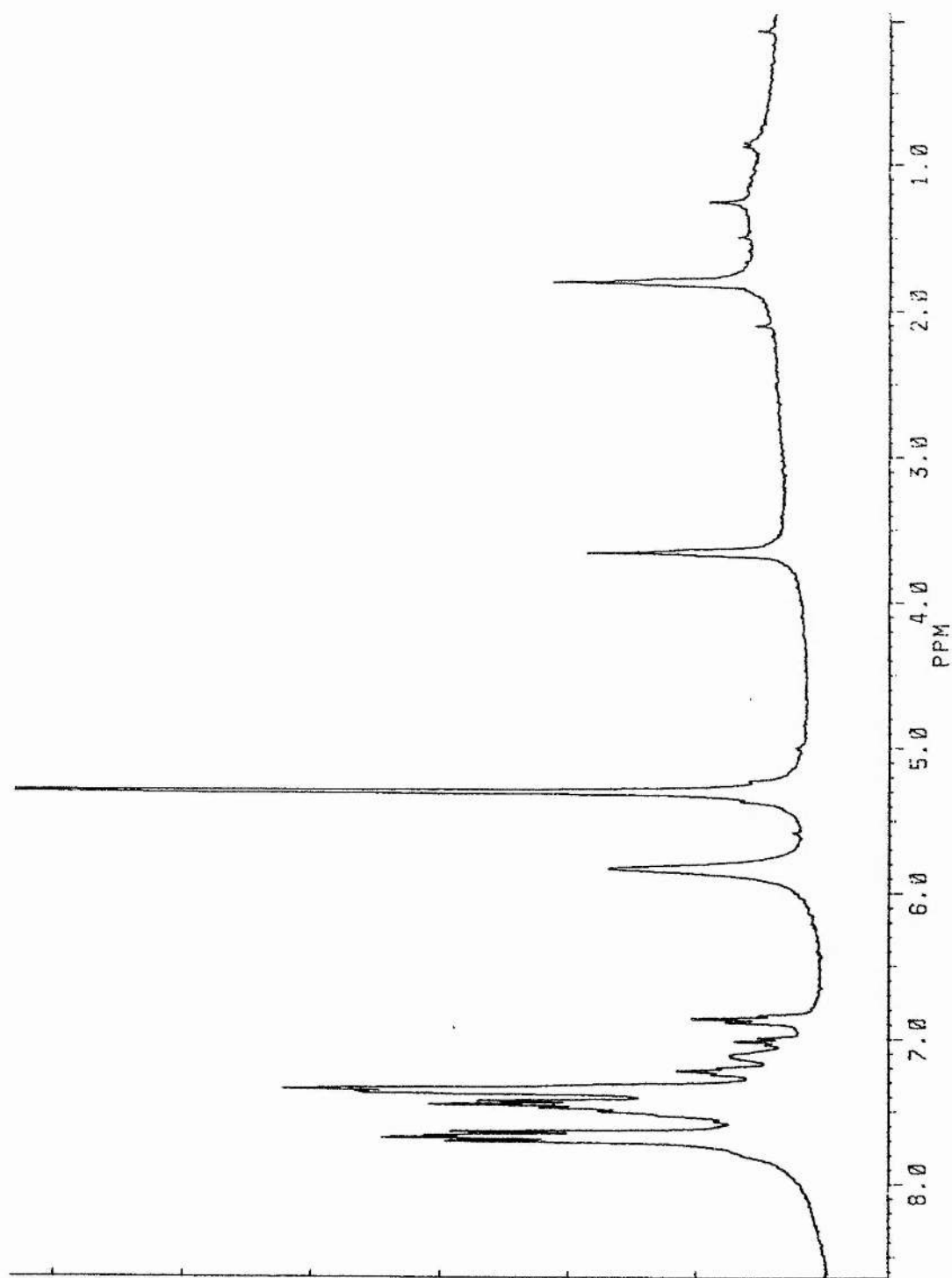


Fig 6.15 ^1H n.m.r. spectrum (300MHz) of $[\text{RuCl}_2(\text{Ph}_2\text{POPPh}_2)(\text{Ph}_2\text{POH})_2]$ (CD_2Cl_2 , 25°C)

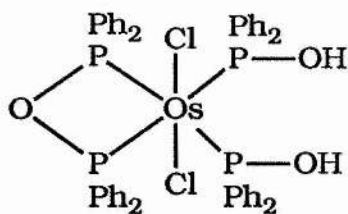


Fig. 6.16

Infra-red Data

This had a $\nu(\text{Os-Cl})$ absorbance at 283 cm^{-1} . The $\nu(\text{P-O-P})$ asym bond is located at 790 cm^{-1} which indicates a chelate tdpd ligand is present. The $\nu(\text{P-O})$ absorbance of the Ph_2PO ligand is located at 860 cm^{-1} . Bands similar to the OH absorbance to the $[\text{Ru}(\text{Ph}_2\text{POPPH}_2)(\text{Ph}_2\text{POH})_2\text{Cl}_2]$ are also observed indicating the presence of inter and intramolecular hydrogen bonding.

^{31}P nmr Data

This complex also exhibits an AA'XX' spin system (Figures 6.17a and b). The resonances in this case are located at 67.3 ppm and 37.5 ppm. The couplings, summarized in Table 6.2, are analogous to those of the ruthenium complex described in Section 6.2.2.

^1H nmr Data

Again, most of the data is located in an uninterpretable

phenyl region, the only feature observed outwith this region being a broad singlet at 3.9 ppm suggesting, as in the ruthenium analogue, the presence of Ph_2POH ligands (Figure 6.18).

F.A.B. Mass Spectrum Data

This indicates the molecular ion is $[\text{Os}(\text{Ph}_2\text{POPPh}_2)(\text{Ph}_2\text{POH})_2\text{Cl}_2]^+$. The full fragmentation pattern is shown in Table 6.3.

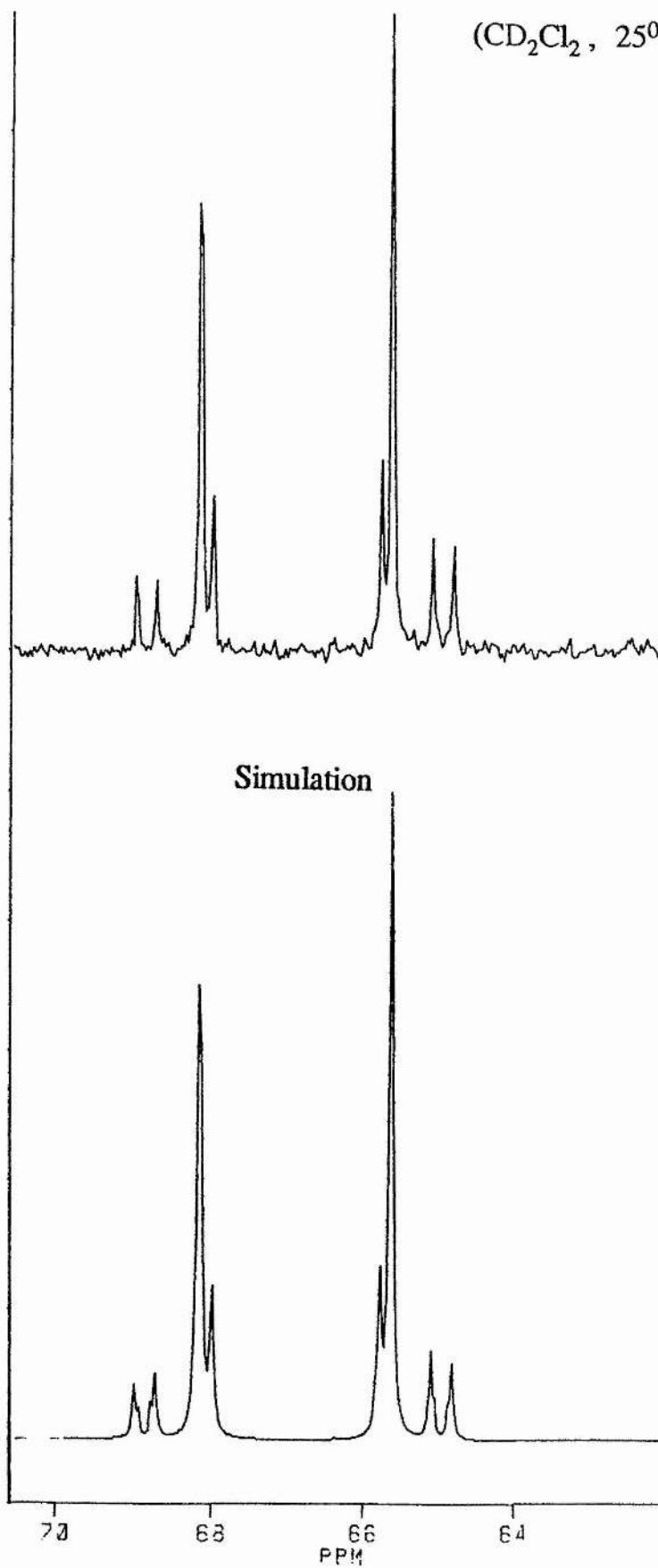
$(\text{CD}_2\text{Cl}_2, 25^\circ\text{C})$ 

Fig. 6.17a ^{31}P n.m.r. spectrum (300MHz) of $[\text{OsCl}_2(\text{Ph}_2\text{POPPh}_2)(\text{Ph}_2\text{POH})_2]$ Part A

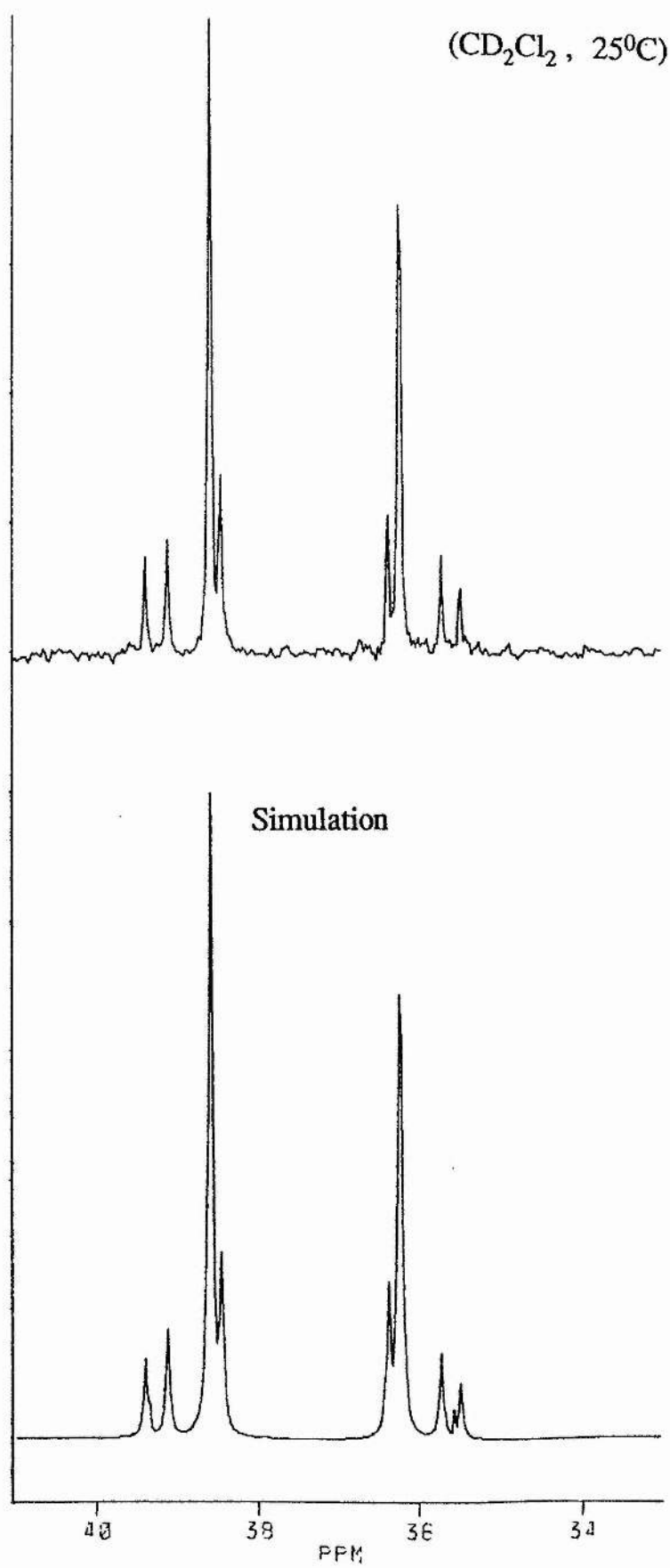


Fig. 6.17b ³¹P n.m.r. spectrum (300MHz) of [OsCl₂(Ph₂POPPh₂(Ph₂POH)₂] Part B

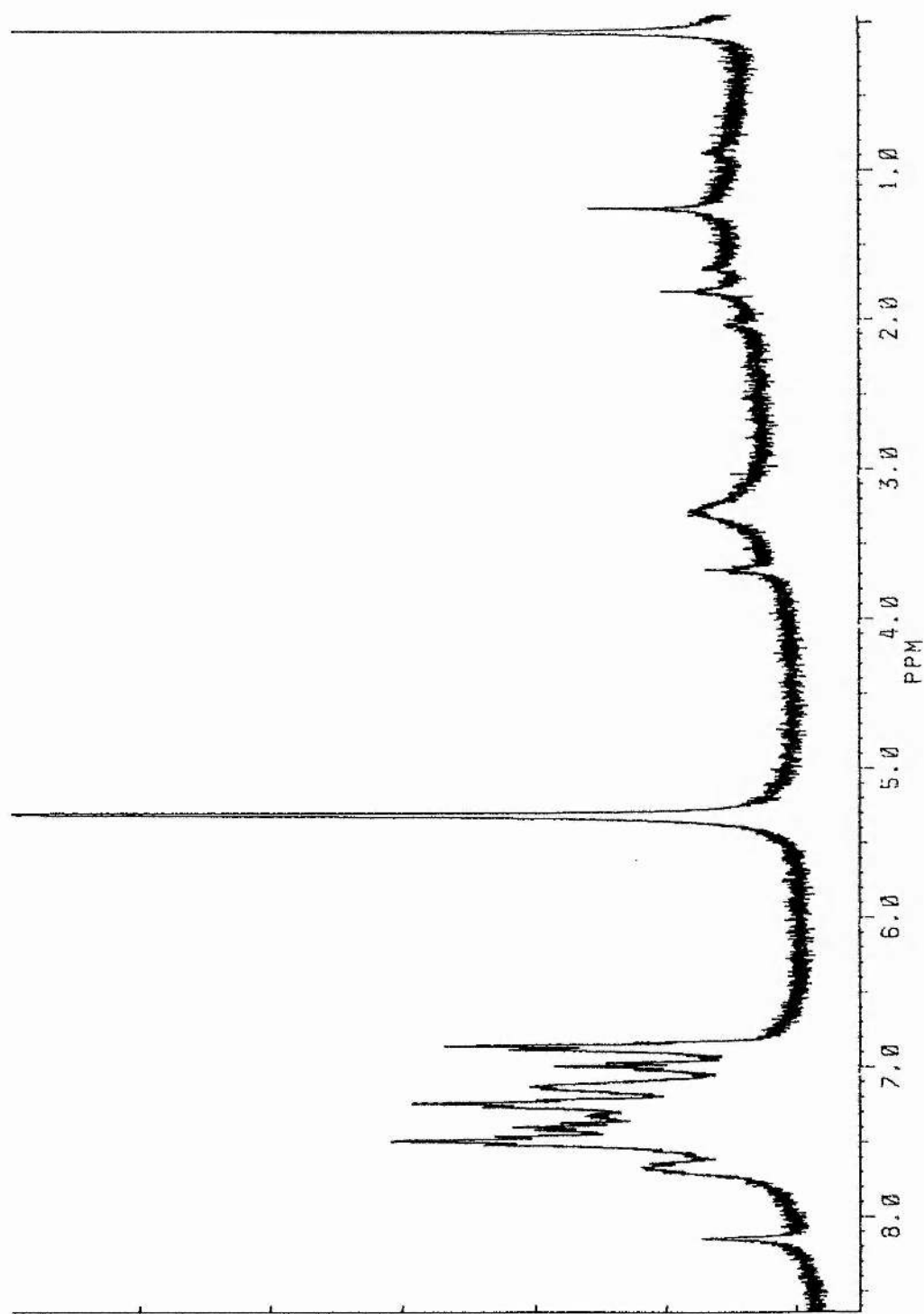


Fig 6.18 ^1H n.m.r. spectrum (300MHz) of $[\text{OsCl}_2(\text{Ph}_2\text{POPPPh}_2)(\text{Ph}_2\text{POH})_2]$ (CD_2Cl_2 , 25°C)

Table 6.1 Spectral Data for Complexes of the Form $[MCl_2(Ph_2POPPh_2)(PPh_2OH)_2]$	
Complex	IR (cm ⁻¹)
	$\nu(OH)^a$ $\nu(OH)^b$ $\nu(P-O)^c$ $\nu(P-O)^d$ $\nu(Ru-Cl)$ 1H (ppm)* δH
$[RuCl_2(Ph_2POPPh_2)(PPh_2OH^{a,b})_2]$	3200br 1680br 863s 780s 280s a, b 5.85s
$[OsCl_2(Ph_2POPPh_2)(PPh_2OH^{a,b})_2]$	3200br 1680br 860s 790s 283s a, b 3.3s

a arising from intermolecular H bonding b arising from intramolecular H bonding
 c of the $Ph_2PHOHOPPh_2$ ring d of the Ph_2POPPh_2 ring * CD_2Cl_2 25°C

Table 6.2		^{31}P Spectral Data for Complexes of the Form $[\text{MCl}_2(\text{Ph}_2\text{POPPh}_2)(\text{PPh}_2\text{OH})_2]^*$									
Complex		Chemical Shifts (ppm)				Coupling Constants (Hz)					
		Pa	Pb	Pc	Pd	PaPb	PaPc	PaPd	PbPc	PbPd	PcPd
$[\text{RuCl}_2(\text{Ph}_2\text{P}^a\text{OP}^b\text{Ph}_2)(\text{P}^{c,d}\text{Ph}_2\text{OH})_2]$		114.18	114.10	84.42	84.40	91.5	-33.8	318.5	327.3	-30.4	30.7
$[\text{OsCl}_2(\text{Ph}_2\text{P}^a\text{OP}^b\text{Ph}_2)(\text{P}^{c,d}\text{Ph}_2\text{OH})_2]$		67.55	67.51	38.88	38.86	81.2	-30.0	289.9	298.6	-24.9	22.3

*(CD_2Cl_2 , 25°C)

Table 6.3Fragmentation Pattern of $[\text{Os}(\text{Ph}_2\text{POPPh}_2)((\text{Ph}_2\text{POH})_2)\text{Cl}_2]$

	m/z
$\text{OsCl}_2(\text{Ph}_2\text{POPPh}_2)(\text{Ph}_2\text{PO})_2\text{H}_2$	1052
$\text{OsCl}_2(\text{Ph}_2\text{POPPh}_2)(\text{Ph}_2\text{PO})\text{H}$	850
$\text{OsCl}(\text{Ph}_2\text{POPPh}_2)(\text{Ph}_2\text{PO})\text{H}$	815
$\text{OsCl}(\text{Ph}_2\text{POPPh}_2)(\text{PhPO})\text{H}$	737
$\text{OsCl}(\text{Ph}_2\text{POPPh}_2)$	648
$\text{OsCl}(\text{Ph}_2\text{POPPh}_2)$	612
$\text{Os}(\text{Ph}_2\text{POPPh}_2)$	576
$\text{Os}(\text{Ph}_2\text{POPPh})$	499
$\text{Os}(\text{Ph}_2\text{PO})\text{H}(\text{P})$	423
$\text{Os}(\text{Ph}_2\text{P})$	375

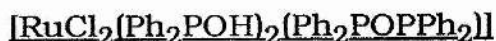
6.3 Experimental

$[\text{RhCl}(\text{PPh}_3)(\text{Ph}_2\text{POPPh}_2)]$

To a tetrahydrofuran solution of $[\text{RhCl}(\text{PPh}_3)_3]$ (0.5g, 0.54 mmol) a quantity of tetraphenyldiphosphine monoxide (0.21g, 0.54 mol) was added and the solution refluxed for 4-5 hours. Also present was a quantity of $[\text{HNEt}_3]\text{Cl}$. The solution once cooled was filtered, concentrated and allowed to stand at -3°C for several days. Orange crystallites were obtained, the analysis of which proved them to be $[\text{RhCl}(\text{Ph}_2\text{POPh}_2)(\text{PPh}_3)]$. Yield 0.29g (69%).

$[\text{RhCl}_2(\text{Ph}_2\text{PO})_3\text{H}][\text{HNEt}_3]$

Following the same method described above the $[\text{RhCl}(\text{PPh}_3)_3]$ (0.5g, 0.54 mmol) reacted with an excess (0.39g, 1 mmol) of tetraphenyl diphosphoxane. The work up procedure described above resulted in yellow crystals which were found spectroscopically to be a mixture of complexes, one of which was found by x-ray analysis to be $[\text{RhCl}_2(\text{Ph}_2\text{PO})_2\text{H}(\text{Ph}_2\text{PO})][\text{HNEt}_3]$.



Following the same method described above a quantity of tetraphenyldiphosphine monoxide (0.32g, 0.82 mmol) was added to a THF solution of $[\text{RuCl}_2(\text{PPh}_3)_4]$ (1.0g, 0.82 mmol). The work up procedure described above did not produce crystallites. In this case a pale yellow precipitate was obtained by the careful addition of petroleum ether (40-60°C). This precipitate upon exhaustive washing with petroleum ether analysed to be $[\text{RuCl}_2(\text{Ph}_2\text{POPPh}_2)(\text{Ph}_2\text{POH})_2]$. Yield 0.30g (38.0%).



Following the previously described method tetraphenyl diphosphine monoxide (0.15g, 0.58 mmol) was added to solution of $[\text{OsCl}_2(\text{PPh}_3)_4]$ (0.5g, 0.38 mmol) and then refluxed. A bright yellow precipitate was obtained upon allowing the filtered and concentrated solution, which was black in colour, to stand at -3°C for several days. This precipitate needed no further purification and analysed to be $[\text{OsCl}_2(\text{Ph}_2\text{POPPh}_2)(\text{Ph}_2\text{POH})_2]$. Yield 0.14g (34.9%).

Theoretical $[\text{OsCl}_2(\text{Ph}_2\text{POPPh}_2)(\text{Ph}_2\text{POH})_2]\cdot\text{thf}$ C 55.6%; H 4.5%

Found $[\text{OsCl}_2(\text{Ph}_2\text{POPPh}_2)(\text{Ph}_2\text{POH})_2]\cdot\text{thf}$ C55.8%; H4.5%

CHAPTER 7

Crystal Structure Determination

The following chapter contains the structural determinations carried out by the author, which were an integral part of the study reported in this thesis. Also included are brief summaries of the techniques and computer programs used during these determinations. Both data sets were collected using a Nicolet P3 Diffractometer (University of Aberdeen) using Ni-filtered $\text{MoK}\alpha$ radiation ($\lambda = 0.71069$) operating in the $\omega/2\theta$ scan mode and the structural determination programs were run on a Prime 6350 computer (University of Dundee).

7.1 Method of Structure Solution

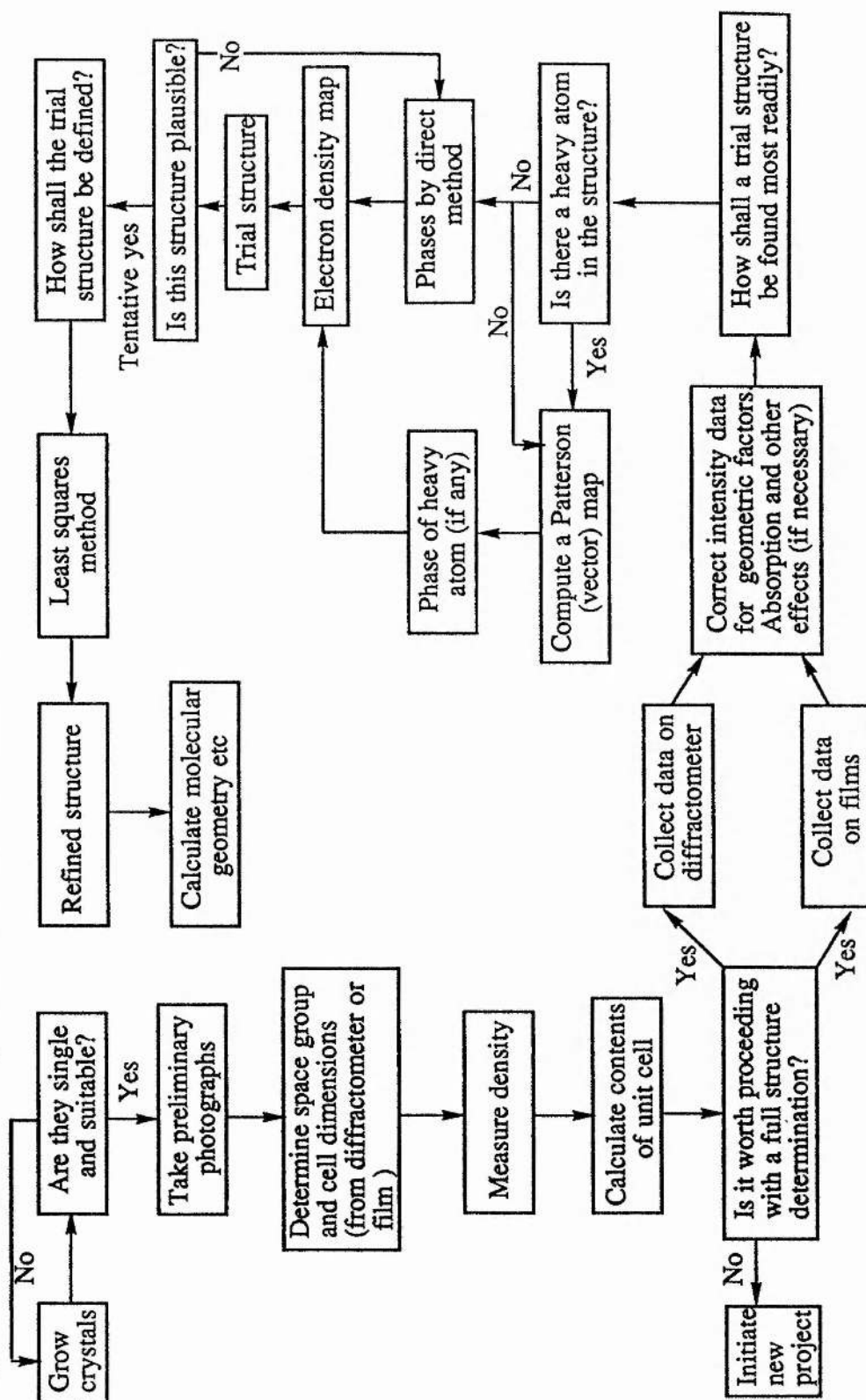
The crystal selected should be of suitable size, which normally entails crystal dimensions which lie between 0.1 and 0.5 mm, and should also be single (i.e. no cracks or overgrowths). The selected crystal is mounted by optical means with what appears to be its principle axis parallel to the axis of the goniometer head. Precise alignment of a crystal can seldom be achieved by optical techniques, the fine adjustment of the setting is achieved by the use of diffraction photographs. The first of these photographs is taken with an oscillation camera (constant rotation between -10° and $+10^\circ$ from the centre of the film) which, as well as allowing corrections to

be made to the initial optical setting, provides information on the symmetry of the structure and one index of reciprocal lattice. Following this a Weissenberg camera is used to take photographs of each of the planes in the oscillation photograph. In a Weissenberg camera both the film and the crystal move, creating festoons of spots from which the values of the remaining two indices can be obtained. These photographs also allow the space group to be assigned. The intensities of the spots are then recorded on a diffractometer (computer operated). This process gives an output of all the intensities of the diffraction spots, the weak of which can be removed leaving the firm data, which is then absorption corrected to produce a file containing h , k , l and F values. The structure programs then basically use intensity statistics to find probable phases for a limited number of h,k,l 's. The limited number of phased h,k,l 's are used to produce an electron density map from which part of the molecule is identified. Upon fixing this section the process is started again until a full structure is obtained. A general summary of the method of structure solution is shown in the flow diagram in figure 7.1(205,206).

Computer Programs

It is in this area that most advances have been made in the development of crystallography in the last few decades. This in turn has resulted in x-ray crystallography becoming a commonly used analytical technique. The computer programs used in this study were:-

Figure 7.1 Flow diagram for the determination of small structures



SHELX76⁽²⁰⁷⁾

This program is used directly after the removal of the weak intensities. It introduces the information obtained from the initial film and chemical studies of the crystals. For example it includes the cell dimensions, the symmetry of the structure, the number and type of the atoms present and the type of lattice present. This essentially takes the raw data of the strong peaks and produces a single output file containing all the strong reflections for the crystal, with the background count removed so that each reflection has a single corrected intensity. The data is now ready for absorption correction⁽²⁰⁸⁾ and least squares refinement.

SHELXS⁽²⁰⁹⁾

This program follows SHELX76 and is responsible for the least squares refinement and the production of electron density, difference Fourier maps, Fourier maps and Patterson maps. The absorption correction process has been summarized in the literature by Walker and Stuart.

XANADU⁽²¹⁰⁾

This carries out the calculations required at the end of a structure determination. The output of this program consists of tables of bond lengths, angles, torsion angles, connectivity data and information on the relative orientations of groups of atoms (e.g.

phenyl groups) in a crystal structure. It also enables a further set of maps to be obtained.

PLUTO⁽²¹¹⁾

Used for molecular drawings. The input is the final coordinate file and by application of this program the molecule can be viewed from any angle or direction.

Equipment

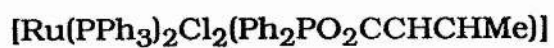
A detailed description of the type of equipment used in the collection x-ray data is not dealt with here as it has been adequately covered in the literature⁽²¹²⁾.

Table 7.1

Attempted Crystal Structure Determinations

Complex/Compound	Outcome
RhD ₄ (Unknown complex, a biproduct of a dimer experiment)	Data collected on a 2 circle diffractometer but of insufficient quality to obtain a structure solution. A further data set will have to be collected using a 4 circle diffractometer.
$[(\text{RhCl}(\text{Ph}_2\text{PO}_2\text{CCHCH}_2))_2(\text{Ph}_2\text{POPPh}_2)]$	Crystals did not diffract over a large enough 2θ range
$[\text{RhCl}(\text{PPh}_3)(\text{Ph}_2\text{POPPh}_2)]$	Molecular structure discussed in Section 7.2 (<i>Polyhedron</i> (1989), 8(12), 1575).
$[\text{Fe}_2(\text{CO})_8(\text{Ph}_2\text{POPPh}_2)_2]$	Data set was not obtainable because the crystals contained an irregularity
$[\text{Rh}(\text{PPh}_3)_2(\text{Ph}_2\text{POPPh}_2)][\text{PF}_6]$	Crystals did not diffract over large enough 2θ range. Also exhibited twinning of the spots.
C ₂₃ H ₃₀ O ₈	Crystal structure included in a paper in press (<i>Journal of Carbohydrate Research</i>) Not included here because it is not of relevance to bulk of thesis ⁽²¹³⁾ .
$[\text{Ru}(\text{PPh}_3)_2(\text{Ph}_2\text{PO}_2\text{CCHCH}_2)\text{Cl}_2]$	Several crystals attempted. On the whole tended not to be single crystals. When a crystal was chosen it gave a very poor spot quality, so

the possibility of data collection.



Crystals diffracted poorly



Molecular Structure discussed in Section 7.3.

7.2 Molecular Structure of $[\text{RhCl}(\text{PPh}_3)(\text{Ph}_2\text{POPPh}_2)]$

7.2.1 Experimental

$[\text{RhCl}(\text{PPh}_3)(\text{tpdp})]$ was prepared by the method described in Chapter 3. Recrystallisation from a concentrated tetrahydrofuran solution, by standing at -3°C for several days, produced crystals of x-ray quality which were found during the structural determination to contain 1 mole of THF as a solvent of crystallisation. From the photographic work the cell dimensions were calculated ($a = 11.294$, $b = 11.475$ and $c = 16.144\text{\AA}$), the crystal was shown to be triclinic ($\alpha = 102.31^\circ$, $\beta = 102.71^\circ$ and $\gamma = 74.11^\circ$) and the space group determined to be P_1 . The calculated cell volume 2056.68\AA^3 was consistent with there being only two molecules in the unit cell. Least squares refinement of the metal and phosphorus atoms was carried out and the remaining non hydrogen atoms were located in the subsequent Fourier difference maps. Isotropic vibrational parameters were refined until all of the non-hydrogen atoms were located, after which the anisotropic vibrational parameters were assigned and refined to convergence. The hydrogen atoms of the phenyl groups were included in calculated positions (C-H bond length fixed at 1.09\AA). The assignment of the oxygen was checked by assigning it as a carbon atom. This however produced an increase in the thermal parameters of this species indicating that our oxygen assignment was the correct one. Latterly the hydrogen atoms were refined anisotropically as was the THF which was found to show some disorder. The final R factor ($R = \sum ||F_0| -$

$|F_0|/|\Sigma|F_0|$) was 0.0718 for 2329 reflections and the maximum peak in the final difference map was 0.873 electron \AA^{-3} . The final positional and thermal parameters of all the atoms are summarised in Tables 7.3, 7.4 and 7.5 whereas bond lengths and angles are in Table 7.6. See Appendix I for the structure factor Tables.

7.2.2 Discussion of Results

The final structure of $[\text{RhCl}(\text{PPh}_3)(\text{tpdp})]$ is shown in Figure 7.2. The most important of the bond lengths and angles are those of the RhPOP ring. The ring angles are all much smaller than the strain free values, most markedly the tight angles at rhodium and oxygen (68.39° and 95.40°) which results in the close approach of the two ring phosphorus atoms (2.457\AA separation). This distance is much less than the sum of the Van der Waals radii of phosphorus (3.4\AA) but longer than the largest found P-P single bond distances (2.35\AA in P_4S_7)⁽²¹⁴⁾, the usual bonded distances are in the region of 2.10\AA - 2.20\AA . The P...P distance is less than those in the related $[\text{M}(\text{CO})_4(\text{Ph}_2\text{POPPh}_2)]$ complexes, $\text{M} = \text{Mo}(2.608\text{\AA})$ or $\text{Cr}(2.533\text{\AA})$, and also those usually observed in bidentate $\text{Ph}_2\text{PCH}_2\text{PPh}_2$ complexes. However MNDO calculations do not indicate any significant P-P bonding⁽²¹⁵⁾. A comparison of the various ring angles in the complexes of Cr, Mo and Rh are shown in Table 7.2⁽²¹⁶⁾.

Table 7.2	Ring angles of Tdpdp complexes				
Metal	M- P ₁ - O	M- P ₂ - O	P- O - P	P- M - P	Ref
Mo	96.9(1)	96.0(1)	103.3(1)	63.82(3)	5
Cr	97.0(1)	96.1(1)	100.2(1)	66.76(4)	5
Rh	98.8(4)	97.3(4)	95.4(5)	68.20(2)	This work

The M-P-O angles are $97.5 \pm 1.5^\circ$ in all cases, suggesting that it is the rigidity of these angles that predetermine the overall ring geometry. The overall structure is found to be distorted square planar about rhodium, the oxygen is found to be 0.083 Å out of the P-Rh-P plane. The Rh-P-O-P ring itself is found to be almost planar. The distortion in the structure most probably results from the slight difference in angles between the left and right side of the structure due in turn to one ring phosphorus being *trans* to the chlorine atom and the second *trans* to the much bulkier triphenyl phosphine group. Hence, the ring geometry is altered slightly to relieve the steric interactions with the PPh₃ group.

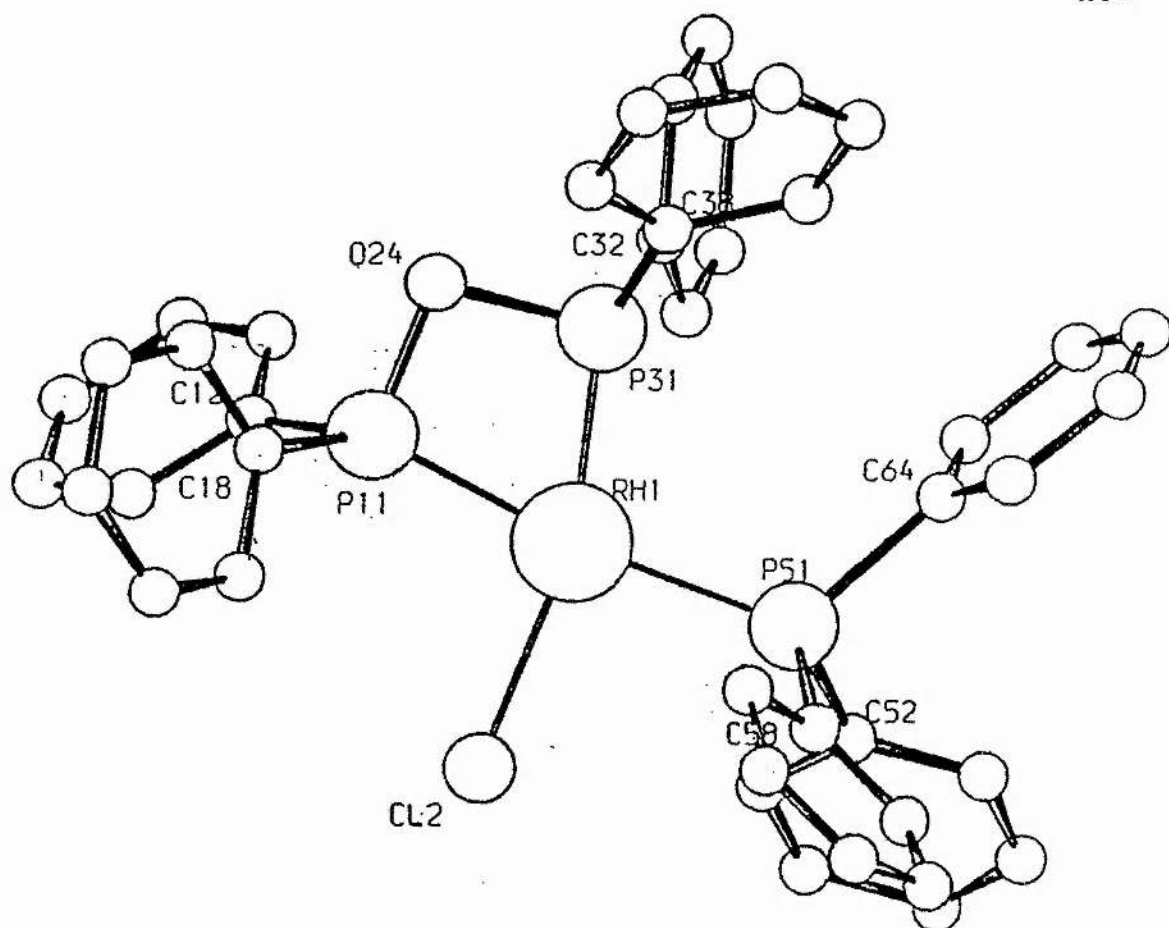


Fig. 7.3

Solid state stereo-projection of $[\text{RhCl}(\text{PPh}_3)(\text{Ph}_2\text{POPPh}_2)]$

TETRAPHENYLDIPHOSPHOXANE TRIPHENYLPHOSPHINE CHLORORHODIUM (I)

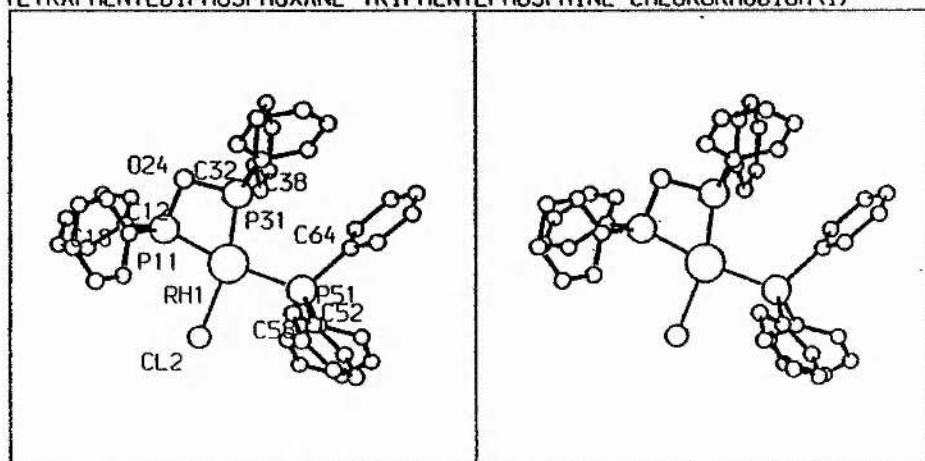


Table 73

Coordinates $\times 10^4$ for non hydrogen atoms
with e.s.d's in parentheses. $U_{eq} \times 10^3$.

$$U_{eq} = (1/3) \sum_i \sum_j U_{ij} a_i^* a_j^* a_i \cdot a_j$$

	x/a	y/b	z/c	U_{eq}
RH1	5967(1)	8782(1)	2173(1)	46(1)
CL2	4749(4)	7317(4)	2035(3)	81(2)
P11	4553(4)	10441(4)	2573(3)	50(1)
C12	3125(14)	11192(15)	1952(10)	51(6)
C13	1971(18)	11065(15)	2036(11)	76(8)
C14	899(18)	11614(17)	1565(11)	83(8)
C15	927(19)	12314(18)	1029(13)	87(9)
C16	2052(22)	12488(18)	951(12)	94(9)
C17	3119(18)	11911(15)	1417(11)	71(8)
C18	4074(13)	10611(17)	3536(10)	55(6)
C19	3837(15)	9598(18)	3754(12)	71(8)
C20	3459(18)	9689(24)	4479(14)	90(10)
C21	3295(19)	10716(26)	5009(14)	95(11)
C22	3519(20)	11748(21)	4787(14)	102(10)
C23	3885(20)	11680(20)	4052(12)	94(10)
O24	5418(9)	11438(8)	2714(6)	53(4)
P31	6653(4)	10420(4)	2384(3)	48(1)
C32	6851(14)	11082(15)	1544(11)	51(6)
C33	7215(16)	12180(16)	1656(12)	71(8)
C34	7228(17)	12653(18)	997(14)	73(8)
C35	6894(17)	12075(20)	242(14)	80(9)
C36	6529(18)	11008(19)	101(11)	81(9)
C37	6504(15)	10491(16)	747(12)	69(7)
C38	7875(16)	10832(14)	3200(11)	54(7)
C39	7648(18)	11390(18)	3937(12)	81(8)
C40	8607(24)	11653(20)	4586(12)	103(10)
C41	9800(20)	11302(23)	4453(15)	107(11)
C42	10069(18)	10795(17)	3711(13)	77(8)
C43	9120(17)	10514(15)	3073(11)	68(7)
P51	7727(4)	7200(4)	1891(3)	55(1)
C52	7549(14)	6201(14)	926(10)	49(6)
C53	6360(15)	6277(15)	416(11)	62(7)
C54	6220(19)	5536(18)	-330(12)	78(9)
C55	7227(21)	4718(16)	-618(11)	71(8)
C56	8364(16)	4664(16)	-107(13)	60(7)
C57	8544(17)	5380(14)	605(11)	63(7)
C58	8213(16)	6120(19)	2626(11)	73(7)
C59	8862(30)	4987(21)	2528(13)	148(15)
C60	9309(30)	4243(25)	3086(18)	146(15)
C61	9067(28)	4654(34)	3799(21)	187(19)
C62	8442(41)	5740(45)	3923(22)	433(36)
C63	8063(29)	6585(26)	3349(18)	237(18)
C64	9244(16)	7653(17)	1852(12)	60(7)
C65	9187(16)	8151(18)	1237(13)	80(9)
C66	10283(30)	8488(22)	1177(17)	122(14)
C67	11244(27)	8233(27)	1748(23)	147(18)
C68	11288(22)	7687(28)	2366(22)	162(19)
C69	10260(22)	7387(17)	2475(14)	98(10)
C71	2734(41)	15208(40)	3835(36)	214(26)
C72	4377(58)	14743(38)	3132(36)	210(28)
C73	3577(48)	15989(28)	4054(19)	263(22)
C74	3176(57)	14656(38)	3019(30)	235(25)
C75	4899(51)	5538(75)	3798(47)	319(44)

Supplementary Table. 7.4

Anisotropic temperature factors $\times 10^3$
with e.s.d.'s in parentheses

	U11	U22	U33	U23	U13	U12
RH1	50 (1)	39 (1)	50 (1)	12 (1)	9 (1)	-8 (1)
CL2	87 (3)	70 (4)	95 (4)	8 (3)	32 (3)	-27 (3)
P11	55 (3)	43 (3)	50 (3)	14 (2)	1 (2)	-8 (2)
C12	55 (10)	54 (12)	42 (11)	7 (9)	17 (9)	-2 (9)
C13	94 (15)	68 (14)	70 (15)	41 (11)	26 (12)	7 (12)
C14	87 (15)	88 (16)	66 (15)	44 (13)	0 (12)	7 (12)
C15	81 (15)	71 (16)	81 (18)	25 (13)	-14 (13)	17 (12)
C16	106 (17)	80 (16)	76 (17)	44 (13)	-16 (15)	8 (15)
C17	91 (14)	53 (13)	72 (15)	15 (11)	15 (12)	-19 (11)
C18	41 (9)	63 (13)	53 (13)	11 (11)	9 (9)	2 (9)
C19	71 (12)	85 (15)	66 (15)	27 (12)	13 (11)	-19 (11)
C20	83 (15)	141 (23)	55 (16)	48 (15)	-6 (13)	-33 (15)
C21	76 (14)	150 (26)	59 (17)	23 (17)	7 (13)	-27 (17)
C22	114 (18)	94 (19)	70 (19)	-17 (15)	8 (14)	-10 (15)
C23	150 (20)	89 (18)	54 (15)	12 (13)	49 (15)	-21 (15)
O24	69 (7)	21 (6)	60 (8)	8 (5)	18 (6)	6 (5)
P31	51 (3)	37 (3)	52 (3)	9 (2)	4 (2)	-7 (2)
C32	55 (10)	39 (11)	53 (13)	10 (9)	6 (9)	-4 (8)
C33	91 (14)	59 (13)	62 (15)	27 (12)	7 (11)	-11 (11)
C34	82 (14)	63 (14)	76 (16)	31 (14)	-17 (12)	-30 (11)
C35	79 (14)	88 (18)	83 (19)	48 (15)	23 (13)	-2 (12)
C36	123 (17)	74 (15)	53 (14)	38 (12)	24 (12)	-6 (13)
C37	79 (13)	62 (13)	69 (15)	12 (12)	13 (11)	-21 (10)
C38	82 (13)	34 (10)	46 (13)	7 (9)	6 (10)	-20 (9)
C39	95 (15)	133 (19)	32 (13)	15 (13)	10 (12)	-57 (14)
C40	135 (21)	132 (21)	43 (15)	-16 (13)	30 (16)	-44 (17)
C41	75 (16)	175 (25)	72 (19)	19 (17)	-1 (14)	-40 (16)
C42	80 (14)	93 (16)	61 (15)	12 (13)	8 (13)	-32 (12)
C43	78 (13)	61 (13)	57 (14)	-2 (10)	5 (11)	-16 (11)
P51	65 (3)	38 (3)	52 (3)	4 (2)	7 (2)	-2 (2)
C52	42 (9)	50 (11)	58 (12)	19 (10)	-2 (9)	-18 (8)
C53	58 (12)	57 (12)	70 (14)	2 (11)	29 (11)	-7 (9)
C54	106 (17)	75 (15)	56 (15)	-5 (12)	13 (13)	-40 (13)
C55	116 (17)	57 (13)	41 (13)	4 (10)	29 (13)	-13 (13)
C56	53 (12)	57 (13)	72 (15)	17 (12)	16 (11)	-5 (10)
C57	98 (15)	29 (10)	44 (13)	8 (9)	3 (11)	6 (10)
C58	65 (11)	71 (15)	52 (14)	-28 (12)	13 (10)	7 (11)
C59	327 (41)	52 (15)	26 (14)	0 (12)	-7 (19)	-17 (21)
C60	250 (37)	90 (20)	78 (22)	23 (20)	-3 (24)	-24 (22)
C61	161 (27)	229 (40)	149 (33)	144 (31)	52 (25)	95 (25)
C62	453 (66)	535 (81)	197 (38)	284 (51)	245 (42)	391 (63)
C63	319 (42)	165 (27)	120 (26)	51 (23)	113 (27)	201 (28)
C64	62 (12)	70 (14)	62 (15)	21 (11)	27 (11)	-20 (10)
C65	59 (12)	87 (16)	99 (19)	-4 (14)	31 (12)	-26 (11)
C66	202 (30)	83 (18)	108 (24)	-37 (17)	87 (22)	-68 (23)
C67	76 (20)	104 (25)	226 (46)	-91 (28)	37 (24)	-49 (20)
C68	18 (12)	178 (32)	294 (48)	89 (28)	22 (19)	8 (15)
C69	103 (18)	72 (15)	115 (21)	50 (14)	11 (16)	7 (14)
C71	279 (49)	127 (33)	270 (56)	26 (34)	60 (41)	-101 (32)
C72	245 (50)	135 (33)	285 (61)	34 (36)	30 (50)	-113 (39)
C73	414 (53)	174 (27)	209 (29)	4 (22)	48 (36)	-109 (34)
C74	274 (55)	154 (36)	150 (37)	-9 (29)	-73 (42)	46 (41)
C75	246 (51)	432 (92)	357 (80)	134 (66)	-78 (52)	-256 (62)

Supplementary Table 75

Coordinates $\times 10^4$ for hydrogen atoms

	x/a	y/b	z/c
H131	1920	10535	2473
H141	12	11484	1623
H151	72	12737	664
H161	2095	13057	536
H171	4003	12043	1356
H191	3952	8732	3346
H201	3286	8885	4621
H211	3007	10766	5578
H221	3404	12609	5201
H231	4018	12492	3895
H331	7481	12650	2260
H341	7511	13503	1080
H351	6917	12477	-269
H361	6262	10569	-512
H371	6220	9638	647
H391	6695	11655	4042
H401	8391	12121	5174
H411	10550	11430	4952
H421	11016	10606	3604
H431	9345	10052	2487
H531	5551	6927	617
H541	5300	5600	-694
H551	7136	4152	-1208
H561	9165	3988	-300
H571	9482	5325	940
H591	9058	4601	1924
H601	9854	3319	2934
H611	9390	4096	4273
H621	8175	6075	4513
H631	7663	7551	3523
H651	8349	8306	788
H661	10317	8926	686
H671	12078	8493	1714
H681	12153	7481	2787
H691	10230	6988	2985

Table 7.6

Interatomic distances (Å) and angles (°)

CL2 ---RH1	2.394 (6)	P11 ---RH1	2.215 (4)
P31 ---RH1	2.156 (5)	P51 ---RH1	2.356 (4)
C12 ---P11	1.831 (15)	C18 ---P11	1.804 (19)
O24 ---P11	1.648 (12)	P31 ---P11	2.457 (7)
C13 ---C12	1.391 (28)	C17 ---C12	1.356 (28)
C14 ---C13	1.372 (24)	C15 ---C14	1.355 (33)
C16 ---C15	1.377 (36)	C17 ---C16	1.376 (26)
C19 ---C18	1.401 (31)	C23 ---C18	1.345 (26)
C20 ---C19	1.375 (33)	C21 ---C20	1.322 (34)
C22 ---C21	1.419 (43)	C23 ---C22	1.390 (35)
P31 ---O24	1.674 (10)	C32 ---P31	1.844 (21)
C38 ---P31	1.819 (17)	C33 ---C32	1.392 (27)
C37 ---C32	1.412 (24)	C34 ---C33	1.359 (34)
C35 ---C34	1.346 (30)	C36 ---C35	1.355 (34)
C37 ---C36	1.373 (32)	C39 ---C38	1.334 (26)
C43 ---C38	1.407 (27)	C40 ---C39	1.418 (29)
C41 ---C40	1.353 (35)	C42 ---C41	1.344 (32)
C43 ---C42	1.404 (26)	C52 ---P51	1.807 (15)
C58 ---P51	1.848 (22)	C64 ---P51	1.940 (22)
C53 ---C52	1.424 (22)	C57 ---C52	1.387 (23)
C54 ---C53	1.380 (25)	C55 ---C54	1.373 (28)
C56 ---C55	1.381 (26)	C57 ---C56	1.328 (25)
C59 ---C58	1.302 (29)	C63 ---C58	1.269 (36)
C60 ---C59	1.341 (38)	C61 ---C60	1.274 (47)
C62 ---C61	1.252 (55)	C63 ---C62	1.444 (58)
C65 ---C64	1.283 (34)	C69 ---C64	1.400 (27)
C66 ---C65	1.424 (43)	C67 ---C66	1.305 (41)
C68 ---C67	1.326 (58)	C69 ---C68	1.359 (43)
C73 ---C71	1.420 (70)	C74 ---C71	1.539 (79)
C74 ---C72	1.356 (93)	C75 ---C72	1.428 (88)
C75 ---C73	1.568 (82)		
P11 -RH1 -CL2	97.4 (2)	P31 -RH1 -CL2	165.7 (2)
P31 -RH1 -P11	68.4 (2)	P51 -RH1 -CL2	91.1 (2)
P51 -RH1 -P11	170.0 (2)	P51 -RH1 -P31	103.1 (2)
C12 -P11 -RH1	127.1 (5)	C18 -P11 -RH1	119.4 (6)
C18 -P11 -C12	102.8 (7)	O24 -P11 -RH1	97.3 (4)
O24 -P11 -C12	101.3 (7)	O24 -P11 -C18	104.9 (7)
P31 -P11 -RH1	54.7 (1)	P31 -P11 -C12	122.8 (7)
P31 -P11 -C18	125.4 (5)	P31 -P11 -O24	42.7 (3)
C13 -C12 -P11	119.8 (14)	C17 -C12 -P11	123.2 (14)
C17 -C12 -C13	116.9 (15)	C14 -C13 -C12	120.0 (19)
C15 -C14 -C13	121.5 (21)	C16 -C15 -C14	119.7 (18)
C17 -C16 -C15	117.9 (22)	C16 -C17 -C12	123.8 (21)
C19 -C18 -P11	119.1 (13)	C23 -C18 -P11	123.4 (18)
C23 -C18 -C19	117.5 (19)	C20 -C19 -C18	121.0 (18)

C21	-C20	-C19	123.1 (27)	C22	-C21	-C20	116.0 (24)
C23	-C22	-C21	121.7 (20)	C22	-C23	-C18	120.6 (23)
P31	-O24	-P11	95.4 (5)	P11	-P31	-RH1	57.0 (2)
O24	-P31	-RH1	98.8 (4)	O24	-P31	-P11	41.9 (4)
C32	-P31	-RH1	121.9 (5)	C32	-P31	-P11	120.2 (5)
C32	-P31	-O24	102.3 (6)	C38	-P31	-RH1	126.4 (6)
C38	-P31	-P11	124.3 (7)	C38	-P31	-O24	98.8 (6)
C38	-P31	-C32	102.8 (8)	C33	-C32	-P31	123.3 (13)
C37	-C32	-P31	117.4 (15)	C37	-C32	-C33	119.0 (19)
C34	-C33	-C32	119.2 (17)	C35	-C34	-C33	120.9 (21)
C36	-C35	-C34	122.2 (24)	C37	-C36	-C35	119.1 (18)
C36	-C37	-C32	119.6 (18)	C39	-C38	-P31	122.4 (15)
C43	-C38	-P31	119.9 (13)	C43	-C38	-C39	117.7 (16)
C40	-C39	-C38	122.6 (20)	C41	-C40	-C39	118.3 (19)
C42	-C41	-C40	121.2 (20)	C43	-C42	-C41	120.1 (20)
C42	-C43	-C38	119.8 (17)	C52	-P51	-RH1	116.5 (5)
C58	-P51	-RH1	112.3 (6)	C58	-P51	-C52	103.0 (8)
C64	-P51	-RH1	118.3 (5)	C64	-P51	-C52	100.0 (8)
C64	-P51	-C58	104.8 (9)	C53	-C52	-P51	121.0 (11)
C57	-C52	-P51	123.4 (12)	C57	-C52	-C53	115.5 (14)
C54	-C53	-C52	121.4 (15)	C55	-C54	-C53	121.3 (17)
C56	-C55	-C54	115.8 (16)	C57	-C56	-C55	124.7 (16)
C56	-C57	-C52	121.1 (16)	C59	-C58	-P51	127.9 (17)
C63	-C58	-P51	116.0 (19)	C63	-C58	-C59	115.2 (22)
C60	-C59	-C58	127.6 (23)	C61	-C60	-C59	118.2 (27)
C62	-C61	-C60	116.6 (38)	C63	-C62	-C61	125.5 (37)
C62	-C63	-C58	116.0 (27)	C65	-C64	-P51	114.6 (14)
C69	-C64	-P51	117.3 (18)	C69	-C64	-C65	128.1 (21)
C66	-C65	-C64	116.7 (19)	C67	-C66	-C65	116.0 (31)
C68	-C67	-C66	126.0 (34)	C69	-C68	-C67	120.8 (25)
C68	-C69	-C64	112.3 (25)	C74	-C71	-C73	92.3 (44)
C75	-C72	-C74	122.4 (53)	C75	-C73	-C71	120.2 (40)
C72	-C74	-C71	106.0 (42)	C73	-C75	-C72	87.7 (45)

7.3 Molecular Structure of $[\text{RhCl}_2(\text{Ph}_2\text{PO})_3\text{H}][\text{Et}_3\text{NH}]$

7.3.1 Experimental

The complex was prepared by the method described in chapter 6, the crystals of x-ray quality were obtained for recrystallisation from a concentrated tetrahydrofuran solution upon standing at -3°C for several days. The stratagem used to solve this structure was largely the same as that described for $[\text{RhCl}(\text{PPh}_3)(\text{Ph}_2\text{POPPH}_2)]$ and gave rise to the crystal data summarised below.

Crystal Data

$\text{C}_{43}\text{H}_{45}\text{O}_3\text{Cl}_2\text{P}_3\text{NRh} \cdot \text{C}_4\text{H}_8\text{O}$ is monoclinic, $M = 878$, space group $P 2_1/n$

$a = 14.866(6)$, $b = 20.676(10)$, $c = 15.239(6) \text{ \AA}$

$\alpha = 90.0(0)^\circ$, $\beta = 103.88(3)^\circ$, $\gamma = 90.0(0)^\circ$, $V = 4553.34 \text{ \AA}^3$

$Z = 4$, $D_X = 1.281 \text{ gcm}^{-3}$, $\lambda(\text{Mo-K}\alpha) = 0.71069 \text{ \AA}$, $\mu = 5.73 \text{ cm}^{-1}$

$F(000) = 2287.99$, $T = 293\text{K}$, $R = 0.0707$ for 2204 reflections.

Final refinement (minimizing $\omega ||F_0| - |F_c||^2$), 449 refined parameters

$\omega R = 0.0690$, $\omega = 1.1986/(\sigma^2(F) + 0.002174F^2)$.

7.3.2 Structural Features in $[\text{Rh}(\text{Ph}_3\text{PO})_3\text{H}(\text{Cl})_2][\text{HNEt}_3]$

This complex is shown to be a hydrogen bonded ion pair, in which the hydrogen bond (2.593 \AA) is between the hydrogen of the

triethylammonium species and the Ph_2PO oxygen atom identified as O2. The structure is found to be square pyramidal with two Ph_2PO and two Cl ligands in the base plane, the third Ph_2PO being the unique ligand in the apical position. The position of the rhodium atom is consistent with this assignment being 0.3268\AA out of the base plane in the direction of the unique Ph_2PO ligand. The two non unique Ph_2PO groups are observed to form a hydrogen bonded six membered ring of the form shown in figure 7.4.

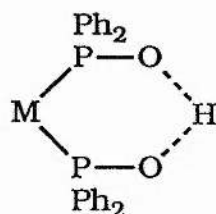


Fig. 7.4

The P-O bond lengths (1.546 and 1.539 \AA respectively) and the O---O interatomic distance⁽²¹⁷⁾ (2.411 \AA) are consistent with those of previously reported MPOHOP ring containing complexes, in which the hydrogen atom lies symmetrically between the two oxygen atoms. The angles between the normals of the phenyl groups are 101.89 , 103.67 and 97.24° , the reason for the latter value being slightly smaller are unknown. The triethylammonium is not symmetrical, two of the β carbon atoms lie below the plane containing the 3α carbon atoms, the third lies above it. The nitrogen itself lies below this plane by 0.4660\AA . A number of different views of the structure are shown in Figures 7.5 to 7.9. These include a view from below the base plane (7.6), a diagram in a better orientation to display the hydrogen bond

interaction (7.7) and a fully labelled diagram (7.8b). Tables of the atom coordinates (Tables 7.7 and 7.8), temperature factors (Table 7.9) and interatomic distances and angles (Table 7.10) are also included. See Appendix II for the structure factor Tables.

Fig. 7.5 Solid state stereo-projection of $[\text{RhCl}_2(\text{Ph}_2\text{PO})_3\text{H}][\text{Et}_3\text{NH}]$

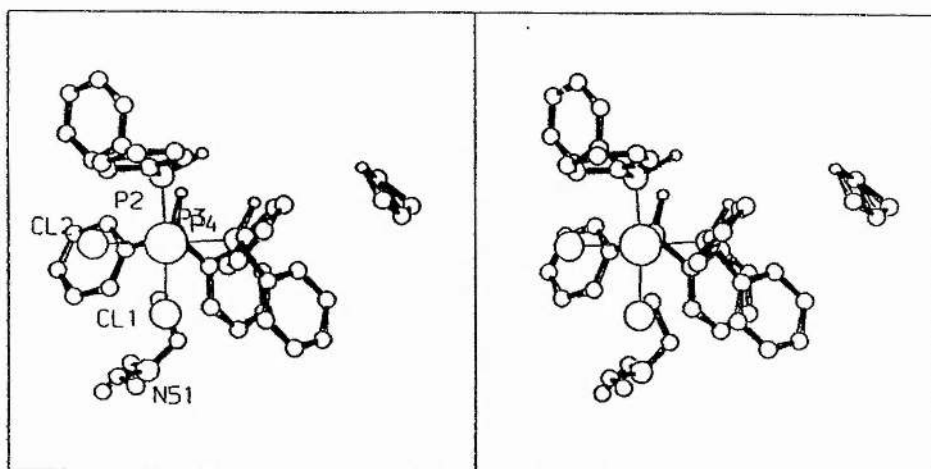
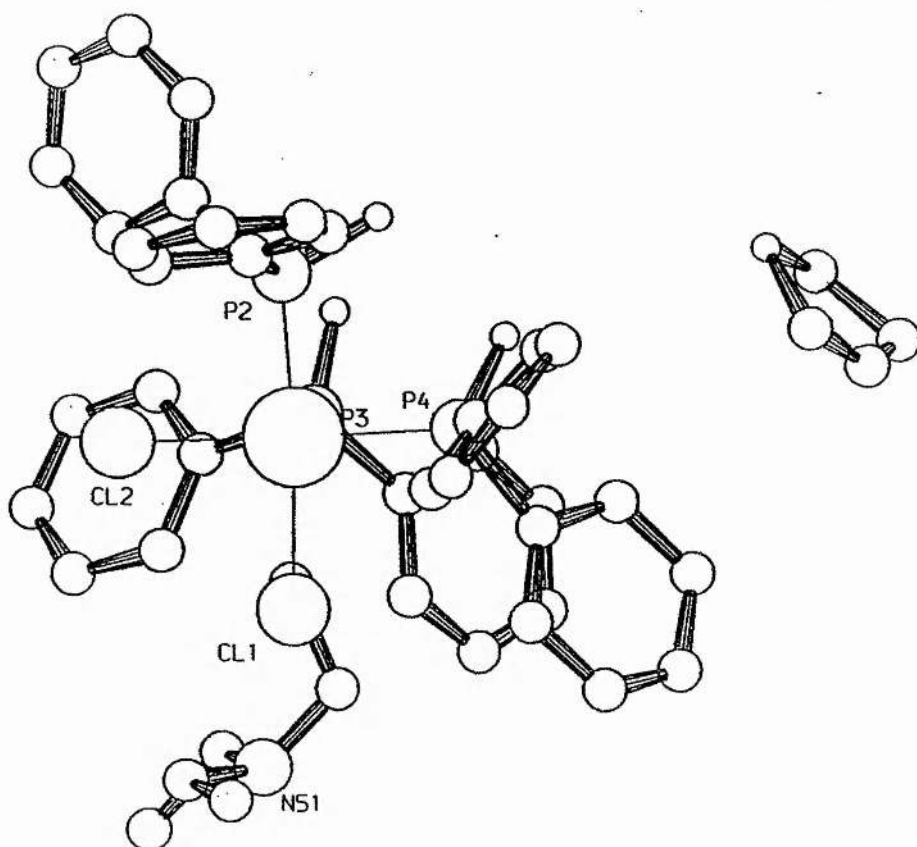


Fig. 7.6 Solid state molecular structure of $[\text{RhCl}_2(\text{Ph}_2\text{PO})_3\text{H}][\text{Et}_3\text{NH}]$



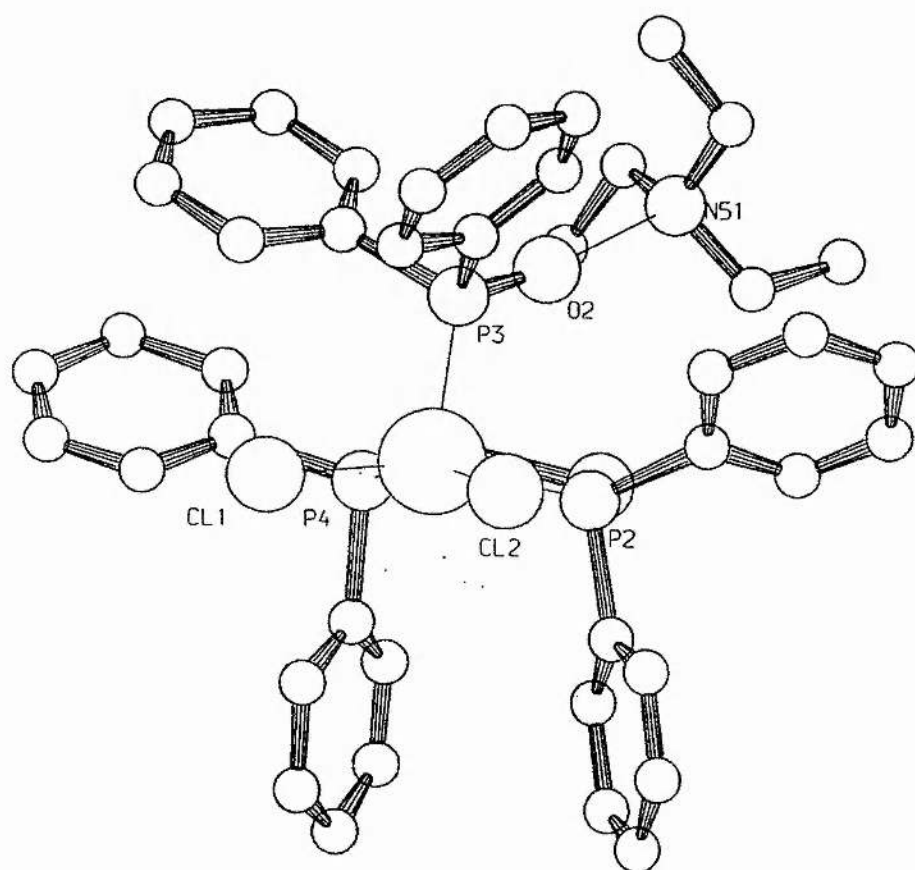


Fig. 7.7 Diagram Displaying Hydrogen Bonding Interaction

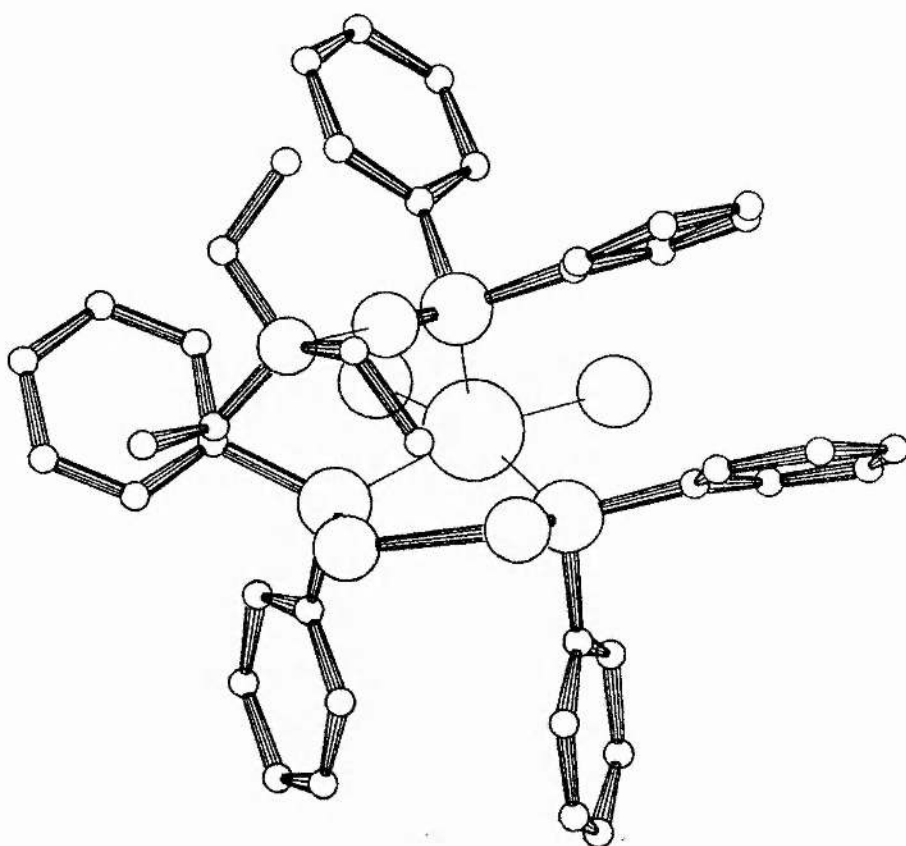


Fig. 7.8a Unlabelled Diagram of $[\text{RhCl}_2(\text{Ph}_2\text{PO})_3\text{H}][\text{EtNH}]$

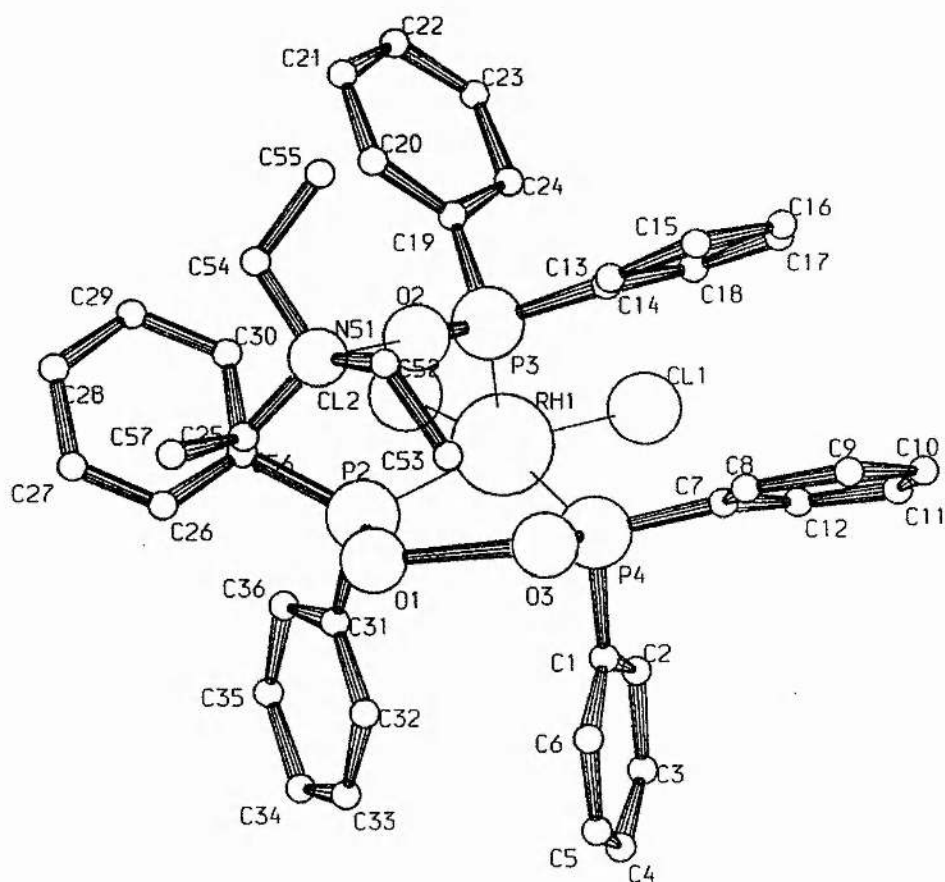


Fig. 7.8b Fully Labelled Diagram of $[\text{RhCl}_2(\text{Ph}_2\text{PO})_3\text{H}][\text{EtNH}]$

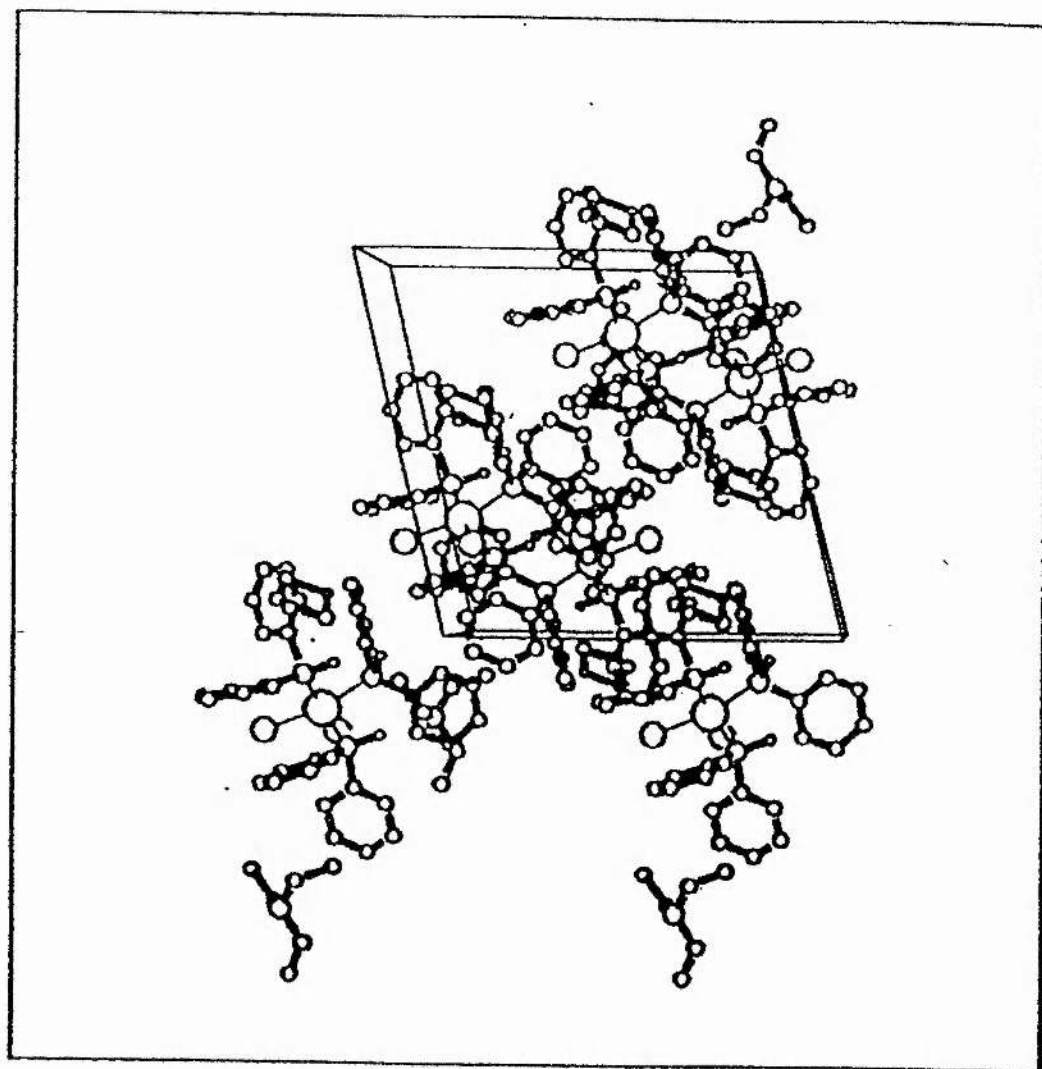


Fig. 7.9 Solid state packing of $[\text{RhCl}_2(\text{Ph}_2\text{PO})_3\text{H}][\text{Et}_3\text{NH}]$

Table 7.7

Coordinates $\times 10^4$ for non hydrogen atoms
with e.s.d's in parentheses. $U_{eq} \times 10^3$.

$$U_{eq} = (1/3) \sum_i \sum_j U_{ij} a_i^* a_j^* a_i \cdot a_j$$

	x/a	y/b	z/c	Ueq
RH1	6983 (1)	944 (1)	8890 (1)	27 (1)
P2	6141 (3)	806 (2)	7444 (3)	33 (1)
P3	7932 (3)	1626 (2)	8414 (3)	31 (1)
P4	6055 (3)	1795 (2)	9056 (3)	31 (1)
Cl1	7575 (3)	831 (2)	10488 (3)	48 (1)
Cl2	7596 (3)	-111 (2)	8764 (3)	45 (1)
O1	5571 (8)	1404 (6)	7032 (7)	48 (4)
O2	7614 (8)	1871 (5)	7461 (7)	39 (4)
O3	5749 (8)	2213 (5)	8200 (7)	35 (4)
C1	5012 (8)	1429 (6)	9268 (8)	37 (6)
C2	5043 (8)	930 (6)	9889 (8)	41 (6)
C3	4223 (8)	663 (6)	10016 (8)	57 (8)
C4	3372 (8)	896 (6)	9522 (8)	56 (8)
C5	3341 (8)	1395 (6)	8901 (8)	61 (9)
C6	4161 (8)	1662 (6)	8773 (8)	58 (9)
C7	6371 (9)	2362 (6)	9994 (8)	48 (7)
C8	6379 (9)	3015 (6)	9763 (8)	64 (9)
C9	6568 (9)	3485 (6)	10439 (8)	73 (10)
C10	6749 (9)	3302 (6)	11346 (8)	72 (11)
C11	6741 (9)	2650 (6)	11577 (8)	75 (11)
C12	6552 (9)	2180 (6)	10901 (8)	57 (8)
C13	8255 (9)	2324 (5)	9157 (7)	34 (6)
C14	8200 (9)	2929 (5)	8742 (7)	49 (8)
C15	8476 (9)	3482 (5)	9261 (7)	66 (9)
C16	8808 (9)	3430 (5)	10196 (7)	52 (8)
C17	8862 (9)	2825 (5)	10611 (7)	50 (8)
C18	8586 (9)	2272 (5)	10092 (7)	44 (7)
C19	9027 (7)	1186 (6)	8548 (9)	31 (6)
C20	9415 (7)	1201 (6)	7801 (9)	62 (9)
C21	10280 (7)	923 (6)	7854 (9)	71 (9)
C22	10757 (7)	629 (6)	8654 (9)	74 (10)
C23	10370 (7)	614 (6)	9402 (9)	74 (10)
C24	9505 (7)	892 (6)	9349 (9)	47 (7)
C25	6645 (8)	503 (5)	6542 (7)	23 (6)
C26	6038 (8)	476 (5)	5689 (7)	49 (7)
C27	6362 (8)	294 (5)	4939 (7)	51 (8)
C28	7294 (8)	138 (5)	5042 (7)	69 (10)
C29	7901 (8)	165 (5)	5894 (7)	67 (9)
C30	7577 (8)	347 (5)	6645 (7)	48 (8)
C31	5259 (10)	190 (7)	7464 (8)	58 (9)
C32	4360 (10)	375 (7)	7474 (8)	51 (8)
C33	3695 (10)	-94 (7)	7505 (8)	84 (11)
C34	3929 (10)	-749 (7)	7525 (8)	96 (13)
C35	4828 (10)	-933 (7)	7514 (8)	88 (10)
C36	5493 (10)	-464 (7)	7484 (8)	68 (9)
C41	4426 (39)	4164 (18)	7851 (29)	180 (25)
C42	4529 (42)	4402 (26)	8918 (40)	234 (33)
C43	3880 (40)	4131 (44)	8820 (49)	361 (52)
C44	3598 (32)	3461 (21)	8612 (31)	162 (23)
O45	3952 (31)	3555 (18)	7842 (27)	270 (25)
N51	12150 (15)	2494 (9)	10921 (12)	80 (8)
C53	11136 (16)	1682 (12)	11497 (21)	102 (13)
C52	11996 (26)	1794 (13)	11054 (18)	135 (16)
C54	13041 (21)	2626 (18)	10534 (17)	118 (16)

C55	13861 (19)	2325 (15)	11105 (18)	101 (13)
C56	11389 (18)	2873 (10)	10338 (17)	76 (10)
C57	11019 (19)	2584 (13)	9337 (17)	95 (11)

Supplementary Table 7.8

Anisotropic temperature factors $\times 10^3$
with e.s.d.'s in parentheses

	U11	U22	U33	U23	U13	U12
RH1	29 (1)	26 (1)	24 (1)	3 (1)	3 (1)	0 (1)
P2	37 (3)	31 (3)	29 (3)	2 (2)	7 (2)	-3 (3)
P3	28 (3)	32 (3)	32 (3)	7 (2)	8 (2)	-2 (2)
P4	39 (3)	29 (3)	26 (3)	-2 (2)	9 (2)	-6 (3)
Cl1	61 (4)	49 (4)	31 (3)	5 (3)	3 (3)	-2 (3)
Cl2	52 (3)	29 (3)	47 (3)	0 (2)	0 (3)	7 (3)
O1	54 (9)	42 (8)	34 (8)	5 (6)	-13 (7)	-6 (7)
O2	38 (8)	42 (8)	34 (7)	15 (6)	4 (6)	11 (7)
O3	39 (8)	50 (8)	22 (6)	14 (6)	18 (6)	15 (6)
C1	52 (14)	26 (11)	32 (11)	0 (9)	9 (10)	5 (10)
C2	51 (12)	36 (11)	35 (10)	13 (11)	10 (9)	1 (12)
C3	66 (16)	56 (15)	60 (15)	5 (12)	39 (14)	-6 (13)
C4	60 (16)	57 (16)	66 (15)	-27 (14)	43 (13)	13 (15)
C5	57 (17)	58 (16)	65 (17)	-17 (14)	10 (14)	22 (15)
C6	92 (19)	58 (16)	26 (12)	-15 (11)	21 (13)	16 (15)
C7	47 (14)	35 (13)	53 (14)	-11 (11)	-4 (11)	6 (11)
C8	75 (19)	51 (16)	68 (16)	1 (13)	20 (14)	-14 (14)
C9	67 (17)	72 (18)	70 (18)	-22 (15)	0 (14)	-21 (15)
Cl0	51 (16)	81 (21)	90 (21)	-41 (16)	27 (15)	-5 (15)
Cl1	71 (18)	98 (22)	65 (17)	-6 (16)	32 (14)	-8 (17)
Cl2	89 (18)	58 (15)	21 (11)	-15 (11)	4 (12)	-22 (13)
Cl3	46 (13)	30 (11)	26 (11)	-12 (9)	9 (9)	7 (10)
Cl4	68 (16)	24 (12)	51 (13)	-1 (10)	4 (12)	25 (11)
Cl5	93 (19)	12 (11)	94 (19)	14 (12)	25 (16)	-15 (12)
Cl6	51 (14)	26 (13)	72 (16)	-7 (12)	2 (12)	2 (11)
Cl7	59 (15)	58 (15)	28 (12)	-11 (11)	-2 (11)	-13 (12)
Cl8	47 (13)	57 (14)	26 (11)	-9 (10)	7 (10)	-28 (11)
Cl9	18 (10)	30 (11)	36 (11)	-12 (9)	-13 (9)	10 (8)
C20	56 (17)	63 (16)	67 (17)	9 (13)	19 (13)	-7 (13)
C21	48 (14)	85 (18)	93 (19)	-21 (17)	44 (14)	14 (16)
C22	51 (16)	61 (17)	104 (21)	-25 (16)	5 (17)	20 (14)
C23	47 (17)	60 (17)	102 (21)	8 (15)	-8 (15)	19 (14)
C24	25 (11)	61 (14)	52 (13)	-12 (13)	5 (9)	-23 (13)
C25	38 (12)	2 (9)	29 (10)	-8 (7)	12 (9)	-7 (8)
C26	38 (13)	65 (15)	36 (12)	-19 (11)	-4 (11)	-8 (12)
C27	47 (15)	60 (16)	46 (14)	10 (11)	14 (12)	-25 (12)
C28	64 (18)	91 (19)	56 (16)	-9 (15)	24 (14)	4 (16)
C29	38 (14)	97 (18)	78 (19)	-5 (15)	41 (14)	30 (14)
C30	25 (12)	75 (16)	41 (13)	-9 (12)	5 (10)	-5 (11)
C31	64 (17)	85 (19)	19 (11)	5 (12)	-4 (11)	-42 (15)
C32	31 (13)	74 (17)	54 (14)	-13 (12)	20 (11)	-11 (13)
C33	62 (18)	140 (26)	58 (16)	-49 (19)	30 (14)	-59 (19)
C34	88 (22)	113 (27)	74 (18)	22 (18)	-8 (16)	-81 (20)
C35	107 (21)	59 (16)	71 (17)	36 (15)	-30 (16)	-41 (20)
C36	70 (19)	67 (17)	53 (15)	14 (14)	-13 (13)	-26 (15)
C41	355 (64)	72 (27)	139 (34)	61 (25)	109 (39)	8 (34)
C42	244 (64)	216 (53)	202 (54)	-14 (46)	-27 (47)	-107 (47)
C43	171 (54)	544 (**)	382 (87)	-403 (92)	94 (52)	30 (65)
C44	231 (46)	149 (37)	160 (39)	103 (32)	153 (39)	22 (32)
O45	330 (54)	181 (35)	253 (43)	51 (34)	-24 (38)	65 (37)
N51	127 (21)	40 (12)	55 (13)	-26 (10)	-15 (13)	10 (13)
C53	57 (17)	90 (21)	188 (30)	-82 (20)	90 (20)	-33 (15)
C52	223 (41)	59 (20)	82 (21)	-36 (17)	-42 (23)	23 (23)
C54	81 (22)	225 (39)	60 (19)	-8 (21)	41 (17)	-39 (25)
C55	62 (19)	150 (28)	90 (21)	-33 (20)	19 (16)	1 (20)

C56	91 (20)	48 (15)	81 (18)	1 (14)	5 (15)	35 (14)
C57	113 (23)	95 (21)	69 (17)	5 (16)	7 (16)	47 (18)

Supplementary Table 7.9

Coordinates $\times 10^4$ for hydrogen atoms

	x/a	y/b	z/c
DUMM	5647	1636	9169
H21	5702	749	10272
H31	4247	276	10498
H41	2737	689	9621
H51	2682	1576	8518
H61	4137	2049	8292
DUMM	6225	1998	9470
H81	6239	3156	9061
H91	6574	3990	10260
H101	6895	3666	11869
H111	6881	2509	12279
H121	6546	1675	11079
DUMM	8040	1896	8756
H141	7943	2969	8018
H151	8434	3950	8940
H161	9022	3858	10598
H171	9119	2785	11335
H181	8628	1804	10414
DUMM	8358	1401	8507
H201	9045	1429	7181
H211	10580	935	7275
H221	11427	413	8695
H231	10739	386	10021
H241	9205	880	9927
DUMM	6395	644	7122
H261	5317	596	5609
H271	5892	273	4278
H281	7545	-3	4461
H291	8622	45	5974
H301	8047	368	7305
DUMM	5774	554	7441
H321	4179	881	7459
H331	3000	48	7512
H341	3415	-1112	7548
H351	5009	-1439	7530
H361	6189	-606	7476
H511	12217	2658	11606

Table 7.10

Interatomic distances (Å) and angles(°) .

P2 ---RH1	2.277(5)	P3 ---RH1	2.236(5)
P4 ---RH1	2.287(5)	C11 ---RH1	2.395(4)
C12 ---RH1	2.390(5)	O1 ---P2	1.546(12)
C25 ---P2	1.828(13)	C31 ---P2	1.834(16)
O2 ---P3	1.504(12)	C13 ---P3	1.826(11)
C19 ---P3	1.835(11)	O3 ---P4	1.540(11)
C1 ---P4	1.824(14)	C7 ---P4	1.821(13)
C42 ---C41	1.670(76)	C43 ---C41	1.849(94)
O45 ---C41	1.442(60)	C43 ---C42	1.097(91)
C44 ---C43	1.461(98)	O45 ---C44	1.410(69)
C52 ---N51	1.487(33)	C54 ---N51	1.599(40)
C56 ---N51	1.485(29)	C52 ---C53	1.602(49)
C55 ---C54	1.458(39)	C57 ---C56	1.607(34)
P3 -RH1 -P2	90.5(2)	P4 -RH1 -P2	89.8(2)
P4 -RH1 -P3	89.8(2)	C11 -RH1 -P2	162.8(2)
C11 -RH1 -P3	106.5(2)	C11 -RH1 -P4	92.7(2)
C12 -RH1 -P2	86.6(2)	C12 -RH1 -P3	105.5(2)
C12 -RH1 -P4	164.3(2)	C12 -RH1 -C11	86.4(2)
O1 -P2 -RH1	114.5(5)	C25 -P2 -RH1	122.7(4)
C25 -P2 -O1	104.7(6)	C31 -P2 -RH1	107.5(4)
C31 -P2 -O1	103.7(7)	C31 -P2 -C25	101.5(6)
O2 -P3 -RH1	116.6(5)	C13 -P3 -RH1	113.0(5)
C13 -P3 -O2	107.9(6)	C19 -P3 -RH1	105.4(4)
C19 -P3 -O2	109.9(7)	C19 -P3 -C13	103.2(6)
O3 -P4 -RH1	113.7(5)	C1 -P4 -RH1	105.3(5)
C1 -P4 -O3	106.9(6)	C7 -P4 -RH1	122.2(5)
C7 -P4 -O3	105.7(6)	C7 -P4 -C1	101.5(7)
C2 -C1 -P4	122.4(9)	C6 -C1 -P4	117.6(10)
C8 -C7 -P4	116.2(9)	C12 -C7 -P4	123.7(10)
C14 -C13 -P3	116.7(8)	C18 -C13 -P3	123.2(8)
C20 -C19 -P3	115.4(8)	C24 -C19 -P3	124.5(10)
C26 -C25 -P2	115.0(9)	C30 -C25 -P2	124.8(8)
C32 -C31 -P2	120.2(11)	C36 -C31 -P2	119.8(11)
C43 -C41 -C42	35.9(32)	O45 -C41 -C42	101.4(39)
O45 -C41 -C43	70.6(39)	C43 -C42 -C41	81.0(55)
C42 -C43 -C41	63.1(51)	C44 -C43 -C41	91.1(48)
C44 -C43 -C42	135.4(74)	O45 -C44 -C43	84.5(42)
C44 -O45 -C41	113.1(37)	C54 -N51 -C52	112.7(24)
C56 -N51 -C52	118.4(20)	C56 -N51 -C54	105.7(19)
C53 -C52 -N51	111.3(24)	C55 -C54 -N51	110.9(23)
C57 -C56 -N51	114.2(19)		

REFERENCES

1. S. G. Davies, "Organotransition Metal Chemistry : Applications to Organic Synthesis", Pergammon Press, 1982.
2. H. M. Colquhoun, H. Holton, D. J. Thompson and M. V. Twigg, "New Pathways for organic Synthesis : Practical Applications of Transition Metals", Plenum Press, 1983.
3. C. Magnus, *Pogg. Ann.*, (1828) **14**, 239.
4. W. C. Zeise, *Pogg. Ann.*, (1831), **21**, 497.
5. (a) W. C. Zeise, *Pogg. Ann.*, (1838), **45**, 332.
(b) W. C. Zeise, (1839), **47**, 478.
6. K. Birnbaum, *Ann. Chem.*, (1868), **145**, 67.
7. K. Birnbaum, *J. Prakt. Chem.* (1868), **104**, 381.
8. W. Prandtl and K. A. Hofmann, *Ber.*, (1900), **33**, 2981.
9. M. Herberhold, "Metal π Complexes, Vol II, Part 2", Chapters VI-VIII, Elsevier Scientific Publishing Company, 1974.
10. S. Winstein and H. J. Lucas, *J. Am. Chem. Soc.*, (1956), **78**, 1665.
11. H. J. Lucas, R. S. Moore and D. Pressman, *J. Am. Chem. Soc.*, (1943), **65**, 227.
12. B. E. Douglas, *J. Am. Chem. Soc.*, (1953), **75**, 4839.
13. M. J. S. Dewar, *Bull. Soc. Chim. Fr.*, **18**, C79, 1951.
14. J. Chatt and L. A. Duncanson, *J. Chem. Soc.*, (1953), 2939.
15. P. Heimbach and R. Traummüller "Chemie der Metall-Olefin Komplexe", Verlag Chemie, Weinheim, 1970.

16. N. Rösh, R. P. Messmer and K. H. Johnson, *J. Am. Chem. Soc.*, (1974), **96**, 3855.
17. S. D. Ittel and J. A. Ibers, *Adv. Organomet. Chem.* (1976), **14**, 33.
18. L. M. Muir, K. W. Muir and J. A. Ibers, *Faraday Discuss. Chem. Soc.*, (1969), **47**, 84.
19. J. M. Baraban and J. A. McGinnety, *J. Am. Chem. Soc.*, (1975), **97**, 4232.
20. R. Cramer, J. B. Cline and J. D. Roberts, *J. Am. Chem. Soc.*, (1969), **91**, 2519.
21. A. J. Shultz, R. K. Brown, J. M. Williams and R. R. Schock, *J. Am. Chem. Soc.*, (1972), **94**, 1451.
22. K. Jones and C. Kruger, *Angew Chem. Int. Ed. Engl.*, (1980), **19**, 520.
23. C. Pedone and E. Benedetti, *J. Organomet. Chem.*, (1971), **29**, 443.
24. S. Merlino, R. Lazzaroni and G. Montagnoli, *J. Organomet. Chem.*, (1971), **30**, C93.
25. A. De Renzi, B. DiBabio, G. Paiaro, A. Panunzi and C. Pedone, *Gazz. Chim. Ital.*, (1976), **106**, 765.
26. S. C. Nyburg, K. Simpson and W. Wong-Ng, *J. Chem. Soc., Dalton Trans.*, (1976), 1865.
27. F. Sartori and L. Leoni, *Acta Crystallogr., Sect B*, (1976), **B32**, 145.
28. F. A. Catton, J. N. Francis, B. A. Frenz and M. Tsutsui, *J. Am. Chem. Soc.*, (1973), **95**, 2483.

29. A. McAdam, J. N. Francis and J. A. Ibers, *J. Organomet. Chem.*, (1971), **29**, 149.
30. L. J. Guggenberger, *Inorg. Chem.*, (1973), **12**, 499.
31. D. J. Sepelak, C. G. Pierpont, E. K. Barfield, J. T. Budz and C. A. Poffenberger, *J. Am. Chem. Soc.* (1976), **98**, 6178.
32. R. Countryman and B. R. Penfold, *Chem. Commun.*, (1971), 1598.
33. A. D. Walsh, *Trans. Faraday Soc.* (1949), **45**, 179.
34. J. A. McGinnety and J. A. Ibers, *Chem. Commun.*, (1968), 235.
35. R. J. Cvetanovic, F. J. Duncan, W. E. Falconer and R. S. Irwin, *J. Am. Chem. Soc.*, (1965), **87**, 1827.
36. M. A. Muhs and F. T. Weiss, *J. Am. Chem. Soc.*, (1962), **84**, 4697.
37. E. Gil-Av and V. Schurig, *Analy. Chem.*, (1971), **43**(14), 2030.
38. R. Cramer, *J. Am. Chem. Soc.*, (1967), **89**, 4621.
39. R. G. Denning, F. R. Hartley and L. M. Venanzi, *J. Chem. Soc. A*, (1967), 328.
40. R. Spagna, L. M. Venanzi and L. Zambonelli, *Inorg. Chem. Acta*, (1970), **4**, 475.
41. P. M. Henry, *J. Am. Chem. Soc.*, (1964), **86**, 3246.
42. S. V. Pestrikov, I. I. Moiseev and B. A. Tswilikhouskaya, *Russ. J. Inorg. Chem.*, (1966), **11**, 931.
43. J. R. Holden and N. C. Baenziger, *J. Am. Chem. Soc.*, (1955), **77**, 4987.

44. A. R. Brause, F. Kaplan and M. Orchin, *J. Am. Chem. Soc.*, (1967), **89**, 2661.
45. B. F. G. Johnson, G. E. Holloway, G. Hulley and J. Lewis, *Chem. Commun.*, (1967), 1143.
46. T. Okuyama, T. Fueno and J. Furukawa, *Bull. Chem. Soc. Jap.*, (1969), **42**, 3106.
47. C. E. Holloway, G. Hulley, B. F. G. Johnson and J. Lewis, *Chem. Abstr.*, (1970), **73**, 35499d.
48. A. R. Brause, *Diss. Abstr. B.*, (1968), **28(8)**, 3215.
49. G. E. Holloway, G. Hulley, B. F. G. Johnson and J. Lewis, *J. Chem. Soc., A*, (1969), 53.
50. R. Cramer, *J. Am. Chem. Soc.*, (1964), **86**, 217.
51. R. W. Taft in "Steric Effects in Organic Chemistry", M. S. Newman, Ed., Wiley, New York, N.Y. 1956, Chapter 3.
52. G. A. Tolman, W. C. Seidel and D. H. Gerlach, *J. Am. Chem. Soc.*, (1972), **94**, 2669.
53. L. Vaska, *Accounts Chem. Res.*, (1968), **1**, 335.
54. R. G. Denning and L. M. Venanzi, *J. Chem. Soc., A*, (1967), 336.
55. T. Yamamoto, A. Yamamoto and S. Ikeda, *J. Am. Chem. Soc.*, (1971), **93**, 3360.
56. H. J. Lucas, F. W. Billmeyer and D. Pressman, *J. Am. Chem. Soc.*, (1943), **65**, 230.
57. A. M. Rubinshtein and G. V. Derbisher, *Dokl. Akad. Nauk. SSSR* (1950), **74**, 283; *Chem. Abstr.*, (1951), **45**, 3280b.

58. A. D. Gelman and L. N. Essen, *Dokl. Akad. Nauk. SSSR*, (1951), **77**, 273; *Chem. Abstr.*, (1951), **45**, 6117g.
59. J. Chatt, L. M. Vallarino and L. M. Venanzi, *J. Chem. Soc.*, (1957), 2496.
60. J. Chatt, L. M. Vallanino and L. M. Venanzi, *J. Chem. Soc.*, (1957), 3413.
61. R. C. Denning and L. M. Wenanzi, *J. Chem. Soc.*, (1963), 3241.
62. R. E. Yingst and B. E. Douglas, *Inorg. Chem.*, (1964), **3**, 1177.
63. M. Dubeck, *J. Am. Chem. Soc.*, (1960), **82**, 6193.
64. D. W. McBride, E. Dudek and F. G. A. Stone, *J. Chem. Soc.*, (1964), 1752.
65. P. M. Treichel and F. G. A. Stone, *Advan. Organometal. Chem.*, (1964), **1**, 143.
66. R. S. Dickson and G. Wilkinson, *Chem. Ind. (London)*, (1963), 1432.
67. J. L. Beston, D. W. A. Sharp and G. Wilkinson, *J. Chem. Soc.*, 3488 (1962).
68. H. C. Clark and J. H. Tsai, *Chem. Commun.*, (1965), 111.
69. I. I. Moiseev, E. A. Feodoroiskaya and Y. K. Syrkin, *Zh. Neorg. Khim.*, (1959), **4**, 2641; *Chem. Abstr.*, (1960), **54**, 13933g.
70. G. W. Parshall and G. Wilkinson, *Inorg. Chem.*, (1962), **1**, 896.
71. R. B. King and A. Fronzaglia, *Inorg. Chem.*, (1966), **5**, 1837.
72. J. Halpern, *Pure Appl. Chem.*, (1983), **55**, 99.

73. M. D. Fryzuk, B. Dosnich, *J. Am. Chem. Soc.*, (1977), **99**, 5946.
74. L. K. Atkinson and D. C. Smith, *J. Chem. Soc., A, Dalton Trans.*, (1971), 3592.
75. L. Malatesta, M. Agoletta and G. Caglio, *J. Organomet. Chem.*, (1977), **129**, 117.
76. B. Bogdanovic, *Angew. Chem.*, (1965), **77**, 1010.
77. E. H. Schubert and R. K. Sheline, *Inorg. Chem.*, (1966), **5**, 1071.
78. H. W. Kouwenhoven, J. Lewis and R. S. Nyhlom, *Proc. Chem. Soc.*, (1961), 220.
79. M. A. Bennett, H. W. Kouwenhoven, J. Lewis and R. S. Nyholm, *J. Chem. Soc.*, (1964), 4570.
80. M. A. Bennett and R. Watt, *Chem. Commun.*, (1971), 94.
81. C. B. Robertson and P. O. Whimp, *J. Organomet. Chem.*, (1973), **49**, C27.
82. M. A. Bennett, R. N. Johnson and I. B. Tomkins, *J. Am. Chem. Soc.*, (1974), **96**, 61.
83. E. Weiss, K. Stark, J. E. Lancaster and H. D. Murdoch, *Helv. Chim. Acta.*, (1963), **46**, 288.
84. G. O. Schenck, E. Koemer von Gustorf and M. J. Jun, *Tetrahedron Lett.*, (1962), 1059.
85. M. A. Bennett, C. B. Robertson, I. B. Tomkins and P. O. Whimp, *Chem. Commun.*, (1971), 341.
86. C. B. Robertson and P. O. Whimp, *J. Chem. Soc. Dalton Trans.*, (1973), 2454.

87. M. A. Bennett, W. R. Kneen and R. S. Nyholm, *J. Organometal Chem.*, (1971), **26**, 293.
88. M. A. Bennett, R. S. Nylom and J. D. Saxby, *J. Organomet. Chem.*, (1967), **10**, 301.
89. L. V. Interrante and G. V. Nelson, *Inorg. Chem.*, (1968), **7**, 2059.
90. L. V. Interante, M. A. Bennett and R. S. Nylom, *Inorg. Chem.*, (1966), **5**, 2212.
91. M. A. Bennett, L. V. Interante and R. S. Nyholm, *Z. Naturforsch, B*, (1965), **20**, 633.
92. M. A. Bennett and E. J. Hann, *J. Organometal. Chem.*, (1971), **29**, C15.
93. M. A. Bennett, R. N. Johnson, I. B. Tomkins, *J. Am. Chem. Soc.*, (1974), **96**, 61.
94. D. I. Hall and R. S. Nyholm, *Chem. Commun.*, (1970), 488.
95. P. W. Clark and G. E. Hartwell, *Inorg. Chem.*, (1970), **9**, 1948.
96. M. A. Bennett and P. W. Clark, *J. Organomet. Chem.*, (1976), **110**, 367.
97. M. A. Bennett, P. W. Clark, G. B. Robertson and P. O. Whimp, *Chem. Commun.*, (1972), 1011.
98. M. A. Bennett and P. A. Longstaff, *J. Am. Chem. Soc.*, (1969), **91**, 6266.
99. M. A. Bennett, R. N. Johnson, G. R. Robertson, I. B. Tomkins and P. O. Whimp, *J. Organomet. Chem.*, (1974), **77**, C43.

100. M. A. Bennett, R. N. Johnson, G. B. Robertson, I. B. Tomkins and P. O. Whimp, *J. Am. Chem. Soc.*, (1976), **98**, 3514.
101. C. Crocker, R. J. Errington, W. S. McDonald, K. J. Odell, B. L. Shaw, *Chem. Commun.*, (1979), 498.
102. M. I. Bruce, G. Shaw and F. G. A. Stone, *J. Chem. Soc. Dalton Trans.*, (1976), 81.
103. J. S. Ricci and J. A. Ibers, *J. Organomet. Chem.*, (1971), **27**, 261.
104. W. Winter, *Angew. Chem.*, (1975), **87**, 172; *Angew. Chem. Int. Ed. Engl.*, (1975), **14**, 170.
105. W. Winter and J. Strähle, *Angew. Chem. Int. Ed. Engl.*, (1978), 17(2), 128.
106. P. W. Clark and G. E. Hartwell, *J. Organometal. Chem.*, (1975), **97**, 117.
107. M. Orrico Visscher, J. C. Huffmann and W. E. Streib, *Inorg. Chem.*, (1974), 13(4), 792.
108. R. R. Ryan, R. Schaeffer, P. Clark and G. Hartwell, *Inorg. Chem.*, (1975), 14(12), 3039.
109. G. E. Hartwell and P. W. Clark, *Chem. Commun.*, (1970), 1115.
110. P. W. Clark and G. E. Hartwell, *J. Organomet. Chem.*, (1977), **139**, 385.
111. P. W. Clark and G. E. Hartwell, *J. Organomet. Chem.*, (1975), **102**, 387.
112. P. W. Clark and G. E. Hartwell, *J. Organomet. Chem.*, (1975), **96**, 451.

113. P. E. Garrou and G. E. Hartwell, *J. Organomet. Chem.*, (1974), **71**, 443.
114. P. E. Garrou and G. E. Hartwell, *J. Organomet. Chem.*, (1973), **55**, 331.
115. J. L. S. Curtis and G. E. Hartwell, *J. Chem. Soc. Dalton*, (1974), 1898.
116. H. Yamazaki, Y. Wakasuki and K. Aoki, *Chem. Lett.*, (1979), 1041.
117. D. C. Cupertino, M. M. Harding and D. J. Cole-Hamilton, *J. Organomet. Chem.*, (1985), **24**, 4433.
118. S. A. Preston, D. C. Cupertino, Pilar Plama-Ramirez and D. J. Cole-Hamilton, *Chem. Commun.*, (1986), 977.
119. D. C. Cupertino, Ph.D. Thesis.
120. A. Barouski, A. Iraqi, D. C. Cupertino, D. J. Irvine, D. J. Cole-Hamilton, *J. Chem. Soc.*, in press.
121. J. D. Morrison and H. S. Mosher, "Asymmetric Organic Reactions", American Chemical Society, Washington D.C., 1976, p.280.
122. J. D. Morrison and H. S. Mosher, "Asymmetric Organic Reactions", American Chemical Society, Washington D.C., 1976, p.40.
123. J. Halpern, A. S. C. Chan, P. P. Reley, J. J. Pluth, *Adv. Chem. Ser.*, (1979), **173**, 16.
124. R. McCrindle, E. C. Alyea, S. A. Dias and A. J. McAlees, *J. Chem. Soc., Dalton Trans.*, (1979), 640.

125. A. S. C. Chan, J. J. Pluth, J Halpern, *J. Am. Chem. Soc.*, (1980), **102**, 5952.
126. W. C. Chrisopfel and B. D. Vineyard, *J. Am. Chem. Soc.*, (1979), **101**, 4406.
127. R. T. De Pue, D B Collum, J. W. Ziller and M. R. Churchill, *J. Am. Chem. Soc.*, (1985), **107**, 2131.
128. A. Oudeman, F. van Rantwyk and H. van Bekkum, *J. Coord. Chem.*, (1974), **4**, 1.
129. L. Simandi, F. Nagy and E. Budo, *Acta. Chem. (Budapest)*, (1968), **58**, 39; *Chem. Abstr.*, (1969), **70**, 56916r.
130. M. Kuwahara, T. Kato and M. Takasumi, *Nippon Kagaku Kaishi*, (1979), 675; *Chem. Abstr.*, (1979), **91**, 56301v.
- 131 D. C. Cupertino and D. J. Cole-Hamilton, *J. Chem. Soc. DaltonTrans.* , (1987), 443
- 132 Aldrich library of Infra red Spectra
- 133 P. E Garrou, *Chem. Rev.*, (1981), **81** , 229
- 134 S. D. Littel and J. A. Ibers, *Adv. Organomet. Chem.*, (1976), **14**, 33
- 135 D. H. Williams and I. Fleming, 'Spectroscopic Methods in Organic Chemistry', second edition, McGraw-Hill (U.K.) ltd
- 136 E. W. Abel, S. K. Baragava, K. G. Orrell, *Prog. Inorg. Chem.*, (1984), **32**, 1 and refs therein
- 137 H. C. Clark, K. R. Dixon and W. J. Jacobs, *Chem Commun.*, (1968), 548
- 138 L. Malatesta. G Caglio and M. Angoletta, *J. Chem. Soc.*, (1965), 6974

- 139 W. Heiber and H. Duchatsch, *Chem. Ber.*, (1965), **98**, 1744
- 140 W. Heiber and V. Frey, *Chem. Ber.*, (1966), **99**, 2614
- 141 R. B. King, M. B. Bisnette and A. Fronzaglia, *J. Organomet. Chem.*, (1965), **3**, 256
- 142 R. B. King, M. B. Bisnette and A. Fronzaglia, *J. Organomet. Chem.*, (1966), **5**, 341
- 143 W. Heiber and V. Frey and P. Joan, *Chem. Ber.*, (1967), **100**, 1961
- 144 T. Kruck, M. Holfer and M. Noack, *Chem. Ber.*, (1966), **99**, 1153
- 145 J. Halpern and S. F. A. Kettle, *Chem. and Ind.*, (1961), 745
- 146 D. Rose, J. D. Gilbert, R. P. Richardson and G. Wilkinson, *J. Chem. Soc. (A)*, (1969), 2610
- 147 P. Legzdins, R. W. Mitchell, G. L. Rempel, J. D. Ruddick and G. Wilkinson, *J. Chem. Soc. (A)*, (1970), 3322
- 148 R. W. Mitchell, J. D. Ruddick and G. Wilkinson, *J. Chem. Soc. (A)*, (1971), 3224
- 149 M. J. Lawrence and G. Foster, G.P. 1,806,293
- 150 R. S. Coffey, *Chem. Commun.*, (1967), 923
- 151 J. J. Byerley, G. L. Rempel, N. Takebe and B. R. James, *Chem. Commun.*, (1971), 1482
- 152 C. A. Agambar and K. G. Orrell, *J. Chem. Soc. (A)*, (1969), 897
- 153 S. D. Robinson and M. F. Uttley, *J. Chem. Soc. Dalton Trans.*, (1973), 1912

- 154 T. H. Brown and P. J. Green, *J. Am. Chem. Soc.*, (1970), **92**, 2359
- 155 K. Bare Private Communication
- 156 D. B. Denney and L. C. Smith, *Chem. Commun.*, (1976), 3404
- 157 V. S. Tsivunin, L. V. Zhegalina, L.N. Krutskii, *Zh. Obshch. Khim.*, (1973), 43(2), 439
- 158 S. W. Ng and J. J. Zuckerman, *J. Organomet. Chem.*, (1982), **234**, 257
- 159 'Chem-X', Chemical modeling program, Chemical Design Ltd
- 160 P. W. Clark and G. E. Hartwell, *J. Chem. Soc. Dalton Trans.*, (1977), **139(3)**, 385
- 161 H. Iuth, M. R. Truter, A. Robson, *J. Chem. Soc. A*, (1969), 28
- 162 S. M. Nelson and M. Sloan, *Chem. Commun.*, (1972), 745
- 163 D. H. Gibson, T. S. Ong, F.G. Khoury, *J. Organomet. Chem.*, (1978), **157**, 81
- 164 C. P. Casey and C. R. Cry, *J. Am. Chem. Soc.*, (1976), **95**, 551
- 165 K. M. Abraham, J. R. van Wazer, *J. Organomet. Chem.*, (1975), **85**, 41
- 166 R. S. Davidson, R. A. Sheldon and S. Trippett, *J. Chem. Soc. C.*, (1967), **16**, 1547
- 167 J. A. Millar and D. Stewart, *Tett. Lett.*, (1977), **12**, 1065
- 168 E. J. Spanier and F. E. Caropreso, *J. Am. Chem. Soc.*, (1970), **92(11)**, 3348
- 169 D. Hunter, J. K. Michie, J. A. Millar, W. Stewart, *Phosphorus and Sulphur*, (1981), **10**, 267

- 170 R. F. Hudson, R. J. G. Searle and F. H. Devitt, *J. Chem. Soc., B*, (1966), **8**, 789
- 171 I. F. Lutsenko, V. L. Foss, *Pure and Applied Chem.*, (1980), **52**, 917
- 172 L. Homer and M. Jordan, *Phosphorus and Sulphur*, (1980), **8**, 235
- 173 J. McKechnie, D. S. Payne and W. Sim, *J. Chem Soc.* (1965), 3500
- 174 D. J. Irvine, D. J. Cole-Hamilton, J. Barnes and P. K. G. Hodgeson., *Polyhedron*, (1989), **8(12)**, 1575
- 175 K. W. Chiu, H. S. Rzepa, R. N. Sheppard, G. Wilkinson and W-K. Wong, *Polyhedron* , (1982), **1**, 809
- 176 E. H. Wong R. M. Ravenelle, E. J. Gabe, F. L. Lee and L. Prasad, *J. Organomet. Chem.*, (1982), **233**, 321
- 177 A. R. Seidle, R. A. Newmark, R. D. Howell, *Inorg. Chem.* (1988), **27**, 2473
- 178 P. W. Clark and G. E. Hartwell, *J. Organomet. Chem.*, (1975), **102**, 387
- 179 H Vahrenkamp, *Chem. Ber.* , (1972), **105** , 3575
- 180 J. Vogt, P.A.N.I.C., n.m.r. parameter fitting program, N.M.R. Software dept, Spectrospin, A.G. Fallanden, Switzerland
- 181 H. Gunter, ' n.m.r. Spectrometry an introduction', John Wiley and sons ltd, (1980)
- 182 S. A. Preston, M.Sc. Thesis
- 183 K. Bare, Private Communication (184) C. S. Kraihanzel and C. M. Bartish, *J. Am. Chem. Soc.*, (1972), **94**, 3572

- 185 E. H. Wong, F. C. Bradley, L. Prasad and E. J. Gabe, *J. Organomet. Chem.*, (1984), **263**, 167 and refs therein
- 186 C. Zeiher, J. Mohyla, I-P. Lorenz and W. Hiller, *J. Organomet. Chem.*, (1985), **286**, 159
- 187 H. W. Choi and E. L. Muettertides, *J. Am. Chem. Soc.*, (1982), **104**, 153
- 188 G. M. Gray and C. S. Kraihanzel, *J. Organomet. Chem.*, (1982), **238**, 209
- 189 E. H. Wong, L. Prasad, E. J. Gabe and F. C. Bradley, *J. Organomet. Chem.* (1984), **236**, 321
- 190 E. H. Wong, R. M. Ravenelle, E. J. Gabe, F. L. Lee and L. Prasad, *J. Organomet. Chem.*, (1984), **233**, 321
- 191 D. M. Roundhill, R. P. Sperline and W. B. Beaulieu, *Coord. Chem. Rev.*, (1978), **26** and refs therein
- 192 K. R. Dixon and A. D. Rattray, *Can. J. Chem.*, (1971), **49**, 3997
- 193 A. Pidcock and C. R. Waterhouse, *J. Chem. Soc., A*, (1970), 2080
- 194 A. Pidcock and C. R. Waterhouse, *J. Chem. Soc., A*, (1970), 2087
- 195 D. V. Navik, G. J. Palenik, S. Jacobson, A. J. Carty, *J. Am. Chem. Soc.*, (1974), **96(7)**, 307
- 196 R. P. Sperline, M. K. Dickson and D. M. Roundhill, *Chem Commun.*, (1977), 62
- 197 R. O. Gould, C. L. Jones, W. J. Sime and T. A. Stephenson, *J. Chem. Soc. Dalton Trans.*, (1977), 669

- 198 I.W. Robertson and T.A. Stephenson, *Inorg. Chim. Acta*, (1980), **45**, L215
- 199 J. A. S. Duncan, D. Hedden, D. M. Roundhill, T. A. Stephenson and M. D. Walkinshaw, *Angew. Chem Int Ed.*, (Eng), (1982), **21**, 452
- 200 J. A. S. Duncan, T. A. Stephenson, M. D. Walkinshaw, D. Hedden, D. M. Roundhill, *J. Chem. Soc. Dalton Trans.*, (1984), 801
- 201 M. A. Bennett and T. R. B. Mitchell, *J. Organomet. Chem.*, (1974), **70**, C30
- 202 H. Werner and R. Feser, *Z. Anorg. Allg. Chem.*, (1979), **458**, 301 (Check this Ref)
- 203 J. A. S. Duncan, T. A. Stephenson, W. B. Beaulieu, D. M. Roundhill, *J. Chem. Soc. Dalton Trans.*, (1983), 1755
- 204 G. C. Pimentel and A. L. McClellan, 'The Hydrogen Bond' W.H. Freeman and co (1960)
- 205 J. P. Glusker, K. N. Trueblood, 'Crystal Structure Analysis - A Primer.' O.U.P., (1972)
- 206 L. S. D. Glasser, *Crystallography and It's Applications*, van Nostrand Reinhold, (1977)
- 207 G. M. Sheldrick, 'SHELX76', program for crystal structure determination, Univ. of Cambridge, (1976)
- 208 N. Walker and D. Stuart, *Acta. Cryst.*, (1983), **39A**, 158
- 209 G. M. Sheldrick, 'SHELXS', program for structure solution, Univ. of Gottigen, (1986)

- 210 P. Roberts and G. M. Sheldrick, 'XANADU', program for crystallographic calculations, Univ. of Cambridge, (1975)
- 211 W. D. S. Motherwell and W. Clegg, 'PLUTO', program for molecular drawings, Univ. of Cambridge, (1978)
- 212 G. H. Stout and L. H. Jensen, 'X-ray determination: A practical guide, MacMillan, New York (1968)
- 213 J. Brimacombe, J. Barnes and D. J. Irvine , *Carbohydr Res*, In Press
- 214 D. E. C. Corbridge, 'Topics in Phosphorus Chemistry vol 3 p54ff and refs therein, interscience publishers
- 215 G. Glidewell, private communication
- 216 D. V. Naik, G. J. Palenik, S. Jacobson and A. Carty, *J. Am. Chem. Soc.*, (1974), **96**, 2286
- 217 M.C. Cornock, R.O. Gould, C.L. Jones and T.A. Stephenson *J. Chem. Soc. Dalton Trans.*, (1977), 1307

Summary

This study has thus shown that both the AAA and VAA ligands can be synthesised but that they can not be isolated because of their further reaction to tetraphenyldiphosphine monoxide. Use of dilute solutions of AAA and VAA, prepared in situ, has, however, allowed these ligands to be used in reactions with metal containing substrates.

In reactions with $[\text{RhCl}(\text{PPh}_3)_3]$ the above ligands were found, along with CAA to produce complexes containing the phosphorus mixed anhydride bound in a bidentate fashion. In all cases the ligands were bound via a σ bond to the phosphorus atom and a π bond to the alkene species. VAA was also observed to take part in a metal promoted double bond migration upon coordination, the complex isolated from the reaction $[\text{RhCl}(\text{PPh}_3)_3]$ and VAA being the same as that produced by the reaction of $[\text{RhCl}(\text{PPh}_3)_3]$ and CAA. The CAA complex was itself noted to be fluxional at room temperature. Altering the mole ratio of the $[\text{RhCl}(\text{PPh}_3)_3]/\text{AAA}$ reaction to 1:2, resulted in a metal promoted rearrangement of the AAA ligand being observed. This rearrangement centred on the formation of a new $\text{Ph}_2\text{POPPh}_2$ (tetraphenyldiphosphoxane) ligand, the complex isolated being $[\text{RhCl}(\text{PPh}_3)(\text{Ph}_2\text{POPPh}_2)]$, the first platinum metal complex containing a chelate $\text{Ph}_2\text{POPPh}_2$ ligand to be isolated. Further reaction with TiPF_6 was used to produce a second complex

$[\text{Rh}(\text{PPh}_3)_2(\text{Ph}_2\text{POPPh}_2)][\text{PF}_6]$ involving replacement of Cl^- with a further PPh_3 ligand. This later process resulted from reaction of an isolated quantity of the initial tdpdp complex. If the complex was not isolated but directly reacted with the thallium reagent the complex isolated was not that mentioned above but $[\text{Rh}(\text{PPh}_3)_3(\text{O}_2\text{CCH}_2\text{CH}_2\text{PPh}_3)][\text{PF}_6]$. A complex in which the zwitterionic ligand is bound to the metal centre via the carbonyl group.

Reaction of the same ligands with rhodium dimers of the form $[\text{Rh}_2\text{Cl}_2(\text{L})_2]$ was also found to produce complexes containing the mixed anhydride ligands coordinated via the phosphorus atom and the double bond. If L is cyclooctadiene, a 1:1 rhodium to ligand reaction produces complexes of the general form, $[\text{Rh}_2\text{Cl}_2(\text{anhydride})_2]$. These are chlorine bridged dimer with the anhydrides bound as described above. With the AAA ligand, if L is ethylene and the reaction is 1:1 or if L is cyclooctadiene and the reaction is 1:2 in favour of the ligand, then the products are $[\text{RhCl}(\text{AAA})_2]$ and $[\text{Rh}_2\text{Cl}_2(\text{AAA})_2(\text{Ph}_2\text{POPPh}_2)]$, the former being a five coordinate square pyramidal complex in which both AAA ligands are bidentate. The later also contained bidentate AAA ligands but also a $\text{Ph}_2\text{POPPh}_2$ ligand bridging the metal centres. This ligand is again thought to be formed by a metal promoted rearrangement.

Similar reactions of DAA, CAA and AAA with $[\text{RuCl}_2(\text{PPh}_3)_4]$ produced complexes in which the ligands are bound via the phosphorus atom

and the oxygen atom of the carbonyl group. These complexes are of the form $[\text{RuCl}_2(\text{PPh}_3)_2(\text{Anhydride})]$. The reactions of the CAA and AAA complexes also produce a second, as yet unidentified, product. Further tdpdp complexes could be isolated from the reactions of tetraphenyldiphosphine monoxide and $[\text{RhCl}(\text{PPh}_3)_4]$, $[\text{RuCl}_2(\text{PPh}_3)_4]$ and $[\text{OsCl}_2(\text{PPh}_3)_4]$ under reflux conditions.

Thus now that it has been shown that bidentate coordination of these mixed anhydrides can be achieved the way is open to study their catalytic properties. The future of this work, in this area will now centre on the reactions of these complexes with simple nucleophiles, in an attempt to gauge their catalytic abilities and also the degree of stereoselectivity it is possible to achieve.

Appendix 1

OBSERVED AND CALCULATED STRUCTURE FACTORS FOR CHA

PAGE 1

H	K	L	FO	FC	H	K	L	FO	FC	H	K	L	FO	FC	H	K	L	FO	FC
3	0	0	53	52	-3	3	0	38	37	6	5	0	36	35	-1	7	1	19	16
4	0	0	57	-56	-2	3	0	73	-73	10	5	0	20	-21	0	7	1	24	26
5	0	0	31	27	0	3	0	131	-120	11	5	0	20	16	-2	10	0	29	-26
6	0	0	22	-20	1	3	0	20	-15	-7	6	0	23	-27	3	10	0	31	-26
-7	1	0	31	-34	2	3	0	48	45	-6	6	0	28	-23	-2	11	0	26	-23
-6	1	0	40	39	3	3	0	65	-61	-3	6	0	18	-16	-1	11	0	28	27
-5	1	0	35	33	4	3	0	120	115	-2	6	0	41	45	3	11	0	25	-25
-4	1	0	87	-89	5	3	0	31	-29	-1	6	0	29	-29	4	11	0	35	33
-3	1	0	123	116	6	3	0	52	50	0	6	0	33	-32	-1	12	0	25	27
-2	1	0	16	18	7	3	0	17	-15	1	6	0	49	51	0	12	0	30	-31
1	1	0	148	-153	8	3	0	36	-41	2	6	0	44	-47	4	12	0	24	15
2	1	0	74	70	9	3	0	22	24	3	6	0	26	28	5	12	0	27	-13
3	1	0	48	49	10	3	0	18	-16	4	6	0	24	-24	0	13	0	24	-20
5	1	0	30	30	-9	4	0	19	18	5	6	0	39	-41	-1	12	1	24	25
6	1	0	64	-62	-5	4	0	30	-24	6	6	0	40	37	-5	11	1	34	-34
7	1	0	44	47	-3	4	0	38	-37	7	6	0	27	-30	-9	10	1	18	18
8	1	0	18	-23	-1	4	0	35	35	9	6	0	24	-22	-5	10	1	47	-43
9	1	0	35	38	0	4	0	21	-21	-6	7	0	35	-33	-4	10	1	52	48
-9	2	0	23	-23	1	4	0	41	41	-5	7	0	33	30	-3	10	1	30	-28
-6	2	0	24	24	2	4	0	46	-44	-2	7	0	31	34	-8	-9	1	30	-30
-5	2	0	28	29	3	4	0	22	-23	-1	7	0	50	-53	-5	-9	1	23	-25
-4	2	0	75	-74	4	4	0	101	94	0	7	0	22	26	-3	-9	1	48	-46
-3	2	0	122	122	5	4	0	111	-108	7	7	0	22	-25	-2	-9	1	29	33
-2	2	0	66	-65	6	4	0	54	50	8	7	0	25	27	2	-9	1	29	-28
-1	2	0	73	-66	7	4	0	20	-17	9	7	0	22	-22	3	-9	1	39	38
0	2	0	33	27	9	4	0	19	13	-6	8	0	25	-18	-8	-8	1	29	-30
1	2	0	45	-44	10	4	0	30	-28	-5	8	0	31	32	-7	-8	1	33	34
2	2	0	85	79	-10	5	0	20	-13	0	8	0	36	34	-2	-8	1	47	52
3	2	0	56	-56	-4	5	0	23	-19	1	8	0	25	-25	-1	-8	1	47	-49
4	2	0	30	-25	-3	5	0	17	-17	3	8	0	27	28	2	-8	1	22	-18
7	2	0	32	35	-2	5	0	32	35	5	8	0	26	18	3	-8	1	29	29
8	2	0	44	-48	0	5	0	59	-61	6	8	0	20	-27	4	-8	1	39	-41
9	2	0	33	34	1	5	0	84	83	7	8	0	20	15	-6	-7	1	19	-21
-10	3	0	20	-20	2	5	0	59	-61	-4	9	0	34	-32	-5	-7	1	25	21
-8	3	0	29	32	3	5	0	28	25	6	9	0	21	-23	-3	-7	1	21	-15
-7	3	0	24	-33	5	5	0	83	-77	7	9	0	30	32	-2	-7	1	55	55

OBSERVED AND CALCULATED STRUCTURE FACTORS FOR CHA

H	K	L	FO	FC	H	K	L	FO	FC	H	K	L	FO	FC	H	K	L	FO	FC	L	FO	FC
5	-8	2	29	-29	-6	-1	2	77	68	6	1	2	37	37	-6	4	2	33	-29	2	33	-29
-10	-7	2	19	-20	-5	-1	2	43	-39	7	1	2	47	-50	-5	4	2	30	-28	2	30	-28
-9	-7	2	31	31	-2	-1	2	56	-57	8	1	2	46	51	-2	4	2	20	-25	2	20	-25
-8	-7	2	18	-19	-1	-1	2	114	109	9	1	2	21	-24	-1	4	2	54	-54	2	54	-54
-7	-7	2	27	29	0	-1	2	155	-162	-7	2	2	17	28	1	4	2	40	-38	2	40	-38
-6	-7	2	25	-29	1	-1	2	37	42	-6	2	2	28	-29	2	4	2	17	23	2	17	23
-5	-7	2	29	23	2	-1	2	96	-93	-5	2	2	50	48	4	4	2	37	-35	2	37	-35
-2	-7	2	30	33	3	-1	2	73	70	-4	2	2	43	40	5	4	2	75	74	2	75	74
0	-7	2	28	-26	4	-1	2	45	44	-3	2	2	134	-133	6	4	2	40	-34	2	40	-34
1	-7	2	39	41	5	-1	2	71	-68	-2	2	2	133	130	10	4	2	26	27	2	26	27
2	-7	2	21	-26	6	-1	2	28	27	-1	2	2	20	-22	-3	5	2	16	18	2	16	18
6	-7	2	29	31	-11	0	2	22	19	0	2	2	64	60	0	5	2	46	44	2	46	44
7	-7	2	18	-21	-7	0	2	18	18	1	2	2	57	58	1	5	2	58	-59	2	58	-59
-9	-6	2	17	14	-6	0	2	22	19	2	2	2	52	-49	2	5	2	37	38	2	37	38
-7	-6	2	30	33	-5	0	2	28	-25	3	2	2	78	75	3	5	2	57	-56	2	57	-56
-6	-6	2	48	-45	-3	0	2	45	44	4	2	2	37	-39	5	5	2	38	40	2	38	40
-5	-6	2	45	47	-2	0	2	70	65	5	2	2	35	37	6	5	2	38	-38	2	38	-38
-3	-6	2	26	-24	-1	0	2	22	23	8	2	2	46	49	8	5	2	20	-27	2	20	-27
-2	-6	2	34	37	0	0	2	166	-173	9	2	2	20	-22	11	5	2	22	-16	2	22	-16
-1	-6	2	62	-64	1	0	2	110	107	-10	3	2	20	21	-7	6	2	24	-28	2	24	-28
0	-6	2	67	67	2	0	2	223	-217	-9	3	2	22	-21	-6	6	2	27	30	2	27	30
7	-6	2	22	65	3	0	2	72	68	-7	3	2	25	29	-2	6	2	32	-35	2	32	-35
-11	-5	2	19	-17	5	0	2	35	-32	-6	3	2	49	-45	-1	6	2	62	67	2	62	67
-10	-5	2	23	17	6	0	2	65	59	-5	3	2	24	21	1	6	2	36	-35	2	36	-35
-6	-5	2	53	-50	7	0	2	30	-32	-2	3	2	53	53	2	6	2	39	40	2	39	40
-5	-5	2	81	76	8	0	2	24	24	-1	3	2	50	-50	6	6	2	28	-23	2	28	-23
-4	-5	2	46	-47	-9	1	2	30	31	-1	3	2	30	30	7	6	2	28	31	2	28	31
-1	-5	2	77	-81	-6	1	2	31	-32	0	3	2	43	43	8	6	2	27	-29	2	27	-29
0	-5	2	75	79	-4	1	2	65	58	1	3	2	60	62	10	6	2	20	-19	2	20	-19
1	-5	2	47	-46	-3	1	2	112	112	3	3	2	74	-73	-6	7	2	28	23	2	28	23
3	-5	2	32	32	-2	1	2	61	-58	4	3	2	67	62	-5	7	2	39	-40	2	39	-40
-9	-4	2	26	-26	-1	1	2	26	27	5	3	2	60	-60	-2	7	2	35	-36	2	35	-36
-6	-4	2	20	-26	0	1	2	50	-50	6	3	2	25	27	-1	7	2	58	57	2	58	57
-5	-4	2	58	56	1	1	2	122	119	7	3	2	25	24	0	7	2	31	-35	2	31	-35
-4	-4	2	141	-130	2	1	2	40	-37	8	3	2	19	22	10	7	2	24	-25	2	24	-25
-3	-4	2	72	71	3	1	2	41	41	-9	4	2	23	-26	-9	7	2	32	-32	2	32	-32

OBSERVED AND CALCULATED STRUCTURE FACTORS FOR CHA

PAGE 4

H	K	L	FO	FC	H	K	L	FO	FC	H	K	L	FO	FC	H	K	L	FO	FC
7	7	2	17	17	-2	-8	3	39	-41	-7	-4	3	21	27	-2	-2	3	84	-78
8	7	2	22	-23	-1	-8	3	38	45	-4	-4	3	21	22	-1	-2	3	67	67
-5	8	2	28	-26	0	-8	3	45	-46	-3	-4	3	83	-86	0	-2	3	233	233
-4	8	2	38	34	-2	-4	3	27	-27	-2	-4	3	77	77	1	-2	3	104	-101
-2	8	2	21	-19	4	-8	3	40	41	-1	-4	3	20	16	2	-2	3	82	81
1	8	2	25	29	-10	-7	3	23	-22	2	-4	3	43	-43	3	-2	3	31	-31
5	8	2	25	-21	-2	-7	3	34	-34	3	-4	3	89	90	4	-2	3	49	-47
6	8	2	18	19	-1	-7	3	43	42	4	-4	3	47	-47	5	-2	3	57	57
7	8	2	26	-28	0	-7	3	101	-107	5	-4	3	33	39	6	-2	3	63	-58
-3	9	2	35	-32	1	-7	3	44	45	6	-4	3	32	-32	7	-2	3	18	19
7	9	2	18	-17	4	-7	3	22	16	8	-4	3	22	25	-12	-1	3	19	-17
-2	10	2	31	34	5	-7	3	33	-33	9	-4	3	24	-26	-10	-1	3	24	25
3	10	2	32	34	-10	-6	3	18	-19	-10	-3	3	33	37	-9	-1	3	31	-34
-1	11	2	30	-29	-7	-6	3	29	34	-9	-3	3	30	-31	-8	-1	3	28	31
4	11	2	31	-28	-5	-6	3	43	-37	-7	-3	3	36	37	-7	-1	3	45	-45
0	12	2	27	21	-4	-6	3	71	72	-6	-3	3	56	-53	-6	-1	3	31	32
1	12	2	30	-25	-3	-6	3	40	-41	-5	-3	3	38	37	-5	-1	3	26	25
0	-12	3	27	23	0	-6	3	58	-60	-4	-3	3	76	-71	-4	-1	3	37	35
-10	-11	3	19	14	1	-6	3	64	67	-3	-3	3	29	28	-3	-1	3	48	47
-5	-11	3	34	32	2	-6	3	32	-35	-2	-3	3	91	88	-2	-1	3	46	-46
-4	-11	3	35	-35	3	-6	3	19	-18	-1	-3	3	18	24	-1	-1	3	88	85
-8	-10	3	18	20	5	-6	3	24	-17	0	-3	3	50	-49	0	-1	3	20	-19
-6	-10	3	22	-23	6	-6	3	39	38	3	-3	3	54	51	1	-1	3	72	-74
-5	-10	3	25	26	-5	-5	3	25	-20	4	-3	3	82	-77	2	-1	3	87	88
-4	-10	3	45	-39	-4	-5	3	88	84	5	-3	3	75	73	3	-1	3	79	-79
-3	-10	3	42	41	-3	-5	3	69	-67	6	-3	3	39	-36	5	-1	3	35	36
-8	-9	3	33	34	-2	-5	3	79	79	9	-3	3	26	-23	6	-1	3	67	-67
-7	-9	3	32	-36	1	-5	3	24	26	10	-3	3	24	22	7	-1	3	35	39
-5	-9	3	28	22	2	-5	3	57	-58	-13	-2	3	21	12	9	-1	3	21	20
-3	-9	3	23	24	3	-5	3	34	34	-10	-2	3	17	18	-9	0	3	30	-30
-2	-9	3	25	-29	7	-5	3	25	-29	-9	-2	3	33	-34	-7	0	3	24	-31
3	-9	3	44	-40	8	-5	3	22	25	-8	-2	3	39	41	-6	0	3	64	64
4	-9	3	27	25	-12	-4	3	20	16	-6	-2	3	49	-43	-3	0	3	38	38
-8	-8	3	23	22	-11	-4	3	24	-22	-5	-2	3	18	20	-2	0	3	90	-87
-7	-8	3	34	-33	-10	-4	3	33	33	-4	-2	3	19	-20	-1	0	3	64	67
-6	-8	3	24	23	-8	-4	3	24	-24	-3	-2	3	48	49	0	0	3	55	-61

OBSERVED AND CALCULATED STRUCTURE FACTORS FOR CHA

PAGE 5

H	K	L	FO	FC	H	K	L	FO	FC	H	K	L	FO	FC	H	K	L	FO	FC	H	K	L	FO	FC
-8	3	3	27	-28	1	6	3	90	-95	-2	10	4	23	21	-4	-5	4	67	66	-7	-2	4	40	43
-5	3	3	62	-57	2	6	3	38	39	4	10	4	38	-31	-3	-5	4	24	-22	-6	-2	4	92	-83
-4	3	3	50	51	4	6	3	22	18	-9	-9	4	18	-19	-1	-5	4	25	25	-4	-2	4	31	-32
-3	3	3	70	-69	6	6	3	33	-26	-6	-9	4	29	-35	1	-5	4	40	45	-2	-2	4	38	-35
-2	3	3	67	69	-4	7	3	45	-41	-5	-9	4	31	26	2	-5	4	38	-40	-1	-2	4	86	-84
0	3	3	121	114	-3	7	3	30	29	-1	-9	4	25	-21	4	-5	4	21	19	0	-2	4	55	57
1	3	3	43	43	0	7	3	23	24	0	-9	4	21	15	7	-5	4	26	-28	1	-2	4	20	-22
2	3	3	65	-61	1	7	3	39	-40	1	-9	4	29	-24	9	-5	4	23	17	4	-2	4	77	-75
3	3	3	71	70	2	7	3	46	52	5	-9	4	24	22	-9	-4	4	28	32	5	-2	4	41	39
4	3	3	59	-55	3	7	3	29	-30	-10	-8	4	25	23	-8	-4	4	20	-24	7	-2	4	20	-21
10	3	3	18	-17	6	7	3	17	-18	-9	-8	4	29	-32	-6	-4	4	47	46	-11	-1	4	18	-17
11	3	3	19	15	7	7	3	31	32	-8	-8	4	19	23	-5	-4	4	45	-42	-6	-1	4	54	-49
-8	4	4	26	-31	8	7	3	21	-23	-7	-8	4	20	-18	-4	-4	4	95	91	-2	-1	4	79	76
-7	4	4	30	33	-3	8	3	45	41	0	-8	4	38	40	-3	-4	4	92	-90	-1	-1	4	136	-144
-2	4	4	40	43	3	8	3	29	-29	1	-8	4	28	-32	-2	-4	4	21	17	0	-1	4	135	144
-1	4	4	38	-42	8	8	3	21	-22	3	-8	4	31	-30	-1	-4	4	48	51	1	-1	4	111	-114
0	4	4	28	31	9	8	3	23	24	-9	-7	4	25	-24	0	-4	4	25	25	3	-1	4	52	-50
1	4	4	20	-21	-2	9	3	29	-23	-8	-7	4	25	26	1	-4	4	23	23	6	-1	4	30	-25
2	4	4	38	-38	4	9	3	34	32	-7	-7	4	27	-32	2	-4	4	46	-45	-7	0	4	26	-27
3	4	4	81	82	5	9	3	40	-33	-6	-7	4	35	40	3	-4	4	49	47	-6	0	4	49	50
4	4	4	121	-114	6	9	3	18	25	-5	-7	4	22	-22	8	-4	4	22	23	-5	0	4	50	48
-7	5	5	29	26	-3	10	3	23	-18	-2	-7	4	26	-29	-12	-3	4	19	13	-4	0	4	68	-69
-6	5	5	32	-27	4	10	3	24	22	-1	-7	4	47	46	-9	-3	4	19	17	-1	0	4	85	-87
-5	5	5	28	-23	5	10	3	28	-26	1	-7	4	42	-43	-8	-3	4	39	-40	0	0	4	59	64
-2	5	5	28	-26	6	10	3	20	24	2	-7	4	30	33	-7	-3	4	25	26	1	0	4	105	-104
-1	5	5	70	-73	0	11	4	25	-25	6	-6	4	29	-25	-6	-3	4	27	-26	2	0	4	67	68
0	5	5	49	52	-4	12	4	31	30	-6	-6	4	46	44	-5	-3	4	42	-42	4	0	4	18	-17
1	5	5	48	-52	1	12	4	23	26	-5	-6	4	44	-44	-3	-3	4	108	101	7	0	4	23	-19
2	5	5	30	30	-3	11	4	31	-30	-2	-6	4	38	-40	-2	-3	4	89	-92	8	0	4	33	36
4	5	5	44	-41	-2	11	4	23	23	-1	-6	4	77	83	-1	-3	4	50	47	8	0	4	26	-31
5	5	5	39	39	3	11	4	25	22	0	-6	4	46	-48	1	-3	4	28	-31	-6	1	4	49	45
-5	6	6	30	29	-7	10	4	21	20	-10	-5	4	22	-19	2	-3	4	90	-93	-4	1	4	52	-53
-4	6	6	25	-25	-6	10	4	24	-32	-9	-5	4	23	23	4	-3	4	54	-51	-3	1	4	73	72
-1	6	6	37	-36	-5	10	4	24	21	-6	-5	4	42	39	11	-3	4	20	13	-2	1	4	104	-102
0	6	6	60	63	-4	10	4	24	-19	-5	-5	4	63	-61	-8	-2	4	23	-26	-1	1	4	33	-35

OBSERVED AND CALCULATED STRUCTURE FACTORS FOR CHA

H	K	L	FO	FC	H	K	L	FO	FC	H	K	L	FO	FC	H	K	L	FO	FC
1	1	4	36	-37	-8	4	4	32	-27	6	7	4	26	-32	-11	-7	5	23	-17
2	1	4	48	49	-6	4	4	22	21	9	7	4	26	-24	-10	-7	5	18	17
4	1	4	35	36	-3	4	4	34	-32	-4	8	4	35	-37	-7	-7	5	17	-18
5	1	4	26	-26	-2	4	4	45	45	-3	8	4	32	27	-4	-7	5	20	-19
7	1	4	33	35	-1	4	4	56	54	4	8	4	22	-15	-1	-7	5	30	-30
8	1	4	43	-47	0	4	4	49	-50	5	8	4	25	19	0	-7	5	82	82
-9	2	4	20	16	2	4	4	37	-34	6	8	4	19	-22	1	-7	5	71	-73
-7	2	4	16	-21	3	4	4	42	42	7	8	4	22	22	5	-7	5	33	35
-6	2	4	25	21	5	4	4	51	-53	-3	9	4	38	35	6	-7	5	26	-21
-5	2	4	32	-30	6	4	4	46	44	-2	9	4	34	-33	-9	-6	5	20	-19
-3	2	4	45	48	-8	5	4	21	-23	3	9	4	30	-27	-7	-6	5	20	-23
-2	2	4	101	-104	-7	5	4	32	38	-2	10	4	24	-23	-6	-6	5	20	17
-1	2	4	34	34	-2	5	4	30	33	-1	10	4	25	25	-4	-6	5	51	-51
1	2	4	38	38	-1	5	4	38	-42	3	10	4	31	-27	-3	-6	5	23	27
2	2	4	40	37	0	5	4	64	-64	4	10	4	33	30	-2	-6	5	71	-71
3	2	4	24	-24	1	5	4	56	57	-1	11	4	24	19	-1	-6	5	24	23
4	2	4	59	60	2	5	4	47	-47	-1	13	5	30	23	0	-6	5	21	23
5	2	4	60	-59	3	5	4	28	30	-5	12	5	29	-25	1	-6	5	48	-49
6	2	4	43	44	6	5	4	54	48	0	12	5	25	-23	2	-6	5	48	52
8	2	4	36	-40	10	5	4	19	14	-6	11	5	19	19	-12	-5	5	18	-14
9	2	4	20	23	-7	6	4	20	22	-4	11	5	41	37	-11	-5	5	25	20
-9	3	4	22	22	-6	6	4	39	-35	-3	11	5	24	-24	-7	-5	5	16	-22
-8	3	4	18	-16	-5	6	4	36	35	-4	10	5	33	32	-5	-5	5	19	-18
-6	3	4	31	28	-3	6	4	18	-15	-3	10	5	43	-38	-4	-5	5	61	-61
-5	3	4	49	-46	-2	6	4	25	27	-8	-9	5	32	-30	-3	-5	5	119	119
-4	3	4	43	44	-1	6	4	67	-69	-7	-9	5	28	29	-2	-5	5	74	-74
-1	3	4	72	76	0	6	4	32	31	-2	-9	5	29	33	0	-5	5	36	-37
1	3	4	38	37	2	6	4	30	-30	1	-9	5	23	-21	1	-5	5	32	-33
2	3	4	38	-36	3	6	4	25	-26	3	-9	5	31	29	2	-5	5	42	46
3	3	4	34	-33	4	6	4	22	-23	4	-9	5	28	-22	3	-5	5	49	-52
4	3	4	96	90	10	6	4	21	20	-7	-8	5	23	25	4	-5	5	24	24
5	3	4	69	-67	-5	7	4	38	38	-6	-8	5	21	-22	8	-5	5	21	-24
6	3	4	44	44	-4	7	4	30	-25	-1	-8	5	57	-58	-11	-4	5	24	21
7	3	4	25	-32	-2	7	4	23	25	0	-8	5	68	69	-10	-4	5	35	-40
9	3	4	26	28	0	7	4	43	42	1	-8	5	27	-26	-9	-4	5	31	32
10	3	4	21	-20	1	7	4	28	-29	4	-8	5	26	-31	-7	-4	5	21	-25

OBSERVED AND CALCULATED STRUCTURE FACTORS FOR CHA

PAGE 7

H	K	L	FO	FC	H	K	L	FO	FC	H	K	L	FO	FC	H	K	L	FO	FC	FO	FC
-9	-1	5	25	28	2	1	5	28	-25	-1	5	5	38	38	3	-9	6	30	28	54	-54
-8	-1	5	33	-39	3	1	5	46	46	0	5	5	63	-68	-9	-8	6	26	23	70	70
-7	-1	5	46	51	5	1	5	71	18	1	5	5	71	73	-8	-8	6	31	-32	70	-69
-6	-1	5	70	-65	6	1	5	24	-32	2	5	5	39	-25	-7	-8	6	30	35	30	-27
-5	-1	5	25	25	7	1	5	27	31	5	5	5	38	-41	-1	-8	6	38	-38	51	52
-3	-1	5	38	-40	9	1	5	17	-14	7	5	5	21	22	0	-8	6	21	-23	56	-57
-2	-1	5	59	60	-9	2	5	31	-31	11	5	5	27	11	1	-8	6	27	31	31	29
-1	-1	5	68	-67	-8	2	5	19	23	-3	6	5	34	-23	6	-8	6	34	30	23	28
2	-1	5	68	-68	-6	2	5	25	-24	0	6	5	20	-48	-12	-7	6	20	13	41	43
3	-1	5	56	56	-5	2	5	64	60	1	6	5	17	86	-9	-7	6	17	18	48	-54
6	-1	5	36	32	-4	2	5	90	-89	2	6	5	48	-48	-6	-7	6	45	-52	28	26
7	-1	5	30	-35	-3	2	5	82	84	-4	7	5	25	28	-2	-7	6	46	47	63	63
8	-1	5	22	27	-2	2	5	59	-60	-3	7	5	40	-38	-1	-7	6	50	-56	19	-20
9	-1	5	18	-17	0	2	5	27	-26	1	7	5	21	26	0	-7	6	30	28	70	-68
-11	0	5	21	-20	2	2	5	34	32	2	7	5	30	-34	-11	-6	6	25	-17	71	66
-6	0	5	33	-36	3	2	5	17	-16	7	7	5	18	-18	-6	-6	6	34	-32	26	-23
-5	0	5	82	78	4	2	5	21	22	8	7	5	21	24	-5	-6	6	74	72	21	18
-4	0	5	32	-34	7	2	5	24	27	-2	8	5	28	29	-4	-6	6	33	-32	46	-49
-3	0	5	50	-49	10	2	5	24	23	3	8	5	28	28	-3	-6	6	25	-26	70	67
-2	0	5	49	51	11	2	5	22	-15	4	8	5	39	-34	-2	-6	6	41	41	31	30
-1	0	5	110	-115	-8	3	5	24	23	5	8	5	41	-42	-1	-6	6	41	-42	39	-41
0	0	5	97	99	-5	3	5	23	22	4	9	5	51	52	0	-6	6	51	52	96	96
1	0	5	51	-48	-4	3	5	40	-40	5	9	5	42	-38	1	-6	6	22	-26	73	-72
2	0	5	29	-26	-3	3	5	67	68	6	9	5	20	29	7	-6	6	17	10	44	46
3	0	5	52	52	-1	3	5	40	44	-3	12	6	24	-20	-9	-5	6	26	-25	46	46
4	0	5	26	-27	3	3	5	90	-88	-10	11	6	21	-16	-8	-5	6	18	19	36	-36
8	0	5	21	25	-2	11	6	24	53	-2	11	6	24	-23	-5	-5	6	68	62	45	-43
10	0	5	24	20	3	4	6	31	-34	3	11	6	26	-21	-4	-5	6	113	-112	22	19
-10	1	5	25	23	-7	4	6	81	85	-6	10	6	31	34	-3	-5	6	87	87	71	73
-9	1	5	28	-27	-1	4	6	39	-40	-4	10	6	36	31	-3	-5	6	49	48	103	-108
-5	1	5	67	67	0	4	6	36	-41	-4	10	6	26	-23	-2	-5	6	30	-32	107	114
-4	1	5	69	-68	3	4	6	67	64	-2	10	6	27	25	-1	-5	6	22	-22	96	-100
-3	1	5	44	42	-8	4	6	45	-41	-9	-9	6	22	-22	1	-5	6	23	-14	23	23
-1	1	5	66	-63	-6	4	6	27	26	-8	-9	6	26	-27	6	-5	6	22	26	24	22
0	1	5	55	58	-5	4	6	27	23	-5	-9	6	36	-31	-8	-4	6	25	33	24	-25
1	1	5	32	-32	2	-9	6	27	-21	2	-9	6	27	-30	-5	-4	6	62	56	33	29

OBSERVED AND CALCULATED STRUCTURE FACTORS FOR CHA

PAGE 8

H	K	L	FO	FC	H	K	L	FO	FC	H	K	L	FO	FC	H	K	L	FO	FC	PAGE
-6	0	6	25	-31	-6	6	6	35	27	-6	-9	7	32	35	5	-5	7	34	32	8
-4	0	6	20	-29	-5	6	6	45	-40	-3	-9	7	24	25	6	-5	7	24	-26	
-3	0	6	23	-29	-1	6	6	33	35	-2	-9	7	26	-22	-10	-4	7	28	30	
-2	0	6	26	25	0	6	6	51	-54	-1	-9	7	24	24	-9	-4	7	36	-37	
0	0	6	47	-45	1	6	6	25	32	0	-9	7	27	-33	-7	-4	7	21	22	
1	0	6	66	69	11	6	6	19	15	4	-9	7	39	38	-6	-4	7	42	-42	
2	0	6	85	-85	-5	7	6	32	-33	-1	-8	7	44	45	-5	-4	7	42	42	
3	0	6	28	29	-4	7	6	36	33	0	-8	7	62	-63	-4	-4	7	29	-29	
5	0	6	24	-21	-2	7	6	24	-30	1	-8	7	52	55	-1	-4	7	21	-20	
6	0	6	30	25	-1	7	6	27	30	5	-8	7	34	-30	0	-4	7	33	-32	
7	0	6	30	-33	0	7	6	24	-24	-11	-7	7	19	14	4	-4	7	57	-54	
10	0	6	19	14	1	7	6	24	28	-10	-7	7	24	-21	5	-4	7	55	52	
-10	1	6	20	17	-4	8	6	34	31	-9	-7	7	18	16	6	-4	7	32	-33	
-7	1	6	18	20	-3	8	6	39	-34	-6	-7	7	21	-26	-13	-3	7	20	15	
-6	1	6	31	-29	-2	8	6	22	13	-2	-7	7	35	34	-10	-3	7	32	30	
-4	1	6	19	21	3	8	6	23	27	0	-7	7	41	-42	-9	-3	7	29	-32	
-3	1	6	61	-58	7	8	6	26	-27	1	-7	7	59	61	-8	-3	7	36	35	
-2	1	6	53	60	-2	9	6	25	17	2	-7	7	27	-29	-6	-3	7	43	-46	
-1	1	6	21	-25	0	9	6	21	22	7	-7	7	24	-17	-5	-3	7	30	29	
0	1	6	80	77	3	9	6	31	30	-6	-6	7	36	-32	-4	-3	7	17	-17	
2	1	6	59	-59	4	9	6	26	-24	-4	-6	7	62	61	-2	-3	7	55	-55	
3	1	6	20	20	-1	11	6	24	-16	-3	-6	7	70	-70	-1	-3	7	20	16	
4	1	6	37	-37	0	11	6	30	28	-2	-6	7	50	49	0	-3	7	31	34	
6	1	6	22	-18	-1	13	7	24	-22	1	-6	7	34	34	1	-3	7	21	-21	
3	1	6	25	27	-4	12	7	28	-27	2	-6	7	54	-56	2	-3	7	27	32	
9	1	6	22	-21	0	12	7	26	21	-11	-5	7	22	-24	3	-3	7	43	-42	
-11	2	6	19	-16	-9	11	7	18	-14	-10	-5	7	33	33	5	-3	7	45	46	
-10	2	6	27	23	-5	11	7	24	20	-9	-5	7	20	-22	6	-3	7	40	-37	
-9	2	6	26	-26	-4	11	7	39	-35	-6	-5	7	21	-20	-12	-2	7	20	-17	
-6	2	6	23	-23	-3	11	7	39	39	-5	-5	7	26	27	-10	-2	7	25	22	
-5	2	6	48	43	-8	10	7	23	24	-3	-5	7	47	-48	-9	-2	7	30	-30	
-3	2	6	39	-36	-3	10	7	49	48	-2	-5	7	78	78	-8	-2	7	29	35	
-2	2	6	70	71	-2	10	7	28	-31	-1	-5	7	47	-48	-7	-2	7	31	-33	
1	2	6	32	-30	3	10	7	24	-18	2	-5	7	44	-44	-6	-2	7	37	35	
3	2	6	19	23	-8	9	7	25	26	3	-5	7	44	44	-2	-2	7	46	-49	
4	2	6	57	-59	-7	9	7	24	-24	4	-5	7	21	-22	-1	-2	7	101	102	

OBSERVED AND CALCULATED STRUCTURE FACTORS FOR CHA

PAGE 9

H	K	L	FO	FC	H	K	L	FO	FC	H	K	L	FO	FC	H	K	L	FO	FC
1	-2	7	64	-64	1	1	7	60	59	-8	-7	8	18	20	-5	-3	8	21	19
2	-2	7	46	46	2	1	7	22	-24	-6	-7	8	26	26	-3	-3	8	30	-28
3	-2	7	54	-52	3	1	7	29	-29	-5	-7	8	41	-41	-1	-3	8	47	-49
6	-2	7	35	-31	10	1	7	19	-14	-2	-7	8	21	-21	0	-3	8	20	25
-12	-1	7	19	-16	11	1	7	20	15	-1	-7	8	44	46	1	-3	8	26	-27
-7	-1	7	18	-17	8	2	7	20	-25	0	-7	8	44	-46	3	-3	8	49	46
-6	-1	7	60	57	-5	2	7	27	-24	1	-7	8	25	21	3	-3	8	42	-41
-5	-1	7	70	-68	-4	2	7	65	64	3	-7	8	22	-26	4	-3	8	37	35
-4	-1	7	30	30	-3	2	7	91	-96	-11	-6	8	24	18	-13	-2	8	19	9
-2	-1	7	58	-60	-2	2	7	74	79	1	-7	8	63	-61	-7	-2	8	25	26
-1	-1	7	103	106	-1	2	7	18	-22	-5	-6	8	78	72	-6	-2	8	41	-36
0	-1	7	48	-51	2	2	7	37	-38	-4	-6	8	26	-30	-5	-2	8	33	34
2	-1	7	49	50	9	2	7	21	22	-3	-6	8	28	28	-4	-2	8	26	-25
7	-1	7	18	22	4	2	7	20	-19	-1	-6	8	36	-35	-1	-2	8	67	-69
10	-1	7	24	-18	8	2	7	18	24	0	-6	8	52	53	0	-2	8	98	103
-11	0	7	20	15	5	2	7	20	15	1	-6	8	18	21	1	-2	8	71	-76
-10	0	7	21	-20	-2	3	7	34	36	-8	-5	8	22	-23	2	-2	8	44	47
-6	0	7	24	21	1	3	7	41	-39	-6	-5	8	21	21	4	-2	8	21	-19
-5	0	7	77	-73	-2	3	7	49	54	-5	-5	8	54	-48	5	-2	8	30	33
-4	0	7	37	33	-1	3	7	61	-63	-4	-5	8	72	68	-3	-1	8	50	52
-3	0	7	18	-5	0	3	7	33	-29	-3	-5	8	68	-66	-2	-1	8	17	12
-2	0	7	21	-24	3	3	7	62	61	-2	-5	8	31	34	-1	-1	8	59	-60
-1	0	7	59	64	4	3	7	55	-55	1	-5	8	19	16	0	-1	8	81	86
0	0	7	81	-81	5	3	7	34	31	2	-5	8	41	-42	1	-1	8	102	-105
1	0	7	59	59	-7	4	7	23	24	3	-5	8	23	16	2	-1	8	54	54
2	0	7	21	20	-6	4	7	32	-24	-8	-4	8	27	-30	6	-1	8	23	-30
6	0	7	30	25	-3	4	7	24	27	-7	-4	8	34	38	7	-1	8	23	24
9	0	7	18	11	-1	4	7	56	-57	-5	-4	8	19	-19	-7	0	8	25	-26
-10	1	7	22	-21	0	4	7	47	48	-4	-4	8	36	36	-6	0	8	40	39
-9	1	7	30	30	1	4	7	21	-25	-3	-4	8	89	-88	-4	0	8	41	-41
-8	1	7	18	-21	2	4	7	21	16	-2	-4	8	38	41	-3	0	8	60	61
-5	1	7	66	-62	4	4	7	36	-35	3	-4	8	45	46	-2	0	8	26	-28
-4	1	7	91	94	5	4	7	47	49	4	-4	8	45	-44	1	0	8	39	-42
-3	1	7	77	-79	-4	5	7	26	-19	8	-3	8	19	-25	2	0	8	61	63
-1	1	7	28	-28	0	5	7	74	77	-7	-3	8	56	60	3	0	8	23	-25
0	1	7	21	-24	1	5	7	46	-49	-6	-3	8	67	-64	7	0	8	25	30

OBSERVED AND CALCULATED STRUCTURE FACTORS FOR CHA

PAGE 10

H	K	L	FO	FC	H	K	L	FO	FC	H	K	L	FO	FC	H	K	L	FO	FC
8	0	8	25	-26	1	4	8	20	21	-7	-10	9	18	19	4	-5	9	32	31
-10	1	8	21	-23	2	4	8	22	-24	-3	-10	9	24	-27	6	-5	9	23	25
-6	1	8	24	19	3	4	8	47	43	-2	-10	9	29	29	-10	-4	9	21	-23
-5	1	8	30	-29	6	4	8	23	24	-1	-10	9	34	-32	-9	-4	9	33	31
-3	1	8	68	70	7	4	8	19	-25	3	-10	9	25	20	-8	-4	9	28	-29
-2	1	8	28	-35	-6	5	8	36	-34	-7	-9	9	18	16	-6	-4	9	30	33
1	1	8	21	22	-5	5	8	41	37	-6	-9	9	25	-31	-5	-4	9	34	-33
3	1	8	43	-43	-1	5	8	32	-37	-2	-9	9	26	28	-4	-4	9	56	54
4	1	8	27	26	0	5	8	42	45	-1	-9	9	37	-42	-3	-4	9	47	-48
6	1	8	28	24	2	5	8	21	-21	0	-9	9	29	29	-1	-4	9	24	21
9	1	8	20	20	7	5	8	20	-18	5	-9	9	31	26	5	-4	9	35	-34
-9	2	8	28	30	-5	6	8	30	25	-5	-8	9	33	34	6	-4	9	28	29
-6	2	8	22	25	-4	6	8	29	-32	-1	-8	9	26	-26	-9	-3	9	22	27
-5	2	8	20	-16	-2	6	8	24	29	0	-8	9	49	47	-8	-3	9	30	-27
-4	2	8	31	34	0	6	8	45	51	1	-8	9	38	-38	-7	-3	9	33	37
-2	2	8	21	-21	1	6	8	47	-48	-10	-7	9	19	19	-5	-3	9	36	-32
-1	2	8	44	45	-4	7	8	29	-18	-9	-7	9	21	-18	-4	-3	9	27	29
0	2	8	22	-23	-3	7	8	33	28	-6	-7	9	21	29	-2	-3	9	35	35
3	2	8	37	-33	1	7	8	24	-26	-3	-7	9	36	37	2	-3	9	42	-40
4	2	8	45	42	7	7	8	21	20	-2	-7	9	20	-21	3	-3	9	34	34
5	2	8	34	-28	-4	8	8	24	-22	0	-7	9	23	24	6	-3	9	26	23
6	2	8	25	29	-3	8	8	30	29	1	-7	9	43	-47	-12	-2	9	24	17
-8	3	8	25	-26	-2	8	8	25	-21	2	-7	9	26	25	-9	-2	9	24	23
-7	3	8	19	19	3	8	8	24	-22	-6	-6	9	30	24	-8	-2	9	29	-34
-6	3	8	27	28	-2	9	8	25	-24	-5	-6	9	31	-25	-7	-2	9	39	44
-4	3	8	21	19	1	9	8	27	18	-3	-6	9	43	45	-2	-2	9	36	36
-3	3	8	45	-45	4	9	8	27	24	-2	-6	9	61	-60	-1	-2	9	53	-54
-2	3	8	25	24	1	11	8	26	19	2	-6	9	37	39	3	-2	9	32	29
2	3	8	34	-35	0	-13	9	25	-22	3	-6	9	19	-17	4	-2	9	31	-28
3	3	8	37	34	-5	-12	9	24	-18	-10	-5	9	22	-22	7	-2	9	17	-18
5	3	8	42	-42	-4	-12	9	33	31	-9	-5	9	26	26	-12	-1	9	20	14
6	3	8	39	36	-3	-12	9	27	-21	-5	-5	9	37	-36	-6	-1	9	26	-28
-8	4	8	25	-20	-4	-11	9	31	30	-4	-5	9	24	24	-5	-1	9	26	29
-7	4	8	29	33	-3	-11	9	35	-34	-2	-5	9	33	-34	-4	-1	9	23	-26
-6	4	8	24	-18	-11	-10	9	18	-7	-1	-5	9	39	35	-3	-1	9	22	22
-1	4	8	24	-28	-8	-10	9	22	-22	3	-5	9	25	-22	-1	-1	9	52	-54

OBSERVED AND CALCULATED STRUCTURE FACTORS FOR CHA

PAGE 11

H	K	L	FO	FC	H	K	L	FO	FC	H	K	L	FO	FC	H	K	L	FO	FC
-6	4	9	37	33	-1	-8	10	33	-33	3	0	10	28	27	-1	12	10	24	4
-5	4	9	43	-43	0	-8	10	31	31	8	0	10	20	16	-5	-12	11	24	16
-1	4	9	24	25	2	-8	10	22	-23	-10	1	10	27	22	-4	-12	11	25	-26
0	4	9	42	-42	4	-8	10	23	-14	-9	1	10	22	-19	-3	-12	11	25	26
1	4	9	28	29	-11	-7	10	24	-16	-5	1	10	34	32	-3	-11	11	27	28
2	4	9	29	-27	-10	-7	10	22	22	-3	1	10	26	-24	-7	-10	11	29	-31
5	4	9	26	-23	-9	-7	10	17	-12	-2	1	10	33	38	-6	-10	11	29	22
-4	5	9	34	34	-7	-7	10	18	21	-1	1	10	28	-32	-1	-9	11	30	33
0	5	9	38	-37	-6	-7	10	19	-20	3	1	10	26	28	0	-9	11	32	-31
1	5	9	55	61	-5	-7	10	46	45	4	1	10	39	-39	-8	-8	11	17	-18
2	5	9	33	-32	-4	-7	10	28	-31	-9	2	10	23	-24	0	-8	11	25	-26
-3	6	9	29	-29	-1	-7	10	22	-29	-4	2	10	26	-25	1	-8	11	35	37
-2	6	9	27	24	0	-7	10	44	46	-3	2	10	28	33	2	-8	11	32	-32
1	6	9	28	31	-10	-6	10	48	-51	2	2	10	28	27	-7	-7	11	18	20
3	6	9	24	22	-6	-6	10	22	23	4	2	10	23	-21	-4	-7	11	23	21
-3	7	9	23	-15	-9	-6	10	25	-27	5	2	10	48	47	-3	-7	11	28	-29
-2	7	9	32	31	-5	-6	10	49	47	6	2	10	25	-24	-2	-7	11	24	20
6	7	9	18	-16	-4	-6	10	67	-63	-8	3	10	20	21	2	-7	11	32	-35
7	7	9	18	6	-3	-6	10	44	46	-2	3	10	29	-31	-11	-6	11	21	-16
5	8	9	25	16	-1	-6	10	22	-16	2	3	10	42	42	-10	-6	11	19	18
7	8	9	21	18	1	-6	10	33	-34	-6	4	10	31	30	-3	-6	11	45	-43
-1	11	9	20	11	-7	-1	10	33	35	-1	4	10	31	34	-2	-6	11	40	38
-2	12	10	25	-23	-8	-5	10	35	36	2	4	10	31	26	3	-6	11	23	24
-9	11	10	19	17	-6	-5	10	26	-22	3	4	10	23	-22	-10	-5	11	19	21
-6	11	10	20	19	-5	-5	10	26	24	6	5	10	25	24	-9	-5	11	23	-20
-9	10	10	20	20	-4	-5	10	64	-63	-5	5	10	26	-27	-8	-5	11	19	19
-8	10	10	19	-15	-3	-5	10	64	65	-1	5	10	30	33	-6	-5	11	25	-27
-6	10	10	18	19	-2	-5	10	33	-33	0	5	10	50	-51	-5	-5	11	23	21
-8	9	10	25	-26	2	-5	10	34	37	-4	6	10	27	23	-4	-5	11	25	-27
-7	9	10	21	20	3	-5	10	29	-28	0	6	10	32	-33	3	-5	11	23	18
1	9	10	29	19	-8	-4	10	20	22	1	6	10	28	25	4	-5	11	26	-26
-12	-8	10	22	12	-7	-4	10	48	-52	-4	7	10	25	20	5	-5	11	27	19
-8	-8	10	20	-20	-3	-4	10	23	17	-3	7	10	27	-27	6	-5	11	24	-23
-7	-8	10	29	-29	-1	-4	10	20	-16	-2	8	10	27	25	-9	-4	11	18	-21
-6	-8	10	36	-41	-3	-4	10	29	29	3	8	10	22	14	-8	-4	11	19	18
5	-8	10	34	30	0	-4	10	53	-54	5	9	10	25	16	-7	-4	11	17	-22

OBSERVED AND CALCULATED STRUCTURE FACTORS FOR CHA

H	K	L	FO	FC	H	K	L	FO	FC	H	K	L	FO	FC	H	K	L	FO	FC
-6	-4	11	24	-24	-3	0	11	52	-49	-3	-11	12	23	16	-1	-3	12	29	-24
-5	-4	11	24	23	1	0	11	24	29	-8	-10	12	26	23	0	-3	12	46	46
-4	-4	11	24	-27	-8	1	11	19	-19	-9	-9	12	21	-15	1	-3	12	48	-45
-3	-4	11	32	30	-7	1	11	20	20	-8	-9	12	19	25	2	-3	12	38	40
-2	-4	11	27	-22	-4	1	11	48	47	-7	-9	12	22	-21	5	-3	12	32	34
3	-4	11	25	-24	-3	1	11	66	-65	-5	-8	12	29	-27	-9	-2	12	20	-17
6	-4	11	30	-27	-2	1	11	59	61	-1	-8	12	22	22	0	-2	12	34	34
-9	-3	11	19	-19	-1	1	11	22	-26	0	-8	12	36	-36	1	-2	12	74	-75
-8	-3	11	25	24	3	1	11	41	44	1	-8	12	25	25	2	-2	12	43	46
-7	-3	11	38	-41	-7	2	11	19	27	-5	-7	12	29	-28	3	-2	12	28	-23
-3	-3	11	24	26	-3	2	11	24	-23	-4	-7	12	42	45	-6	-1	12	34	31
-2	-3	11	37	-40	-2	2	11	54	55	-3	-7	12	35	-30	-2	-1	12	31	-37
-1	-3	11	25	22	-1	2	11	31	-31	0	-7	12	39	-41	1	-1	12	48	-56
3	-3	11	34	-36	1	2	11	26	-17	1	-7	12	34	35	2	-1	12	55	54
6	-3	11	32	-27	3	2	11	33	33	-9	-6	12	23	20	7	-1	12	18	14
-12	-2	11	19	-14	4	2	11	41	-40	-4	-6	12	57	56	8	-1	12	18	-13
-8	-2	11	18	23	5	2	11	28	29	-3	-6	12	62	-62	-10	0	12	18	-12
-7	-2	11	22	-28	-7	3	11	21	19	-2	-6	12	32	33	-5	0	12	33	-33
-6	-2	11	50	49	-6	3	11	34	-31	1	-6	12	32	35	-3	0	12	27	28
-5	-2	11	30	-28	-5	3	11	28	26	-7	-5	12	22	27	-2	0	12	41	-42
-2	-2	11	21	-26	-1	3	11	35	-36	-4	-5	12	35	36	-1	0	12	27	28
-1	-2	11	47	46	0	3	11	26	28	-3	-5	12	52	-51	3	0	12	31	-33
0	-2	11	46	-48	4	3	11	30	-26	-2	-5	12	42	42	4	0	12	26	22
3	-2	11	23	-18	5	3	11	23	25	-1	-5	12	21	-20	-9	1	12	20	21
-11	-1	11	19	17	-4	4	11	25	-26	2	-5	12	22	-24	-1	1	12	24	23
-6	-1	11	31	-43	-3	4	11	29	27	3	-5	12	25	21	5	1	12	19	-27
-5	-1	11	44	33	0	4	11	47	47	4	-4	12	40	40	7	2	12	21	21
-4	-1	11	34	-34	1	4	11	52	-55	-7	-4	12	28	-25	-9	2	12	19	-19
-2	-1	11	22	-34	-2	5	11	22	-23	-6	-4	12	43	42	-8	2	12	33	-29
-1	-1	11	35	-39	-1	5	11	27	-41	-2	-4	12	27	-28	-4	2	12	23	17
0	-1	11	33	36	2	5	11	23	-28	4	-4	12	25	-25	-8	3	12	24	-21
1	0	11	19	21	3	5	11	23	-28	5	-4	12	33	28	1	3	12	23	18
-9	0	11	22	24	-6	6	11	28	14	5	-4	12	27	-26	-4	5	12	25	-19
-7	0	11	39	-37	-3	6	11	22	-18	-7	-3	12	32	-30	2	6	12	25	19
-5	0	11	5	-37	-2	6	11	22	-28	-6	-3	12	32	-30	6	6	12	25	19

OBSERVED AND CALCULATED STRUCTURE FACTORS FOR CHA

H	K	L	FO	FC	H	K	L	FO	FC	H	K	L	FO	FC	H	K	L	FO	FC	H	K	L	FO	FC
-6	-4	13	24	20	5	2	13	28	-26	2	-2	14	29	-29	-5	-7	15	23	18	-6	-4	16	29	-25
-3	-4	13	27	-29	0	3	13	29	-29	3	-2	14	30	22	-10	-6	15	19	20	0	-4	16	32	-29
2	-4	13	22	-17	1	3	13	33	36	-5	-1	14	23	22	-8	-6	15	20	12	-2	-3	16	22	-14
3	-4	13	29	22	5	3	13	29	-29	-2	-1	14	24	23	-1	-6	15	23	-17	0	-3	16	27	24
-8	-3	13	29	-27	1	4	13	38	35	-1	-1	14	24	-24	-9	-5	15	20	-23	1	-3	16	38	-41
-7	-3	13	32	31	2	4	13	34	-32	0	-1	14	30	28	-8	-5	15	24	24	-6	-2	16	30	28
-6	-3	13	33	-28	3	4	13	23	21	2	-1	14	24	-23	-8	-4	15	28	27	-6	-1	16	25	20
-1	-3	13	24	-25	2	5	13	27	-24	3	-1	14	23	23	-7	-4	15	18	17	0	4	16	27	25
3	-3	13	28	27	3	5	13	24	20	-4	0	14	35	-26	-7	-3	15	18	17	-9	-6	17	19	21
4	-3	13	26	-29	-4	-11	14	25	14	-2	0	14	32	-34	-7	-3	15	23	-22	-8	-5	17	21	-15
-8	-2	13	21	-20	-8	-10	14	20	-19	-1	0	14	35	-17	-6	-3	15	32	30	-8	-4	17	19	-19
-7	-2	13	19	-12	0	-9	14	23	18	5	0	14	25	14	0	-3	15	31	-35	-6	-4	17	26	-18
-6	-2	13	43	-42	-5	-8	14	29	26	-9	1	14	19	-17	-5	-2	15	32	-32	-6	-3	17	24	-17
-5	-2	13	25	27	-4	-8	14	29	-23	-8	1	14	23	18	0	-2	15	26	-27	0	-3	17	32	31
-1	-2	13	26	-25	-4	-7	14	35	-36	-5	1	14	24	29	1	-2	15	27	26	-4	-2	17	23	-16
0	-2	13	55	60	-4	-6	14	25	-28	-4	1	14	29	-28	-4	-1	15	22	22	1	-2	17	22	-19
-7	-1	13	17	-17	-3	-6	14	39	40	-1	1	14	30	-29	-3	-1	15	25	-20	-4	-1	17	27	-28
-5	-1	13	32	31	3	-6	14	22	-21	-8	2	14	22	21	-4	0	15	23	19	-1	1	17	24	19
-4	-1	13	38	-40	-3	-5	14	23	24	-2	2	14	23	-25	-3	0	15	43	-43	1	3	17	24	19
-3	-1	13	32	27	-2	-5	14	30	-34	-1	3	14	23	23	-2	0	15	30	35	2	4	17	25	-16
0	-1	13	45	46	4	-5	14	23	25	4	3	14	25	17	2	0	15	29	-28	-5	-8	18	24	13
1	-1	13	47	-49	-7	-4	14	19	-19	-6	4	14	24	20	-3	1	15	31	-31	-4	-8	18	23	-18
-8	0	13	21	23	-6	-4	14	42	35	-4	4	14	22	13	-2	1	15	31	29	-3	-7	18	23	26
-4	0	13	48	-48	-4	-4	14	25	17	-1	4	14	24	22	5	2	15	28	19	-2	-6	18	28	-23
-3	0	13	60	61	-1	-4	14	27	25	0	4	14	26	-23	1	4	15	24	-21	0	-4	18	23	-15
-8	1	13	21	21	0	-4	14	28	-33	-4	5	14	24	21	2	5	15	23	19	-4	-6	19	23	-17
-4	1	13	22	-26	-5	-3	14	25	-29	0	5	14	25	-27	-7	-10	16	21	-17	-3	-6	19	27	13
-3	1	13	42	41	-1	-3	14	28	26	1	5	14	28	23	-4	-10	16	23	-4	-5	-4	19	24	-8
-2	1	13	36	-38	0	-3	14	34	-35	-4	6	14	25	21	-4	-8	16	25	24	0	-3	19	24	-21
1	1	13	26	28	1	-3	14	39	39	-3	6	14	24	-18	-4	-7	16	40	38	1	-2	19	25	17
-7	2	13	18	-16	3	-3	14	24	23	1	8	14	25	-10	-3	-7	16	27	-25	-4	-1	19	25	17
-1	2	13	23	22	-7	-2	14	19	19	1	-9	15	27	24	-8	-6	16	19	-13	-3	0	19	24	-17
1	2	13	28	29	-6	-2	14	25	-19	-9	-8	15	19	11	-3	-6	16	33	-33	0	-2	22	24	6
4	2	13	38	32	1	-2	14	52	53	1	-8	15	23	19	-2	-6	16	24	21	-2	0	22	24	6

Appendix 11

OBSERVED AND CALCULATED STRUCTURE FACTORS FOR DJC.DAT

PAGE 1

H	K	L	10FO	10FC	H	K	L	10FO	10FC	H	K	L	10FO	10FC	H	K	L	10FO	10FC	H	K	L	10FO	10FC	PAGE	
2	0	0	2135	-2204	4	5	0	508	517	11	10	0	480	-482	5	21	0	562	-607	3	2	1	1115	955	1	
4	0	0	1190	-1126	5	5	0	2135	2181	3	11	0	0	787	798	0	22	0	589	594	4	1	1	598	608	1
6	0	0	694	-695	7	5	0	623	-662	4	11	0	0	576	560	6	23	0	576	-500	5	1	1	438	-489	1
10	0	0	721	764	9	5	0	468	474	5	11	0	0	520	-512	-15	0	1	592	-664	6	1	1	558	-564	1
12	0	0	456	-449	0	6	0	1448	-1519	9	11	0	0	420	-299	-9	0	1	727	-659	8	1	1	397	-359	1
1	1	0	1567	-1696	2	6	0	334	-301	11	11	0	0	546	-555	-3	0	1	771	-698	10	1	1	680	637	1
2	1	0	907	-792	5	6	0	900	-891	13	11	0	0	680	616	-1	0	1	2191	2035	12	1	1	866	-958	1
3	1	0	1223	1178	6	6	0	362	-398	0	12	0	0	1972	2028	1	0	1	3262	-3087	-13	1	1	624	622	1
11	1	0	566	-601	7	6	0	489	-501	1	12	0	0	558	585	3	0	1	1949	1929	-11	1	1	750	-797	1
13	1	0	632	614	8	6	0	742	781	2	12	0	0	1135	-1233	5	0	1	1657	-1635	-10	1	1	763	-766	1
1	2	0	3025	2859	9	6	0	566	633	4	12	0	0	507	479	9	0	1	694	696	-9	1	1	434	373	1
2	2	0	382	390	10	6	0	481	-574	9	12	0	0	541	-559	11	0	1	1461	-1449	-5	1	1	1616	-1530	1
3	2	0	469	-415	1	7	0	670	670	10	12	0	0	552	626	13	0	1	542	531	-3	1	1	3552	3571	1
4	2	0	2335	2080	3	7	0	1702	-1611	11	12	0	0	499	513	-12	1	1	660	-608	-2	1	1	490	431	1
5	2	0	958	950	6	7	0	1000	-1094	2	13	0	0	721	-784	-11	1	1	518	-467	-1	1	1	1046	-838	1
6	2	0	771	-789	7	7	0	1469	1488	4	13	0	0	760	746	-10	1	1	493	495	0	1	1	1041	-965	1
9	2	0	846	-808	7	7	0	553	-592	5	13	0	0	479	511	-8	1	1	522	-566	2	1	1	326	-292	1
11	2	0	982	1024	8	7	0	572	-539	12	13	0	0	549	-601	-6	1	1	698	-655	9	1	1	811	-825	1
2	3	0	370	-435	9	7	0	558	575	1	14	0	0	1105	1062	-5	1	1	1452	1462	10	1	1	545	-548	1
3	3	0	520	516	0	8	0	604	-489	7	14	0	0	446	503	-4	1	1	1351	1352	15	1	1	467	-346	1
4	3	0	1415	1402	1	8	0	1823	-1747	9	14	0	0	621	-567	-3	1	1	460	279	-16	1	1	536	526	1
6	3	0	664	-657	4	8	0	506	501	10	14	0	0	595	-495	-2	1	1	1808	-1691	-14	1	1	450	-395	1
12	3	0	818	-847	6	8	0	419	373	11	14	0	0	611	690	-1	1	1	2196	-2345	-9	1	1	820	882	1
14	3	0	661	573	2	9	0	1125	1142	6	15	0	0	463	-330	0	1	1	2000	1977	-7	1	1	367	-394	1
0	4	2	1010	-978	3	9	0	636	715	0	16	0	0	1115	-1132	2	1	1	422	441	-6	1	1	1674	1736	1
1	4	0	1898	1787	4	9	0	602	-589	2	16	0	0	536	563	4	1	1	1473	1410	-5	1	1	1382	1350	1
2	4	0	862	-864	5	9	0	1175	-1166	6	16	0	0	445	-576	7	1	1	447	421	-4	1	1	1300	-1356	1
3	4	0	496	-539	12	9	0	692	729	8	16	0	0	499	449	12	1	1	474	421	-3	1	1	1291	-1305	1
5	4	0	776	-698	14	9	0	548	-476	12	16	0	0	545	419	14	1	1	462	-358	-2	1	1	457	-400	1
6	4	0	516	-507	15	9	0	571	-465	3	17	0	0	593	-508	-10	2	1	783	839	-1	1	1	733	709	1
8	4	0	714	783	0	10	0	782	815	5	17	0	0	748	749	-8	2	1	1246	-1312	0	1	1	278	242	1
10	4	0	931	-913	1	10	0	707	-723	1	18	0	0	450	-479	-7	2	1	360	426	1	1	1	769	730	1
11	4	0	580	536	2	10	0	1122	-1099	3	18	0	0	708	807	-5	2	1	881	-897	3	1	1	486	-483	1
1	5	0	516	-436	3	10	0	871	850	7	18	0	0	474	-425	-3	2	1	566	-459	4	1	1	359	321	1
2	5	0	1271	-1284	4	10	0	810	847	1	20	0	0	637	-707	0	2	1	2543	2698	5	1	1	461	445	1
3	5	0	1664	-1635	7	10	0	580	463	6	20	0	0	534	482	2	2	1	1121	-1038	6	1	1	389	-376	1

OBSERVED AND CALCULATED STRUCTURE FACTORS FOR DJC.DAT

PAGE 2

H	K	L	10FO	10FC	H	K	L	10FO	10FC	H	K	L	10FO	10FC	H	K	L	10FO	10FC	H	K	L	10FO	10FC
11	4	1	852	788	7	7	1	977	-940	0	10	1	389	-423	3	13	1	447	495	-1	19	1	589	627
13	4	1	460	-521	8	7	1	911	914	1	10	1	1206	-1227	4	13	1	551	679	1	19	1	427	-292
-5	5	1	416	-386	-16	8	1	603	-583	2	10	1	1026	1072	7	13	1	674	692	7	19	1	469	-439
-4	5	1	1384	-1793	-14	8	1	545	495	3	10	1	1051	1056	9	13	1	718	-750	3	20	1	592	493
-3	5	1	779	785	-8	8	1	574	568	5	10	1	627	-632	-10	14	1	652	625	-2	21	1	579	-538
-2	5	1	1923	1951	-6	8	1	1029	-1001	6	10	1	365	-214	-8	14	1	756	-773	5	21	1	454	-412
-1	5	1	1254	1217	-4	8	1	1330	1250	7	10	1	454	442	-6	14	1	597	570	6	21	1	539	576
0	5	1	2105	-2005	0	8	1	582	-531	11	10	1	446	-468	0	14	1	401	537	-6	22	1	490	436
1	5	1	529	-581	2	8	1	754	733	12	10	1	537	570	1	14	1	523	542	-3	22	1	465	347
4	5	1	540	484	4	8	1	493	-529	-12	11	1	733	-725	2	14	1	577	-678	1	22	1	516	-494
5	5	1	633	-580	5	8	1	1049	-1059	-10	11	1	589	462	3	14	1	555	-569	5	23	1	552	-476
6	5	1	1191	-1212	6	8	1	898	924	-5	11	1	460	-470	10	14	1	514	538	-14	0	2	611	644
7	5	1	609	614	7	8	1	448	-362	-4	11	1	849	857	12	14	1	595	-674	-12	0	2	522	-445
8	5	1	1139	1158	10	8	1	490	-571	-3	11	1	508	-497	-4	15	1	429	-340	-8	0	2	1293	1388
10	5	1	734	-770	12	8	1	670	645	-2	11	1	1201	-1287	-2	15	1	618	550	-4	0	2	827	-849
-15	6	1	604	652	-11	9	1	562	541	0	11	1	1724	1701	-1	15	1	633	-785	-2	0	2	702	-684
-9	6	1	774	786	-5	9	1	573	612	2	11	1	549	-589	0	15	1	659	-744	0	0	2	981	892
-7	6	1	843	-918	-4	9	1	574	612	3	11	1	583	600	7	15	1	494	531	2	0	2	2752	-2407
-5	6	1	2114	2244	-3	9	1	1825	-1776	5	11	1	520	-490	-7	16	1	779	-786	6	0	2	1037	959
-4	6	1	490	452	-2	9	1	500	-414	7	11	1	651	539	-5	16	1	843	870	8	0	2	378	-432
-3	6	1	1171	-1133	-1	9	1	1798	1813	8	11	1	421	-462	2	16	1	526	514	12	0	2	684	670
3	6	1	603	-622	0	9	1	593	558	10	11	1	538	517	5	16	1	596	582	14	0	2	452	-442
4	6	1	680	-672	1	9	1	1346	-1401	-8	12	1	451	-577	11	16	1	495	595	-11	1	2	433	525
8	6	1	378	357	2	9	1	592	-614	-6	12	1	407	581	-9	17	1	507	-407	-10	1	2	924	973
9	6	1	438	-450	4	9	1	442	-478	-4	12	1	677	-645	-4	17	1	987	-934	-9	1	2	943	-979
11	6	1	458	437	5	9	1	516	-452	1	12	1	1079	-1021	-3	17	1	462	-428	-8	1	2	901	-933
-5	7	1	1630	1527	6	9	1	998	1010	2	12	1	727	-738	-2	17	1	648	651	-7	1	2	367	297
-4	7	1	487	-535	8	9	1	458	-470	3	12	1	820	838	-1	17	1	465	561	-4	1	2	469	-471
-3	7	1	1503	-1456	9	9	1	504	644	4	12	1	719	685	-2	17	1	752	-720	-2	1	2	307	300
-2	7	1	1576	1487	-15	10	1	617	-465	11	12	1	938	-901	-1	17	1	502	-464	-1	1	2	1861	1687
-1	7	1	927	845	-13	10	1	458	395	12	12	1	566	-553	-2	18	1	440	351	0	1	2	1735	1733
0	7	1	1365	-1304	-8	10	1	407	-213	-11	13	1	529	-611	2	18	1	652	643	1	1	2	1303	-1060
1	7	1	1360	-1624	-7	10	1	388	407	-3	13	1	539	565	4	18	1	753	-777	3	1	2	947	958
2	7	1	687	-665	-6	10	1	371	310	-2	13	1	709	-705	-8	19	1	458	-436	5	1	2	479	-500
4	7	1	430	417	-5	10	1	570	-596	-1	13	1	738	-806	-5	19	1	546	573	8	1	2	538	-570
5	7	1	580	592	-3	10	1	452	447	0	13	1	596	695	-3	19	1	865	-804	9	1	2	635	662

H	K	L	10FO	10FC	H	K	L	10FO	10FC	H	K	L	10FO	10FC	H	K	L	10FO	10FC	H	K	L	10FO	10FC
10	1	2	748	736	-11	4	2	441	399	-3	6	2	1096	-1137	11	8	2	483	316	-4	12	2	715	830
11	1	2	891	-940	-7	4	2	412	505	-2	6	2	1964	1956	15	8	2	545	504	-3	12	2	513	550
-11	2	2	399	-476	-6	4	2	555	646	0	6	2	799	-752	-8	9	2	468	469	-1	12	2	703	-755
-8	2	2	436	-483	-5	4	2	2485	-2519	1	6	2	683	672	-2	9	2	1145	1119	3	12	2	1030	1102
-6	2	2	1642	-1688	-4	4	2	1925	-1947	2	6	2	323	-293	-1	9	2	684	693	5	12	2	448	-473
-5	2	2	1709	-1755	-3	4	2	1696	1735	4	6	2	435	461	0	9	2	1477	-1461	7	12	2	650	682
-4	2	2	3018	3180	-2	4	2	551	-509	6	6	2	1295	-1296	1	9	2	742	-699	9	12	2	476	-505
-3	2	2	2851	2769	-1	4	2	649	595	7	6	2	539	379	2	9	2	438	383	-12	13	2	495	-577
-2	2	2	1124	-1128	0	4	2	813	808	8	6	2	866	895	4	9	2	639	-636	-10	13	2	611	702
-1	2	2	721	728	1	4	2	1820	1709	16	6	2	489	-465	5	9	2	554	-539	-8	13	2	811	-870
0	2	2	1341	-1140	2	4	2	578	610	-11	7	2	436	-259	8	9	2	668	670	-4	13	2	518	-534
1	2	2	713	-725	4	4	2	674	701	-8	7	2	510	549	10	9	2	628	-655	-3	13	2	398	-443
2	2	2	439	-309	5	4	2	520	-629	-7	7	2	576	-545	12	9	2	573	397	-1	13	2	437	498
3	2	2	530	491	6	4	2	986	-1022	-5	7	2	612	556	-12	10	2	541	-460	0	13	2	680	722
5	2	2	1017	-1009	7	4	2	680	695	-4	7	2	393	-329	-6	10	2	807	-814	7	13	2	430	-431
6	2	2	507	539	8	4	2	399	349	-2	7	2	1784	1579	-4	10	2	1510	1471	2	13	2	466	-298
7	2	2	569	544	15	4	2	486	-427	0	7	2	1189	-1085	-3	10	2	685	-707	10	13	2	813	813
11	3	2	530	-490	-13	5	2	548	555	1	7	2	579	-634	-2	10	2	1303	-1495	12	13	2	642	-516
-12	3	2	707	-688	-11	5	2	464	-458	3	7	2	563	643	1	10	2	751	743	-5	14	2	662	-647
-11	3	2	788	-796	-7	5	2	1225	-1283	4	7	2	552	-497	2	10	2	629	682	-3	14	2	988	1042
-10	3	2	495	486	-5	5	2	1137	1115	6	7	2	466	-459	4	10	2	928	-908	2	14	2	446	-562
-9	3	2	917	1034	-4	5	2	417	356	7	7	2	547	631	5	10	2	865	-842	4	14	2	580	733
-8	3	2	987	-990	-3	5	2	799	783	8	7	2	651	673	6	10	2	735	766	7	14	2	436	493
-6	3	2	1463	1505	-2	5	2	718	736	9	7	2	941	-881	8	10	2	588	-648	-12	15	2	540	-288
-5	3	2	468	458	0	5	2	1274	-1330	10	7	2	574	-400	-7	11	2	715	704	-11	15	2	573	-658
-3	3	2	790	-778	1	5	2	438	439	11	7	2	461	415	-5	11	2	523	-480	-9	15	2	934	918
-2	3	2	1034	-962	2	5	2	1203	1259	-15	8	2	803	636	-3	11	2	706	-709	-7	15	2	478	-503
0	3	2	2603	2307	4	5	2	370	-369	-13	8	2	569	-491	-1	11	2	1337	1369	-6	15	2	834	833
1	3	2	2347	2099	7	5	2	1010	1058	-7	8	2	686	-727	1	11	2	1495	-1424	-2	15	2	834	-767
8	3	2	1041	-1000	8	5	2	749	-765	-5	8	2	1463	1487	2	11	2	424	-439	-1	15	2	701	-765
9	3	2	438	-395	9	5	2	1324	-1317	-3	8	2	1824	-1682	3	11	2	382	409	1	15	2	1075	1170
10	3	2	1221	1226	11	5	2	748	805	-1	8	2	732	702	6	11	2	434	447	3	15	2	442	-500
11	3	2	740	686	-14	6	2	639	-542	1	8	2	643	-636	9	11	2	826	834	4	15	2	462	495
12	3	2	645	-626	-6	6	2	1384	1379	2	8	2	759	-697	11	11	2	694	-633	6	15	2	466	486
-15	4	2	563	-577	-5	6	2	856	851	5	8	2	1212	1248	-7	12	2	584	574	7	15	2	581	590
-13	4	2	475	426	-4	6	2	2112	-2242	7	8	2	1320	-1343	-5	12	2	598	-627	-	15	2	804	-794

OBSERVED AND CALCULATED STRUCTURE FACTORS FOR DJC.DAT

H	K	L	10FO	10FC	H	K	L	10FO	10FC	H	K	L	10FO	10FC	H	K	L	10FO	10FC	H	K	L	10FO	10FC
9	15	2	556	-476	-7	1	3	1099	1091	-4	3	3	1160	-1091	-1	5	3	522	477	-12	8	3	475	420
10	15	2	525	532	-6	1	3	375	-448	-3	3	3	1119	997	0	5	3	923	-873	-10	8	3	641	-552
-6	16	2	537	485	-5	1	3	381	-321	-1	3	3	732	-618	1	5	3	726	702	-8	8	3	818	763
-5	16	2	775	-639	-4	1	3	969	959	0	3	3	987	839	2	5	3	533	-518	-6	8	3	475	467
-4	16	2	484	-536	-3	1	3	622	-537	1	3	3	637	-568	3	5	3	630	-611	-5	8	3	585	545
-3	16	2	660	768	-2	1	3	415	337	3	3	3	1082	1085	4	5	3	1008	1065	-4	8	3	1343	-1232
3	16	2	433	-456	-1	1	3	343	-355	5	3	3	973	-978	6	5	3	675	-670	-3	8	3	1300	-1311
4	16	2	455	609	0	1	3	701	-641	6	3	3	365	-178	8	5	3	404	-349	-2	8	3	1542	1395
6	16	2	699	-735	1	1	3	665	-715	9	3	3	461	431	10	5	3	493	504	-1	8	3	622	590
-4	17	2	494	-528	2	1	3	1614	1573	11	3	3	910	-892	12	5	3	470	-348	0	8	3	532	-502
-2	17	2	677	598	3	1	3	974	958	12	3	3	451	-363	13	5	3	687	553	1	8	3	789	-723
0	17	2	695	-723	4	1	3	707	-722	13	3	3	513	490	-9	6	3	643	588	3	8	3	532	547
2	17	2	844	880	5	1	3	642	-667	15	3	3	473	-356	-7	6	3	744	-746	6	8	3	1369	-1296
4	17	2	548	-588	6	1	3	568	597	-11	4	3	585	-668	-5	6	3	906	-894	8	8	3	1165	1152
-5	18	2	819	801	10	1	3	658	-718	-9	4	3	580	-597	-4	6	3	1197	-1116	9	8	3	483	-363
-4	18	2	732	-700	11	1	3	492	-465	-7	4	3	517	-449	0	6	3	975	1072	-14	9	3	646	541
0	19	2	482	-543	12	1	3	569	611	-6	4	3	380	-306	-3	6	3	693	-668	-7	9	3	951	-931
2	19	2	582	591	-12	2	3	434	-408	-5	4	3	887	858	2	6	3	1348	1328	-5	9	3	974	972
3	19	2	546	550	-10	2	3	1056	1071	-4	4	3	1167	-1154	5	6	3	744	-857	-3	9	3	497	-558
-5	20	2	479	391	-8	2	3	799	-909	-2	4	3	1226	1194	7	6	3	1995	2151	-2	9	3	453	393
-3	20	2	475	-422	-6	2	3	902	852	-1	4	3	639	583	9	6	3	955	-930	0	9	3	444	-426
-9	21	2	564	-466	-5	2	3	1018	1074	0	4	3	685	688	-8	7	3	998	-949	1	9	3	1121	1032
-2	22	2	498	-474	-3	2	3	602	-639	3	4	3	637	-579	-7	7	3	472	-597	3	9	3	828	-884
-13	0	3	533	-508	-2	2	3	913	-818	5	4	3	1406	1465	-6	7	3	1314	1172	4	9	3	789	-810
-11	0	3	1076	1046	0	2	3	1569	1477	6	4	3	761	783	-5	7	3	1808	1769	5	9	3	560	547
-9	0	3	1031	-1122	1	2	3	850	-766	7	4	3	1419	-1386	-4	7	3	768	-730	6	9	3	720	685
-7	0	3	610	574	2	2	3	613	571	8	4	3	621	-629	-2	7	3	801	754	-9	10	3	598	-559
-5	0	3	470	-527	4	2	3	599	-590	9	4	3	526	545	-1	7	3	682	-606	-8	10	3	523	519
-3	0	3	2032	-1823	5	2	3	482	471	11	4	3	499	492	0	7	3	936	-874	-5	10	3	746	721
-1	0	3	2214	1962	6	2	3	905	894	-16	5	3	445	-344	1	7	3	349	389	-3	10	3	625	-597
1	0	3	1373	-1311	-14	2	3	843	-913	-14	5	3	1212	-1191	2	7	3	572	582	-1	10	3	849	963
7	0	3	629	-666	-8	2	3	907	961	8	5	3	1439	-1520	3	7	3	376	-404	0	10	3	456	-460
9	0	3	1054	1104	10	2	3	853	786	-6	5	3	2203	2249	5	7	3	1626	1575	1	10	3	685	-701
11	0	3	721	-731	-10	3	3	493	-533	-5	5	3	668	-764	6	7	3	854	-809	2	10	3	371	-374
-9	1	3	1603	-1714	-7	3	3	728	776	-4	5	3	1439	-1520	9	7	3	579	-534	5	10	3	394	380
-8	1	3	550	595	-5	3	3	2207	-2308	-3	5	3	1167	1103	-14	8	3	588	-477	7	10	3	1165	-1112

OBSERVED AND CALCULATED STRUCTURE FACTORS FOR DJC.DAT

PAGE 5

H	K	L	10FO	10FC	H	K	L	10FO	10FC	H	K	L	10FO	10FC	H	K	L	10FO	10FC	H	K	L	10FO	10FC
-8	11	3	730	738	-10	15	3	546	485	8	0	4	531	554	-6	3	4	684	-762	0	5	4	298	-295
-6	11	3	774	-787	-8	15	3	744	-714	10	0	4	640	-715	-4	3	4	809	825	3	5	4	977	1031
-4	11	3	549	619	-7	15	3	573	577	-11	1	4	681	670	-1	3	4	823	-787	4	5	4	380	-284
-3	11	3	795	838	-5	15	3	832	-838	-9	1	4	694	-610	0	3	4	745	747	5	5	4	1879	-1932
0	11	3	625	-665	-4	15	3	453	-425	-8	1	4	432	374	1	3	4	1366	-1315	6	5	4	1209	1208
2	11	3	1094	1096	2	15	3	563	-553	-5	1	4	1108	1081	2	3	4	378	364	7	5	4	1451	1530
4	11	3	869	-939	4	15	3	494	497	-1	1	4	1662	-1521	3	3	4	693	691	-8	6	4	977	-1019
6	11	3	445	427	10	15	3	463	401	1	1	4	938	-907	4	3	4	1049	-1118	-6	6	4	777	793
12	11	3	597	574	12	15	3	515	-512	2	1	4	707	685	6	3	4	1514	1598	-5	6	4	421	397
-12	12	3	531	-478	-9	16	3	515	474	3	1	4	917	-888	8	3	4	746	-753	-3	6	4	501	517
-11	12	3	444	533	-3	16	3	642	704	4	1	4	753	-689	-12	4	4	502	-509	-2	6	4	945	-927
-9	12	3	547	-576	-1	16	3	547	-585	5	1	4	1008	1089	-10	4	4	616	618	0	6	4	525	-538
-2	12	3	668	-635	0	16	3	770	-752	6	1	4	970	940	-9	4	4	486	-514	1	6	4	1857	1763
-1	12	3	679	625	6	16	3	490	434	7	1	4	601	-658	-8	4	4	1149	-1217	3	6	4	806	-847
0	12	3	326	325	7	16	3	801	815	8	1	4	462	-477	-7	4	4	977	1010	4	6	4	732	704
1	12	3	462	-482	-6	17	3	946	990	-17	2	4	483	307	-6	4	4	1264	1285	6	6	4	559	513
4	12	3	842	-935	-4	17	3	849	-903	-11	2	4	472	606	-4	4	4	425	-461	8	6	4	980	-1012
6	12	3	427	472	1	17	3	578	668	-9	2	4	1229	-1294	-1	4	4	873	786	-14	7	4	681	-702
7	12	3	559	-603	4	17	3	502	498	-7	2	4	1103	1219	0	4	4	468	461	-10	7	4	525	-421
10	12	3	600	709	-4	18	3	619	-648	-5	2	4	1189	-1089	1	4	4	825	-796	-8	7	4	456	376
-9	13	3	608	-678	-2	18	3	633	637	-4	2	4	461	-536	2	4	4	863	-837	-6	7	4	627	597
-7	13	3	1074	1074	0	18	3	572	-604	-2	2	4	1515	1429	3	4	4	1125	1078	-5	7	4	830	-803
-5	13	3	938	-1013	7	18	3	539	600	-1	2	4	392	-328	4	4	4	387	-379	-4	7	4	1374	-1315
-3	13	3	423	471	-5	19	3	764	762	0	2	4	964	910	7	4	4	1015	-1010	-3	7	4	1018	944
-2	13	3	788	775	3	19	3	525	-577	1	2	4	1469	-1480	9	4	4	562	627	-2	7	4	399	351
1	13	3	670	-733	5	19	3	577	640	2	2	4	892	860	10	4	4	471	553	3	7	4	696	689
3	13	3	809	834	1	20	3	590	-532	3	2	4	1352	1326	12	4	4	562	-529	4	7	4	1213	1127
11	13	3	627	-507	6	20	3	489	-397	4	2	4	935	-946	14	4	4	496	353	5	7	4	1427	-1386
-10	14	3	488	550	-5	22	3	487	187	5	2	4	568	-533	-13	5	4	683	730	6	7	4	1538	-1443
-8	14	3	813	-792	-10	0	4	1518	-1654	6	2	4	485	401	-10	5	4	498	488	7	7	4	818	764
-2	14	3	523	-610	-8	0	4	2175	2265	7	2	4	421	-371	-9	5	4	454	546	8	7	4	729	721
-1	14	3	696	-683	-6	0	4	785	-815	9	2	4	618	704	-6	5	4	514	-547	9	7	4	512	-499
0	14	3	427	382	-2	0	4	1722	1579	11	2	4	825	-779	-5	5	4	1720	-1757	11	7	4	534	511
1	14	3	539	619	0	0	4	1124	-1035	-14	3	4	621	629	-4	5	4	493	461	-9	8	4	815	784
6	14	3	643	726	2	0	4	3638	3603	-10	3	4	697	745	-3	5	4	828	894	-8	8	4	435	-393
8	14	3	704	-780	4	0	4	739	-783	-7	3	4	466	518	-2	5	4	481	-446	-7	8	4	877	-806

OBSERVED AND CALCULATED STRUCTURE FACTORS FOR DJC.DAT

PAGE 6

H	K	L	10FO	10FC	H	K	L	10FO	10FC	H	K	L	10FO	10FC	H	K	L	10FO	10FC	H	K	L	10FO	10FC
-6	8	4	396	233	-7	11	4	584	-575	11	14	4	485	-366	3	0	5	2087	-2051	-8	3	5	410	-415
-4	8	4	639	-640	-5	11	4	470	448	-4	15	4	486	425	5	0	5	1019	1068	-7	3	5	598	637
-3	8	4	1066	1030	-4	11	4	550	537	-2	15	4	442	499	7	0	5	483	-590	-5	3	5	782	818
-2	8	4	672	679	-2	11	4	541	-612	6	15	4	551	544	13	0	5	560	-624	-4	3	5	757	-770
-1	8	4	1270	-1152	2	11	4	500	-511	7	15	4	479	507	-10	1	5	988	-970	-3	3	5	542	-495
0	8	4	407	-332	3	11	4	857	-793	-10	16	4	473	501	-9	1	5	849	-810	-2	3	5	819	756
2	8	4	389	358	5	11	4	607	589	-8	16	4	944	-940	-8	1	5	594	609	-1	3	5	1576	1489
3	8	4	823	-782	7	11	4	747	-771	-6	16	4	608	622	-4	1	5	785	-760	0	3	5	763	729
6	8	4	495	524	-11	12	4	446	408	-2	16	4	783	-803	-2	1	5	1461	1476	1	3	5	1324	-1300
7	8	4	508	519	-9	12	4	692	-727	-1	16	4	648	-690	-1	1	5	384	393	4	3	5	432	-448
-15	9	4	496	450	-8	12	4	1056	1029	1	16	4	491	489	0	1	5	1874	-1826	5	3	5	622	617
-12	9	4	517	561	-7	12	4	485	491	2	16	4	555	-631	1	1	5	433	-473	7	3	5	470	-415
-10	9	4	523	-623	-3	12	4	497	471	4	16	4	604	675	2	1	5	1145	1173	10	3	5	485	522
-6	9	4	555	587	-2	12	4	441	402	-5	17	4	720	-845	3	1	5	482	439	-9	4	5	427	-481
-5	9	4	584	564	0	12	4	599	-636	3	17	4	483	519	7	1	5	529	-443	-7	4	5	1287	1392
-4	9	4	552	-573	1	12	4	538	-564	5	17	4	461	-562	-15	2	5	453	389	-6	4	5	499	-549
-3	9	4	937	-895	2	12	4	1005	1021	7	17	4	570	632	-11	2	5	642	559	-5	4	5	780	-769
-2	9	4	609	626	4	12	4	633	-685	-1	18	4	868	-858	-9	2	5	497	-484	-2	4	5	490	530
-1	9	4	548	525	5	12	4	412	405	1	18	4	796	808	-8	2	5	1199	1231	-1	4	5	446	-437
2	9	4	470	-407	11	12	4	632	-616	3	18	4	694	-712	-6	2	5	627	-703	0	4	5	354	-309
4	9	4	1214	1221	-6	13	4	530	-566	5	18	4	512	611	-5	2	5	656	635	1	4	5	1226	-1146
5	9	4	472	466	-3	13	4	640	672	-6	19	4	458	415	-4	2	5	420	429	2	4	5	976	957
6	9	4	831	-835	-1	13	4	698	-722	-4	19	4	492	-518	-3	2	5	566	599	3	4	5	1184	1109
7	9	4	743	-733	2	13	4	520	519	0	19	4	385	-366	-1	2	5	972	-984	4	4	5	968	-1004
8	9	4	604	629	4	13	4	1234	-1283	6	19	4	531	-602	0	2	5	453	-446	5	4	5	674	-653
-8	10	4	836	868	8	13	4	489	-451	-2	20	4	535	467	1	2	5	1039	961	6	4	5	812	823
-7	10	4	421	-456	-9	14	4	1006	-1027	1	20	4	489	453	2	2	5	2201	2208	11	4	5	475	-493
-2	10	4	670	648	-7	14	4	1024	926	-5	21	4	487	426	3	2	5	1724	-1672	-12	5	5	553	-609
0	10	4	545	-466	-5	14	4	583	-591	-3	21	4	706	-612	4	2	5	1439	-1488	-10	5	5	760	858
1	10	4	794	795	-4	14	4	505	-587	-1	21	4	494	509	5	2	5	980	930	-8	5	5	1076	-1200
2	10	4	785	756	0	14	4	622	632	-4	23	4	565	458	6	2	5	914	883	-5	5	5	357	348
3	10	4	797	-868	2	14	4	495	-476	-2	23	4	695	-633	14	2	5	647	-581	-4	5	5	379	401
4	10	4	536	-485	3	14	4	935	908	-13	0	5	760	-715	-13	3	5	648	-636	-3	5	5	436	-452
12	10	4	461	413	7	14	4	532	-518	-9	0	5	606	615	-11	3	5	530	534	-2	5	5	451	-445
-13	11	4	553	-472	9	14	4	481	499	-1	0	5	593	-595	-10	3	5	531	522	0	5	5	291	297
-11	11	4	642	582	10	14	4	558	532	1	0	5	2184	2194	-9	3	5	1015	-1096	2	5	5	752	-761

OBSERVED AND CALCULATED STRUCTURE FACTORS FOR DJC.DAT

PAGE 7

H	K	L	10FO	10FC	H	K	L	10FO	10FC	H	K	L	10FO	10FC	H	K	L	10FO	10FC	H	K	L	10FO	10FC
3	5	5	428	473	3	8	5	638	599	9	11	5	516	482	3	16	5	858	934	8	1	6	428	-307
5	5	5	638	655	4	8	5	1587	1514	10	11	5	595	-476	11	16	5	817	-793	11	1	6	486	562
6	5	5	1101	1136	6	8	5	668	-603	-8	12	5	585	512	12	17	5	714	-650	12	1	6	625	565
7	5	5	608	-589	7	8	5	617	-530	-7	12	5	464	-506	-13	17	5	394	304	-13	2	6	668	-534
8	5	5	898	-1001	8	8	5	429	323	-6	12	5	582	-520	-12	17	5	543	469	-12	2	6	694	713
10	5	5	545	536	-11	9	5	635	-668	-4	12	5	813	811	-11	18	5	556	-517	-11	2	6	694	727
12	5	5	480	-449	-9	9	5	802	671	-2	12	5	710	-813	-9	18	5	865	930	-9	2	6	428	-240
-13	6	5	658	642	-5	9	5	438	-446	1	12	5	694	734	-7	18	5	507	-465	-7	2	6	1199	-1201
-7	6	5	578	626	-4	9	5	779	-865	2	12	5	494	519	-5	19	5	556	555	-5	2	6	536	542
-5	6	5	776	-738	-2	9	5	1559	1597	3	12	5	1127	-1209	-4	19	5	503	-561	-4	2	6	387	-356
-3	6	5	404	358	-1	9	5	1133	-1142	4	12	5	448	-473	-2	20	5	588	573	-2	2	6	349	352
-2	6	5	401	-455	1	9	5	1278	1262	5	12	5	568	549	-1	20	5	507	-376	-1	2	6	1856	1695
-1	6	5	776	730	3	9	5	857	-766	12	12	5	475	457	-4	21	5	540	-428	0	2	6	544	-591
0	6	5	428	409	5	9	5	576	-601	-11	13	5	573	606	0	21	5	556	-548	2	2	6	1039	-1002
3	6	5	764	881	7	9	5	501	475	-7	13	5	432	207	1	21	5	486	351	3	2	6	837	-868
5	6	5	1169	-1254	8	9	5	537	559	-1	13	5	669	665	3	22	5	474	-386	4	2	6	505	514
6	6	5	655	-656	-13	10	5	543	-566	1	13	5	554	-502	-12	22	5	714	721	6	2	6	419	-348
-13	7	5	604	478	-8	10	5	703	-723	7	13	5	440	-414	-10	22	5	731	-785	8	2	6	461	350
-10	7	5	794	748	-7	10	5	740	-683	9	13	5	518	579	-6	22	5	738	688	13	2	6	597	-597
-9	7	5	678	709	-5	10	5	552	563	-8	14	5	792	696	0	22	5	2133	-2048	-10	3	6	755	-774
-5	7	5	890	-852	-4	10	5	660	623	-7	14	5	457	440	2	22	5	420	-371	-9	3	6	631	-737
-4	7	5	418	415	-3	10	5	592	-607	-6	14	5	606	-553	14	22	5	843	890	-8	3	6	930	931
-3	7	5	929	877	0	10	5	334	295	-4	14	5	501	443	-13	1	6	639	-570	-5	3	6	772	-801
-2	7	5	1389	-1257	1	10	5	480	525	-3	14	5	530	524	-10	1	6	876	-836	-3	3	6	1142	1153
-1	7	5	772	-778	2	10	5	930	-952	4	14	5	624	659	-9	1	6	493	621	-2	3	6	388	367
1	7	5	368	410	3	10	5	1058	-1060	4	14	5	1050	-1162	-8	1	6	932	911	0	3	6	1391	-1395
3	7	5	611	-662	4	10	5	787	802	6	14	5	536	522	-5	1	6	639	-599	1	3	6	421	-367
4	7	5	573	-564	5	10	5	674	718	-10	15	5	624	593	-4	1	6	482	384	2	3	6	1788	1767
5	7	5	397	-274	-10	11	5	770	-742	-8	15	5	599	-518	-3	1	6	423	459	3	3	6	627	587
6	7	5	958	977	-8	11	5	501	553	-2	15	5	622	-576	-2	1	6	532	498	4	3	6	587	-511
7	7	5	950	955	-6	11	5	449	561	0	15	5	410	461	-1	1	6	939	-852	11	3	6	465	-438
8	7	5	529	-560	-2	11	5	678	714	1	15	5	444	-363	0	1	6	1165	-1187	12	3	6	538	634
-12	8	5	676	601	-1	11	5	397	225	7	15	5	573	-595	1	1	6	2773	2606	-13	4	6	612	-768
-7	8	5	663	581	0	11	5	1149	-1190	-7	16	5	576	502	2	1	6	1211	1190	-11	4	6	619	529
1	8	5	435	286	2	11	5	1013	943	-5	16	5	611	-539	3	1	6	1576	-1684	-6	4	6	725	-736
2	8	5	790	-688	7	11	5	453	-510	1	16	5	613	-678	5	1	6	499	548	-5	4	6	805	846

OBSERVED AND CALCULATED STRUCTURE FACTORS FOR DJC.DAT

PAGE 8

H	K	L	10FO	10FC	H	K	L	10FO	10FC	H	K	L	10FO	10FC	H	K	L	10FO	10FC	H	K	L	10FO	10FC
-4	4	6	443	499	-1	7	6	628	630	-9	11	6	526	554	-2	7	6	617	604	-2	7	6	820	800
-2	4	6	893	-892	0	7	6	638	664	-1	11	6	989	-1010	-1	7	6	513	602	-1	7	6	678	-675
-1	4	6	467	493	1	7	6	625	-622	1	11	6	1615	1654	0	7	6	458	524	0	7	6	1041	-1020
0	4	6	468	503	2	7	6	1073	-1122	3	11	6	1364	-1348	1	7	6	500	408	1	7	6	451	484
1	4	6	409	-468	3	7	6	589	615	-8	12	6	438	-183	2	7	6	657	-579	2	7	6	1206	1149
2	4	6	515	570	4	7	6	794	804	-5	12	6	561	544	3	7	6	478	535	3	7	6	676	-663
4	4	6	646	-596	5	7	6	630	621	-3	12	6	529	-584	-15	7	6	647	-519	-15	7	6	489	466
5	4	6	653	703	-13	8	6	711	735	-2	12	6	449	476	-13	7	6	499	-523	-13	7	6	599	-636
6	4	6	757	807	-8	8	6	703	589	-1	12	6	770	823	-9	7	6	624	493	-9	7	6	527	496
7	4	6	535	-578	-5	8	6	1044	-1043	0	12	6	580	-629	-8	7	6	473	-455	-8	7	6	701	700
-9	5	6	776	-849	-3	8	6	1374	1315	3	12	6	470	-521	-7	7	6	841	-818	-7	7	6	722	-762
-7	5	6	988	1086	-1	8	6	1433	-1310	4	12	6	543	593	-5	7	6	621	688	-5	7	6	478	578
-5	5	6	588	-621	1	8	6	1045	945	5	12	6	438	407	-4	7	6	755	767	-4	7	6	504	487
-4	5	6	413	-442	5	8	6	786	-779	-10	13	6	587	-622	-3	7	6	2522	-2332	-3	7	6	1339	-1423
-2	5	6	453	476	6	8	6	706	-613	-8	13	6	752	800	-1	7	6	1553	1596	-1	7	6	1006	1000
-1	5	6	863	883	7	8	6	625	750	-6	13	6	547	-478	1	7	6	1338	-1371	1	7	6	377	354
1	5	6	721	-773	-16	9	6	512	252	0	13	6	438	-434	3	7	6	684	643	2	7	6	509	457
3	5	6	956	971	-1	9	6	811	-821	2	13	6	975	991	-12	7	6	610	608	3	7	6	711	-778
9	5	6	485	443	0	9	6	948	948	-9	13	6	744	-782	11	7	6	593	617	11	7	6	551	540
11	5	6	514	-595	2	9	6	1941	-1843	3	13	6	450	-442	12	7	6	511	-639	12	7	6	490	375
-14	6	6	537	344	3	9	6	501	-581	-8	13	6	435	440	-12	7	6	1027	-1063	-12	7	6	552	578
-12	6	6	839	-833	4	9	6	640	629	-7	13	6	477	532	-9	7	6	663	677	-9	7	6	720	-703
-10	6	6	550	592	-12	10	6	805	720	12	14	6	477	-527	-4	7	6	763	-734	-4	7	6	401	-465
-6	6	6	578	-617	-7	10	6	754	778	-9	15	6	607	-639	-3	7	6	422	-403	-2	7	6	1284	1349
-5	6	6	517	-517	-6	10	6	589	597	-7	15	6	895	894	-1	7	6	682	679	-1	7	6	691	667
-4	6	6	1071	1099	-4	10	6	757	-822	-5	15	6	574	-606	0	7	6	418	436	0	7	6	939	-971
-2	6	6	1507	-1590	-3	10	6	549	-499	-1	15	6	460	387	1	7	6	401	441	1	7	6	487	-532
0	6	6	880	922	-2	10	6	1115	1179	0	15	6	472	-362	5	7	6	731	-730	5	7	6	570	530
4	6	6	648	-695	-1	10	6	919	-899	1	15	6	625	-626	8	7	6	725	-782	8	7	6	824	881
6	6	6	651	658	0	10	6	870	-895	2	15	6	551	442	10	7	6	423	498	10	7	6	595	-594
7	6	6	563	587	2	10	6	458	264	3	15	6	603	619	11	7	6	453	488	11	7	6	517	-477
8	6	6	658	-730	3	10	6	750	750	-4	16	6	587	642	-8	7	6	635	-624	-8	7	6	690	688
10	6	6	490	378	4	10	6	619	656	11	16	6	526	-579	-6	7	6	466	447	-6	7	6	1009	-1035
-16	7	6	545	348	6	10	6	444	-509	12	16	6	694	658	-5	7	6	555	-594	-5	7	6	569	546
-6	7	6	614	594	7	10	6	612	-573	13	16	6	375	444	-4	7	6	679	-542	-4	7	6	1588	1626
-2	7	6	1181	-1187	-13	11	6	468	-604	-10	17	6	403	-408	-3	7	6	752	-730	-3	7	6	1110	-1168

OBSERVED AND CALCULATED STRUCTURE FACTORS FOR DJC.DAT

PAGE 9

H	K	L	10FO	10FC	H	K	L	10FO	10FC	H	K	L	10FO	10FC	H	K	L	10FO	10FC	H	K	L	10FO	10FC
1	5	7	391	-427	-13	9	7	590	732	-1	14	7	450	222	-3	2	8	675	-702	5	5	8	444	329
2	5	7	569	605	-8	9	7	538	534	0	14	7	526	-510	0	2	8	1032	1075	7	5	8	915	-959
3	5	7	545	528	-7	9	7	666	675	-6	15	7	642	-740	1	2	8	735	734	9	5	8	773	730
4	5	7	463	-553	-4	9	7	481	-527	-5	15	7	479	482	3	2	8	1058	-1029	-10	6	8	597	-657
10	5	7	477	-407	3	9	7	849	817	-3	15	7	478	-495	4	2	8	441	481	-9	6	8	530	-523
-13	6	7	530	-557	-11	10	7	473	-475	2	15	7	503	489	6	2	8	427	-409	-6	6	8	831	-872
-11	6	7	482	498	-5	10	7	512	-586	4	15	7	606	-661	8	2	8	489	-257	-4	6	8	770	822
-8	6	7	486	-539	-3	10	7	690	685	-11	16	7	479	420	11	2	8	893	867	-1	6	8	393	474
-3	6	7	948	-987	-1	10	7	1334	-1303	-4	17	7	716	688	13	2	8	588	-401	1	6	8	376	-427
-2	6	7	751	-827	0	10	7	1080	1016	4	17	7	485	-409	-7	3	8	410	-465	5	6	8	501	-435
-1	6	7	1380	1762	1	10	7	1184	1230	5	17	7	599	-620	-4	3	8	1308	-1370	8	6	8	616	585
0	6	7	538	509	3	10	7	695	-685	-2	18	7	570	-551	-2	3	8	1523	1547	10	6	8	765	-974
1	6	7	569	-575	6	10	7	667	-733	-1	18	7	589	528	-1	3	8	583	-536	-14	7	8	594	582
5	6	7	496	487	9	10	7	570	-562	-2	20	7	677	-682	0	3	8	832	-837	-12	7	8	498	-643
7	6	7	649	-725	-12	11	7	657	547	0	20	7	712	705	3	3	8	489	-514	-8	7	8	461	-421
9	6	7	984	1046	-6	11	7	505	563	-10	0	8	571	639	8	3	8	671	698	-5	7	8	482	449
-11	6	7	621	-548	-2	11	7	805	798	-8	0	8	587	-586	-11	4	8	511	-520	-4	7	8	973	985
-13	7	7	688	638	1	11	7	414	-400	-6	0	8	689	624	-10	4	8	830	-933	-3	7	8	474	-541
-5	7	7	1069	-1035	2	11	7	1147	-1184	-4	0	8	1184	-1260	-8	4	8	927	904	-2	7	8	1225	-1155
-4	7	7	835	827	4	11	7	836	841	0	0	8	1791	1813	-7	4	8	655	-700	-1	7	8	1361	1297
-3	7	7	1198	1219	-10	12	7	600	-642	2	0	8	1093	-1143	-6	4	8	517	-667	0	7	8	542	536
-2	7	7	1044	-1028	-8	12	7	577	585	4	0	8	796	710	-5	4	8	1089	1121	1	7	8	472	-501
-1	7	7	499	486	-1	12	7	1116	-1209	10	0	8	465	460	-4	4	8	1017	1143	6	7	8	746	780
0	7	7	391	386	0	12	7	918	-900	12	0	8	677	-714	-3	4	8	405	-419	7	7	8	532	-418
1	7	7	391	-372	1	12	7	901	954	-5	1	8	782	-762	-1	4	8	754	-783	8	7	8	710	-673
3	7	7	453	420	-13	13	7	484	-320	-4	1	8	620	-592	2	4	8	405	427	9	7	8	463	363
5	7	7	458	-522	-9	13	7	505	541	-3	1	8	1022	1014	9	4	8	783	-867	-4	8	8	413	415
7	7	7	571	524	-7	13	7	1041	-1080	-1	1	8	1489	-1453	10	4	8	700	-706	-2	8	8	604	-620
-12	8	7	571	-586	-5	13	7	575	637	0	1	8	521	-586	11	4	8	603	670	-1	8	8	1073	1034
-4	8	7	1263	1202	-3	13	7	643	-722	4	1	8	817	861	-13	5	8	698	-652	1	8	8	604	-598
-3	8	7	491	429	-1	13	7	548	498	9	1	8	483	-306	-10	5	8	439	343	9	8	8	648	481
-2	8	7	1792	-1694	0	13	7	485	427	-17	2	8	515	-413	-5	5	8	688	765	11	8	8	629	-542
0	8	7	1113	1056	1	13	7	703	681	-9	2	8	703	713	-4	5	8	873	-908	-13	9	8	551	625
2	8	7	1091	-1079	3	13	7	870	-893	-7	2	8	756	-789	-3	5	8	1327	-1370	-12	9	8	701	-673
9	8	7	417	129	-8	14	7	479	373	-5	2	8	1207	1245	-2	5	8	798	855	-10	9	8	467	461
10	8	7	471	421	-6	14	7	467	-326	-4	2	8	494	-484	-1	5	8	1196	1255	-4	9	8	478	-404

OBSERVED AND CALCULATED STRUCTURE FACTORS FOR DJC.DAT

H	K	L	10FO	10FC	H	K	L	10FO	10FC	H	K	L	10FO	10FC	H	K	L	10FO	10FC
-5	9	8	519	-587	-2	2	9	436	472	-5	6	9	1287	1296	1	10	9	456	-446
-4	9	8	538	470	2	2	9	1053	-1012	-4	6	9	483	577	2	10	9	529	591
-3	9	8	583	688	4	2	9	800	853	-3	6	9	1115	-1150	5	10	9	477	-499
-2	9	8	1109	-1090	5	2	9	414	-590	7	6	9	476	-521	-10	11	9	784	758
0	9	8	637	653	6	2	9	751	-720	-13	7	9	561	-604	0	11	9	487	447
1	9	8	469	527	8	2	9	470	515	-12	7	9	553	512	1	11	9	439	443
-10	10	8	510	521	-11	3	9	452	-455	-10	7	9	567	-563	8	11	9	504	-504
-6	10	8	459	527	-9	3	9	629	693	-9	7	9	537	-453	10	11	9	627	517
0	10	8	1006	980	-7	3	9	588	-635	-7	7	9	719	693	-8	12	9	475	-390
1	10	8	565	-677	-3	3	9	380	485	-6	7	9	653	-692	-2	12	9	559	643
2	10	8	805	-837	-2	3	9	404	-496	-3	7	9	933	-888	5	12	9	569	-593
3	10	8	451	430	-1	3	9	490	-480	-2	7	9	687	675	-9	13	9	679	645
4	10	8	487	557	4	3	9	618	709	-1	7	9	863	884	-6	13	9	580	534
-11	11	8	573	-452	7	3	9	789	704	0	7	9	359	-434	-7	14	9	455	-356
-1	11	8	1197	-1213	9	3	9	834	-888	1	7	9	516	-582	-6	14	9	968	926
-9	12	8	564	688	11	3	9	479	524	2	7	9	461	-369	-4	14	9	880	-931
-7	12	8	646	-659	-9	4	9	587	547	3	7	9	494	404	4	14	9	499	423
-3	12	8	454	-399	-7	4	9	772	-782	7	7	9	539	-539	6	14	9	526	-546
0	12	8	667	697	-6	4	9	539	572	9	7	9	581	588	-10	15	9	510	-388
2	12	8	655	651	-5	4	9	1046	1153	10	7	9	579	-611	-3	15	9	465	472
-6	13	8	445	-510	-4	4	9	1017	-1026	-6	8	9	549	-635	0	15	9	471	-500
-2	13	8	706	712	-3	4	9	860	-919	-4	8	9	966	983	2	15	9	467	319
-2	13	8	689	745	-2	4	9	826	825	4	8	9	576	-452	-7	16	9	486	-466
0	13	8	463	-431	3	4	9	614	-653	6	8	9	819	753	-5	16	9	825	821
1	13	8	437	-338	5	4	9	488	601	-12	9	9	684	-622	-3	16	9	581	-508
4	13	8	494	505	6	4	9	551	-464	-9	9	9	568	-506	3	16	9	461	-428
6	13	8	501	-469	7	4	9	672	-657	-7	9	9	748	741	5	16	9	584	591
-9	14	8	512	550	-12	5	9	447	473	-4	9	9	559	532	7	16	9	530	-414
-7	14	8	908	-905	-10	5	9	595	-554	-2	9	9	998	-898	1	17	9	461	-430
-5	14	8	881	914	-8	5	9	586	626	-1	9	9	726	761	-6	18	9	475	-469
-3	14	8	555	-530	-7	5	9	503	-496	0	9	9	710	674	-4	18	9	517	559
2	14	8	433	417	-6	5	9	941	-939	1	9	9	460	-462	2	18	9	479	402
-5	15	8	510	446	-2	5	9	597	632	2	9	9	493	-388	-3	19	9	525	-460
-4	15	8	508	-493	-1	5	9	688	-678	9	9	9	560	563	-1	19	9	610	574
-2	15	8	624	620	8	5	9	1105	1174	-5	10	9	515	-619	0	21	9	576	563

OBSERVED AND CALCULATED STRUCTURE FACTORS FOR DJC.DAT

PAGE 11

H	K	L	10FO	10FC	H	K	L	10FO	10FC	H	K	L	10FO	10FC	H	K	L	10FO	10FC
-12	0	10	512	-485	4	3	10	561	630	-3	8	10	815	-819	4	13	10	648	667
-10	0	10	558	539	6	3	10	442	-604	-2	8	10	499	-467	-3	14	10	582	528
-8	0	10	637	-691	-13	4	10	617	619	-1	8	10	660	582	0	14	10	453	-397
-4	0	10	677	741	-9	4	10	501	426	0	8	12	453	487	5	14	10	735	-744
4	0	10	836	-889	-7	4	10	697	-712	5	8	10	732	723	-9	15	10	591	455
6	0	10	822	811	-4	4	10	474	-511	7	8	10	677	-641	-6	15	10	702	632
8	0	10	618	-589	-3	4	10	943	923	9	8	10	641	476	-5	15	10	531	501
-8	1	10	778	-769	3	4	10	584	-532	-6	9	10	641	-713	-4	15	10	467	-481
-7	1	10	811	783	6	4	10	679	-662	-1	9	10	527	469	3	15	10	617	-573
-6	1	10	821	875	7	4	10	723	754	0	9	10	483	-501	-2	16	10	460	455
-5	1	10	533	-582	8	4	10	678	709	2	9	10	503	526	6	16	10	616	-479
-1	1	10	642	580	9	4	10	533	-496	3	9	10	474	471	-5	17	10	616	569
1	1	10	653	-629	-9	5	10	527	487	4	9	10	879	-791	-3	18	10	477	-446
2	1	12	646	-705	-7	5	10	856	-895	-12	10	10	574	-492	-2	20	10	539	-477
3	1	10	982	988	-5	5	10	981	1059	-10	10	10	617	654	-9	0	11	883	-930
4	1	10	459	484	-2	5	10	582	-594	-8	10	10	510	-543	-7	0	11	701	702
5	1	10	750	-715	1	5	10	497	452	-4	10	10	467	415	1	0	11	1018	-1053
6	1	10	452	-364	5	5	10	516	492	-2	10	10	472	-476	3	0	11	521	546
7	1	10	496	471	9	5	10	493	-567	0	10	10	470	474	-7	1	11	527	608
-10	2	10	630	608	11	5	10	460	392	1	10	10	500	374	-5	1	11	444	-414
-9	2	10	514	595	-12	6	10	575	522	6	10	10	485	531	-1	1	11	671	-640
-5	2	10	519	-588	-8	6	10	579	576	-9	11	10	647	-584	2	1	11	474	575
-3	2	10	433	423	-4	6	10	816	-901	-7	11	10	786	717	3	1	11	886	916
-2	2	10	637	-620	-3	6	10	501	-528	-5	11	10	509	-491	4	1	11	991	-929
0	2	10	398	-363	-2	6	10	753	759	1	11	10	574	-606	5	1	11	622	-761
3	2	10	657	646	6	6	10	980	-1022	3	11	10	781	776	6	1	11	918	957
5	2	10	858	-889	8	6	10	616	708	5	11	10	500	-498	-10	2	11	484	342
7	2	10	862	916	-7	7	10	663	-628	6	11	10	489	326	-8	2	11	742	-793
9	2	10	486	-416	-6	7	10	665	-704	-11	12	10	517	-486	-3	2	11	543	-642
-8	3	10	528	-526	-5	7	10	550	468	6	12	10	499	517	0	2	11	380	365
-7	3	10	664	-632	-2	7	10	551	502	9	12	10	490	-427	2	2	11	633	-702
-6	3	10	938	957	0	7	10	647	-616	-8	13	10	656	-601	3	2	11	604	635
-4	3	10	669	-699	4	7	10	749	-742	-6	13	10	619	687	-15	3	11	471	-390
-3	3	10	520	-571	9	7	10	445	-346	-5	13	10	472	-405	-13	3	11	469	339
-1	3	10	1089	1095	-9	8	10	538	-552	-2	13	10	439	426	-6	3	11	591	532
0	3	10	640	624	-7	8	10	673	677	2	13	10	508	-472	-5	3	11	583	-651

OBSERVED AND CALCULATED STRUCTURE FACTORS FOR DJC.DAT

PAGE 12

H	K	L	10FO	10FC	H	K	L	10FO	10FC	H	K	L	10FO	10FC	H	K	L	10FO	10FC	H	K	L	10FO	10FC
2	8	11	964	868	1	1	12	949	-1039	-3	8	12	507	472	-4	2	13	615	676	-6	14	13	698	-629
4	8	11	741	-752	-7	2	12	857	817	1	8	12	830	826	-4	14	13	545	-901	-4	14	13	545	582
-11	9	11	512	480	-1	2	12	619	-611	3	8	12	820	-841	-2	14	13	529	510	-2	14	13	529	-409
-2	9	11	486	-422	2	2	12	618	658	-10	9	12	556	-523	0	14	13	479	-483	0	14	13	479	421
3	9	11	560	-488	3	2	12	989	904	-4	9	12	473	-364	-8	16	13	610	-427	-3	16	13	610	608
5	9	11	738	756	4	2	12	459	-482	-3	9	12	743	-647	-10	0	14	513	732	-10	0	14	513	-456
-9	10	11	585	-651	5	2	12	569	-561	0	9	12	668	-746	1	0	14	501	-952	-4	0	14	501	-579
-7	10	11	514	414	-10	3	12	679	677	2	9	12	518	450	3	0	14	664	486	-2	0	14	664	675
-1	10	11	694	740	-7	3	12	484	439	-8	10	12	476	414	-4	0	14	749	351	0	0	14	749	-776
1	10	11	1076	-1138	-5	3	12	479	-379	-6	10	12	454	-570	-3	0	14	488	835	2	0	14	488	388
3	10	11	697	713	-2	3	12	741	-818	0	10	12	586	-518	-2	1	14	496	-677	-2	1	14	496	-450
-12	11	11	473	-489	0	3	12	623	684	2	10	12	816	788	5	1	14	463	-457	1	1	14	463	493
-7	11	11	440	-162	2	3	12	536	-546	3	10	12	498	-547	0	1	14	526	547	3	1	14	526	-458
-6	11	11	649	-664	6	3	12	631	636	6	10	12	585	347	2	2	14	721	-701	-3	2	14	721	-699
-3	11	11	440	357	-8	4	12	686	-651	-1	11	12	593	546	-5	2	14	637	-424	-1	2	14	637	654
2	11	11	549	483	-4	4	12	509	-552	-12	12	12	534	-430	-1	2	14	500	-517	1	2	14	500	-505
4	11	11	757	-733	0	4	12	511	485	-7	12	12	595	561	-11	3	14	610	-494	-8	3	14	610	561
6	11	11	551	549	1	4	12	660	-734	-5	12	12	533	-594	-10	3	14	449	397	-6	3	14	449	-491
-3	12	11	532	-454	2	4	12	504	-499	2	12	12	620	570	0	3	14	690	438	-4	3	14	690	721
0	12	11	445	398	3	4	12	532	551	4	12	12	614	-606	2	3	14	486	-464	-2	3	14	486	-374
3	12	11	466	374	-9	5	12	457	374	-4	13	12	481	573	3	4	14	559	-536	-2	4	14	559	-513
-5	13	11	556	-657	-3	5	12	754	802	0	13	12	535	496	5	4	14	475	337	-1	4	14	475	504
-1	13	11	446	-380	-1	5	12	686	-733	-3	15	12	516	432	-2	4	14	429	523	0	4	14	429	360
3	13	11	569	630	0	5	12	374	395	-2	17	12	487	303	-9	5	14	474	521	-11	5	14	474	348
5	13	11	525	-602	1	5	12	653	641	-11	0	13	645	591	1	5	14	489	874	-9	5	14	489	-605
-4	15	11	641	-613	-6	6	12	559	513	-7	0	13	764	-791	2	5	14	589	468	-7	5	14	589	541
0	18	11	406	-516	-1	6	12	499	-603	-5	0	13	566	643	3	5	14	733	-462	-5	5	14	733	-728
-14	0	12	485	521	2	6	12	604	-635	-3	0	13	762	-864	0	10	13	691	-335	-3	5	14	691	727
-12	0	12	555	-525	4	6	12	669	687	-1	0	13	1033	1134	4	10	13	772	413	-2	6	14	772	-896
-8	0	12	812	799	-12	7	12	696	563	3	0	13	658	-674	0	11	13	445	-653	0	6	14	445	481
2	0	12	1312	1275	-9	7	12	605	535	-2	1	13	573	556	2	11	13	462	784	3	6	14	462	-151
4	0	12	964	-897	-5	7	12	596	-602	0	1	13	822	-806	-5	12	13	511	341	-10	7	14	511	165
-9	1	12	487	-446	-2	7	12	731	716	1	1	13	459	-397	-4	12	13	615	431	-4	7	14	615	-496
-5	1	12	511	514	0	7	12	372	-322	2	1	13	851	894	-1	12	13	693	534	-3	7	14	693	539
-4	1	12	456	310	1	7	12	570	612	-8	2	13	587	604	0	12	13	533	336	2	7	14	533	-496
0	1	12	513	471	-9	8	12	458	340	-6	2	13	731	-806	1	13	13	771	-499	-1	8	14	771	-726

OBSERVED AND CALCULATED STRUCTURE FACTORS FOR DJC.DAT

PAGE 13

H	K	L	10FO	10FC	H	K	L	10FO	10FC	H	K	L	10FO	10FC	H	K	L	10FO	10FC
1	8	14	533	572	-4	15	14	543	484	-4	5	15	671	646	1	10	15	619	560
-8	9	14	480	-595	-4	1	15	436	-324	-2	5	15	654	-692	3	10	15	589	-477
-2	9	14	545	429	-2	1	15	586	521	-9	6	15	560	-480	-4	11	15	559	-458
1	9	14	581	483	-1	1	15	486	404	-5	6	15	644	-657	-7	1	16	487	-279
2	9	14	574	-513	-8	2	15	477	533	-3	7	15	656	743	-8	3	16	508	442
0	10	14	694	-669	-5	3	15	502	379	-8	8	15	506	-397	-6	3	16	463	-440
-9	11	14	466	392	-3	3	15	724	-708	-6	8	15	601	497	-2	3	16	632	588
0	12	14	467	-451	-10	4	15	477	-513	0	8	15	490	553	-5	4	16	578	558
-1	14	14	563	461	-6	4	15	527	-536	-7	10	15	555	-516	-6	5	16	509	-355